Seasonal variations in the ecological impacts of compound climate events

vorgelegt von
Master of Science
Johannes Joscha Vogel
ORCID: 0000-0002-0654-9673

an der Fakultät VI - Planen Bauen Umwelt
der Technischen Universität Berlin
zur Erlangung des akademischen Grades

Doktor der Naturwissenschaften
- Dr. rer. nat. -

genehmigte Dissertation

Promotionsausschuss:

Vorsitzende:	Prof. Dr. Galina Churkina
Gutachterin:	Prof. Dr. Eva Paton
Gutachter:	Prof. Dr. Christoph Hinz
Gutachterin:	Prof. Dr. Annegret Thieken

Tag der wissenschaftlichen Aussprache: 22. Februar 2022

Berlin 2022

Acknowledgments

The work of this thesis was supported and made possible by many people and I wish to express my deep gratitude in these following lines.

I would like to thank Eva Paton for helping me all the way through the process of crafting this dissertation, for taking the time to discuss thoughts together as well as for her openness and support to let me follow own ideas. Axel Bronstert is always in high spirits, which makes meetings with him enjoyable every time. I am also grateful to Valentin Aich for being my mentor in his kind and helpful way.

I had the opportunity to take part in two collaborative works, which was a great pleasure and definitively the highlight of this endeavour. One group project emerged from the Training School on Statistical Modelling in 2019 at Lake Como. It was a great group of PhD students and I would like to thank Cristina Deidda, Leila Rahimi, Christoph Sauter and Elisabeth Tschumi for this shared experience. I was always looking forward to our meetings and I learned a lot during this project. Special thanks go to Pauline Rivoire who was always very enthusiastic about this work and is simply a great person for exchanging ideas and working together. Jakob Zscheischler and Karin van der Wiel were very determined supervisors who put a lot of effort and time in supporting this work. I am very grateful to them for their part in organizing the training school and supervising the development of our group article.

The other group work during my PhD thesis, a task force created by my graduate school NatRiskChange on the Australian Black Summer was a further great opportunity to create a joint project from scratch. It was a very nice group to work with and I am very glad to have shared this work with my colleagues Melanie Fischer, Matthias Kemter, Elisabeth Schönfeldt and Lisa Luna. I am very thankful for our joint time in and outside of work.

I also want to express my gratitude to the other PhD students both in NatRiskChange and the department of Ecohydrology. Many thanks to Lukas Schoppa, Shubham Sharma, Katharina Schmidt as well as Nasrin Haacke, Moreen Willaredt, Pedro Alencar, Sidra Bibi and Karin Hoffmann for all the nice chats and their friendship. It is saddening that our time together was shortened so much due to the pandemic. Furthermore, I would like to thank Michael Facklam for his cheerful nature.

Finally, I would like to thank my family, especially my mother and sister, Michaela and Alena Vogel for always believing in me and supporting me in everything I pursue.

Berlin, December 20, 2021

Abstract

Climate change alters the relationship between climate regimes and ecosystems in manifold ways. The interplay of multiple climatic drivers as well as the seasonal timing of extreme weather events is essential in determining the magnitude of detrimental impacts on ecosystems. Thus, this thesis analyses changes in compound hot and dry conditions in the face of climate change and investigates which combinations of temperature and water availability lead to adverse effects on ecosystems at certain stages during the course of the year. For this purpose, low states of ecosystem productivity in the Mediterranean Basin as well as crop failure in the Northern Hemisphere are attributed to their meteorological drivers.

The Mediterranean Basin is a climate change hot spot with strong land-atmosphere feedbacks, where temperature increases at a faster rate than the global average, which leads to substantial changes in ecosystem composition, productivity and phenology in this region. Therefore, one focus is put on changes in the frequency of compound warm spells and droughts and the impact of temperature and soil moisture anomalies on ecosystem productivity in the Mediterranean Basin. Changes in compound warm spells and droughts over the last four decades are analysed, considering events that are extreme in both their absolute value as well as respective to the time of their seasonal occurrence. Furthermore, seasonal ecosystem vulnerability in the Mediterranean Basin is analysed. Low states of ecosystem productivity – indicated by the fraction of absorbed photosynthetically active radiation – are attributed to temperature and soil moisture anomalies during the course of the year.

The results show that the number of compound warm spells and droughts in the Mediterranean has significantly increased over the last four decades. This increase is primarily driven by rising temperatures, rather than lack of precipitation. Especially the compound events with high duration and magnitude are strongly increasing, indicating the emergence of novel climatic conditions, which are exceeding the previous climatic variability. Compound events, which are extreme relative to their seasonal time of occurrence, are increasing in particular in spring and early summer. This is concerning, since this is the main growing season in the Mediterranean Basin and thus potentially harmful for agricultural and natural ecosystems. Moreover, three main vulnerability regimes of Mediterranean ecosystems are identified: a) vulnerability to hot and dry conditions in late spring to midsummer, b) vulnerability to cold and dry conditions from the end of summer to mid-autumn and c) vulnerability during cold and wet conditions from the end of autumn to mid-spring. However, there are also prominent regional differences within the Mediterranean Basin. The period of vulnerability to hot and dry conditions is particularly long in Turkey, ranging from spring to autumn. On the other hand, the Balkans are mostly energy-limited throughout the course of the year and ecosystems rarely show vulnerability to hot anomalies.

A further aspect of this work addresses the drivers of declines in wheat yield in the Northern Hemisphere. Winter wheat is one of the most cultivated crops in the world and plays an

essential role in human diet and food security, which highlights the importance of gaining a better understanding of environmental conditions leading to crop failure. Therefore, an automated variable selection approach to detect the most relevant meteorological drivers leading to crop failure of winter wheat in the Northern Hemisphere using 1600 years of simulated weather and crop yield data is presented.

Crop failure of winter wheat in the Northern Hemisphere is often related to vapour pressure deficit during the reproductive phase. In addition, diurnal temperature range and the number of frost days in the growing season are identified as further relevant predictors. Both monthly means of common climate variables as well as climate extreme indicators play an important role in the prediction of crop failure.

The methodology used in this thesis is flexible and can easily be transferred to other ecoclimatological settings with a focus on seasonality. Both satellite-derived data sets as well as data from model observations are considered in this work. The increasing maturity and long-term availability of remote sensing time series make satellite products a valuable asset for assessing the interplay of ecosystems and meteorological drivers at large spatial scales. In addition, model simulations allow to examine a large range of environmental conditions, which is crucial for the investigation of the impacts of climatic extremes and thus model data is used to complement satellite observations.

The work presented here can facilitate monitoring of changes in environmental drivers and detect corresponding detrimental impacts on ecosystems, which can be useful to take measures to adapt crop choice, cropping calendars and irrigation management.

Zusammenfassung

Der Klimawandel verändert die Wechselwirkungen zwischen klimatischen Bedingungen und Ökosystemen auf vielfältige Weise. Das Zusammenspiel mehrerer klimatischer Einflussfaktoren sowie das jahreszeitliche Auftreten von Extremwetterereignissen spielt eine wesentliche Rolle für das Ausmaß negativer Auswirkungen auf Ökosysteme. Daher untersucht diese Arbeit klimawandelbedingte Änderungen zeitgleich auftretender heißer und trockener Bedingungen und erforscht, welche Kombinationen von Temperatur und Wasserverfügbarkeit im Jahresverlauf zu nachteiligen Auswirkungen auf Ökosysteme führen. Zu diesem Zweck werden niedrige Ökosystemproduktivität im Mittelmeerraum und Ernteausfälle in der nördlichen Hemisphäre ihren meteorologischen Einflussfaktoren zugeordnet.

Der Mittelmeerraum ist ein klimatischer Brennpunkt und gekennzeichnet durch starke Rückkopplungen zwischen Landoberfläche und Atmosphäre. Die Temperatur steigt schneller an als im globalen Durchschnitt, was grundlegende Änderungen in der Phänologie, Zusammensetzung und Produktivität der dortigen Ökosysteme zur Folge hat. Aus diesem Grund liegt ein Schwerpunkt dieses Werks auf der Untersuchung von Veränderungen in der Häufigkeit zeitgleichen Auftretens von Hitze- und Trockenphasen sowie den Auswirkungen von Temperatur- und Bodenfeuchteanomalien auf die Ökosystemproduktivität im Mittelmeergebiet. Veränderungen in der Koinzidenz von Hitze- und Trockenphasen in den letzten vier Jahrzehnten werden untersucht. Hierbei werden sowohl solche Ereignisse betrachtet, die absolut gesehen als extrem eingestuft werden, als auch Ereignisse, die relativ zu ihrem saisonalen Erscheinen im Jahresgang als extrem gelten. Darüber hinaus wird die saisonale Vulnerabilität von Ökosystemen im Mittelmeergebiet untersucht. Der Anteil der absorbierten photosynthetisch aktiven Strahlung wird als Indikator für niedrige Ökosystemproduktivität verwendet und Temperatur- und Bodenfeuchteanomalien im Jahresverlauf zugeordnet.

Die Ergebnisse zeigen, dass die Anzahl der zeitgleich auftretenden Hitze- und Trockenphasen im Mittelmeerraum in den letzten vier Jahrzehnten signifikant angestiegen ist. Diese Zunahme ist in erster Linie auf steigende Temperaturen zurückzuführen und nicht auf mangelnden Niederschlag. Insbesondere bei Ereignissen mit langer Dauer und hoher Magnitude ist ein starker Anstieg zu verzeichnen. Dies deutet auf das Vorkommen neuartiger klimatische Bedingungen außerhalb der bisherigen klimatischen Variabilität hin. Ereignisse, die im Bezug zu ihrem zeitlichen Auftreten als extrem anzusehen sind, nehmen vor allem im Frühling und zu Beginn des Sommers zu, der Hauptvegetationsperiode im Mittelmeergebiet. Ein Anstieg zu dieser Jahreszeit ist daher besorgniserregend, da er ungünstige Auswirkungen auf landwirtschaftliche und natürliche Ökosysteme zur Folge haben könnte. Der Jahresgang der ökologischen Vulnerabilität ist durch drei Phasen charakterisiert: a) Vulnerabilität während heißer und trockener Bedingungen im späten Frühling bis zum Hochsommer, b) Vulnerabilität während kalter und trockener Bedingungen von Ende Sommer bis Mitte Herbst und c) Vulnerabilität während kalter und feuchter Bedingungen von Ende Herbst bis Mitte Frühling. Es

gibt jedoch regionale Abweichungen von diesem Muster. Der Zeitraum der Vulnerabilität bei heißen und trockenen Bedingungen in der Türkei ist besonders lang und erstreckt sich vom Frühling bis in den Herbst. Die Balkanhalbinsel ist hingegen fast ganzjährig energielimitiert und Vulnerabilität unter heißen Bedingungen tritt kaum auf.

Ein weiterer Fokus dieser Arbeit liegt auf der Untersuchung von Einflussfaktoren, die Ertragsminderungen der Weizenernte in der nördlichen Hemisphäre verursachen können. Winterweizen ist eine der meistangebauten Feldfrüchte weltweit und von grundlegender Bedeutsamkeit für die menschliche Ernährungssicherheit. Aus diesem Grund ist es essenziell, ein besseres Verständnis der Umweltbedingungen zu erlangen, die Ernteausfälle verursachen können. Zur Identifikation der wichtigsten meteorologischen Einflussfaktoren, die zu Missernten von Winterweizen in der nördlichen Hemisphäre führen können, wird ein automatisiertes Verfahren zur Variablenselektion auf simulierte Wetter- und Ernteertragsdaten über einen Zeitraum von 1600 Jahren angewandt.

Ernteausfälle von Winterweizen in der nördlichen Hemisphäre stehen oftmals im Zusammenhang mit einem Wasserdampfsättigungsdefizit in der Luft während der generativen Wachstumsphase. Weiterhin stellen die tägliche Temperaturspanne und die Anzahl an Frosttagen innerhalb der Vegetationsperiode wichtige Prädiktoren dar. Sowohl monatliche Mittelwerte üblicher Klimavariablen als auch Indikatoren für Klimaextrema spielen eine bedeutsame Rolle für die Prognose von Missernten.

Die in dieser Arbeit verwendete Methodik ist flexibel und leicht auf andere ökoklimatologische Forschungsfragen mit einem Fokus auf Saisonalität anwendbar. Es fanden sowohl satellitenbasierte als auch modellgestützte Datensätze Verwendung. Fernerkundungsdaten sind zunehmend ausgereift und mittlerweile über lange Zeiträume verfügbar, was ihren herausragenden Wert für die Untersuchung von Wechselwirkungen zwischen Ökosystemen und meteorologischen Einflussfaktoren auf großen räumlichen Skalen unterstreicht. Modellsimulationen sind darüber hinaus von großem Nutzen, um Fernerkundungsdaten zu komplementieren. Sie ermöglichen es, eine große Spannweite von Umweltbedingungen zu untersuchen, was von hoher Bedeutung für die Beobachtung der Auswirkungen von klimatischen Extrema ist.

Das hier vorgelegte Werk kann dazu beitragen, Änderungen von Umweltbedingungen und damit verbundene negative Auswirkungen auf Ökosysteme zu überwachen. Auf dieser Basis können Maßnahmen ergriffen werden, um die Auswahl geeigneter Feldfrüchte, den Zeitpunkt des Anbaus und das Bewässerungsmanagement zu optimieren.

Contents

List of Abbreviations

ABL	Atmospheric Boundary Layer
AgMERRA	AgMIP Modern-Era Retrospective Analysis for Research and Applications
AgMIP	Agricultural Model Intercomparison and Improvement Project
APSIM	Agricultural Production Systems sIMulator
AVHRR	Advanced Very-High-Resolution Radiometer
CDO	Climate Data Operators
CGLS	Copernicus Global Land Service
CRNS	Cosmic-Ray Neutron Sensing
CSI	Critical Success Index
ECMWF	European Centre for Medium-Range Weather Forecasts
ECV	Essential Climate Variable
ERA5	ECMWF Reanalysis 5th Generation
ESA CCI	European Space Agency's Climate Change Initiative
FAOSTAT	Food and Agriculture Organization Corporate Statistical Database
FAPAR	Fraction of Absorbed Photosynthetically Active Radiation
GCOS	Global Climate Observing System
GLM	Generalized Linear Model
HadCRUT	Hadley Centre / Climatic Research Unit Temperature
IPCC	Intergovernmental Panel on Climate Change
LASSO	Least Absolute Shrinkage and Selection Operator
NDVI	Normalised Difference Vegetation Index
PROBA–V	Project for On-Board Autonomy – Vegetation
RCP	Representative Concentration Pathway
RUE	Radiation Use Efficiency
SIF	Sun-Induced Fluorescence
SPEI	Standardised Precipitation Evapotranspiration Index
SPI	Standardised Precipitation Index
SPOT/VGT	Satellite Pour l'Observation de la Terre / Vegetation
SREX	Special Report on Climate Extremes
VOD	Vegetation Optical Depth
VPD	Atmospheric Vapour Pressure Deficit

Chapter 1

Introduction

1.1 Motivation

1.1.1 A short introduction to compound events

There is a rising awareness of the importance of compound events since the first introduction of the term in 2012 in the Intergovernmental Panel on Climate Change (IPCC) Special Report on Climate Extremes (SREX) (Seneviratne et al., 2012). Zscheischler et al. (2018) define compound weather and climate events as "the combination of multiple drivers and/or hazards that contributes to societal or environmental risk". However, several other definitions exist, which are addressed in more detail in section 1.3.2. The joint occurrence of multiple drivers and/or hazards can often lead to amplified impacts (Liu et al., 2016, Zscheischler et al., 2020b). Research on compound events is a recently emerging scientific field with substantial societal relevance, yet the available scientific literature is still scarce and knowledge on the changes of such events in regard to global warming is still limited (Horton et al., 2016, Hoegh-Guldberg et al., 2018).

One of the most addressed examples of compound events so far is the joint occurrence of heat and drought (Zscheischler et al., 2021). Climate change will strengthen land-atmosphere feedbacks, which augments the negative interannual correlation between temperature and precipitation over land areas (Fischer and Knutti, 2013, Zscheischler and Seneviratne, 2017). Further details hereof are given in section 1.3.3. The amount of extremely hot and dry warm seasons in many regions is 10-fold higher in the period 2001–2100 compared to 1870–1969 assuming climate projections based on the Representative Concentration Pathway (RCP) 8.5 scenario (Zscheischler and Seneviratne, 2017). Some of the most severe compound droughts and heat waves on record have been occurring in recent history, e.g. in Europe (2003), Russia (2010), California (2014) and the "Black Summer" in Australia (2019–2020) (Ciais et al., 2005, Rahmstorf and Coumou, 2011, AghaKouchak et al., 2014, van Oldenborgh et al., 2021). Many compound events will become more frequent due to global warming including concurrent heat waves and droughts. Compound events, which have been rare or even unobserved in the past have an increased likelihood of occurrence at 2 °C global warming (Masson-Delmotte et al.,

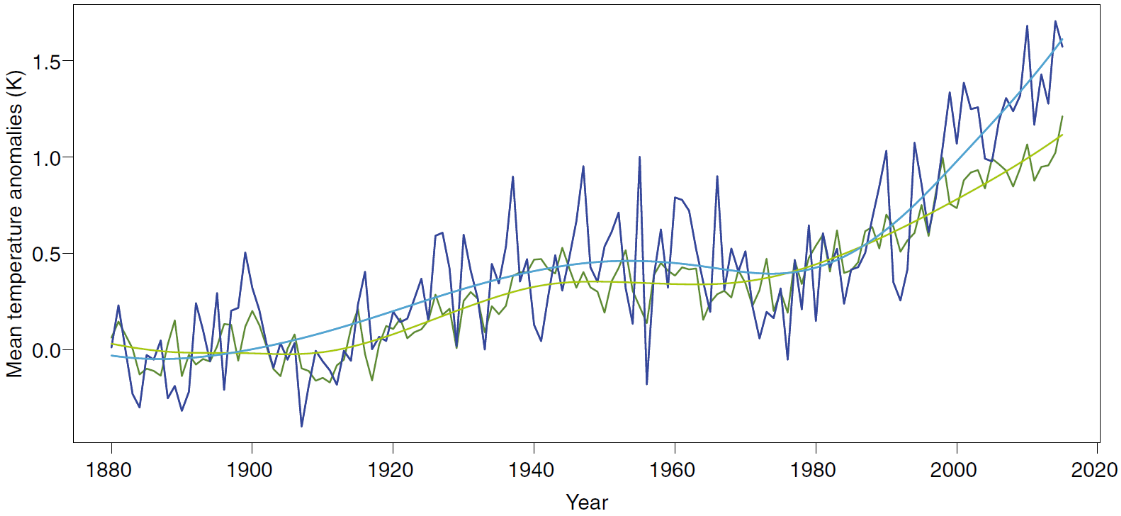

Figure 1.1: Historical atmospheric warming in the Mediterranean Basin (green) and globally (blue) with (light curves) and without (dark curves) smoothing. The figure is obtained from Cramer et al. (2018).

2021). This highlights that detailed knowledge of dependence and impact of droughts and heat waves is crucial (Manning et al., 2018).

1.1.2 Climate change in the Mediterranean

Mediterranean ecosystems are particularly affected by climate change and the region is considered to be a climate change hot spot (Giorgi, 2006, Gao and Giorgi, 2008, Diffenbaugh and Giorgi, 2012). The temperature rise in the Mediterranean exceeds the global average rate and the mean temperature is currently at approximately 1.4 °C above pre-industrial levels (see Fig. 1.1) (Cramer et al., 2018). Increases in hot extremes and soil moisture droughts have been observed in the Mediterranean during the last decades (Perkins-Kirkpatrick and Gibson, 2017, Tramblay et al., 2020, Masson-Delmotte et al., 2021). Precipitation is projected to decreases for all seasons in the Mediterranean for the twenty-first century, except for precipitation in northern regions during winter where changes are insignificant (Lionello and Scarascia, 2018). Temperature extremes are projected to increase at faster rates than the mean temperature in the Mediterranean (Lewis et al., 2019, Masson-Delmotte et al., 2021). Intensification of extreme events is one of the most worrisome aspects of climate change and society is potentially more vulnerable to changes in extremes compared to changes in the mean of climatic conditions (Jentsch et al., 2007, Sedlmeier et al., 2018). Therefore, a focus is put on the Mediterranean Basin in this thesis.

1.1.3 The role of climatic drivers and their seasonal timing as causes of adverse ecosystem impacts

Increasing frequency and intensity of droughts and heat waves in the Mediterranean Basin can affect its ecosystems in many ways. The associated changes include e.g. increasing tree mortality and fire risk (Sarris et al., 2011, Ruffault et al., 2018), pronounced shifts in the occurrence of phenological phases (Gordo and Sanz, 2009, 2010), reductions in agricultural yields and the ability to provide ecosystem services (Peñuelas et al., 2017, Peña-Gallardo et al., 2019, Fraga et al., 2020). The identification of ecological effects of compound events is thus a crucial research gap (Hegerl et al., 2011, Mahony and Cannon, 2018), which motivates the investigation of ecosystem responses to temperature and soil moisture anomalies in this work.

The seasonal timing of climatic anomalies forms another main aspect throughout this thesis. Ecosystem responses depend on the seasonal timing of events and small temporal shifts can affect the magnitude of the corresponding ecosystem response substantially (Sippel et al., 2016, Denton et al., 2017, Sippel et al., 2018b). Particularly the impact of heat and drought stress on crop yield depends highly on the timing of the climatic stressors (Zhu et al., 2021). Moreover, the combined effect of heat and drought stress is more severe for cereal growth and productivity than the individual effects of these stressors (Jagadish et al., 2014, Schauberger et al., 2017, Ribeiro et al., 2020a, Hamed et al., 2021). Agricultural production has been increasingly negatively affected by compound hot and dry events over the course of the last decades (Feng et al., 2021). In addition to the focus on Mediterranean ecosystems, the relationship of climatic conditions on crop failure in the Northern Hemisphere is therefore a further aspect emphasized in this thesis, due to its high relevance for food security.

1.2 Perils associated with climate change in the Mediterranean Basin

1.2.1 Mediterranean climate

The Mediterranean Basin is located in a transition zone between arid subtropical and mesic mid-latitude regimes and does not form a homogeneous biogeographical unit (Blondel and Aronson, 1995, Lionello et al., 2006, 2012). It should be noted that the term “Mediterranean” does not only refer to a geographical region but also to a climatic zone. Aside from the Mediterranean Basin, which encompasses more than half of the world’s regions with Mediterranean climate (Archibold, 1995), Mediterranean climate can be found on the west sites of continents between 30° and 40° in California, Chile, South Africa and Australia (Archibold, 1995, Rubio, 2009). The area of the Mediterranean Basin with Mediterranean climate according to the Köppen-Geiger classification encompasses most areas located at the coast around the Mediterranean Sea as well as the Atlantic coast of Portugal, whereas the coasts of Libya, Egypt and north-eastern Spain do not form part of the Mediterranean climate regime due to their aridity. The climate of the Mediterranean Basin is characterised by mild, wet winters and hot and dry summers, thus exhibiting a strong annual seasonality in both temperature and precipitation (Lionello et al., 2006, Bonada and Resh, 2013). Periods of frost occur in the northern part of the Basin, while they are seldom in the south (Schönfelder and Schönfelder, 2018). Heat waves are a frequent characteristic of the Mediterranean summer (Conte et al., 2002) and are often connected to persistent anti-cyclonic regimes (Ulbrich et al., 2012). There is also a large interannual and seasonal variability of precipitation (Bonada and Resh, 2013, Spano et al., 2013). This is related to the influence of several large-scale atmospheric oscillation patterns and the transitional climate regime of the Mediterranean Basin as well as the substantial circulation changes from summer to winter (Lionello et al., 2006, Tramblay et al., 2020). In addition, the land use, soil type and topography exhibit a large spatial heterogeneity (Thornes, 2002, Lionello et al., 2012, Bonada and Resh, 2013).

The vegetation is dominated by sclerophyllous plants, while woody deciduous plants as well as succulents and perennial and annual herbs are also present (Archibold, 1995, Cherubini et al., 2003, Bonada and Resh, 2013, Spano et al., 2013). Scrublands are the dominant vegetation type, whereas evergreen forests occur mainly at relatively wet sites (Cherubini et al., 2003). Maquis and garrigue are typical examples of Mediterranean scrublands, while *Quercus ilex*, an evergreen oak species, is the characteristic main species of Mediterranean forests (Spano et al., 2013, Schönfelder and Schönfelder, 2018).

Vegetation growth is primarily constrained by water scarcity in summer and low temperatures in winter (however, the latter limitation is primarily affecting northern regions and higher altitudes) (Terradas and Savé, 1992, Archibold, 1995, Cherubini et al., 2003). This so-called double stress results in a bimodal vegetation growth pattern (Terradas and Savé, 1992, Cherubini et al., 2003, Camarero et al., 2010, Gutiérrez et al., 2011). The main growing phase usually occurs during spring, while there is also a minor growing season during autumn (Gutiérrez et al., 2011, Camarero et al., 2021). Some species shed their leaves during the dry season in summer (Spano et al., 2013). The onset of photosynthetic activity after summer is triggered once a sufficient amount of precipitation is reached (Luo et al., 2020).

1.2.2 Land degradation and land cover change in the Mediterranean Basin

The combination of torrential rains occurring in the period from October to March, hot and dry summers, overgrazing, deforestation and wildfires makes the Mediterranean particularly prone to land degradation (Zdruli, 2011). Mediterranean soils are susceptible to soil erosion, their profile development is slow and due to seasonal drying and salinization, clay and organic colloids are often prone to shrinking and swelling processes (Postiglione, 2002, Spano et al., 2013). High levels of evaporation during summer lead to salt accumulation, which causes reduced soil fertility. In combination with soil moisture depletion accompanied by sparse vegetation cover in summer, this enhances soil erosion and subsequently causes land degradation (Postiglione, 2002, Thornes, 2002). Such processes can be potentially irreversible since soil depth of eroded areas might no longer be sufficient to support the prior vegetation cover (Basso et al., 2002).

The Mediterranean vegetation is adapted to high temperatures and water deficits during the dry season (Bonada and Resh, 2013). Nevertheless, an intensification of climate extreme events and increasing aridity imperil the delicate equilibrium of Mediterranean ecosystems and might lead to loss of ecosystem resilience, soil erosion and ultimately desertification (Conte et al., 2002, Rubio, 2009). Already an incremental decrease in water resources can evoke transformations of semiarid to arid drylands and of non-dryland to drylands in the Mediterranean (Rubio, 2009). By the end of the 21st century, the Mediterranean climate zone is projected to expand northward and eastward into formerly temperate zones, while it will likely be substituted by arid climate at the southern margin (Alessandri et al., 2014). At 2 °C warming, the Mediterranean biome area is projected to shrink by approximately 12–15% (Guiot and Cramer, 2016). Increasing temperature accompanied by water deficits due to climate change might render the Mediterranean Basin unsuitable for olive and wine cultivation (Moriondo et al., 2013a,b, Fraga et al., 2020). The length of the Mediterranean growing season is also changing: winter and spring are becoming shorter, whereas autumn potentially extends (Kotsias et al., 2020).

Currently, there is still a greening trend in the Mediterranean due to migration from rural to urban areas (Pausas and Millán, 2019). This land abandonment leads to conversion of agricultural areas to wildlands and grazing reduction due to the absence of livestock. The following biomass increase leads to higher fuel availability and consequently a heightened fire hazard. Unprecedented fire weather with simultaneously hot, dry and windy conditions is likely in the near future in the northern Mediterranean (Ruffault et al., 2018). Therefore, fire and drought risk might revert this greening trend in future (Pausas and Millán, 2019). Furthermore, the increased vegetation density and plant competition due to this biomass increase may cause additional drought vulnerability (Vilà-Cabrera et al., 2011, Lloret et al., 2012, Vayreda et al., 2012)

Besides compound heat waves and droughts, increasing drought lengths combined with a rising number of heavy precipitation events (Seneviratne et al., 2012, Toreti and Naveau, 2015, Samaniego et al., 2018) increases the susceptibility of Mediterranean ecosystems to degradation. Droughts followed by heavy precipitation might increase tree mortality and reduced vegetation cover, rendering the soil prone to erosion, which further reduces ecosystem productivity (Frank et al., 2015).

1.2.3 Societal relevance of droughts in the Mediterranean Basin

Increasing drought severity in the Mediterranean can be primarily linked to rising atmospheric evaporative demand caused by higher temperatures rather than changes in the precipitation patterns (Tramblay et al., 2020, Vicente-Serrano et al., 2020). In addition, the development of anomalous surface anticyclones is projected to drive precipitation declines in the Mediterranean Basin. These anomalies are caused by a reduced land-sea temperature gradient and changes in the circulation in the upper troposphere of the Northern Hemisphere (Tuel and Eltahir, 2020). Regional climate model simulations indicate earlier starting and longer-lasting droughts in the Mediterranean until the end of the 21st century (Beniston et al., 2007). Given a 1.5 °C and 2 °C warming, the length of dry spells in the Mediterranean is projected to increase by 7% to 11%, respectively (Schleussner et al., 2016). The projected risks linked to higher drought frequency and magnitude in the Mediterranean region are much more severe at 2 °C warming compared to 1.5 °C warming (Allen et al., 2018). Furthermore, water demand is likely to increase further in future (Cramer et al., 2018). The Mediterranean is considered one of the regions with the highest socio-economic exposure to drought in the world and this will potentially worsen in the future (Gu et al., 2020). Thus, climate change will likely lead to increasing social instability (Guiot and Kaniewski, 2015, Schilling et al., 2020).

There have been several multi-year droughts in recent decades in the Mediterranean Basin, most of which have occurred in the western Mediterranean, Greece and the Levant (Kelley et al., 2015, Cook et al., 2016). The recent persistent droughts in the Western Mediterranean and Greece are the most severe since the beginning of records in 1100. For the Levant, there is a 98% probability that the recent drought (1998–2012) is the driest on record within the last 500 years (Cook et al., 2016).

The high precipitation variability and subsequently crop yield variability are an important risk factor for the economy in the region (Lionello et al., 2006, Kaniewski et al., 2012, Gouveia et al., 2016). Mediterranean countries are heavily dependent on irrigation for agriculture (Thornes, 2002). Also the provision of seasonal precipitation is of great importance for non-irrigated winter crops, which depend on the accessibility of deep soil moisture (Trigo et al., 2010). Declining agricultural productivity due to drought conditions has been identified as a crucial factor in both historical and recent societal crises in the Mediterranean Basin (Guiot and Cramer, 2016).

Water resources are distributed unevenly among Mediterranean countries, which causes international conflicts (Cramer et al., 2018, Tramblay et al., 2020). Concurrent heat waves and droughts and the subsequent crop failures in the years 1998–2010 might have played a role in the Syrian crisis (Trigo et al., 2010, Kelley et al., 2015, Guiot and Cramer, 2016), which points out the societal relevance of such compound events. Also social conflicts during the Arab Spring in North Africa are partially related to insufficient supply of food and water for the population (Schilling et al., 2020). Moreover, ancient Mediterranean societies were highly susceptible to crop failure caused by droughts. It is assumed that prolonged droughts have led to migration, socio-economic crises and the collapse of societies, such as the "Late Bronze Age collapse" (Kaniewski et al., 2015, Guiot and Cramer, 2016).

1.3 Terminology

1.3.1 Definition of extremeness

According to a review by McPhillips et al. (2018) definitions of extreme events are often incoherent. The term "disturbance" is commonly used instead of the terms "extreme event" or “extreme impact” in ecology, although this has changed in recent years (Frank et al., 2015, McPhillips et al., 2018). Hegerl et al. (2011) elaborate on the difficulties of defining extreme events: Definitions can be based on statistical rareness (regarding historical data) or the impact of extremes. They can include frequency, intensity, duration or all three of them.

The distinction between climate and weather extremes is imprecise; usually, events lasting up to a few days are referred to as extreme weather events, whereas longer events are called extreme climate events, which also can encompass several extreme weather events (Seneviratne et al., 2012). According to this definition, heat waves (usually lasting up to several days) are considered weather extremes, whereas droughts (usually lasting several months) are considered climate extremes.

1.3.2 Definitions and importance of compound events

The term “compound event” was first defined by the IPCC SREX (Seneviratne et al., 2012) as “(1) two or more extreme events occurring simultaneously or successively, (2) combinations of extreme events with underlying conditions that amplify the impact of the events, or (3) combinations of events that are not themselves extremes but lead to an extreme event or impact when combined” (Seneviratne et al., 2012). Leonard et al. (2014) define a compound event as “an extreme impact that depends on multiple statistically dependent variables or events”. The authors criticize the definition of the IPCC SREX report because of a) the artificial boundaries created by coining three distinct classes and b) the imprecise definition of the temporal and spatial scale attributed to the terms “successive” and “simultaneous”.

Compound events can be correlated by a) a common external forcing factor, b) mutual reinforcements due to feedback mechanisms and c) conditional dependence of the occurrence of one event on the occurrence of another event (Seneviratne et al., 2012). However, according to the definition by the IPCC SREX special report (Seneviratne et al., 2012), compound events can also be causally unrelated, whereas Leonard et al. (2014) point out in their definition that the variables or events have to be statistically dependent. Note that according to the definition by Leonard et al. (2014) a compound event can be composed of several events such as a compound drought and heat wave, but an event itself – e.g. a drought – also can be seen as a compound of several coinciding extreme variables.

Finally, Zscheischler et al. (2020a) proposed a more refined typology of compound events, which classifies these events into the four categories a) preconditioned events, b) multivariate events, c) temporally compounding events and d) spatially compounding events, while acknowledging that the boundaries between these groups are sometimes ambiguous.

The assessment of the occurrence probability of compound events is often challenging because the sample size for such events is usually small (Hao et al., 2018, Zscheischler et al., 2020a). Furthermore, standardised assessment approaches are still scarce (Kappes et al., 2012).

If environmental drivers are statistically dependent, the probabilities of the individual drivers cannot be simply multiplied to infer their joint occurrence probability. Analysing the variables' marginal distributions in isolation would underestimate the tail risks (Leonard et al., 2014, Little et al., 2015, AghaKouchak et al., 2020). Furthermore, the joint impact of several drivers or hazards can be much larger than the effect of the individual components in isolation (Liu et al., 2016, Zscheischler et al., 2020b) and many disasters can be traced to a combination of climatic drivers (AghaKouchak et al., 2018, Zscheischler et al., 2018). Nevertheless, studies often focus on single drivers or hazards, whereas multivariate analyses accounting for the dependence of drivers and/or hazards are required for an adequate assessment of the risk associated with compound events.

1.3.3 Feedback mechanisms of heat waves and drought

In many regions of the world, the number of hot days in the hottest month is correlated with antecedent precipitation deficits, indicating that heat waves are strongly linked to surface moisture deficits, particularly for long duration times (Mueller and Seneviratne, 2012). The increased incoming shortwave radiation heating during conditions of reduced cloud cover (and vice versa reduced heating during high cloud cover) is one reason for the anticorrelation of temperature and precipitation over land (Berg et al., 2015). In addition, land-atmosphere feedbacks play a crucial role in the co-occurrence and intensification of heat waves and droughts (see Fig. 1.2) (Miralles et al., 2019). There is strong coupling between heat waves and droughts in transitional zones between wet and dry climate such as the Mediterranean Basin (Green et al., 2017). This is due to two feedback mechanisms: a) increasing evapotranspiration caused by heat waves leading to soil dryness and b) sensible heat increasing at the expense of latent heat, which gets limited by the soil moisture deficit (Seneviratne et al., 2010, 2012). The persistence of such compound hot and dry spells in southern Europe is especially long during the occurrence of stationary anticyclones, so-called atmospheric blocks (Röthlisberger and Martius, 2019).

These land-atmosphere feedbacks lead to increased climate variability, making high intra- and interannual climate variability a typical feature of the Mediterranean (Dünkeloh and Jacobeit, 2003, Lionello et al., 2006, Seneviratne et al., 2010, Gouveia et al., 2016), which in turn increases the likelihood of ecological disturbance events (Potter et al., 2003). Soil moisture is the main driver of vegetation growth in the Mediterranean (Wu et al., 2021) and strongly influenced by land-atmosphere coupling (Seneviratne et al., 2010), which further illustrates the strong influence of such feedback mechanisms on plant functioning (Tramblay et al., 2020).

Climate change will alter the occurrence of compound events in various ways (AghaKouchak et al., 2020, Zscheischler et al., 2020a). For example, there is an increasing frequency in the occurrence of compound hot and dry events due to land-atmosphere feedbacks (Zscheischler and Seneviratne, 2017, AghaKouchak et al., 2020). Due to the intensification of heat waves by droughts via feedback mechanisms, increases in temperature extremes exceed the rise in mean temperatures (Mueller and Seneviratne, 2012, Seneviratne et al., 2014). Furthermore, current droughts are likely to be amplified by high evaporation rates due to more frequent heat waves (Sheffield and Wood, 2008). This is illustrated by the Syrian droughts in 1960

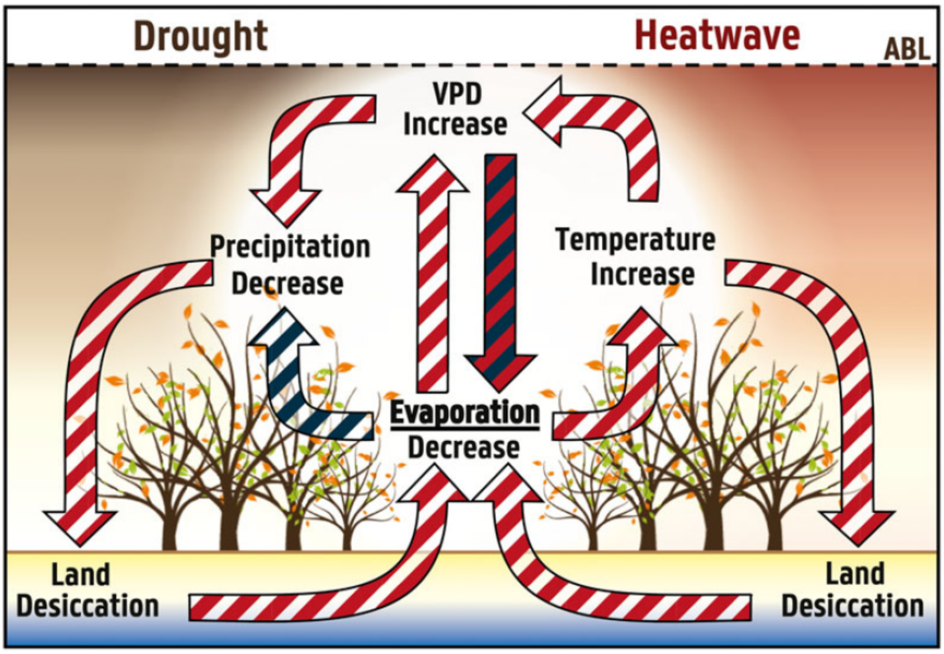

Figure 1.2: Schematic display of land-atmosphere feedback cycles leading to the intensification of hydro-meteorological extremes in the atmospheric boundary layer (ABL). Arrows with red colouring indicate a positive relation (for example temperature increases leading to increasing vapour pressure deficit), whereas arrows with blue colouring indicate a negative relation. The figure is obtained from Miralles et al. (2019).

and 2008: While the temperatures during the 1960 drought were within the typical range, the 2008 drought was characterised by especially high temperatures (Kelley et al., 2015).

1.3.4 Identification and attribution of extremes

The interlinkages of climate extremes to corresponding ecosystem responses are poorly understood; there is a need for knowledge on how magnitude, type and combination of climate extremes might lead to the surpassing of ecosystem response thresholds (Smith, 2011). Frank et al. (2015) point out the need for consistent definitions of climatic extreme conditions and their corresponding ecological impacts. The authors state that comparative meta-analyses are challenging due to this lack of well-defined studies. The impact of climatic drivers on ecosystems can be addressed using either a forward or a backward assessment. The former first identifies climate extremes and then investigates their respective impacts from a driver perspective, whereas the latter identifies extreme impacts and investigates their respective drivers from an impact perspective (Zscheischler et al., 2014). McPhillips et al. (2018) give an overview of extreme event definitions based on 10 years of scientific literature in six academic disciplines. They suggest that events should be defined based on drivers rather than their impact because the effectiveness of measures taken to increase system resilience cannot be assessed adequately otherwise.

On the other hand, definitions of extreme events based on climatic data alone might be inadequate for assessments of ecosystem impacts (Reichstein et al., 2013). Moreover, in a forward assessment one defines a priori which drivers – and combinations thereof – are important for an extreme impact, which inhibits revealing potential unexpected combinations of driver variables. In addition, not every climate extreme triggers an extreme ecosystem response (Kreyling et al., 2008, Smith, 2011, Rolinski et al., 2015). It is crucial to identify those climatic events that have a relevant influence on ecosystem processes (Kreyling et al., 2008, Jentsch et al., 2011, Niu et al., 2014) and a backward approach also allows to determine when an environmental driver cannot explain a certain ecosystem response and other potential drivers might have to be considered (Rolinski et al., 2015). Moreover, a backward assessment allows to identify multiple causes of a single outcome, which makes such an approach particularly appropriate to assess compound events (Zscheischler et al., 2018). As an example, heat waves in combination with droughts can be particularly detrimental for ecosystem productivity, but their impacts can also cancel each other out with regard to ecosystem respiration (von Buttlar et al., 2018). The impact of such variables should thus be addressed jointly rather than independently, due to the positive feedback mechanisms via which they are connected (Mueller and Seneviratne, 2012). For these reasons, backward approaches from an impact perspective have been recommended by several members of the scientific community (Reichstein et al., 2013, Leonard et al., 2014, Ribot, 2014, Ahlström et al., 2015, Rolinski et al., 2015, Zscheischler et al., 2018, 2020a).

However, definitions based on the impact of climatic events on ecosystems depend on the respective ecosystem's functioning and the seasonal timing (Hegerl et al., 2011, von Buttlar et al., 2018). Furthermore, ecosystem impacts can also vary substantially on a temporal scale from e.g. temporary changes in productivity to persistent regime shifts (Crausbay et al., 2017). Smith (2011) provides a more holistic framework to attribute the effects of climate extreme events to ecosystem responses from an ecological perspective. Considering both driver and impact, the author terms a climate extreme that provokes an extreme ecosystem response an "extreme climatic event". Reichstein et al. (2013) refined this definition further describing biosphere-relevant climate extremes as "conditions where an ecosystem function (such as carbon uptake) is higher or lower than a defined extreme percentile during a defined time period and over a certain area, traceable to single or multivariate anomalous meteorological variables". This definition specifically includes compound events such as combined heat waves and droughts. Furthermore, the authors put an emphasis on the impact perspective, suggesting to first identify ecosystem extremes and then attribute them to the corresponding meteorological variables. This definition is applied in chapter 3 in a modified form.

1.3.5 Definitions of droughts and heat waves

A drought is defined as "a period of abnormally dry weather long enough to cause a serious hydrological imbalance" (Field et al., 2012). Generally, four categories of droughts are distinguished: meteorological, agricultural or soil moisture, hydrological and socio-economic droughts (Wilhite and Glantz, 1985, Mishra and Singh, 2010, Seneviratne et al., 2012). These drought types are interrelated. A meteorological drought relates to a precipitation deficit for a certain period of time. Such droughts have usually few direct impacts, however, they can further propagate into agricultural and hydrological droughts. Agricultural or soil moisture droughts are characterised by a deficit of root-zone soil moisture. Hydrological droughts refer to deficits of surface and subsurface water resources, usually indicated by reductions in streamflow and/or groundwater levels. Finally, a socio-economic drought refers to water demand exceeding the supply of water resources (Heim, 2002, Mishra and Singh, 2010, Seneviratne et al., 2012, West et al., 2019). There are also attempts to encompass several drought types comprehensively within one multivariate drought index (Hao and AghaKouchak, 2014, AghaKouchak et al., 2015, Rajsekhar et al., 2015, Mathbout et al., 2021). Drought is a relative term, indicating a temporary deviation from a state and can thus occur in any region. This discriminates it from aridity, a term characterizing a permanent climate with low rainfall and high potential evapotranspiration (Heim, 2002, Rubio, 2009).

Drought definitions are usually anthropocentric and need to be broadened to include e.g. the ecological dimension of drought (Crausbay et al., 2017). As proposed by Seneviratne et al. (2012), the term “soil moisture drought” is used preferentially in this thesis for describing a deficit of root-zone soil moisture instead of the more commonly used term “agricultural drought”, to emphasize its holistic nature, which is not restrained to agricultural systems solely.

There are numerous definitions of heat waves and almost every study uses a different definition for what comprises a heat wave (Perkins, 2015, Fenner et al., 2019). Often the applied metric is tailored for a specific impact group (Perkins, 2015). This renders the comparison of studies a difficult task. The definition of heat waves is not trivial, since magnitude, spatial and temporal scale, relevant variables and choice of relative or absolute thresholds have to be decided on (Horton et al., 2016). Sometimes, the term “heat wave” is restricted only to temperature extremes during the warm season, but it can also be used in a broader sense year-round including warm anomalies during the cold season (Perkins and Alexander, 2013, Horton et al., 2016). Calendar-day based percentiles can serve to link each event with the respective time of the year (Perkins, 2015, Horton et al., 2016).

Horton et al. (2016) state that a heat wave definition should encompass several metrics because essential information is neglected otherwise. For this reason, Perkins and Alexander (2013) created a universally applicable framework with multiple characteristics. The framework consists of three definitions of heat waves (the 90^{th} percentile of daily minimum and maximum temperature and the Excess Heat Factor) applied on five characteristics (number of heat wave days, number of discrete events, length of the longest event, mean event magnitude and highest magnitude). The 90^{th} percentile was considered as the optimum balance to ensure on the one hand that data points can be regarded as extreme and on the other hand not to have too few data points. Nonetheless, the complexity of this framework makes it infeasible to apply it in the joint assessment of warm spells and droughts in this thesis.

1.4 Ecological impacts of climate extremes

1.4.1 Impacts on ecosystem productivity

Extreme events can accelerate ongoing ecosystem changes evoked by shifts in mean values of climate parameters (Jentsch et al., 2007). Increasing severity of climate extremes can lead to irreversible shifts in ecosystems (Bahn et al., 2014). A transition from analyses focussing on the impact of changes in mean climate on ecosystems to an emphasis on the effects of extreme events on ecosystems has occurred in the last years. Extreme responses in ecosystems related to climate extreme events receive increasing attention (Zscheischler et al., 2013).

Climate extremes will become more frequent due to climate change and therefore events considered currently extreme will be part of the future interannual climatic variability (Bahn et al., 2014). These changes in frequency might affect resilience, functionality and sensitivity of ecosystems (Hegerl et al., 2011). There is still a knowledge gap about how the intensification of climate extremes will impact ecosystem recovery long-term (Piao et al., 2019), as well as regarding the impacts on ecosystems caused by sequential events and interactions of several drivers (Miao et al., 2009, Sippel et al., 2018b, Shukla et al., 2019). Due to increasing frequency of climate extremes, plants may not be able to fully recover in the shortened regeneration phases between two events. However, ecological stress memory could mitigate the adverse effects partially (Walter et al., 2013). Decreases in the survival rate of the affected vegetation might finally lead to a single drought event triggering a regime shift in the ecosystem (Lloret et al., 2004, Hegerl et al., 2011, Gouveia et al., 2016).

The impacts of compound events on ecosystem productivity are complex. The impacts of droughts on plant mortality have been studied primarily in consideration of increasing temperature so far, whereas studies, where the increasing number and intensity of heat waves is also incorporated, are missing (Matusick et al., 2018). It is difficult to disentangle the individual effects of temperature and precipitation extremes and there are strong differences depending on the respective ecosystem (Lloret et al., 2012, Niu et al., 2014, Sippel et al., 2016, Vogel et al., 2019). For example, the combination of a warm winter followed by a wet spring in 2015–2016 led to extreme crop yield reductions in northern France, whereas vegetation productivity on the Iberian Peninsula was exceptionally high during that time (Ben-Ari et al., 2018, Sippel et al., 2018a). Gross primary productivity in grasslands and agricultural areas shows higher sensitivity to heat waves and drought in comparison to forests (Flach et al., 2021). Sensible heat increases more over forests than grasslands under heat waves due to higher evapotranspiration rates over grasslands compared to forests, which exhibit stronger stomata control. However, this might lead to quicker soil moisture depletion in grasslands, therefore in the long term, the sensible heat can become higher over grasslands compared to forests (Teuling et al., 2010). In a simulation by de Boeck et al. (2016) heat waves alone did not evoke heat stress on grasslands. Nonetheless, they found signs of heat stress in combination with drought. The occurrence of heat stress only under drought conditions can likely be explained by the reduced heat mitigation by transpiration in this case. The amplifications

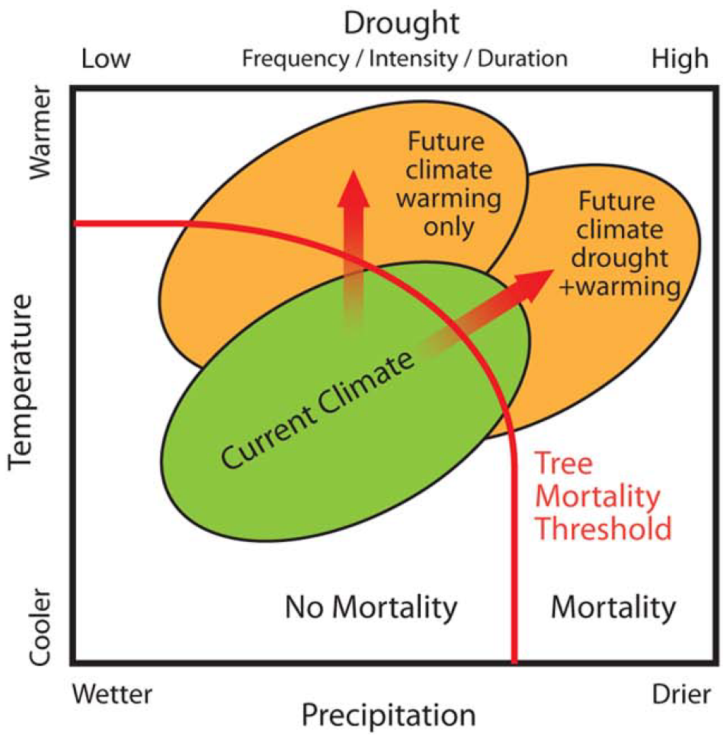

Figure 1.3: Conceptual display showing the current (green) and future (orange) climate variability for temperature, drought and precipitation, where the red line indicates a threshold beyond which plant mortality is induced. The figure is obtained from Allen et al. (2015), who modified it based on Allen et al. (2010).

of heat waves and droughts in forests can lead to tree mortality (Teskey et al., 2015) and climate change might exacerbate the vulnerability of forests towards droughts and heat waves further (see Fig. 1.3) (Anderegg et al., 2013, Allen et al., 2015). However, impacts potentially differ between various forest ecosystems. For example, transpirational cooling is used by some tree species to reduce heat stress, but it remains unclear how many species use this strategy (Teskey et al., 2015). The compound event literature usually focuses on climatic compound events (see e.g. Zscheischler et al. (2020a)). However, interactions between climate extremes and non-climatic disturbances such as pests and diseases are also relevant and seldom researched (Frank et al., 2015, Piao et al., 2019). As an example, grazing pressure can reduce ecosystem resilience to drought (He et al., 2017). Furthermore, hot and dry conditions often foster bark beetle outbreaks (Breshears et al., 2005, Kurz et al., 2008, Allen et al., 2010).

Droughts reduce gross primary productivity and ecosystem respiration, while heat waves do not significantly affect gross primary productivity and increase ecosystem respiration in Mediterranean and temperate ecosystems (Teskey et al., 2015, von Buttlar et al., 2018, Piao et al., 2019). In combination, both drivers lead to negligible changes in ecosystem respiration, but gross primary productivity gets reduced, which results in a reduced net ecosystem productivity. As a consequence, compound heat waves and droughts result in a much more pronounced decline in net ecosystem productivity than heat waves or droughts in isolation (von

Buttlar et al., 2018). An increasing number of droughts might turn carbon sinks to sources, and therefore counteract the effect of extended growing seasons due to warming (Ciais et al., 2005).

Increasing levels of CO_2 in the atmosphere lower stomatal conductance and thus transpiration, while increasing photosynthesis rates, thereby improving water use efficiency – defined as the ratio of net photosynthesis to transpiration. This way, plants save water and can partially mitigate the effects of heat waves and droughts (Ainsworth and Long, 2005, Norby and Zak, 2011, Lemordant et al., 2016).

Moreover, extreme events can have different effects depending on the season (de Boeck et al., 2011, Denton et al., 2017, Piao et al., 2019), which is illustrated by the compound heat wave and drought in the USA in 2012: while vegetation activity in spring was enhanced due to the earlier onset of the vegetation period caused by higher spring temperatures, it was reduced during summer by mutually reinforcing biosphere-atmosphere feedbacks. The elevated activity in spring led to increased water uptake, which in combination with the high temperatures resulted in high evapotranspiration rates and subsequently depletion of soil moisture storages in summer. The dry conditions further exacerbated the heat wave and vice versa (Wolf et al., 2016). In addition, interactions over time also have to be accounted for: wet conditions early in the season might lead to smaller root depths, which constraints the ability of plants to cope with dry conditions at later stages during the growing season (Raymond et al., 2020).

In addition, elevation plays also an important role in determining the ecological effects. Reduction in net primary productivity was observed in the majority of Anatolian Forests for the period from 2000–2010, with the exception of high-elevation coniferous ecosystems, where productivity increased in response to rising temperatures (Erşahin et al., 2016). Furthermore, the increasing anthropogenic nitrogen deposition also has effects on the functioning of ecosystems (Phoenix et al., 2012): higher amounts of nitrogen lead to an accelerated depletion of water during spring, which causes earlier drying of the Mediterranean vegetation (Luo et al., 2020).

1.4.2 Physiological and structural effects

Heat waves and droughts have a variety of physiological and structural effects on vegetation and often amplify each other's effects (Teskey et al., 2015). Heat waves heighten the atmospheric evaporative demand, leading to increased evapotranspiration, which in turn favours the emergence of soil moisture droughts. Therefore, drought stress has a higher intensity and starts earlier under heat wave conditions. Heat stress is exacerbated if transpirational cooling is minimised due to closing of stomata under drought conditions (de Boeck et al., 2011, Teskey et al., 2015). Plants close their stomata to reduce transpiration, which increases the temperature inside their leaves and causes heat stress (de Boeck et al., 2011). In addition, the reduced mesophyll and stomatal conductance evoked by droughts slows CO_2 fixation (Rennenberg et al., 2006, Keenan et al., 2010). These processes can ultimately lead to plant mortality via two ways: Either hydraulic failure – in case the water demand exceeds the supply – or else carbon starvation (Bréda et al., 2006, McDowell et al., 2008). In the latter case, autotrophic respiration exceeds the rate of photosynthesis and as a consequence carbohydrate reserves are depleted and the plant's metabolism can no longer be sustained (van der Molen et al., 2011). It is hypothesized that carbon starvation is more likely to occur in isohydric species, which reduce stomatal conductance under drought conditions, whereas hydraulic failure is more common for anisohydric species, which have little control over stomatal conductance under drought conditions (McDowell et al., 2008). However, there is also evidence that carbon starvation is less usual than hydraulic failure in isohydric forest ecosystems (Hartmann et al., 2013, Rowland et al., 2015).

In the context of the influence of heat and drought on plant functioning and photosynthesis, the atmospheric vapour pressure deficit (VPD) also plays a crucial role. Heat and soil moisture drought are associated with high vapour pressure deficits and it remains challenging to disentangle the individual effects of the variables temperature, radiation, VPD and atmospheric CO_2 concentrations on vegetation (Grossiord et al., 2020). Increased VPD exacerbates water stress by increasing the demand of plants for soil water and the subsequent heightened transpiration rates then lead to earlier depletion of soil water resources (Lobell et al., 2013). Nevertheless, the impact of VPD is often neglected in agricultural studies and still not fully understood (Novick et al., 2016, Zhang et al., 2017). Global warming will potentially lead to increasing VPD and it is projected that VPD will become a limiting factor for ecosystem productivity (Novick et al., 2016, Zhang et al., 2017, Grossiord et al., 2020).

Plant physiology is affected by hot and dry conditions in many ways, e.g. via Rubisco inactivation, worsened functioning of thylakoid membranes and heightened photo-oxidative stress (Crafts-Brandner and Salvucci, 2000, Schrader et al., 2004, García-Plazaola et al., 2008, Teskey et al., 2015). In addition, there is a reduction of net photosynthesis and chlorophyll concentration and osmolyte production is heightened to sustain water uptake (Rennenberg et al., 2006, García-Plazaola et al., 2008, Teskey et al., 2015). Moreover, the photosystem II is particularly susceptible to heat stress and damages are considered irreversible above air temperature of 40 °C for trees (Yordanov, 1992, Allakhverdiev et al., 2008). Furthermore, heat waves and droughts can lead to reduced leaf area, leaf shedding, growth reduction and changes in biomass allocation (Reichstein et al., 2013, Teskey et al., 2015, Denton et al., 2017).

Increased leaf temperature can provoke accelerated phenological development in some species (Bernal et al., 2011). Nonetheless, mortality caused by climatic events can be attenuated by stabilizing processes in plant communities. Such an event can lead to enhanced recruitment as well as increased growth and survival rate in the remaining population in the aftermath (Lloret et al., 2012). Climate extreme events can also be beneficial and potentially cause reductions in pest and pathogens, while at the same time they can also be favourable for pollinators and seed dispersers and consequently alleviate vegetation stress (Dale et al., 2001, Rosenzweig et al., 2001, Lloret et al., 2012).

1.4.3 Importance of climate extremes for agricultural production

Wheat covers the largest area worldwide of all crops and is ranked third in the amount of annual production. It contributes approximately one fifth of daily calories and protein in the human diet (Shiferaw et al., 2013, FAOSTAT, 2019). It is the main crop in temperate zones but is also grown in a wide range of other climate zones (Monneveux et al., 2012, Peña-Bautista et al., 2017, Mäkinen et al., 2018).

Climate change has negatively affected wheat yield in lower latitudes in the last decades, whereas the effects have been positive in higher latitudes (Iizumi et al., 2018, Mbow et al., 2019). A wheat yield reduction by 6% per °C is estimated (Asseng et al., 2015). According to a counterfactual analysis by Iizumi et al. (2018), global average wheat yield was reduced by 1.8% between 1981 and 2010. A significant part of yield increases due to technological advancements and carbon dioxide fertilization were counterbalanced during this time by global warming (Lobell et al., 2011). In future, the frequency of unfavourable climatic conditions for crop production is projected to increase, which will lead to larger temporal and spatial variability of yields (Trnka et al., 2011, 2014, Asseng et al., 2015, Ben-Ari et al., 2018). However, the higher exposure to extreme events also might lead to acclimation and thus better adapted crops (Hegerl et al., 2011, Mäkinen et al., 2018), which could attenuate yield reductions.

Heat and drought stress can impair growth and development at most developmental stages of the growth cycle (Jagadish et al., 2014), but the impact on crop yield depends highly on the timing of climatic stressors (Zhu et al., 2021). The life cycle of cereals consists of three broad stages, the vegetative, reproductive and the grain filling stage. The latter two are primarily important in determining crop yield, whereas negative effects during the vegetative stage can potentially still be compensated later on (Jagadish et al., 2014). For example, drought during the vegetative phase only reduces the photosynthesis rate and thus plant growth, whereas drought during the reproductive phase may induce ovule abortion and pollen sterility, which directly limits crop yield (Barnabás et al., 2008). Thus, wheat is particularly vulnerable to heat stress during anthesis and grain filling and less so in its vegetative phase (Porter and Gawith, 1999, Luo, 2011). While most studies highlight the vulnerability to drought during the reproductive phase, there is nevertheless also evidence that the vegetative phase, e.g. during stem elongation is equally sensitive (Daryanto et al., 2016, Le Gouis et al., 2020) The vulnerability to heat is likely to exacerbate and the regions for wheat production will shift due to climate change (Schlenker and Roberts, 2009, Rezaei et al., 2015, Lischeid et al., 2022). While it will be challenging to sustain productivity in low-latitude areas with increasing temperatures, wheat is comparatively well adapted to water stress and might thus become more competitive in arid regions than the crops which are currently grown there (Shiferaw et al., 2013).

The frequency of days during the reproductive stage exceeding critical temperature thresholds is projected to increase more than threefold by 2050 in Europe (Gourdji et al., 2013). Due to the high vulnerability of crops to heat stress during this phase, this poses a large threat to crop production (Porter and Gawith, 1999, Trnka et al., 2014). Anthesis might advance by 2 weeks by 2060 due to accelerated crop growth under warmer conditions (Trnka et al., 2014). Global warming accelerates the development of plants, leading to a shorter time span until maturity. This way, the reproductive period occurs earlier and thus under comparatively cooler temperatures, so crops might avoid the exposure to heat and drought stress during the reproductive phase (Trnka et al., 2014, Rezaei et al., 2015). However, it remains unclear if an earlier vegetation period can actually compensate for increased heat stress in summer during anthesis. For example, the reduced effective global radiation due to a shift to shorter day lengths might offset the benefits of warmer spring temperatures for plant growth (Trnka et al., 2014, Rezaei et al., 2015). Furthermore, the potential for heat stress mitigation by advancement of the reproductive stage is limited for spring crops in comparison to winter crops (Rezaei et al., 2015, Strer et al., 2018). Moreover, according to a study by Gourdji et al. (2013), this strategy would likely be less effective for other crops like maize, rice and soybean compared to wheat. In addition, while higher temperatures increase the grain growth rate, the grain filling period is also shortened, which in summary leads to reduced grain size (Prasad et al., 2008, Rezaei et al., 2015).

Wheat yield reductions are primarily driven by heat and droughts, whereas water logging and frost are less frequent causes, although they can be regionally important (Lesk et al., 2016, Zampieri et al., 2017, van der Velde et al., 2018). Indicators of meteorological drought such as the Standardised Precipitation Index (SPI) are insufficient for predicting yield anomalies and indicators that incorporate soil moisture drought like the Standardised Precipitation-Evapotranspiration Index (SPEI) or gridded soil moisture data sets might be more appropriate (Vogel et al., 2019). Nevertheless, in a study by Lischeid et al. (2022) soil moisture was a less relevant driver of crop yield than precipitation. However, the soil moisture data set was simulated based on meteorological variables and thus its information content might be already mostly contained in the meteorological predictors used in this study. Therefore, a satellite-based soil moisture data set could potentially add further predictive power compared to a simulated soil moisture data set. It is unclear if heat or drought stress is the main driver of crop failure. In some cases, temperature is more important (Lobell et al., 2011, Vogel et al., 2019), while in other cases precipitation dominates (Ribeiro et al., 2020b). Under current conditions, exceedances of critical temperatures are still rare (Schauberger et al., 2017). However, according to Zhu et al. (2021), a paradigm shift from water limitation to extreme temperatures as the primary cause of crop failure is projected.

In addition to the detrimental effects of heat waves and droughts in isolation, the combined effect of heat and drought stress can be particularly detrimental for growth and productivity (Jagadish et al., 2014, Schauberger et al., 2017, Ribeiro et al., 2020a, Hamed et al., 2021). Wheat canopy temperature rises during heat stress, particularly when additionally evaporative cooling is reduced due to the lack of water availability during drought conditions (Mäkinen et al., 2018). According to findings by Ribeiro et al. (2020a), in comparison to heat stress, less extreme levels of drought stress cause an equivalent detrimental impact on crop yield, indicating that drought is the dominant driver in compound events. Climate change will not only lead to warming temperatures but also to changes in the coupling of heat and moisture, which will affect crop yield negatively (Lesk et al., 2021). In addition, temporally compounding events, like the combination of a warm winter and a wet spring leading to crop failure have not been addressed adequately so far (Ben-Ari et al., 2018, Zscheischler et al., 2020a)

The increasing intensity and frequency of extreme events need to be accounted for in the breeding of new cultivars (Mäkinen et al., 2018). For this aim, it is crucial to maintain a large genetic variability to be able to deal with the uncertain nature of future extreme events (Le Gouis et al., 2020). Adaptation measures, such as shifts in cropping calendars will also be required (Strer et al., 2018), e.g. earlier spring wheat cultivars could potentially prevent negative impacts of heat and drought during reproductive phases (Mäkinen et al., 2018).

1.5 Objectives and structure of the thesis

This thesis consists of one study with a climatological focus and two interdisciplinary studies at the interface of climatology and ecology. The first two studies are located in the Mediterranean Basin, while the third study comprises the entire Northern Hemisphere. The Mediterranean Basin was chosen as a focus region for this thesis because it is a climate change hot spot with strong land-atmosphere feedbacks, which faces substantial changes in ecosystem composition, productivity and phenology. This combination of climatological and ecological transformations makes it a particularly interesting study region for the ecoclimatological context of this thesis. In the final study, unfavourable weather conditions leading to crop failure for winter wheat are investigated, which is of major interest due to the tremendous importance of this crop for global food security.

Objective of the first study (chapter 2): Quantification of changes in the number of compound warm spells and droughts from 1979 to 2018 in the Mediterranean Basin
In the first study, the ERA5 reanalysis data set is used to detect changes in compound warm spells and droughts in the Mediterranean over the last four decades in the Mediterranean Basin. The study aims to a) assess if there are significant trends in compound warm spells and droughts, b) quantify the magnitude of these trends and identify the regions with the largest increases, c) identify which component – namely warm spells and droughts – primarily drives increases in compound events and d) identify months with the highest increases in warm spells, droughts and compound events. The study investigates both warm season events – events during the time span from May to October, which are extreme in their absolute value – as well as year-round deseasonalised events – which are extreme relative to the time of their occurrence.

Objective of the second study (chapter 3): Identification of seasonal ecosystem vulnerability to temperature and soil moisture anomalies in the Mediterranean Basin
The second study investigates the seasonal ecosystem vulnerability to climatic drivers in the Mediterranean Basin by attributing states of low ecosystem productivity to the related climatic

conditions during the course of the year. For this purpose, significant deviations of temperature and soil moisture during periods with low levels of the fraction of absorbed photosynthetically active radiation (FAPAR) are identified for each month of the year. Temperature is obtained from the ERA5 Land reanalysis data set, soil moisture is retrieved from both ERA5 Land and the satellite-based European Space Agency's Climate Change Initiative (ESA CCI) product and the FAPAR is acquired from the Copernicus Global Land Service (CGLS) for the time span 1999–2019. The study aims to identify during which time of the year ecosystem are vulnerable to certain combinations of temperature and soil moisture deviations for various subregions and land cover classes.

Objective of the third study (chapter 4): Automated detection of the main meteorological drivers of crop failure in the Northern Hemisphere
In the third study, least absolute shrinkage and selection operator (LASSO) logistic regression is applied to predict crop failure in the Northern Hemisphere based on a set of meteorological variables. Weather data from the global climate model EC-Earth and annual winter wheat yield data from the Agricultural Production Systems sIMulator (APSIM) crop model for 1600 simulated growing seasons are applied in this study. The objective of this study is to assess the usability of LASSO regression to accurately predict crop failure and identify relevant meteorological drivers in an automated way, which allows its usage in other applications where extreme impacts are attributed to their drivers. To assess the performance of LASSO regression, the model is compared to a generalized linear model and a random forest binary classification. The key drivers of crop failure are identified from a large variable set encompassing monthly meteorological variables including maximal temperature, VPD, precipitation as well as several climate extreme indicators for the entire growing season.

Chapter 5 condenses the results of the articles from the chapters 2, 3 and 4 and draws conclusions thereof. Finally, challenges in regard to the work of this thesis are presented and future research directions are indicated.

1.6 Author contributions

The main body of this thesis consists of three peer-reviewed publications, which are displayed below. In addition, the contributions of all participating authors are indicated here.

1. **Chapter 2:** Vogel, J., Paton, E., Aich, V., Bronstert, A. Increasing compound warm spells and droughts in the Mediterranean Basin. Weather and Climate Extremes 32, 100312; 10.1016/j.wace.2021.100312 (2021).

   Johannes Vogel: Data analysis (Lead), Conceptualization (Lead), Visualization (Lead), Writing – original draft (Lead), Writing – review and editing (Lead)
   Eva Paton: Conceptualization (Supporting), Supervision (Lead), Writing – review and editing (Supporting)

Valentin Aich: Conceptualization (Supporting), Writing – review and editing (Supporting)
Axel Bronstert: Writing – review and editing (Supporting)

2. **Chapter 3:** Vogel, J., Paton, E., Aich, V. Seasonal ecosystem vulnerability to climatic anomalies in the Mediterranean. Biogeosciences 18, 5903–5927; 10.5194/bg-18-5903-2021 (2021).

   Johannes Vogel: Data analysis (Lead), Conceptualization (Lead), Visualization (Lead), Writing – original draft (Lead), Writing – review and editing (Lead)
   Eva Paton: Conceptualization (Supporting), Supervision (Lead), Writing – review and editing (Supporting)
   Valentin Aich: Conceptualization (Supporting), Writing – review and editing (Supporting)

3. **Chapter 4:** Vogel, J., Rivoire, P., Deidda, C., Rahimi, L., Sauter, C.A., Tschumi, E., van der Wiel, K., Zhang, T., Zscheischler, J. Identifying meteorological drivers of extreme impacts: an application to simulated crop yields. Earth Syst. Dynam. 12, 151–172; 10.5194/esd-12-151-2021 (2021).

   Johannes Vogel: Data analysis including the Lasso logistic regression (Lead), Visualization (Lead), Writing – original draft (Lead), Writing – review and editing (Lead)
   Pauline Rivoire: Data analysis including the Lasso logistic regression (Lead), Visualization (Lead), Writing – original draft (Lead), Writing – review and editing (Lead)
   Cristina Deidda: Data analysis (Supporting), Visualization (Supporting), Writing – original draft (Supporting), Writing – review and editing (Supporting)
   Leila Rahimi: Data analysis (Supporting), Visualization (Supporting), Writing – original draft (Supporting), Writing – review and editing (Supporting)
   Christoph A. Sauter: Data analysis (Supporting), Visualization (Supporting), Writing – original draft (Supporting), Writing – review and editing (Supporting)
   Elisabeth Tschumi: Data analysis (Supporting), Visualization (Supporting), Writing – original draft (Supporting), Writing – review and editing (Supporting)
   Karin van der Wiel: Climate model simulations with EC-Earth (Lead), Conceptualization (Equal), Supervision (Equal), Writing – original draft (Supporting), Writing – review and editing (Supporting)
   Tianyi Zhang: Crop model simulations with APSIM (Lead), Writing – review and editing (Supporting)
   Jakob Zscheischler: Conceptualization (Equal), Supervision (Equal), Writing – original draft (Supporting), Writing – review and editing (Supporting)

In addition, I contributed to the following articles, which are not included in this thesis:

1. Paton, E., Vogel, J., Kluge, B., Nehls, T. Ausmaß, Trends und Extrema von Dürren in der Stadt – Extent, trend and extremes of droughts in urban areas. Hydrologie & Wasserbewirtschaftung 65, 5–16; 10.5675/HyWa_2021.1_1 (2021).

2. Kemter, M., Fischer, M., Luna, L.V., Schönfeldt, E., Vogel, J., Banerjee, A., Korup, O., Thonicke, K. Cascading Hazards in the Aftermath of Australia's 2019/2020 Black Summer Wildfires. Earth's Future 9; 10.1029/2020EF001884 (2021).

Furthermore, an article on the meteorological drivers of phenological changes in the Mediterranean Basin is in preparation.

Chapter 2

Increasing compound warm spells and droughts in the Mediterranean Basin

Johannes Vogel, Eva Paton, Valentin Aich and Axel Bronstert

Weather and Climate Extremes, 32, 100312, https://doi.org/10.1016/j.wace.2021.100312, 2021

Weather and Climate Extremes 32 (2021) 100312

Contents lists available at ScienceDirect

Weather and Climate Extremes

journal homepage: http://www.elsevier.com/locate/wace

Increasing compound warm spells and droughts in the Mediterranean Basin

Johannes Vogel[a,b,*], Eva Paton[b], Valentin Aich[c], Axel Bronstert[a]

[a] *Institute of Environmental Science and Geography, University of Potsdam, Potsdam, Germany*
[b] *Institute of Ecology, Technical University of Berlin, Berlin, Germany*
[c] *Potsdam Institute for Climate Impact Research, Potsdam, Germany*

ARTICLE INFO

Keywords:
Compound events
Warm spells
Droughts
Mediterranean basin
Extreme events
Climate change

ABSTRACT

The co-occurrence of warm spells and droughts can lead to detrimental socio-economic and ecological impacts, largely surpassing the impacts of either warm spells or droughts alone. We quantify changes in the number of compound warm spells and droughts from 1979 to 2018 in the Mediterranean Basin using the ERA5 data set. We analyse two types of compound events: 1) warm season compound events, which are extreme in absolute terms in the warm season from May to October and 2) year-round deseasonalised compound events, which are extreme in relative terms respective to the time of the year. The number of compound events increases significantly and especially warm spells are increasing strongly – with an annual growth rates of 3.9 (3.5) % for warm season (deseasonalised) compound events and 4.6 (4.4) % for warm spells –, whereas for droughts the change is more ambiguous depending on the applied definition. Therefore, the rise in the number of compound events is primarily driven by temperature changes and not the lack of precipitation. The months July and August show the highest increases in warm season compound events, whereas the highest increases of deseasonalised compound events occur in spring and early summer. This increase in deseasonalised compound events can potentially have a significant impact on the functioning of Mediterranean ecosystems as this is the peak phase of ecosystem productivity and a vital phenophase.

1. Introduction

1.1. Climate change in the mediterranean

The Mediterranean Basin is a region particularly prone to the effects of climate change and was characterized as one of the climate change hot-spots areas of the 21st century (Giorgi, 2006; Orlowsky and Seneviratne, 2012; Lionello and Scarascia, 2018). Temperature increases at a faster pace in the Mediterranean compared to the global average due to regional feedback mechanisms enhancing changes in extreme temperatures (Diffenbaugh et al., 2007; Orlowsky and Seneviratne, 2012). A global increase in 1.5 and 2 °C is thought to correspond to a 2.2 and 3 °C increase of the daily maximum temperature in the Mediterranean Basin, respectively (Seneviratne et al., 2016). Future warming rates in the Mediterranean are expected to be 20% higher than globally – in summer even up to 50% –and increasing inter-annual variability in the warm season is projected (Giorgi, 2006; Lionello and Scarascia, 2018). Increases in extreme events were observed in the past decades and are projected to continue in the 21st century in the Mediterranean Basin (Giannakopoulos et al., 2009; Hartmann et al., 2013; IPCC, 2019) for heat wave intensity and duration (Diffenbaugh et al., 2007; Fischer and Schär, 2010; Lionello et al., 2012; Christidis et al., 2015), as well as drought and aridity (Sousa et al., 2011; Dai, 2013; Cook et al., 2016; Samaniego et al., 2018; Spinoni et al., 2018). Heat wave intensity in the Mediterranean shows the largest growths worldwide and particularly extremely intense heat waves are becoming more frequent (Perkins-Kirkpatrick and Gibson, 2017). Soil water content also decreases in all seasons due to global warming, with the largest reductions in winter and spring (Samaniego et al., 2018).

1.2. Socio-economic and ecological relevance

Increases in hot and dry days have manifold detrimental impacts, including forest mortality (Allen et al., 2010), decreasing crop yields (World Bank, 2014; Zscheischler et al., 2017; IPCC, 2019), increasing fire risk (Ruffault et al., 2018), vegetation stress, rising energy demand, declining summer tourism (Giannakopoulos et al., 2009; van Lanen et al., 2016) and health effects (Poumadère et al., 2005; Fischer and Schär, 2010).

In addition, severe climatic changes are likely to provoke land cover

* Corresponding author. Institute of Environmental Science and Geography, University of Potsdam, Potsdam, Germany.
E-mail address: joschavogel@uni-potsdam.de (J. Vogel).

https://doi.org/10.1016/j.wace.2021.100312
Received 23 March 2020; Received in revised form 25 January 2021; Accepted 9 February 2021
Available online 17 February 2021

changes and ecosystem regime shifts (Feng and Fu, 2013). Above 2 °C warming, desertification is projected to take place in the Mediterranean Basin until the end of the 21st century, rendering it inappropriate for e.g. olive cultivation (Moriondo et al., 2013; Guiot and Cramer, 2016; Fraga et al., 2020). Reduced water availability accompanied by increasing aridity elicited primarily by changes in precipitation and temperature will result in loss of Mediterranean ecosystems and their current biodiversity in the next decades (Guiot and Cramer, 2016; Cramer et al., 2018). Moreover, the increasing severity of heat and drought will lead to the loss of the function of semiarid ecosystems as carbon sink (Ciais et al., 2005; Ma et al., 2015).

Jentsch and Beierkuhnlein (2008) point out that changes in the disturbance regime associated with extreme weather events might be more harmful to ecosystem functioning than trends and shifts in mean conditions. Short-term events are likely to affect the long-term ecosystem state by shifting it to an alternate stable state (Kreyling et al., 2011). Changes in frequency and amplitude of extreme climatic events potentially result in non-linear alterations in ecosystem resilience, functionality and sensitivity (Hegerl et al., 2011). The effects of such disturbance regime shifts on ecosystem resilience and resistance are not yet well understood and therefore need to be addressed in further research (Jentsch and Beierkuhnlein, 2008; Hegerl et al., 2011; Mahony and Cannon, 2018).

1.3. Definition and importance of compound events

A dependence structure between variables increases the occurrence probability of multivariate extremes. For example, high temperatures and low precipitation are usually negatively correlated, i.e. that the probability of an extreme hot and dry summer is much higher compared to an extremely hot and wet summer (Zscheischler et al., 2018). This illustrates that univariate analyses might fall short of precisely representing the potential risks associated with compound events (AghaKouchak et al., 2014; Zscheischler and Seneviratne, 2017). In addition, the impacts of combinations of extremes can be much higher than the summed up impact of their individual components (Hegerl et al., 2011; Zscheischler et al., 2020). Many past hazard-related climatological studies focused on single drivers, while the majority of recent meteorological and climatological events with extreme impacts are compound effects by multiple drivers – often in the form of compound heat waves and droughts (Zscheischler et al., 2018; Collins et al., 2013; Sedlmeier et al., 2018). The risk of concurrent droughts and heat waves was not analysed extensively to date (AghaKouchak et al., 2014; Kong et al., 2020), although their thermodynamical relationship through soil moisture is well-known (Horton et al., 2016). Recent studies investigated concurrent droughts and heat waves e.g. in the USA (Mazdiyasni and AghaKouchak, 2015), India (Sharma and Mujumdar, 2017), Europe (Manning et al., 2019), China (Wu et al., 2019; Ye et al., 2019; Kong et al., 2020) and globally (Zscheischler and Seneviratne, 2017; Hao et al., 2018). The amplification of risks from interlinked impacts are particularly pronounced in the Mediterranean Basin (Cramer et al., 2018), e.g. increased fire risk due to heat waves and droughts (Gouveia et al., 2016). In addition, the interaction of drivers and corresponding hazards is likely to change due to climate change, leading to the occurrence of novel climatic conditions (Zscheischler et al., 2018).

Several definitions of compound events were framed in recent years (Seneviratne et al., 2012; Leonard et al., 2014; Zscheischler et al., 2018). Here, we follow the confined definition according to the workshop on correlated extremes, held in New York City from May 29–31, 2019, which defined compound/multivariate events as events occurring at the same time and in the same place (Horton and Raymond, 2018). In this study, a compound event is termed as the co-occurrence of warm spells and droughts at the same time.

We investigate two types of compound events: 1) compound events defined by the extremeness of their absolute values and 2) compound events, which are extreme in relation to the respective time of the year. We call the first category warm season compound events and the latter deseasonalised compound events. Warm season compound events are analysed only for the period May–October, whereas deseasonalised compound events are investigated year-round (for further details see section 2.3). We analyse deseasonalised compound events in addition to warm season compound events because extremes outside the warm season are rarely assessed in comparison to summertime events (Perkins, 2015). Moreover, the impact of events on agriculture and ecosystems depends on their seasonal timing and thus requires a year-round analysis. (de Boeck et al., 2011; Hegerl et al., 2011; Sippel et al., 2016; Ben-Ari et al., 2018). To assess the risks imposed by these events on the Mediterranean Basin, it is therefore crucial to incorporate also events, which might not be high in absolute values, however are considered extreme in regard of the time of the year of their occurrence (de Boeck et al., 2011). While compound warm spells and droughts have been assessed in the Mediterranean Basin before (Russo et al., 2019), this is the first paper encompassing a year-round investigation according to our knowledge.

1.4. Research questions

Within this article, the following research questions are examined. Does the number of warm season and deseasonalised compound events increase significantly in the Mediterranean Basin over the last 40 years (cf. section 3.1)? If so, how large is the increase and in which countries is it largest? Which is the major component – namely warm spells and droughts – for increases of warm season and deseasonalised compound events (cf. section 3.2)? Which months show the highest increase in the number of warm season and deseasonalised warm spells, droughts and compound events (cf. section 3.3)?

2. Methods

2.1. Study area

The study area is refined to the zones, which are part of the Köppen-Geiger categories Csa and Csb within the Mediterranean Basin (cf. Fig. 1). The Csa and Csb categories refer to “Warm temperate climate with dry and hot summer” and “Warm temperate climate with dry and warm summer”, respectively. The Köppen-Geiger classification map was obtained from Kottek et al. (2006) and Rubel et al. (2017).

2.2. Data

Hourly 2 m air temperature, total precipitation and potential evaporation were obtained from the ERA5 reanalysis data set with a spatial resolution of $0.25° \times 0.25°$ – encompassing 2 883 pixels in total – for the 40-year period from 1979 to 2018 (Copernicus Climate Change Service, 2017; Hersbach et al., 2019). The daily maximum 2 m air temperature was extracted from hourly data. Hourly total precipitation and potential evaporation were summed up monthly.

2.3. Definition of events

The typical time scales of droughts and warm spells diverge – droughts typically are investigated on a monthly to yearly scale, whereas warm spells are observed on a daily to weekly scale (Miralles et al., 2019). Therefore, using a single time scale might not capture all relevant temporal dynamics (Le Page and Zribi, 2019) and separate time scales for both phenomena are required. We use a peak over threshold approach to define extremes. Here, we define daily maximum temperature above the 90th percentile of the daily maximum 2 m air temperature of the period 1979–2018 with a duration of at least 5 days for each pixel as the standard case for a warm spell. In addition to that, also warm spells defined by the 85-, 90-, 95th percentile and a duration of 3, 5 and 7 days (leading to nine cases of warm spells in total) are investigated for

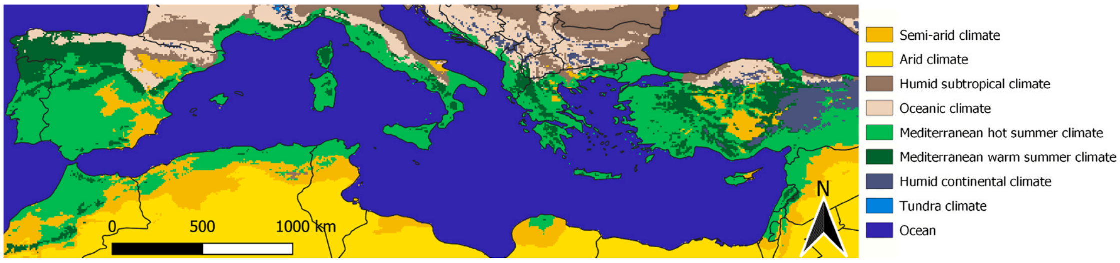

Fig. 1. Mediterranean study area for which the Köppen-Geiger climate category is "Mediterranean hot summer climate" (light green) or "Mediterranean warm summer climate" (dark green). (For interpretation of the references to colour in this figure legend, the reader is referred to the Web version of this article.)

assessing the impact of the choice of duration and magnitude on the obtained changes in the number of events. For the definition of droughts, two indices are applied, the Standardised Precipitation Index (SPI) (McKee et al., 1993) and the Standardised Precipitation Evapotranspiration Index (SPEI) (Vicente-Serrano et al., 2010).

For the calculation of the SPI, precipitation is summed monthly, a probability distribution function is fitted (a gamma distribution for the SPI and a log-logistic distribution for the SPEI, respectively) and transformed to a normal distribution with mean of 0 and standard deviation equal to 1, where positive values indicate wet conditions and negative values indicate dry conditions. The SPEI is calculated similarly to the SPI, but it is based on the difference of precipitation and potential evapotranspiration – not solely on precipitation as it is the case for the SPI. Both indices are calculated monthly based on the current and the two preceding months separately for each pixel. This means, that e.g. the SPI and SPEI value for the month of July always includes also precipitation data from May and June. This 3-month SPI and SPEI is abbreviated as SPI-3 and SPEI-3 hereafter, respectively. According to Szalai et al. (2000), soil moisture drought is correlated best with SPI-2 and SPI-3, thus the SPI-3 can serve as a proxy for soil moisture conditions (WMO, 2012). A drought is defined as SPI-3 < -0.8 and SPEI-3 < -0.8 respectively following the methodology of Mueller and Seneviratne (2012) and Mazdiyasni and AghaKouchak (2015).

Compound warm spells and droughts are defined as warm spells coinciding with SPI-3 droughts according to the approach by Mazdiyasni and AghaKouchak (2015). We analyse first the changes in compound events (cf. section 3.1) and then examine their individual components – namely warm spells and SPI-3 droughts (cf. section 3.2). In the latter part, also SPEI-3 droughts – which are not part of the definition of compound events – are included in addition to SPI-3 droughts to cover not only the precipitation aspect of droughts, but also the influence of potential evapotranspiration to acquire a more comprehensive characterisation of the drought regime in the Mediterranean.

Compound events are categorized in two ways regarding absolute extremes – which we refer to as warm season compound events – and extremes relative to their respective timing of the year – which we refer to as deseasonalised compound events.

Warm season compound events are defined as the joint occurrence of a warm season warm spell and a warm season SPI-3 drought. A warm season warm spell is defined as the 5-day exceedance of the 90th percentile threshold of the daily maximum temperature values of the 40-year period (Mazdiyasni and AghaKouchak, 2015). For the calculation of the warm season SPI-3 drought, the entire distribution of the respective time span from March to October is used (Note: March and April are included because they are required for the calculation of the SPI-3 in May and June. Otherwise, their values are neglected in this study.). Therefore, a warm season SPI-3 drought is a representative measure for a drought condition during the period from March to October. The process is performed similarly for SPEI-3 droughts.

Deseasonalised compound events are defined as the joint occurrence of a deseasonalised warm spell and a deseasonalised SPI-3 drought. A deseasonalised warm spell is defined as the 5- day exceedance of the 90th percentile threshold of the deviation of the daily maximum temperature from the long-term mean condition of the respective date of the year. Daily maximum temperature is deseasonalised by subtracting the mean of the respective calendar day k of the year as stated below (cf. equation (1)).

The deseasonalised temperature $T^{des}_{n\kappa}$ is defined as:

$$\forall n \in N(T^{des}_{n\kappa} = T_{n\kappa} - \overline{T}_{nk}) \tag{1}$$

where $T_{n\kappa}$ is the temperature of the given day κ and $\overline{T}_{nk}$ is the mean temperature for the given calendar day k for all pixels $n \in N$, where N denotes the set of all pixels in the Mediterranean Basin belonging to the Köppen-Geiger categories Csa and Csb. $\overline{T}_{nk}$ is calculated by averaging over all days κ with the same calendar day k (e.g. the first day of January 01.01.) within the time span 1979–2018 and subsequently smoothing the obtained curve of the mean annual temperature cycle for each pixel $n \in N$ to minimise stochastic fluctuations in the annual temperature curve.

For the calculation of the deseasonalised SPI-3 drought, the SPI is calculated based on the distribution of each month of year – and its 2 preceding months – separately, i.e. it is representative for the extremeness with respect to the given time of the year. The process is performed similarly for SPEI-3 droughts.

2.4. *Challenges of the SPI and the SPEI*

All drought indices have certain limitations. The applicability of the SPI in dry seasons has been questioned because in such cases, periods without rainfall are the norm and cannot be considered as a drought (Wu et al., 2007). If there are too many zero precipitation values, it is infeasible to fit a suitable gamma distribution and thus to yield normally distributed SPI values (Mishra and Singh, 2010). In addition, relatively small deviations can lead to disproportionately large changes in the SPI value in case of periods with scarce rain (WMO, 2012). In the Mediterranean Basin such periods without precipitation are common during summer time (Palutikof et al., 1994; Manning et al., 2019). This is the reason why there are particularly few droughts detected for the deseasonalised summer months. In our study, this limitation is partially alleviated by using the SPI-3 to avoid covering a period with insufficient length for rainfall occurrence.

The SPEI is highly correlated with temperature (Kong et al., 2020) and is thus to a certain degree also already an indicator for a compound event. For this reason SPEI droughts are not investigated in co-occurrence with warm spells in this study. Nevertheless, it can serve as good additional indicator to verify the analyses of warm spells and SPI droughts as it is related to both measures – directly to SPI, because it has a precipitation component and indirectly to warm spells because temperature is a driver of potential evapotranspiration.

Furthermore, estimations of potential evaporation can vary depending on the applied method (Zhao et al., 2013). Potential evaporation of a vegetated land surface, which may be partially water-limited, cannot be measured routinely for large regions. Therefore, several approaches exist for its calculation or estimation, e.g. physically-based (i.e. based on the energy budget of the land surface) ones like the Penman-Monteith equation and temperature-based estimation approaches like the Thornthwaite and the Hargreaves equation (Thornthwaite, 1948; Monteith, 1965; Hargreaves, 1975; Zhao et al., 2013). Potential evaporation values from ERA5 are based on surface energy balance calculations (such as the Penman-Monteith equation) with the vegetation parameters set for well watered agricultural land (Copernicus Climate Change Service, 2017). The Penman-Monteith equation is energy-balance-based and requires air temperature, relative air humidity, net radiation and wind speed as input atmospheric variables and estimates for water conductance through the vegetation cover (Allen et al., 1998; Bonan, 2016). It usually yields rather realistic estimations of evapotranspiration with a high spatial and temporal resolution. However, due to its comprehensive data requirements its usage is limited in many regions (Donohue et al., 2010). In such cases the application of the empirical Hargreaves equation can be recommended, which was designed for simplicity and is based solely on temperature (Allen et al., 1998; Hargreaves and Allen, 2003). Another widely applied method in cases of data scarcity is the Thornthwaite equation (Garcia et al., 2004).

2.5. Detection of temporal change

The number of compound events are aggregated yearly and divided by the number of pixels to obtain the average yearly number of compound events per pixel. Using this aggregation, autocorrelation is reduced. Trend detection is performed using the non-parametric Mann-Kendall test for the aggregated time series from 1979 to 2018. A modified version of the Mann-Kendall Test was used to account for temporal autocorrelation based on the Hamed and Rao (1998) variance correction approach. Additionally, we corrected for multiple testing using the Benjamini and Hochberg (1995) correction.

Moreover, the 40-year time span from 1979 to 2018 is divided into two 20-year periods to analyse changes over time. The percentage change in the number of events between both time spans 1979–1998 and 1999–2018 is investigated by calculating the proportion of compound events E_{prop} from the total number of compound events that occurred in each 20-year period as stated in equation (2), where N_{79-98}, N_{99-18}, N_{79-18} are events occurring in the time spans 1979–1998, 1999–2018 and 1979–2018, respectively.

$$E_{\mathrm{prop}} = \frac{N_{99-18} - N_{79-98}}{N_{79-18}} \tag{2}$$

Furthermore, the two-sample Cramér-von-Mises test and the two-sample Kolmogorov-Smirnov test are applied for comparing the differences in the distributions of compound events between the two time spans 1979–1998 and 1999–2018. These tests evaluate the distance between the cumulative distribution functions of the two time spans 1979–1998 and 1999–2018. The tests indicate, whether the two sample distributions stem from the same population based on the rejection of the null hypothesis indicated by the significance level of the p-value. A p-value < 0.05 (5% significance level) is considered to be significant for the Mann-Kendall test, Cramér-von-Mises test and the Kolmogorov-Smirnov test. In addition, we apply a change vector analysis to compare the relative increases of warm spells in relation to droughts between the time periods 1979–1998 and 1999–2018. The change vector analysis is a visualisation technique often used for display of temporal changes in two spectral bands in satellite imagery (Malila, 1980; Johnson and Kasischke, 1998). A more detailed explanation of this visualisation tool is given in section 3.2 and Fig. 9.

The analysis was carried out using R version 3.6.1 and Python version 3.7.3. The R package 'SPEI' was applied for calculating SPI-3 and SPEI-3 (Beguería and Vicente-Serrano, 2017) and the R package 'RStoolbox' was used to perform the change vector analysis (Leutner et al., 2019).

3. Results

3.1. Temporal changes in compound events over the period 1979–2018

The development over time of compound events from 1979 to 2018 shows a significant increase for both warm season and deseasonalised compound events (cf. Fig. 2). According to the slope of the fitted regression, the number of events rises from 0.27 (0.29) events per year in 1979 to 1.22 (1.16) in 2018 with an average standard deviation of 0.99 (1.06) for warm season (deseasonalised) compound events. The average annual growth rate is 3.9% (3.5%) for warm season (deseasonalised) compound events. These trends are statistically significant (cf. Table 1). Extreme hot and dry years such as 2003, 2012 and 2017 show notable peaks in the number of warm season compound events. Another striking feature is the high number of deseasonalised compound events in the years 2014–2017, which all rank among the highest six years within the entire 40-year period.

The average yearly number of warm season (deseasonalised) compound events per pixel in the entire period 1979–2018 is 0.72 (0.72), with an average event number of 0.46 (0.48) in the first period from 1979 to 1998 and 0.98 (0.96) in the second period from 1999 to 2018 (cf. Fig. 3). The boxplots and the empirical cumulative distribution functions of the average yearly number of events per pixel deviate strongly between the two time periods for both warm season and deseasonalised compound events (cf. Figs. 3 and 4). Particularly in the upper tail of the distribution of warm season compound events the divergence is highly pronounced (cf. left panel in Fig. 4), indicating that especially the years with the highest number of extreme events are getting more frequent. This increase in the upper tail – i.e. increase in years with substantially high numbers of events and/or particularly long events – can also be seen in Fig. 3 in the large extension of the right whisker of warm season compound event in the period 1999–2018.

The spatial patterns of changes in event number are mostly consistent for warm season compound events compared to deseasonalised compound events (cf. Fig. 5). The number of compound events has increased substantially in the years 1999–2018 compared to 1979–1998 in most areas of the Mediterranean Basin. For warm season (deseasonalised) compound events, 86.7% (91.1%) of all pixels have a higher number of events in the time period from 1999 to 2018 compared to 1979–1998 with the increases being most pronounced in Morocco, south-eastern Spain and western Turkey. There are only few pixels, where the number of (warm season/deseasonalised) compound events has not changed (4.4%/2.0%) or decreased (8.9%/6.9%) from the first to the second period, notably in southern Turkey and the north-eastern region of the Iberian Peninsula.

The highest increases over the 40-year period have occurred in the Western Balkan countries (Albania, Bosnia and Herzegovina, Croatia, Montenegro and North Macedonia) for warm season compound events (cf. Fig. 6), followed by Italy, Morocco, France and Spain. Libya is the only country showing decreases over time. Interestingly, on the other hand, Libya has the second highest increases regarding deseasonalised compound events – only superseded by Syria –, which is in contrast to the temporal decrease for warm season compound events. However, we consider this contrast between warm season and deseasonalised compound events insignificant, because the Mediterranean region in Libya is fairly small and the strong increase in deseasonalised compound events is mainly driven by a few events in the last decade (cf. Fig. A11). The

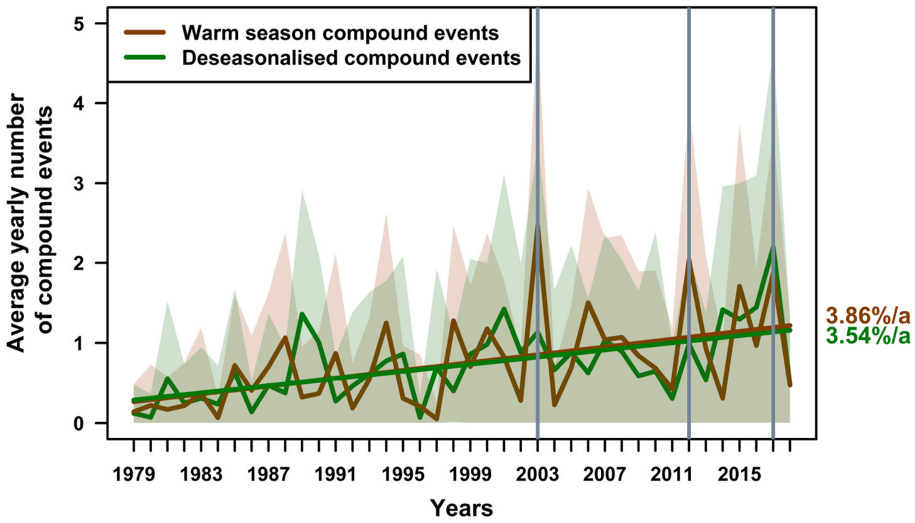

Fig. 2. Number of warm season (brown) and deseasonalised (green) compound events in the Mediterranean averaged yearly over all pixels for the 40-year period 1979–2018. The standard deviation is displayed as shaded area in the respective colour. The average annual growth rate in percentage is stated adjacent to the regression lines for warm season (brown) and deaseasonalised (green) compound events. The three years with the highest number of warm season compound events (2003, 2012 and 2017) are marked by grey vertical lines. (For interpretation of the references to colour in this figure legend, the reader is referred to the Web version of this article.)

Table 1
First column: Mann-Kendall (MK) trend detection for the number of compound events, SPI-3 and SPEI-3 droughts and warm spells averaged yearly over all pixels in the Mediterranean over the period 1979–2018. Second and third column: Statistical analysis of changes in event distributions for the periods from 1979 to 1998 and 1999–2018 for compound events, SPI-3 and SPEI-3 droughts and warm spells averaged yearly over all pixels in the Mediterranean using the Cramér-von-Mises test (CvM) and the Kolmogorov-Smirnov test (KS). Significant p-values are depicted bold. Forth column: Average annual growth rate (AAGR) in percentage.

	p-value			AAGR
	MK	CvM	KS	
Compound events				
warm season	$\mathbf{1.47 \cdot 10^{-3}}$	$\mathbf{3.00 \cdot 10^{-3}}$	$\mathbf{1.23 \cdot 10^{-2}}$	3.86%
deseasonalised	$\mathbf{1.53 \cdot 10^{-4}}$	$\mathbf{\leq 2.2 \cdot 10^{-16}}$	$\mathbf{3.97 \cdot 10^{-3}}$	3.54%
Droughts				
SPI-3, warm season	$7.71 \cdot 10^{-1}$	$6.83 \cdot 10^{-1}$	$8.32 \cdot 10^{-1}$	$-1.92 \cdot 10^{-1}$%
SPI-3, deseasonalised	$8.00 \cdot 10^{-1}$	$9.85 \cdot 10^{-1}$	$9.83 \cdot 10^{-1}$	$-4.55 \cdot 10^{-2}$%
SPEI-3, warm season	$\mathbf{3.45 \cdot 10^{-3}}$	$\mathbf{3.00 \cdot 10^{-3}}$	$\mathbf{2.71 \cdot 10^{-4}}$	$6.28 \cdot 10^{-1}$%
SPEI-3, deseasonalised	$\mathbf{5.90 \cdot 10^{-3}}$	$\mathbf{1.80 \cdot 10^{-2}}$	$8.11 \cdot 10^{-2}$	1.58%
Warm spells				
warm season	$\mathbf{5.22 \cdot 10^{-6}}$	$\mathbf{\leq 2.2 \cdot 10^{-16}}$	$\mathbf{5.57 \cdot 10^{-5}}$	4.57%
deaseasonalised	$\mathbf{7.02 \cdot 10^{-9}}$	$\mathbf{\leq 2.2 \cdot 10^{-16}}$	$\mathbf{9.55 \cdot 10^{-6}}$	4.38%

only country with a significant trend for both warm season and deseasonalised compound events is Turkey indicated by an asterisk in Fig. 6. Additionally, for warm season compound events, a significant trend occurs in Israel and Palestinian territories (Palest. ter.), Italy, Morocco and Spain, as well as in France, Syria and Tunisia for deseasonalised compound events. The peak of 2003 compound event in the Western Mediterranean stands out clearly in France, Italy, Tunisia and the Western Balkan, whereas the most pronounced event in the Eastern Mediterranean occurs in 2010, clearly observable in Cyprus, Israel and Palestinian territories, Lebanon and Syria (cf. Fig. A11).

3.2. Investigation of the drought and the warm spell component of compound events

There is a significant trend from 1979 to 2018 for the number of compound events, warm spells and SPEI-3 droughts for both warm season and deseasonalised compound events (cf. Table 1). Only SPI-3 droughts show no significant trend. Likewise, the distribution of events differs significantly between 1979 - 1998 and 1999–2018 for the number of compound events, warm spells and SPEI-3 droughts for both warm season and deseasonalised compound events – except for deaseasonalised compound events according to the Kolmogorov-Smirnov test –, but not for SPI-3 droughts. The average number of events increases from 0.40 (0.62) events per year in 1979 to 2.39 (3.44) events per year in 2018 for warm season (deseasonalised) warm spells according to the fitted linear regression. For SPEI-3 droughts, the average number of events rises from 2.02 (1.94) to 2.59 (3.63), respectively. For SPI-3 droughts, none of the tests shows any significance, i.e. there are no indications of changes over time.

Compound events are increasing – indicated by an annual growth

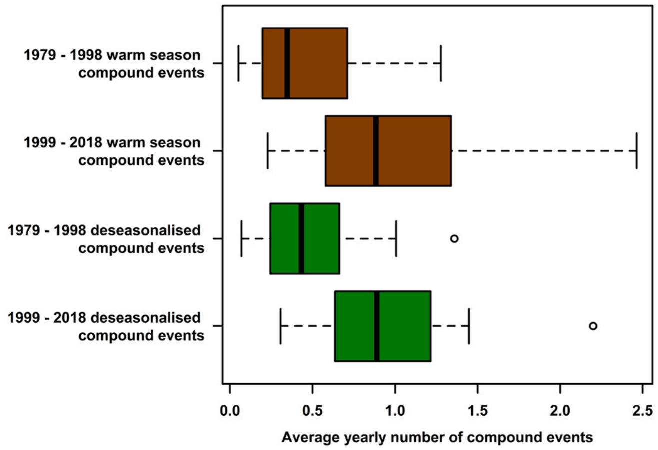

Fig. 3. Boxplots of the number of warm season (brown) and deseasonalised (green) compound events in the Mediterranean for the time periods 1979–1998 and 1999–2018 averaged yearly over all pixels. (For interpretation of the references to colour in this figure legend, the reader is referred to the Web version of this article.)

rate of 3.9 (3.5) % for warm season (deseasonalised) compound events –, but to a lesser degree than warm spells alone – indicated by an annual growth rate of 4.6 (4.4) % for warm season (deseasonalised) warm spells (cf. Table 1). SPI-3 droughts on the other hand show no notable increases. Therefore, the changes in compound events can likely be mostly attributed to increases in warm spells alone. However, in contrast to SPI-3 droughts, SPEI-3 droughts are increasing substantially. This means while precipitation is not showing large changes, potential evapotranspiration is increasing because of the higher frequency of warm spells.

Finally, it should be noted that, the choice of duration and magnitude in the definition of warm spells affects the obtained annual growth rates in the number of events substantially. Notably, the higher the chosen definition for the respective warm spell duration and magnitude is, the higher are the changes in number of compound events over time (cf. Fig. 7), ranging from an annual growth rate of 2.4% (2.2%) for the 3-day duration and 85th percentile to 7.4% (5.8%) for the 7-day and 95th percentile for warm season (deaseasonalised) compound events. Interestingly, for the most extreme events defined by 7-days durations above the 95th percentile, in many regions these events occur only in the time period from 1999 to 2018. This indicates that novel climatic conditions are emerging; producing extremes with a magnitude and duration, which did not occur in earlier times.

Increases of deseasonalised and warm season warm spells are highly consistent (cf. Fig. 8). Except for Portugal and Galicia, warm spells increase throughout the entire Mediterranean. SPI-3 droughts decrease in many regions, especially in southern Italy, Albania, Greece and western and southern Turkey. SPEI-3 droughts show also decreases at some locations in these regions, however to a lesser degree. In general, SPEI-3 droughts slightly increase throughout the Mediterranean, but not as pronounced as warm spells.

Fig. 9 shows how droughts and warm spells change in relation to each other in space between the first (1979–1998) and second period (1999–2018), qualitatively and quantitatively. The direction of change given by the angle indicates how both components are changing over time, e.g. if both warm spells and SPI-3 droughts are increasing (cyan colouring), mostly SPI-3 droughts are increasing, while warm spells are stagnant (green colouring) or mostly warm spells are increasing with stagnant SPI-3 droughts (dark blue colouring). For warm season compound events the average angle of all pixels is 82.5°, i.e. the prevailing case in the Mediterranean Basin are increasing warm spells with stagnant SPI-3 droughts over time (indicated by dark blue colouring) or sometimes even with decreasing SPI-3 droughts, e.g. in Cyprus, southern Turkey and southern Italy (purple colouring). By contrast, in the Iberian Peninsula and the Maghreb states often also SPI-3 droughts are increasing (cyan colouring) and sometimes only droughts are increasing, whereas warm spells remain stagnant (green colouring). Decreases and stagnation in warm spells are rare, but occur e.g. in southern Turkey and Portugal (yellow, orange, red and rose colouring).

For deseasonalised compound events primarily the warm spells increase, whereas SPI-3 droughts remain constant, illustrated by an average angle of all pixels of 86.5°(indicated by dark blue colouring in the lower left panel in Fig. 9). In Morocco, eastern Turkey and Libya, both droughts and warm spells are increasing (cyan colouring). Moreover, regions with decreasing SPI-3 droughts and increasing warm spells are prominent in southwestern Spain, southern Italy and Greece (purple colouring). A remarkable different behaviour is detectable near the Atlantic Coast of the Iberian Peninsula, where many pixels with increasing SPI-3 droughts are located (indicated by cyan, green and yellow colouring). Northwestern Iberia was also identified as a region with increasing moisture availability during the 20th century by Sousa et al. (2011). However, the magnitude of the change is often not very

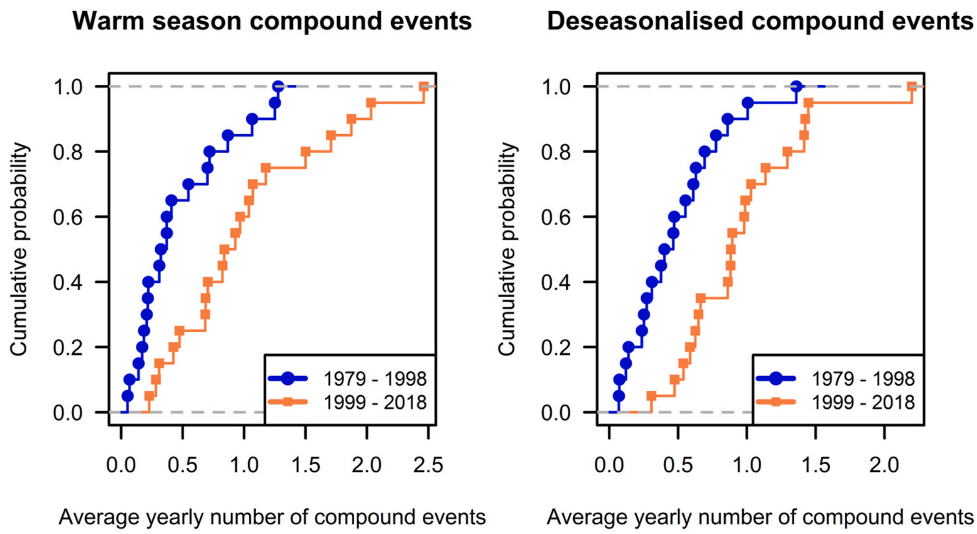

Fig. 4. Event frequency specified by the empirical cumulative distribution functions of the number of warm season (left panel) and deseasonalised (right panel) compound events in the Mediterranean averaged yearly over all pixels for both time periods 1979–1998 (green) and 1999–2018 (brown). (For interpretation of the references to colour in this figure legend, the reader is referred to the Web version of this article.)

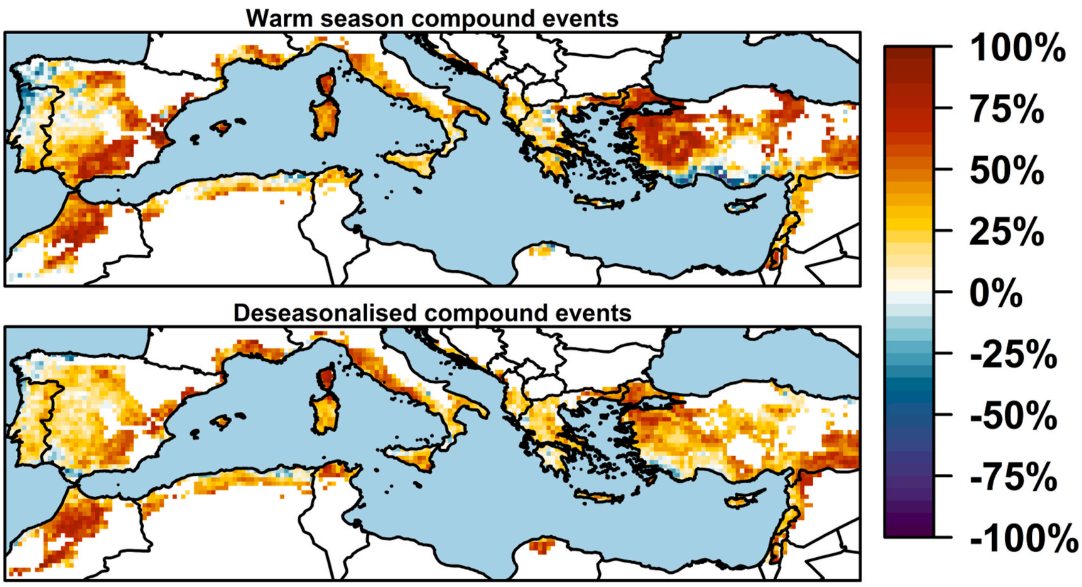

Fig. 5. Regional change detection of compound events between the two periods 1979–1998 and 1999–2018 showing the proportion of compound events from the total number of compound events that occurred in each 20-year period for warm season (upper panel) and deseasonalised (lower panel) compound events in the Mediterranean. The percentage is given by the difference between both periods divided by the entire time span 1979–2018 (cf. equation (2)). A value of 100% indicates all events occurred in the period 1999–2018, a value of −100% indicates all events occurred in the period 1979–1998 and a value of 0% indicates an equal number of events in both periods.

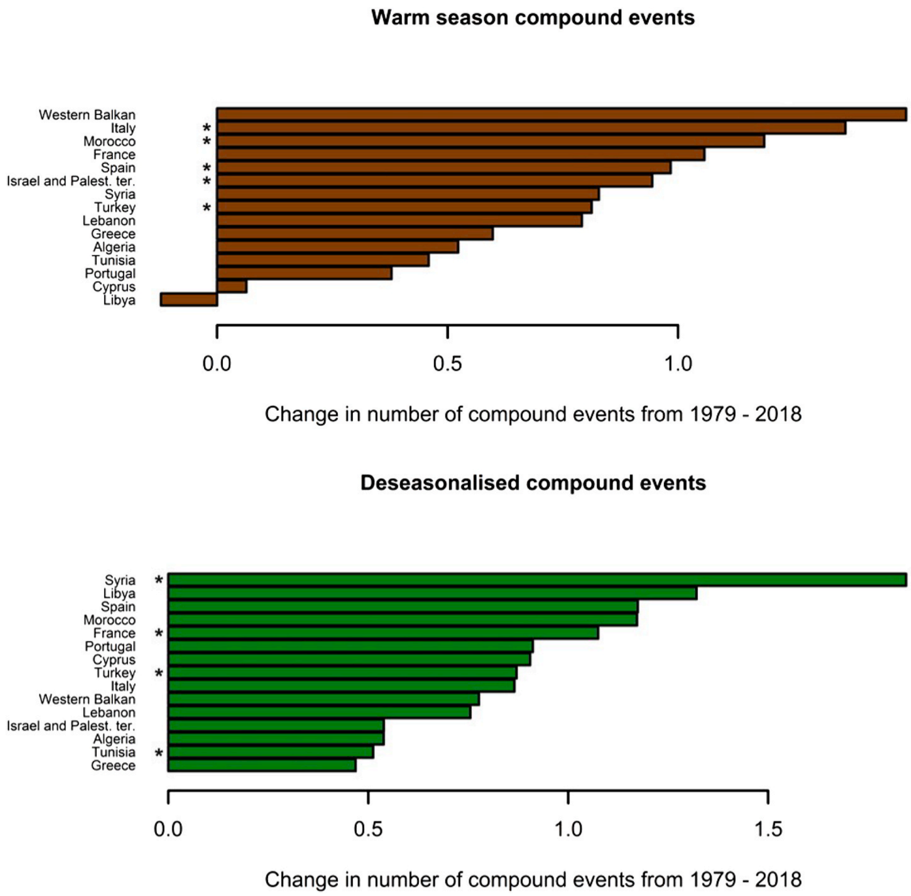

Fig. 6. Absolute change in the number of warm season (upper panel) and deseasonalised (lower panel) compound events over the 40-year-period 1979–2018 for each country. Note that only the regions located within the study area (cf. Fig. 1) of the respective countries are incorporated. Significant trends based on the Mann-Kendall test are marked with an asterisk. The corresponding time series are shown in Fig. A11.

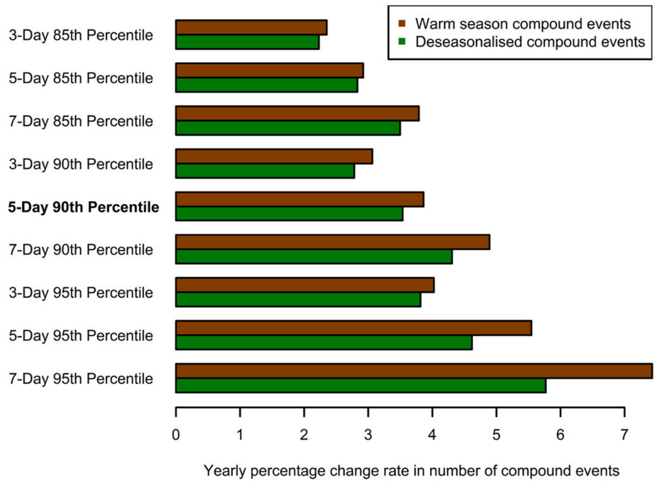

Fig. 7. Comparison of the effect of different warm spell lengths and magnitudes on change rates of compound events in the Mediterranean: Percentage change in the number of warm season (brown) and deseasonalised (green) compound events averaged yearly over all pixels from 1979 to 2018 for nine warm spell definitions using all nine combinations of the three warm spell durations (3, 5 and 7 days) and three warm spell intensities (85th, 90th and 95th percentile). The 5-Day 90th percentile is the standard case used in this article and is highlighted in bold. (For interpretation of the references to colour in this figure legend, the reader is referred to the Web version of this article.)

pronounced, so the behaviour of the warm spells has to be carefully interpreted here.

Quantitatively, the increase for both warm season and deseasonalised compound events is highest in western Turkey and Andalusia, whereas the smallest changes occur at the Atlantic coast of the Iberian Peninsula and southern Turkey (cf. right panels in Fig. 9). This shows that within Turkey, there is a substantial gradient in the change of the number of compound events on a relatively small spatial scale.

3.3. Monthly assessment of compound events, warm spells and droughts

The absolute number of warm season compound events increased from 1979 to 2018 by 0.19 events per pixel in July and 0.69 in August, whereas the other months showed virtually no changes (cf. Fig. 10). According to Conte et al. (2002), two thirds of all heat waves happen within July and August, which explains why these are also the months where compound events are predominantly increasing. However, the number of deseasonalised compound events increases most in February, May and June by 0.11, 0.11 and 0.17 events per pixel from 1979 to 2018, respectively, whereas July, August and September have rather small increases by only $3.8{\cdot}10^{-1}$, $6.2{\cdot}10^{-1}$ and $1.8{\cdot}10^{-1}$ events per pixel, respectively (cf. Fig. 10).

Both deseasonalised and warm season warm spells have increased over the 40-years time period in all months (cf. Fig. 10 and Table 1). Warm season warm spells particularly increased in July and August – with the maximum increase in August of 1.10 in the number of events from 1979 to 2018, whereas deseasonalised warm spells increased most in the months from April to June – with a maximum increase of 0.44 in April. SPI-3 and SPEI-3 droughts show varying behaviours. Warm season (desasonalised) SPI-3 droughts show decreases in a third of the months, especially in autumn with a minimum of −0.13 in September (−0.14 in October). Warm season SPEI-3 droughts have a maximum of 0.29 in July – and are much smaller in all other months. Deseasonalised SPEI-3 droughts increase in all months except March and November, where the difference is approximately zero, with maximum increases during the summer months – up to an increase of 0.34 events in August.

4. Discussion

4.1. Changes in the number of warm spells, droughts and compound events

The increases in the number of compound events confirms the findings by Manning et al. (2019), who found an increasing number in dry and hot events in Europe for the period 1950–2013, which is primarily driven by increases in temperature. Especially warm spells have been increasing strongly, whereas SPEI droughts have been increasing – presumably because of increases in the potential evapotranspiration – to a lesser degree and SPI droughts are generally constant over time. This indicates that the rise in the number of compound events is primarily driven by temperature changes and not lack of precipitation. A notable exception are the findings of Gudmundsson and Seneviratne (2015), who state there are few significant changes in southern Europe over the 30-year period 1961–1990 based on an analysis of SPI droughts. Notably, the detection of changes in the number of droughts in the Mediterranean Basin is dependent on the choice of drought index and

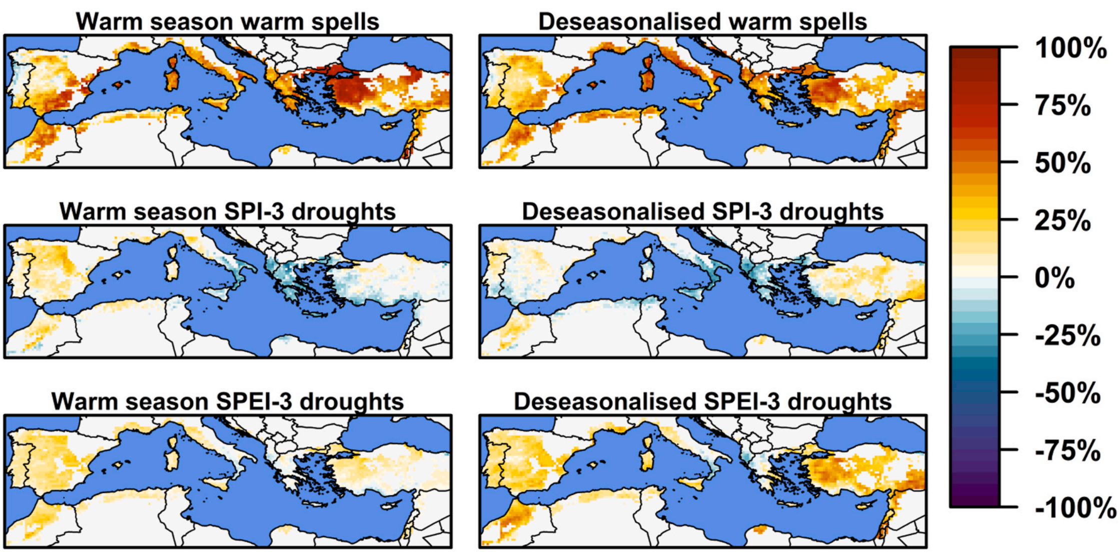

Fig. 8. Same as Fig. 5 for warm season (left column) and deseasonalised (right column) warm spells (upper panels), SPI-3 (central panels) and SPEI-3 (lower panels) droughts in the Mediterranean.

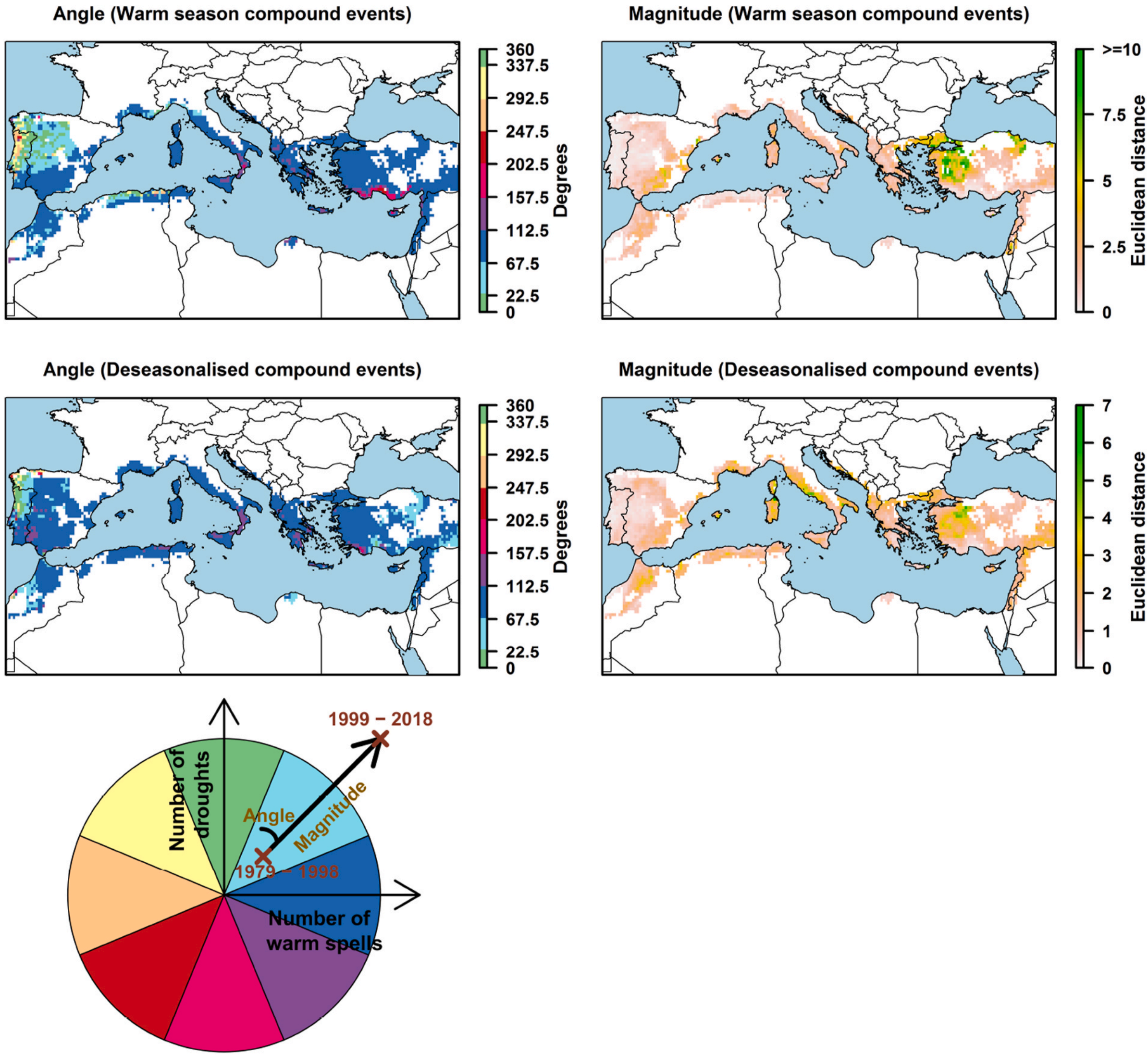

Fig. 9. Detection of change in the number of warm spells and SPI-3 droughts in the Mediterranean between the time periods 1979–1998 and 1999–2018 using a change vector analysis: A change vector is defined by two points given by the number of warm spells and the number of SPI-3 droughts in the period from a) 1979–1998 and b) 1999–2018. The angle (left column) and the magnitude (right column) of the change vector are displayed, where the angle is defined by the vector and the y-axis – the y-axis displays the number of droughts in this case – and the magnitude is given by the length of the vector, i.e. the Euclidean distance between both points. Warm spells and SPI-3 droughts are normalised by division through the number of droughts and warm spells in the first period (1979–1998), respectively. The colouring of the angular plot divides the angles into eight 45°sections (see schematic illustration of the change vector analysis with an exemplary vector at the bottom of the plot).

the reference time period (Spinoni et al., 2017). Therefore, the non-significant trends for SPI droughts in this study have to be interpreted with caution.

The increase rate of warm spells depends on the choice of percentile used for defining the warm spell magnitude in the Mediterranean, with larger increases at higher percentiles. The most extreme compound events - i.e. those with the highest heat wave duration and magnitude – occur primarily in the period from 1999 to 2018, which indicates the emergence of novel unprecedented climatic conditions in the Mediterranean in recent decades. This is consistent with previous findings indicating that temperatures at the hot tail, i.e. the highest percentiles, increase much faster than mean temperature, up to 6 °C for 1.5 °C mean warming due to surface moisture and atmospheric feedbacks in the Mediterranean Basin, (Diffenbaugh et al., 2007; Fischer and Schär, 2010; Mueller and Seneviratne, 2012; Orlowsky and Seneviratne, 2012; Lewis et al., 2019).

4.2. Discrepancy between SPI and SPEI droughts

Lack of precipitation and high evapotranspiration rates are the general drivers of Mediterranean droughts (Sousa et al., 2011; Spinoni et al., 2017). In contrast to SPI droughts, SPEI droughts are increasing substantially (cf. Fig. 10 and Table 1), indicating that while precipitation is not showing large changes, potential evapotranspiration is increasing. This is in line with Vicente-Serrano et al. (2020) who link increasing drought severity in the Mediterranean primarily to increasing atmospheric evaporative demand rather than precipitation deficits. Therefore, the Mediterranean is likely getting drier in spite of unchanged precipitation patterns. The SPEI is particularly suitable to detect the warming impact by climate change (Vicente-Serrano et al., 2010), whereas the SPI cannot show such warming-induced changes in droughts as it is based solely on precipitation (Dubrovsky et al., 2009). This leads to the conclusion that, while compound events are strongly

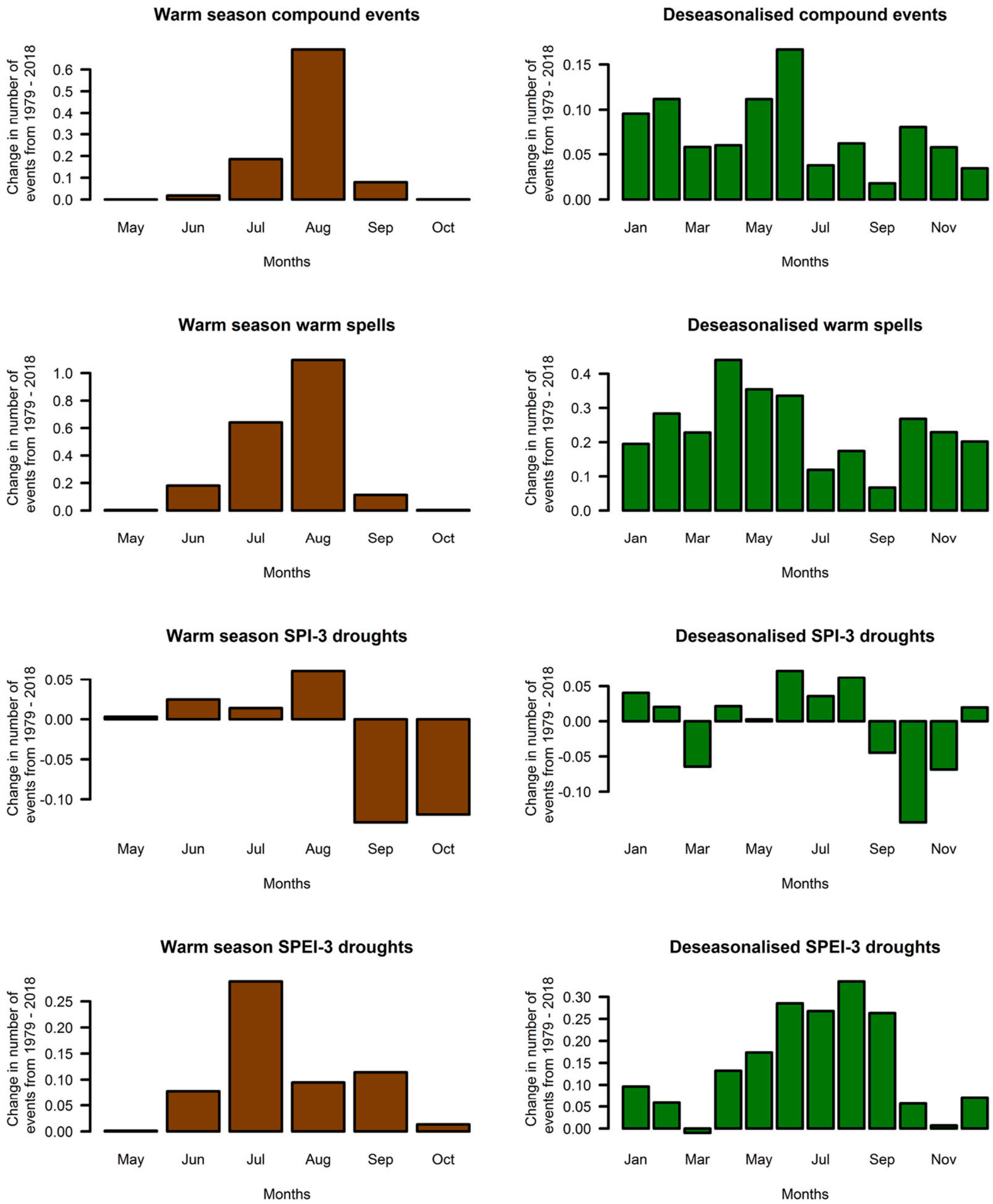

Fig. 10. Absolute change in the number of warm season (left column) and deseasonalised (right column) events in the Mediterranean averaged yearly over all pixels over the 40-year-period 1979–2018 for each month for compound events (first line), warm spells (second line), SPI-3 droughts (third line), SPEI-3 drought (fourth line).

increasing in the Mediterranean, the increases of compound events calculated by the definition based on the SPI used here is presumably underestimating the drought component. Future research should aim for adequately incorporating the water balance and land-atmosphere feedbacks by using direct measurements of soil moisture droughts and actual evapotranspiration, e.g. based on remote sensing (Sharma and Mujumdar, 2017; Toulios et al., 2020). However, such an approach can be presumably only be undertaken reliably for the last two to three decades due to the scarce spatio-temporal satellite coverage before (Dorigo et al., 2017). Furthermore, remote sensing only retrieves surface soil moisture, but users are often requiring deeper reaching root-zone soil moisture (Albergel et al., 2008; Dorigo et al., 2017).

Increases in SPEI-3 droughts are highly relevant, as heat waves jointly with increasing evapotranspiration can lead to a drier climate state, potentially leading to desertification in the Mediterranean Basin with drastic impacts on its ecosystems (Conte et al., 2002; Gao and Giorgi, 2008; Guiot and Cramer, 2016; Samaniego et al., 2018). The Mediterranean biome will extend northwards in future due to global warming (Seneviratne et al., 2006; Feng and Fu, 2013), potentially leading to similar exacerbations in the number of compound events in those regions.

4.3. Timing of events

The rate of change in number of events differs between warm season and deseasonalised compound events. The months July and August show the highest increases in warm season compound events by far, whereas the highest change rates of deseasonalised compound events occur in spring and early summer and are relatively low from July to September. It has been noted that the onset of droughts is starting earlier in the year, shifting towards spring (Beniston et al., 2007; Giannakopoulos et al., 2009; Trenberth et al., 2014; Samaniego et al., 2018). Spinoni et al. (2017, 2018) found that changes in the number of drought frequency and severity differed substantially depending on the season and are highest in spring and summer in the Mediterranean Basin. This increase in deseasonalised compound events in spring is potentially very relevant for Mediterranean ecosystems and agriculture as this is the peak phase of ecosystem productivity and a vital phenophase. This is in line with findings by Samaniego et al. (2018), stating plant development is affected negatively due to decreasing soil moisture availability during the growing season in Europe. This shows the importance of incorporating deseasonalised compound events, because these patterns are not visible for warm season compound events and might be missed if only warm season compound events are investigated. Compound warm spells and droughts may occur earlier in the year than they used to in the past, which potentially explains the high rate of change in spring and early summer compared to the relatively low rate of change in late summer for deseasonalised compound events. This shift could be due to earlier depletion of water resources in the ecosystems (e.g. soil moisture) caused by increased temperatures and the associated ecosystem productivity and evapotranspiration in springtime (Buermann et al., 2018; Bastos et al., 2020). Mediterranean winter and spring droughts are linked to the occurrence of subsequent summer heat anomalies in the Mediterranean and central Europe (Vautard et al., 2007; Russo et al., 2019). For example, the increased evapotranspiration in spring contributed roughly as much as evapotranspiration in summer to the summer heat wave and drought in 2018 (Bastos et al., 2020). This soil moisture deficit can in turn fortify the development of heat waves due to lack of evaporative cooling (Lian et al., 2020). So far, the evidence supporting this mechanism is scarce (Lian et al., 2020) and this study contributes to add to evidence supporting this hypothesis. Drought impacts also depend on seasonality. However, seasonal differences were rarely analysed for Europe up to this point (Spinoni et al., 2017, 2018).

Further research is crucial for a better understanding of the effect of weather extremes on transpiration rates in European ecosystems (Teuling et al., 2010), as the effects of warm spells and droughts on vegetation dynamics are not one-sided and vegetation dynamics in turn also influence magnitude and duration of warm spells and droughts (Lemordant et al., 2016).

5. Conclusion

Our research supports prior findings that increases in the number of compound events in the Mediterranean Basin in the last four decades are mostly driven by temperature changes. A continuing and regular combined monitoring of the changes in warm spells and droughts and their future development is crucial to provide the necessary data and information base for an adequate risk management. Such a risk management might include adaptation of crop choice, sowing schedules, and irrigation options. The interdependence between warm spells and droughts and the associated feedback mechanisms for warm spells and droughts are still under debate and the question if droughts primarily drive warm spells or vice versa is nontrivial (Sheffield et al., 2012). In this respect, the onset and development of compound warm spells and droughts is still not well understood and it remains unclear how these events and their interactions will be altered by climate change (Sheffield and Wood, 2008; Miralles et al., 2019) and thus how these compound events will evolve in future. A better insight into these intertwined mechanisms and feedbacks of such compound events might be derived from detailed coupled local or regional meteorological and soil-hydrological modelling experiments, where energy fluxes and water storages can be modelled and analysed under observed boundary conditions, such as conducted e.g. by Niu et al. (2014) and Senatore et al. (2015). Such modelling experiments, however, require data from comprehensive on-site measurements campaigns for meteorological and soil-hydrological variables to enable a model validation of both energy and water fluxes.

Increases in deseasonalised compound warm spells and droughts might have major implications for Mediterranean ecosystems and agriculture. An earlier onset of compound events in the year is likely to affect the growing season length and ecosystem productivity and in turn evapotranspiration rates. This might lead to unforeseen changes in the complex land-atmosphere feedbacks in this region. This highlights the importance of incorporating deseasonalised compound events, because these patterns are not visible for warm season compound events and might be missed if only warm season compound events are investigated.

CRediT authorship contribution statement

Johannes Vogel: Conceptualization, Software, Formal analysis, Writing - review & editing, Visualization. **Eva Paton:** Conceptualization, Writing - review & editing, Supervision. **Valentin Aich:** Writing - review & editing. **Axel Bronstert:** Writing - review & editing.

Declaration of competing interest

The authors declare that they have no known competing financial interests or personal relationships that could have appeared to influence the work reported in this paper.

Acknowledgments

The authors would like to thank Omid Mazdiyasni and Amir AghaKouchak for providing support for this research project. Furthermore, we would like to thank Benjamin Leutner for helping to implement the change vector analysis in our study. This research was funded by the DFG research training group “Natural Hazards and Risks in a Changing World” (NatRiskChange GRK 2043).

AppendixA

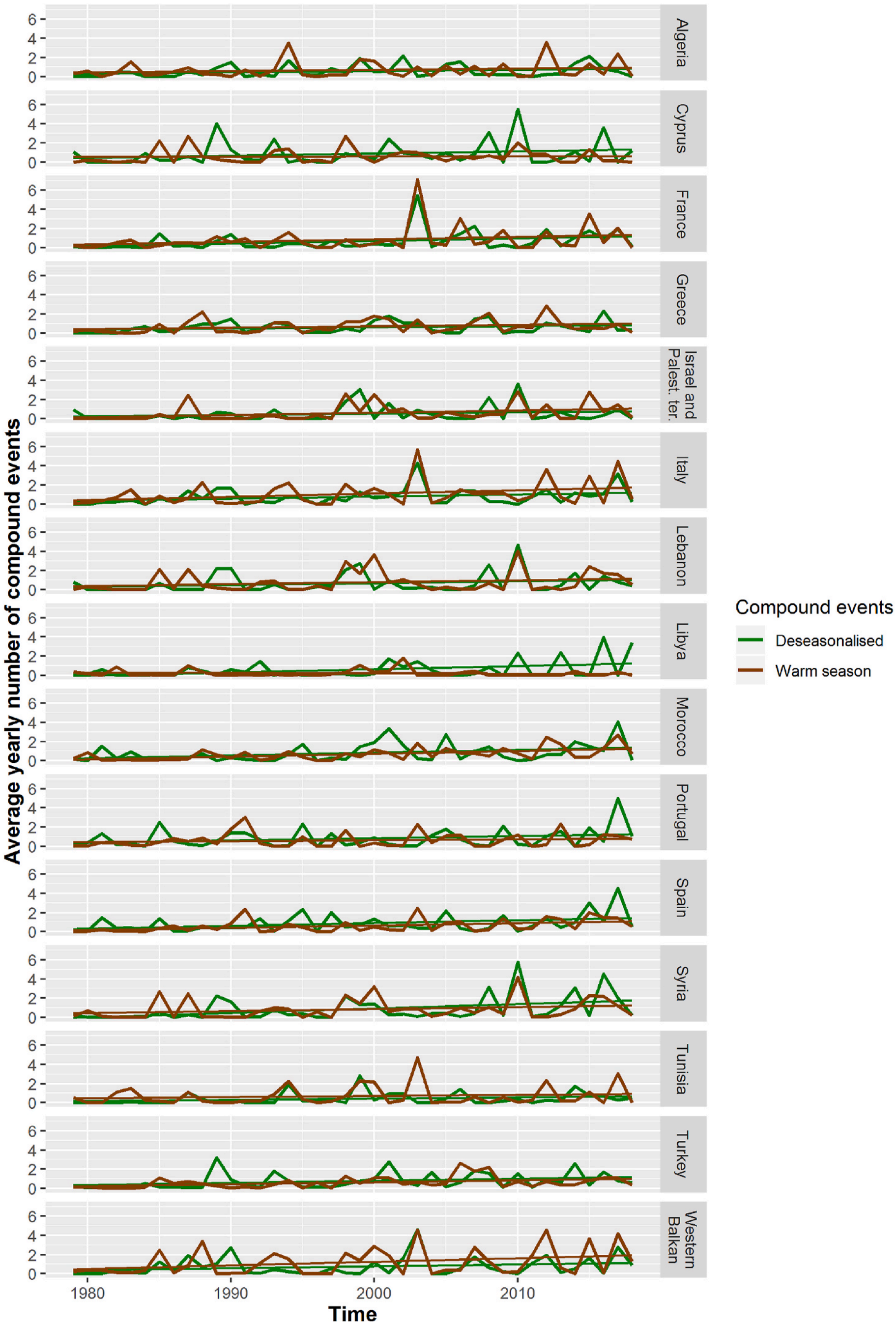

Fig. A.11. Number of warm season (brown) and deseasonalised (green) compound events for each country averaged yearly over all pixels for the 40-year period 1979–2018. Note that only the regions located within the study area (cf. Fig. 1) of the respective countries are incorporated.

References

AghaKouchak, A., Cheng, L., Mazdiyasni, O., Farahmand, A., 2014. Global warming and changes in risk of concurrent climate extremes: Insights from the 2014 California drought. Geophys. Res. Lett. 41 (24), 8847–8852.

Albergel, C., Rüdiger, C., Pellarin, T., Calvet, J.-C., Fritz, N., Froissard, F., Suquia, D., Petitpa, A., Piguet, B., Martin, E., 2008. From near-surface to root-zone soil moisture using an exponential filter: an assessment of the method based on in-situ observations and model simulations. Hydrol. Earth Syst. Sci. Discuss. 5 (3), 1603–1640.

Allen, C.D., Macalady, A.K., Chenchouni, H., Bachelet, D., McDowell, N., Vennetier, M., Kitzberger, T., Rigling, A., Breshears, D.D., Hogg, E.H., Gonzalez, P., Fensham, R., Zhang, Z., Castro, J., Demidova, N., Lim, J.-H., Allard, G., Running, S.W., Semerci, A., Cobb, N., 2010. A global overview of drought and heat-induced tree mortality reveals emerging climate change risks for forests. For. Ecol. Manag. 259 (4), 660–684.

Allen, R.G., Pereira, L.S., Raes, D., Smith, M., 1998. Crop Evapotranspiration: Guidelines for Computing Crop Water Requirements: FAO Irrigation and Drainage Paper 56. Food and Agriculture Organisation of the United Nations, Rome.

Bastos, A., Ciais, P., Friedlingstein, P., Sitch, S., Pongratz, J., Fan, L., Wigneron, J.P., Weber, U., Reichstein, M., Fu, Z., Anthoni, P., Arneth, A., Haverd, V., Jain, A.K., Joetzjer, E., Knauer, J., Lienert, S., Loughran, T., McGuire, P.C., Tian, H., Viovy, N., Zaehle, S., 2020. Direct and seasonal legacy effects of the 2018 heat wave and drought on european ecosystem productivity. Science advances 6 (24), eaba2724.

Beguería, S., Vicente-Serrano, S.M., 2017. Spei: Calculation of the Standardised Precipitation-Evapotranspiration Index. https://CRAN.R-project.org/package=SPEI. last accessed on 03/03/20.
Ben-Ari, T., Boé, J., Ciais, P., Lecerf, R., van der Velde, M., Makowski, D., 2018. Causes and implications of the unforeseen 2016 extreme yield loss in the breadbasket of France. Nat. Commun. 9 (1), 1627.
Beniston, M., Stephenson, D.B., Christensen, O.B., Ferro, C.A.T., Frei, C., Goyette, S., Halsnaes, K., Holt, T., Jylhä, K., Koffi, B., Palutikof, J., Schöll, R., Semmler, T., Woth, K., 2007. Future extreme events in european climate: an exploration of regional climate model projections. Climatic Change 81 (S1), 71–95.
Benjamini, Y., Hochberg, Y., 1995. Controlling the false discovery rate: a practical and powerful approach to multiple testing. J. Roy. Stat. Soc. B 57 (1), 289–300.
Bonan, G.B., 2016. Ecological Climatology: Concepts and Applications, third ed. Cambridge University Press, New York.
Buermann, W., Forkel, M., O'Sullivan, M., Sitch, S., Friedlingstein, P., Haverd, V., Jain, A.K., Kato, E., Kautz, M., Lienert, S., Lombardozzi, D., Nabel, J.E.M.S., Tian, H., Wiltshire, A.J., Zhu, D., Smith, W.K., Richardson, A.D., 2018. Widespread seasonal compensation effects of spring warming on northern plant productivity. Nature 562 (7725), 110–114.
Christidis, N., Jones, G.S., Stott, P.A., 2015. Dramatically increasing chance of extremely hot summers since the 2003 european heatwave. Nat. Clim. Change 5 (1), 46–50.
Ciais, P., Reichstein, M., Viovy, N., Granier, A., Ogée, J., Allard, V., Aubinet, M., Buchmann, N., Bernhofer, C., Carrara, A., Chevallier, F., de Noblet, N., Friend, A.D., Friedlingstein, P., Grünwald, T., Heinesch, B., Keronen, P., Knohl, A., Krinner, G., Loustau, D., Manca, G., Matteucci, G., Miglietta, F., Ourcival, J.M., Papale, D., Pilegaard, K., Rambal, S., Seufert, G., Soussana, J.F., Sanz, M.J., Schulze, E.D., Vesala, T., Valentini, R., 2005. Europe-wide reduction in primary productivity caused by the heat and drought in 2003. Nature 437 (7058), 529–533.
Collins, M., Knutti, R., Arblaster, J., Dufresne, J.-L., Fichefet, T., Friedlingstein, P., Gao, X., Gutowski, W.J., Johns, T., Krinner, G., et al., 2013. Long-term climate change: projections, commitments and irreversibility. In: Stocker, T.F., Qin, D., Plattner, G.K., Tignor, M., Allen, S.K., Boschung, J., Nauels, A., Xia, Y., Bex, V., Midgley, P.M. (Eds.), Climate Change 2013. Cambridge University Press, New York, pp. 1029–1136.
Conte, M., Sorani, N., Piervitali, E., 2002. Extreme climatic events over the mediterranean. In: Geeson, N., Brandt, C.J., Thornes, J.B. (Eds.), Mediterranean Desertification, vol. 1. John Wiley & Sons, Chichester West Sussex England and Hoboken NJ USA, pp. 15–31.
Cook, B.I., Anchukaitis, K.J., Touchan, R., Meko, D.M., Cook, E.R., 2016. Spatiotemporal drought variability in the mediterranean over the last 900 years. Journal of geophysical research. Atmospheres : JGR 121 (5), 2060–2074.
Copernicus Climate Change Service, 2017. ERA5: Fifth generation of ECMWF atmospheric reanalyses of the global climate: Copernicus climate change service climate data store (cds). https://cds.climate.copernicus.eu last accessed on 03/03/20.
Cramer, W., Guiot, J., Fader, M., Garrabou, J., Gattuso, J.-P., Iglesias, A., Lange, M.A., Lionello, P., Llasat, M.C., Paz, S., Peñuelas, J., Snoussi, M., Toreti, A., Tsimplis, M.N., Xoplaki, E., 2018. Climate change and interconnected risks to sustainable development in the mediterranean. Nat. Clim. Change 8 (11), 972–980.
Dai, A., 2013. Increasing drought under global warming in observations and models. Nat. Clim. Change 3 (1), 52–58.
de Boeck, H.J., Dreesen, F.E., Janssens, I.A., Nijs, I., 2011. Whole-system responses of experimental plant communities to climate extremes imposed in different seasons. New Phytol. 189 (3), 806–817.
Diffenbaugh, N.S., Pal, J.S., Giorgi, F., Gao, X., 2007. Heat stress intensification in the mediterranean climate change hotspot. Geophys. Res. Lett. 34 (11), 1–6.
Donohue, R.J., McVicar, T.R., Roderick, M.L., 2010. Assessing the ability of potential evaporation formulations to capture the dynamics in evaporative demand within a changing climate. J. Hydrol. 386 (1–4), 186–197.
Dorigo, W., Wagner, W., Albergel, C., Albrecht, F., Balsamo, G., Brocca, L., Chung, D., Ertl, M., Forkel, M., Gruber, A., Haas, E., Hamer, P.D., Hirschi, M., Ikonen, J., de Jeu, R., Kidd, R., Lahoz, W., Liu, Y.Y., Miralles, D., Mistelbauer, T., Nicolai-Shaw, N., Parinussa, R., Pratola, C., Reimer, C., van der Schalie, R., Seneviratne, S.I., Smolander, T., Lecomte, P., 2017. ESA CCI soil moisture for improved earth system understanding: state-of-the art and future directions. Rem. Sens. Environ. 203, 185–215.
Dubrovsky, M., Svoboda, M.D., Trnka, M., Hayes, M.J., Wilhite, D.A., Zalud, Z., Hlavinka, P., 2009. Application of relative drought indices in assessing climate-change impacts on drought conditions in Czechia. Theor. Appl. Climatol. 96 (1–2), 155–171.
Feng, S., Fu, Q., 2013. Expansion of global drylands under a warming climate. Atmos. Chem. Phys. 13 (19), 10081–10094.
Fischer, E.M., Schär, C., 2010. Consistent geographical patterns of changes in high-impact european heatwaves. Nat. Geosci. 3 (6), 398–403.
Fraga, H., Pinto, J.G., Viola, F., Santos, J.A., 2020. Climate change projections for olive yields in the mediterranean basin. Int. J. Climatol. 40 (2), 769–781.
Gao, X., Giorgi, F., 2008. Increased aridity in the mediterranean region under greenhouse gas forcing estimated from high resolution simulations with a regional climate model. Global Planet. Change 62 (3–4), 195–209.
Garcia, M., Raes, D., Allen, R., Herbas, C., 2004. Dynamics of reference evapotranspiration in the bolivian highlands (altiplano). Agric. For. Meteorol. 125 (1–2), 67–82.
Giannakopoulos, C., Le Sager, P., Bindi, M., Moriondo, M., Kostopoulou, E., Goodess, C. M., 2009. Climatic changes and associated impacts in the mediterranean resulting from a 2 ° c global warming. Global Planet. Change 68 (3), 209–224.
Giorgi, F., 2006. Climate change hot-spots. Geophys. Res. Lett. 33 (8), 1–4.
Gouveia, C.M., Bistinas, I., Liberato, M.L., Bastos, A., Koutsias, N., Trigo, R., 2016. The outstanding synergy between drought, heatwaves and fuel on the 2007 southern Greece exceptional fire season. Agric. For. Meteorol. 218–219, 135–145.
Gudmundsson, L., Seneviratne, S.I., 2015. European drought trends. Proceedings of the International Association of Hydrological Sciences 369, 75–79.
Guiot, J., Cramer, W., 2016. Climate change: the 2015 paris agreement thresholds and mediterranean basin ecosystems. Science (New York, N.Y.) 354 (6311), 465–468.
Hamed, K.H., Rao, A.R., 1998. A modified mann-kendall trend test for autocorrelated data. J. Hydrol. 204, 182–196.
Hao, Z., Hao, F., Singh, V.P., Zhang, X., 2018. Changes in the severity of compound drought and hot extremes over global land areas. Environ. Res. Lett. 13 (12), 124022.
Hargreaves, G.H., 1975. Moisture availability and crop production. Transactions of the ASAE 18, 980–984.
Hargreaves, G.H., Allen, R., 2003. History and evaluation of hargreaves evapotranspiration equation. J. Irrigat. Drain. Eng. 129 (1), 53–63.
Hartmann, D.L., Tank, A.M.K., Rusticucci, M., Alexander, L.V., Brönnimann, S., Charabi, Y.A.R., Dentener, F.J., Dlugokencky, E.J., Easterling, D.R., Kaplan, A., et al., 2013. Observations: atmosphere and surface. In: Stocker, T.F., Qin, D., Plattner, G.K., Tignor, M., Allen, S.K., Boschung, J., Nauels, A., Xia, Y., Bex, V., Midgley, P.M. (Eds.), Climate Change 2013. Cambridge University Press, New York, pp. 159–254.
Hegerl, G.C., Hanlon, H., Beierkuhnlein, C., 2011. Elusive extremes. Nat. Geosci. 4 (3), 142–143.
Hersbach, H., Bell, W., Berrisford, P., Horányi, A., J, M.-S., Nicolas, J., Radu, R., Schepers, D., Simmons, A., Soci, C., Dee, D., 2019. Global reanalysis: goodbye era-interim, hello era5. ECMWF (European Centre for Medium-Range Weather Forecasts) Newsletter 159, 17–24. Spring 2019.
Horton, R., Raymond, C., 2018. Workshop on correlated extremes at columbia university. new york. https://web.archive.org/web/20181222015430/http://extremeweather.columbia.edu/workshop-on-correlated-extremes. last accessed on 03/03/20.
Horton, R.M., Mankin, J.S., Lesk, C., Coffel, E., Raymond, C., 2016. A review of recent advances in research on extreme heat events. Current Climate Change Reports 2 (4), 242–259.
IPCC, 2019. Summary for policymakers. In: IPCC (Ed.), Climate Change and Land: an IPCC Special Report on Climate Change, Desertification, Land Degradation, Sustainable Land Management, Food Security, and Greenhouse Gas Fluxes in Terrestrial Ecosystems, pp. 1–34 (in press).
Jentsch, A., Beierkuhnlein, C., 2008. Research frontiers in climate change: effects of extreme meteorological events on ecosystems. Compt. Rendus Geosci. 340 (9–10), 621–628.
Johnson, R.D., Kasischke, E.S., 1998. Change vector analysis: a technique for the multispectral monitoring of land cover and condition. Int. J. Rem. Sens. 19 (3), 411–426.
Kong, Q., Guerreiro, S.B., Blenkinsop, S., Li, X.-F., Fowler, H.J., 2020. Increases in summertime concurrent drought and heatwave in eastern China. Weather and Climate Extremes 28, 100242.
Kottek, M., Grieser, J., Beck, C., Rudolf, B., Rubel, F., 2006. World map of the Köppen-geiger climate classification updated. Meteorol. Z. 15 (3), 259–263. URL. http://koeppen-geiger.vu-wien.ac.at/present.htm.
Kreyling, J., Jentsch, A., Beierkuhnlein, C., 2011. Stochastic trajectories of succession initiated by extreme climatic events. Ecol. Lett. 14 (8), 758–764.
Le Page, M., Zribi, M., 2019. Analysis and predictability of drought in northwest africa using optical and microwave satellite remote sensing products. Sci. Rep. 9 (1), 1466.
Lemordant, L., Gentine, P., Stéfanon, M., Drobinski, P., Fatichi, S., 2016. Modification of land-atmosphere interactions by CO2 effects: implications for summer dryness and heat wave amplitude. Geophys. Res. Lett. 43 (19), 10,240–10,248.
Leonard, M., Westra, S., Phatak, A., Lambert, M., van den Hurk, B., McInnes, K., Risbey, J., Schuster, S., Jakob, D., Stafford-Smith, M., 2014. A compound event framework for understanding extreme impacts. Wiley Interdisciplinary Reviews: Climate Change 5 (1), 113–128.
Leutner, B., Horning, N., Schwalb-Willmann, J., 2019. Rstoolbox: Tools for remote sensing data analysis. http://bleutner.github.io/RStoolbox last accessed on 03/03/20.
Lewis, S.C., King, A.D., Perkins-Kirkpatrick, S.E., Mitchell, D.M., 2019. Regional hotspots of temperature extremes under 1.5 °c and 2 °c of global mean warming. Weather and Climate Extremes 26, 100233.
Lian, X., Piao, S., Li, L.Z.X., Li, Y., Huntingford, C., Ciais, P., Cescatti, A., Janssens, I.A., Peñuelas, J., Buermann, W., Chen, A., Li, X., Myneni, R.B., Wang, X., Wang, Y., Yang, Y., Zeng, Z., Zhang, Y., McVicar, T.R., 2020. Summer soil drying exacerbated by earlier spring greening of northern vegetation. Science advances 6 (1) eaax0255.
Lionello, P., Abrantes, F., Congedi, L., Dulac, F., Gacic, M., Gomis, D., Goodess, C., Hoff, H., Kutiel, H., Luterbacher, J., Planton, S., Reale, M., Schröder, K., Struglia, M. V., Toreti, A., Tsimplis, M., Ulbrich, U., Xoplaki, E., 2012. Mediterranean climate: Background information. In: Lionello, P. (Ed.), The Climate of the Mediterranean Region. Elsevier insights. Elsevier Science, Amsterdam (xxxv–xc).
Lionello, P., Scarascia, L., 2018. The relation between climate change in the mediterranean region and global warming. Reg. Environ. Change 18 (5), 1481–1493.
Ma, X., Huete, A., Moran, S., Ponce-Campos, G., Eamus, D., 2015. Abrupt shifts in phenology and vegetation productivity under climate extremes. J. Geophys. Res.: Biogeosciences 120 (10), 2036–2052.
Mahony, C.R., Cannon, A.J., 2018. Wetter summers can intensify departures from natural variability in a warming climate. Nat. Commun. 9 (1), 783.
Malila, W.A., 1980. Change vector analysis: an approach for detecting forest changes with landsat. In: Proceedings, Symposium on Machine Processing of Remotely Sensed Data. Purdue University, West Lafayette, Indiana, pp. 326–335.

Manning, C., Widmann, M., Bevacqua, E., van Loon, A.F., Maraun, D., Vrac, M., 2019. Increased probability of compound long-duration dry and hot events in europe during summer (1950–2013). Environ. Res. Lett. 14 (9), 094006.
Mazdiyasni, O., AghaKouchak, A., 2015. Substantial increase in concurrent droughts and heatwaves in the United States. Proc. Natl. Acad. Sci. U.S.A. 112 (37), 11484–11489.
McKee, T.B., Doesken, N.J., Kleist, J., 1993. The relationship of drought frequency and duration to time scales: Preprints, eighth conference on applied climatology, anaheim, ca. Amer. Meteor. Soc. 179–184.
Miralles, D.G., Gentine, P., Seneviratne, S.I., Teuling, A.J., 2019. Land-atmospheric feedbacks during droughts and heatwaves: state of the science and current challenges. Ann. N. Y. Acad. Sci. 1436 (1), 19–35.
Mishra, A.K., Singh, V.P., 2010. A review of drought concepts. J. Hydrol. 391 (1–2), 202–216.
Monteith, J.L., 1965. Evaporation and environment. Symp. Soc. Exp. Biol. 19, 205–234.
Moriondo, M., Trombi, G., Ferrise, R., Brandani, G., Dibari, C., Ammann, C.M., Lippi, M. M., Bindi, M., 2013. Olive trees as bio-indicators of climate evolution in the mediterranean basin. Global Ecol. Biogeogr. 22 (7), 818–833.
Mueller, B., Seneviratne, S.I., 2012. Hot days induced by precipitation deficits at the global scale. Proc. Natl. Acad. Sci. U.S.A. 109 (31), 12398–12403.
Niu, G.-Y., Paniconi, C., Troch, P.A., Scott, R.L., Durcik, M., Zeng, X., Huxman, T., Goodrich, D.C., 2014. An integrated modelling framework of catchment-scale ecohydrological processes: 1. model description and tests over an energy-limited watershed. Ecohydrology 7 (2), 427–439.
Orlowsky, B., Seneviratne, S.I., 2012. Global changes in extreme events: regional and seasonal dimension. Climatic Change 110 (3–4), 669–696.
Palutikof, J.P., Goodess, C.M., Guo, X., 1994. Climate change, potential evapotranspiration and moisture availability in the mediterranean basin. Int. J. Climatol. 14, 853–869.
Perkins, S.E., 2015. A review on the scientific understanding of heatwaves–their measurement, driving mechanisms, and changes at the global scale. Atmos. Res. 164–165, 242–267.
Perkins-Kirkpatrick, S.E., Gibson, P.B., 2017. Changes in regional heatwave characteristics as a function of increasing global temperature. Sci. Rep. 7 (1), 12256.
Poumadère, M., Mays, C., Le Mer, S., Blong, R., 2005. The 2003 heat wave in France: dangerous climate change here and now. Risk Anal. : an official publication of the Society for Risk Analysis 25 (6), 1483–1494.
Rubel, F., Brugger, K., Haslinger, K., Auer, I., 2017. The climate of the european alps: shift of very high resolution Köppen-geiger climate zones 1800–2100. Meteorol. Z. 26 (2), 115–125.
Ruffault, J., Curt, T., Martin-StPaul, N.K., Moron, V., Trigo, R.M., 2018. Extreme wildfire events are linked to global-change-type droughts in the northern mediterranean. Nat. Hazards Earth Syst. Sci. 18 (3), 847–856.
Russo, A., Gouveia, C.M., Dutra, E., Soares, P.M.M., Trigo, R.M., 2019. The synergy between drought and extremely hot summers in the mediterranean. Environ. Res. Lett. 14 (1), 014011.
Samaniego, L., Thober, S., Kumar, R., Wanders, N., Rakovec, O., Pan, M., Zink, M., Sheffield, J., Wood, E.F., Marx, A., 2018. Anthropogenic warming exacerbates european soil moisture droughts. Nat. Clim. Change 8 (5), 421–426.
Sedlmeier, K., Feldmann, H., Schädler, G., 2018. Compound summer temperature and precipitation extremes over central europe. Theor. Appl. Climatol. 131 (3–4), 1493–1501.
Senatore, A., Mendicino, G., Gochis, D.J., Yu, W., Yates, D.N., Kunstmann, H., 2015. Fully coupled atmosphere-hydrology simulations for the central mediterranean: impact of enhanced hydrological parameterization for short and long time scales. J. Adv. Model. Earth Syst. 7 (4), 1693–1715.
Seneviratne, S.I., Donat, M.G., Pitman, A.J., Knutti, R., Wilby, R.L., 2016. Allowable CO2 emissions based on regional and impact-related climate targets. Nature 529 (7587), 477–483.
Seneviratne, S.I., Lüthi, D., Litschi, M., Schär, C., 2006. Land-atmosphere coupling and climate change in europe. Nature 443 (7108), 205–209.
Seneviratne, S.I., Nicholls, N., Easterling, D., Goodess, C.M., Kanae, S., Kossin, J., Luo, Y., Marengo, J., McInnes, K., Rahimi, M., 2012. Changes in climate extremes and their impacts on the natural physical environment. In: IPCC (Ed.), Managing the Risks of Extreme Events and Disasters to Advance Climate Change Adaptation. Cambridge University Press, Cambridge, UK, and New York, NY, USA, pp. 109–230.
Sharma, S., Mujumdar, P., 2017. Increasing frequency and spatial extent of concurrent meteorological droughts and heatwaves in India. Sci. Rep. 7 (1), 15582.
Sheffield, J., Wood, E.F., 2008. Projected changes in drought occurrence under future global warming from multi-model, multi-scenario, ipcc ar4 simulations. Clim. Dynam. 31 (1), 79–105.
Sheffield, J., Wood, E.F., Roderick, M.L., 2012. Little change in global drought over the past 60 years. Nature 491 (7424), 435–438.
Sippel, S., Zscheischler, J., Reichstein, M., 2016. Ecosystem impacts of climate extremes crucially depend on the timing. Proc. Natl. Acad. Sci. U.S.A. 113 (21), 5768–5770.
Sousa, P.M., Trigo, R.M., Aizpurua, P., Nieto, R., Gimeno, L., Garcia-Herrera, R., 2011. Trends and extremes of drought indices throughout the 20th century in the mediterranean. Nat. Hazards Earth Syst. Sci. 11 (1), 33–51.
Spinoni, J., Naumann, G., Vogt, J.V., 2017. Pan-european seasonal trends and recent changes of drought frequency and severity. Global Planet. Change 148, 113–130.
Spinoni, J., Vogt, J.V., Naumann, G., Barbosa, P., Dosio, A., 2018. Will drought events become more frequent and severe in europe? Int. J. Climatol. 38 (4), 1718–1736.
Szalai, S., Szinell, C., Zoboki, J., 2000. Drought monitoring in Hungary. In: WMO (Ed.), Early Warning Systems for Drought Preparedness and Drought Management, pp. 182–199. Geneva, Switzerland.
Teuling, A.J., Seneviratne, S.I., Stöckli, R., Reichstein, M., Moors, E., Ciais, P., Luyssaert, S., van den Hurk, B., Ammann, C., Bernhofer, C., Dellwik, E., Gianelle, D., Gielen, B., Grünwald, T., Klumpp, K., Montagnani, L., Moureaux, C., Sottocornola, M., Wohlfahrt, G., 2010. Contrasting response of european forest and grassland energy exchange to heatwaves. Nat. Geosci. 3 (10), 722–727.
Thornthwaite, C.W., 1948. An approach toward a rational classification of climate. Geogr. Rev. 38 (1), 55–94.
Toulios, L., Spiliotopoulos, M., Papadavid, G., Loukas, A., 2020. Observation methods and model approaches for estimating regional crop evapotranspiration and yield in agro-landscapes: a literature review. In: Mirschel, W., Terleev, V.V., Wenkel, K.-O. (Eds.), Landscape Modelling and Decision Support. Vol. 8 of Innovations in Landscape Research. Springer International Publishing, Cham, pp. 79–100.
Trenberth, K.E., Dai, A., van der Schrier, G., Jones, P.D., Barichivich, J., Briffa, K.R., Sheffield, J., 2014. Global warming and changes in drought. Nat. Clim. Change 4 (1), 17–22.
van Lanen, H.A., Laaha, G., Kingston, D.G., Gauster, T., Ionita, M., Vidal, J.-P., Vlnas, R., Tallaksen, L.M., Stahl, K., Hannaford, J., Delus, C., Fendekova, M., Mediero, L., Prudhomme, C., Rets, E., Romanowicz, R.J., Gailliez, S., Wong, W.K., Adler, M.-J., Blauhut, V., Caillouet, L., Chelcea, S., Frolova, N., Gudmundsson, L., Hanel, M., Haslinger, K., Kireeva, M., Osuch, M., Sauquet, E., Stagge, J.H., van Loon, A.F., 2016. Hydrology needed to manage droughts: the 2015 european case. Hydrol. Process. 30 (17), 3097–3104.
Vautard, R., Yiou, P., D'Andrea, F., de Noblet, N., Viovy, N., Cassou, C., Polcher, J., Ciais, P., Kageyama, M., Fan, Y., 2007. Summertime european heat and drought waves induced by wintertime mediterranean rainfall deficit. Geophys. Res. Lett. 34 (7), 3661.
Vicente-Serrano, S.M., Beguería, S., López-Moreno, J.I., 2010. A multiscalar drought index sensitive to global warming: the standardized precipitation evapotranspiration index. J. Clim. 23 (7), 1696–1718.
Vicente-Serrano, S.M., McVicar, T.R., Miralles, D.G., Yang, Y., Tomas-Burguera, M., 2020. Unraveling the influence of atmospheric evaporative demand on drought and its response to climate change. WIREs Climate Change 11 (2).
WMO, 2012. Standardized Precipitation Index: User Guide.
World Bank, 2014. Turn down the heat : Confronting the New climate normal. World Bank, Washington, DC. URL. https://openknowledge.worldbank.org/bitstream/10986/20595/3/9781464804373.pdf.
Wu, H., Svoboda, M.D., Hayes, M.J., Wilhite, D.A., Wen, F., 2007. Appropriate application of the standardized precipitation index in arid locations and dry seasons. Int. J. Climatol. 27 (1), 65–79.
Wu, X., Hao, Z., Hao, F., Li, C., Zhang, X., 2019. Spatial and temporal variations of compound droughts and hot extremes in China. Atmosphere 10 (2), 95.
Ye, L., Shi, K., Xin, Z., Wang, C., Zhang, C., 2019. Compound droughts and heat waves in China. Sustainability 11 (12), 3270.
Zhao, L., Xia, J., Xu, C.-Y., Wang, Z., Sobkowiak, L., Long, C., 2013. Evapotranspiration estimation methods in hydrological models. J. Geogr. Sci. 23 (2), 359–369.
Zscheischler, J., Orth, R., Seneviratne, S.I., 2017. Bivariate return periods of temperature and precipitation explain a large fraction of european crop yields. Biogeosciences 14, 3309–3320.
Zscheischler, J., Seneviratne, S.I., 2017. Dependence of drivers affects risks associated with compound events. Science advances 3 (6), e1700263.
Zscheischler, J., van den Hurk, B., Ward, P.J., Westra, S., 2020. Multivariate extremes and compound events. In: Sillmann, J., Sippel, S., Russo, S. (Eds.), Climate Extremes and Their Implications for Impact and Risk Assessment. Elsevier, Amsterdam, pp. 59–76.
Zscheischler, J., Westra, S., van den Hurk, B.J.J.M., Seneviratne, S.I., Ward, P.J., Pitman, A., AghaKouchak, A., Bresch, D.N., Leonard, M., Wahl, T., Zhang, X., 2018. Future climate risk from compound events. Nat. Clim. Change 8 (6), 469–477.

Chapter 3

Seasonal ecosystem vulnerability to climatic anomalies in the Mediterranean

Johannes Vogel, Eva Paton and Valentin Aich

Biogeosciences, 18, 5903–5927, https://doi.org/10.5194/bg-18-5903-2021, 2021

Biogeosciences, 18, 5903–5927, 2021
https://doi.org/10.5194/bg-18-5903-2021

Biogeosciences
Open Access

Seasonal ecosystem vulnerability to climatic anomalies in the Mediterranean

Johannes Vogel[1,2]**, Eva Paton**[2]**, and Valentin Aich**[3]

[1]Institute of Environmental Science and Geography, University of Potsdam, Potsdam, Germany
[2]Institute of Ecology, Technical University of Berlin, Berlin, Germany
[3]Global Water Partnership, Geneva, Switzerland

Correspondence: Johannes Vogel (joschavogel@uni-potsdam.de)

Received: 23 February 2021 – Discussion started: 8 March 2021
Revised: 4 October 2021 – Accepted: 11 October 2021 – Published: 17 November 2021

Abstract. Mediterranean ecosystems are particularly vulnerable to climate change and the associated increase in climate anomalies. This study investigates extreme ecosystem responses evoked by climatic drivers in the Mediterranean Basin for the time span 1999–2019 with a specific focus on seasonal variations as the seasonal timing of climatic anomalies is considered essential for impact and vulnerability assessment. A bivariate vulnerability analysis is performed for each month of the year to quantify which combinations of the drivers temperature (obtained from ERA5-Land) and soil moisture (obtained from ESA CCI and ERA5-Land) lead to extreme reductions in ecosystem productivity using the fraction of absorbed photosynthetically active radiation (FAPAR; obtained from the Copernicus Global Land Service) as a proxy.

The bivariate analysis clearly showed that, in many cases, it is not just one but a combination of both drivers that causes ecosystem vulnerability. The overall pattern shows that Mediterranean ecosystems are prone to three soil moisture regimes during the yearly cycle: they are vulnerable to hot and dry conditions from May to July, to cold and dry conditions from August to October, and to cold conditions from November to April, illustrating the shift from a soil-moisture-limited regime in summer to an energy-limited regime in winter. In late spring, a month with significant vulnerability to hot conditions only often precedes the next stage of vulnerability to both hot and dry conditions, suggesting that high temperatures lead to critically low soil moisture levels with a certain time lag. In the eastern Mediterranean, the period of vulnerability to hot and dry conditions within the year is much longer than in the western Mediterranean. Our results show that it is crucial to account for both spatial and temporal variability to adequately assess ecosystem vulnerability. The seasonal vulnerability approach presented in this study helps to provide detailed insights regarding the specific phenological stage of the year in which ecosystem vulnerability to a certain climatic condition occurs.

1 Introduction

Drought frequency and intensity are increasing in the Mediterranean, accompanied by rising temperatures and heat wave intensities (Perkins-Kirkpatrick and Gibson, 2017; Samaniego et al., 2018; IPCC, 2019; Tramblay et al., 2020). These climatic changes are linked to vulnerability of ecosystems in various ways, e.g. to reductions in forest growth and increasing tree mortality (Sarris et al., 2007, 2011) as well as extended fire risk (Sarris et al., 2014; Ruffault et al., 2018) and declining agricultural yields (Peña-Gallardo et al., 2019; Fraga et al., 2020). Furthermore, the ability to provide ecosystem services is impaired due to alterations in functioning and structure of Mediterranean ecosystems (Ogaya and Peñuelas, 2007; Peñuelas et al., 2017). Broad-scale vegetation shifts and replacement of species are projected, and ultimately desertification is expected in many Mediterranean regions (Gao and Giorgi, 2008; Zdruli, 2011; Feng and Fu, 2013; Liu et al., 2018).

The Mediterranean climate is characterised by great spatial and temporal variability, which makes the investigation of ecosystem impacts challenging. The Mediterranean Basin is marked by complex topography and is influenced

Published by Copernicus Publications on behalf of the European Geosciences Union.

by several large-scale atmospheric patterns (Lionello et al., 2006, 2012). Furthermore, the Mediterranean climate has an intricate seasonal cycle, alternating between water-limited conditions in summer and energy-limited conditions in winter (Spano et al., 2013). An assessment of ecosystem vulnerability in the Mediterranean therefore needs to account for both its spatial and temporal variability.

In this study, we build on the ecosystem vulnerability analysis proposed by van Oijen et al. (2013, 2014) and Rolinski et al. (2015), adapted with a focus on seasonal and multivariate impacts using remote sensing and reanalysis data. We enhance the ecosystem vulnerability concept with a focus on the seasonal timing of impacts. Ecosystem responses differ depending on the seasonal timing of the event (de Boeck et al., 2011; Smith, 2011; Sippel et al., 2016). Shifts of only a few weeks in drought occurrence can make the difference between negligible and detrimental impacts (Denton et al., 2017; Sippel et al., 2017, 2018). Even though accounting for seasonality is crucial in investigating climatic impacts on ecosystems, it is still often neglected (Piao et al., 2019). Studies are frequently limited to particular periods of interest within the year – usually a period of up to half a year centred around summer – when investigating seasonality (van Oijen et al., 2014; Baumbach et al., 2017; Nicolai-Shaw et al., 2017; Karnieli et al., 2019) but rarely investigate the seasonality year-round. In addition, combinations of climatic events in the seasonal cycle are seldom addressed (Smith, 2011; Hatfield and Prueger, 2015). Due to the pronounced land–atmosphere feedback mechanisms in the Mediterranean (Seneviratne et al., 2006; Green et al., 2017; Tramblay et al., 2020), it is particularly important to analyse the impacts of climatic anomalies in soil moisture and temperature jointly rather than in isolation (Mueller and Seneviratne, 2012). Such joint impacts of multiple stressors on ecosystems are still little researched (IPCC, 2019). Relationships between climatological and ecological variables at the tails of the distribution can show distinctly different behaviour compared to the findings based on conventional linear correlation, which makes it especially important to investigate the impact of climate anomalies on ecosystems, not only their mean behaviour (Jentsch et al., 2007; Reyer et al., 2013; Baumbach et al., 2017; Ribeiro et al., 2020).

Soil moisture is a particularly relevant variable for assessing the state of ecosystems as it is directly related to plant activity, biomass and agricultural yields (McWilliam, 1986; Sherry et al., 2008; Seneviratne et al., 2010; Zscheischler et al., 2013), especially in seasonally water-limited areas such as the Mediterranean (Szczypta et al., 2014). However, large-scale soil moisture data covering long time spans are scarce. Therefore, soil moisture proxies are applied in most cases, e.g. land surface models or drought indicators such as the standardised precipitation index (SPI) (Dorigo et al., 2017; Nicolai-Shaw et al., 2017). However, the SPI is primarily an indicator for meteorological droughts, which do not necessarily propagate into soil moisture droughts (de Boeck et al., 2011). Only a few studies use soil moisture data derived from satellite imagery because long-term coverage was not available until recently. Individual satellites do not cover sufficiently long time spans, but long-term coverage can be achieved by merging soil moisture data from several satellites. The European Space Agency's Climate Change Initiative (ESA CCI) soil moisture data set provides a unique, globally consistent multi-decadal time series based on several active and passive microwave sensors (Dorigo and de Jeu, 2016; Dorigo et al., 2017). It was first published in 2012 and has continuously improved since (Dorigo et al., 2017). It has proven capability to assess land–vegetation–atmosphere dynamics (de Jeu and Dorigo, 2016; Dorigo and de Jeu, 2016; Nicolai-Shaw et al., 2017; Gruber et al., 2019). So far, satellite-based soil moisture data are still rarely used in ecosystem research (Dorigo et al., 2017), and Rolinski et al. (2015), for example, point out the need to use observational data in the assessment of ecosystem vulnerability. Therefore, we seek to put greater emphasis on the possibilities arising from newly available remote sensing products within the last years. In addition, we also performed the analysis using the soil moisture product from the ERA5-Land reanalysis data set. The fraction of absorbed photosynthetically active radiation (FAPAR) is used as an indicator of ecosystem productivity in our study. The FAPAR is crucial for monitoring climatic impacts on terrestrial ecosystems and is directly related to the photosynthetic activity of vegetation and thus to its greenness and health (Potter et al., 2003; Gobron et al., 2010; Ivits et al., 2016). Vegetation indices such as the normalised difference vegetation index (NDVI) are closely related to the FAPAR and can be seen as proxies (Myneni and Williams, 1994; Pinty et al., 2009).

This study aims to quantify ecosystem vulnerability by assessing which combinations of climatic drivers lead to extreme reductions in ecosystem productivity in the Mediterranean Basin using a bivariate vulnerability analysis with a specific focus on seasonal variations. Soil moisture and temperature are investigated as climatic drivers, and the FAPAR is used to assess the ecological response. Furthermore, ecosystem vulnerability is calculated separately by land cover class and subregion to account for the spatial complexity of the Mediterranean Basin.

2 Methods

2.1 Study area

The study area is constrained to all grid points in the Mediterranean Basin belonging to the Köppen–Geiger classes Csa ("warm temperate climate with dry and hot summer") and Csb ("warm temperate climate with dry and warm summer"; cf. Fig. 1) to ensure a certain level of comparability within the study area. Furthermore, the study area is subdivided into land cover classes and subregions. The land cover classes

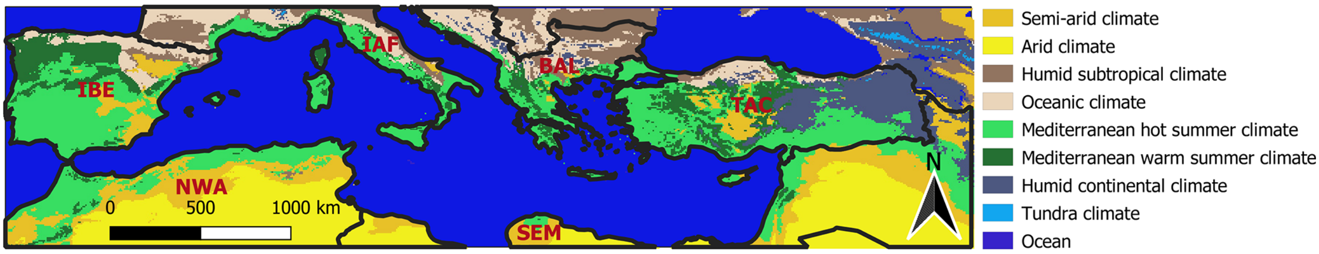

Figure 1. Study area in the Mediterranean Basin: the Köppen–Geiger climate categories "Mediterranean hot summer climate" (light green) and "Mediterranean warm summer climate" (dark green) are included in this study. The study area was divided into six subregions: the Iberian Peninsula (IBE), Italy and France (IAF), the Balkan Peninsula (BAL), Turkey and Cyprus (TAC), the south-eastern Mediterranean (SEM), and north-western Africa (NWA)

were aggregated according to Table B1 using the ESA CCI land cover classification map of 2018. Grid points where the land cover changed between 1999 and 2018 were excluded in this study as well as grid points belonging to the land cover classes "water bodies'' and "urban areas''. The countries belonging to each subregion are listed in Table B2.

2.2 Data

Daily satellite-based soil moisture data from ESA CCI were obtained at a resolution of 0.25° from 1978–2019 (Gruber et al., 2019). The merged data set (v04.7), containing data from both active and passive sensors, is used. The quality of this data set has continuously improved over the years due to the incorporation of an increasing number of satellites (Dorigo et al., 2017). The data set is representative of the topsoil surface layer of up to 2 cm thickness (Kidd and Haas, 2018). Monthly air temperature and soil moisture reanalysis data are retrieved from ERA5-Land produced by the European Centre for Medium-Range Weather Forecasts (ECMWF) at a resolution of 9 km from 1981–2019 (Muñoz-Sabater, 2019). The three soil moisture layers corresponding to the depths 0–7, 7–28 and 28–100 cm are used in the analysis. This study is conducted using the ESA CCI soil moisture data set as well as the ERA5-Land soil moisture data set to verify the robustness of our results. The FAPAR is obtained from the Copernicus Global Land Service (CGLS) (Baret et al., 2013; Verger et al., 2014). It is derived from SPOT/VGT from 1999–2013 and PROBA-V from 2014–2019 and is provided in 10 d steps (Verger et al., 2019). Furthermore, the ESA CCI land cover classification for the years 1999 and 2018 with a spatial resolution of 300 m (v2.1.1) was used (ESA, 2017). The Köppen–Geiger classification map was acquired from Kottek et al. (2006) and Rubel et al. (2017).

2.3 Data preprocessing

All data sets are resampled to a common spatial and temporal resolution of 0.25° and a monthly time step, respectively. The investigated time span encompasses 21 years from 1999–2019. Grid points with more than 60 months of missing soil moisture data within the period from 1999–2019 were excluded from this study (see Fig. 2). These are primarily grid points located close to the coast. In a next step, all variables are deseasonalised by subtracting the annual cycle to account for extremeness relative to the respective time of the year. The variables are z-transformed by subtracting the monthly mean and dividing by the year-round standard deviation of the deseasonalised time series (Eq. 1); z-score transformation allows for a direct comparison of values despite their different physical units (Orth et al., 2020).

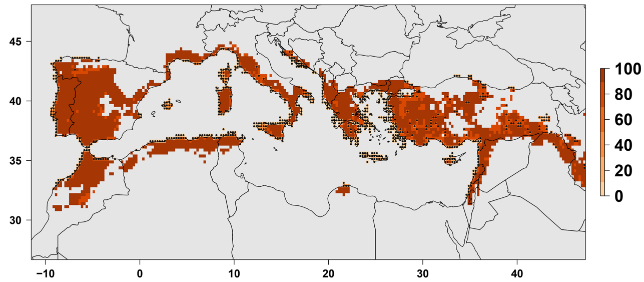

Figure 2. Percentage of available monthly soil moisture values from 1999–2019. All grid points excluded from this study are marked with a dot.

$$z_i = \frac{X_i - \mu_{i,\text{month}}}{\sigma_i} \tag{1}$$

The impact of environmental drivers on ecosystems may show a time lag of up to a few months – so-called "legacy effects" (von Buttlar et al., 2018; Piao et al., 2019). Hence, a moving average of 3 months $n = 3$ is applied to the environmental driver variables env temperature and soil moisture; i.e. the preceding 2 months are included with equal weight for each monthly time step i in the time span of $m = 21$ years (Eq. 2) to account for lagged effects.

$$\text{env}_i = \frac{1}{n} \sum_{k=i-2}^{i} \text{env}_k \text{ for } i \in (1, \ldots, m \times 12) \tag{2}$$

2.4 Derivation of ecosystem vulnerability

In the context of our study, ecosystem vulnerability depicts if ecosystems are susceptible or sensitive to a certain hazard. It allows states of low ecosystem productivity to be attributed to certain climatic conditions by linking such states to corresponding deviations in temperature and soil moisture. The terminology on ecosystem vulnerability is confusing since several partially ambiguous terms exist due to the concept being still rather new in ecological research (van Oijen et al., 2013; Weißhuhn et al., 2018). Following the definition by Rolinski et al. (2015), "ecosystem vulnerability V_E is the average deviation of the environmental variable under hazardous ecosystem conditions from values under non-hazardous ecosystem conditions" in our approach. Here, the environmental variable env is either temperature or soil moisture, respectively, and the ecosystem variable sys is the FAPAR. Ecosystem vulnerability V_E is calculated according to Eq. (3) as the difference in the expectation value E_{nonhaz} of the environmental variable env under non-hazardous conditions of the ecosystem variable sys and the respective value E_{haz} under hazardous conditions of the ecosystem variable sys (van Oijen et al., 2013; Rolinski et al., 2015).

$$V_E = E(\text{env}|\text{sys nonhaz}) - E(\text{env}|\text{sys haz}), \qquad (3)$$

with conditional expectational values defined following Eq. (4):

$$E(\text{env}|\circ) = \int \text{env}\,\mathbb{P}(\text{env}|\circ)\,\text{d}\,\text{env}, \qquad (4)$$

where $\mathbb{P}$ is the probability of env under the specified condition $\circ$ (sys nonhaz or sys haz). The probability of hazard occurrence $\mathbb{P}_H$ is given by the number of data points under hazardous conditions N_{haz} divided by the total number of data points N, which gives $\mathbb{P}_H = N_{\text{haz}}/N$. The discrimination threshold between non-hazardous and hazardous ecosystem conditions is set as the 10th percentile of the FAPAR values for each grid point individually; i.e. $\mathbb{P}$(sys haz) is fixed to 0.1 in this study. Such a threshold is commonly used in ecoclimatological studies (Ahlström et al., 2015; Baumbach et al., 2017; Nicolai-Shaw et al., 2017). To investigate the robustness of our results, we also performed the analysis using the 5th and 15th percentile for discrimination of hazardous and non-hazardous ecosystem conditions. The spatial and temporal patterns for these cases were in agreement with the 10th percentile chosen in our study (results not shown), which indicates that our results are not sensitive to the choice of the percentile. Every grid point has the same number of months with hazardous ecosystem conditions; i.e. the same risk of exceeding the threshold is assumed uniformly for all grid points.

We used the Mann–Whitney U test to investigate significant deviations in climatic conditions during non-hazardous and hazardous ecosystem conditions, which was adjusted for multiple testing using the Benjamini and Hochberg (1995) correction. Significant positive values indicate ecosystem vulnerability V_E to cold (dry) conditions for the climatic driver temperature (soil moisture). Similarly, significant negative values are associated with vulnerability to hot (wet) conditions. In the case of two climatic drivers, this leads to nine possible vulnerability conditions (see Fig. 3). The corresponding p values are not shown throughout the article due to the large number of data. A schematic display of the calculation of ecosystem vulnerability V_E is given in Fig. 4 for an exemplary grid point with vulnerability to hot and dry conditions for the month of July. The two drivers temperature and soil moisture are assessed for their effects on ecosystem vulnerability. In this example, the average temperature in July during non-hazardous ecosystem conditions E_{nonhaz} is lower than the average during hazardous ecosystem conditions E_{haz}, leading to a negative vulnerability to temperature, i.e. vulnerability to hot conditions (Fig. 4a). For soil moisture, the average soil moisture during non-hazardous ecosystem conditions E_{nonhaz} is higher than soil moisture during hazardous conditions E_{haz}; therefore vulnerability is positive, indicating vulnerability to dry conditions (Fig. 4b). Our approach is impact-based; i.e. it focusses on the extremeness of the impact rather than the extremeness of the driver as this enables relating multiple drivers to a single outcome (Zscheischler et al., 2014, 2018). According to the framework by Smith (2011), vulnerability to extreme climatic events is defined as a climate extreme leading to an extreme ecological response. Therefore, our definition differs in that regard in that it comprises extremeness only for the ecological response, not necessarily for the climatic driver. The definition used here is broader than the one by Smith (2011) because it includes significant deviations in

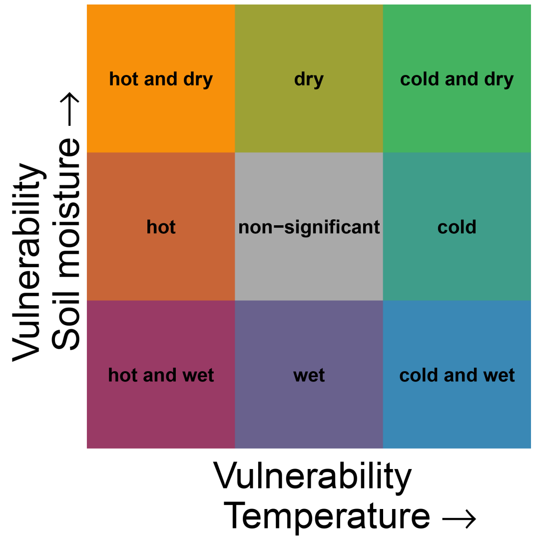

Figure 3. Illustration of the vulnerability to all potentially occurring climatic conditions.

the driver variable in general, not only extremes. In our case, ecosystem vulnerability rather shows if the ecosystem variable is susceptible to certain climatic conditions (which do not need to be extreme). The analysis was carried out using R version 3.6 and Climate Data Operators (CDO) version 1.9 (Schulzweida, 2019; R Core Team, 2020).

3 Results

3.1 Ecosystem vulnerability by land cover

Figure 5 displays the ecosystem vulnerability to soil moisture and temperature for each land cover class and each month of the year as well as the corresponding statistical significance indicated by the background colour (see explanation in Fig. 3). The vulnerability to temperature and soil moisture can be summarised into three major regimes during the course of the year (see Fig. 5). From May to July, the vegetation is especially prone to hot and dry conditions. From August to October, there is a shift to a vulnerability to cold and dry conditions in general. Finally, from November to April cold and wet conditions are usually associated with high vulnerability of the vegetation. There are sharp transitions in ecosystem vulnerability from April to May, from July to August, and from October to November for most land cover classes.

In the period from November to March the vast majority of land covers are vulnerable to cold conditions. From March to May there is a transition phase from cold to hot conditions. While in March almost all land covers are vulnerable to cold conditions, in April only four of them still remain vulnerable ("forest (broadleaved)", "forest (needleleaved)", " mixed" and "shrubland"), and none are vulnerable in May, when the majority shift to vulnerability to hot conditions. In summer, a period with significant vulnerability to hot conditions only precedes the next phase of vulnerability to both hot and dry conditions, e.g. for "crops (rainfed)" and "grassland", indicating that the heat desiccates the soil first until it reaches critically low soil moisture levels in the following months. The cycle reverses around July and August. While four land cover classes are still vulnerable to hot conditions in July, none of the classes are in August. Vulnerability to high temperatures is almost entirely restricted to the period from May to July. From August to October, most land cover classes exhibit vulnerability to cold and dry conditions, and from midsummer to the beginning of autumn almost all land cover classes are prone to drought. In the following period from November to March, cold and wet conditions prevail on average. The vulnerability to wet conditions is highest from November to January, whereas many land cover classes are insensitive to soil moisture during most of the time from February to May. Exemptions are, for example, " forest (broadleaved)", "crops (rainfed)" and "mixed", where low ecosystem productivity coincides with wet conditions, e.g. in March to April.

The vulnerability to hot conditions of "grassland" is 1 month ahead of most other land classes, starting already in April. This could indicate a faster response of this land cover class to environmental drivers than other land cover classes. Sparse vegetation is probably well adapted to high temperatures as it never shows vulnerability to hot conditions, which means that temperature during extreme ecosystem conditions is not significantly higher than during non-extreme ecosystem conditions. It also never coincides with significantly wet conditions, which might point out that transpiration in these areas is never so high that it could contribute substantially to the desiccation of the soil, and thus its influence on soil moisture is negligible.

3.2 Ecosystem vulnerability by subregions

Similarly to Fig. 5, ecosystem vulnerability for each subregion is shown in Fig. 6. There is more variability than regarding land cover classes, and the general pattern of most land cover classes with a "hot and dry" regime followed by a "cold and dry" regime and subsequently by a "cold and wet" regime does not hold true for most of the Mediterranean subregions. The vulnerability to soil moisture usually peaks during summer or autumn and reaches a minimum in spring or winter – exceptions are Italy and France as well as the south-eastern Mediterranean. The yearly development of vulnerability to temperature is characterised by a minimum around late spring or summer.

There is an extended period of time in which ecosystems are prone to hot conditions from March to October in Turkey, whereas in other regions this period often only lasts for 2 to 3 months in spring and summer. North-western Africa and the south-eastern Mediterranean are prone to dry conditions 9 and 8 months of the year, respectively, indicating that these regions are usually soil-moisture-limited. Italy and France have the lowest sensitivity to soil moisture, with only small deviations from zero. Nevertheless, these deviations are significant for half of the months in the year. Interestingly, the Balkan Peninsula is never prone to hot conditions. Outside of the summer season, wet conditions particularly coincide with low ecosystem productivity in Italy and France, the Balkans, and the Iberian Peninsula.

The number of events per month is not equally distributed throughout the year. There is a decline from June to November with a minimum usually around September in which only few events are detected. This reflects the time span of the dormant season since these months are usually too dry for ecosystem activity. There are some notable exceptions for land covers involving trees ("forest (broadleaved)", "forest (needleleaved)", 'mixed" and "crops (irrigated)") (see Fig. 5) as well as the northernmost subregions of the Mediterranean, Italy and France, and the Balkan Peninsula (see Fig. 6), where the number only decreases slightly during this period.

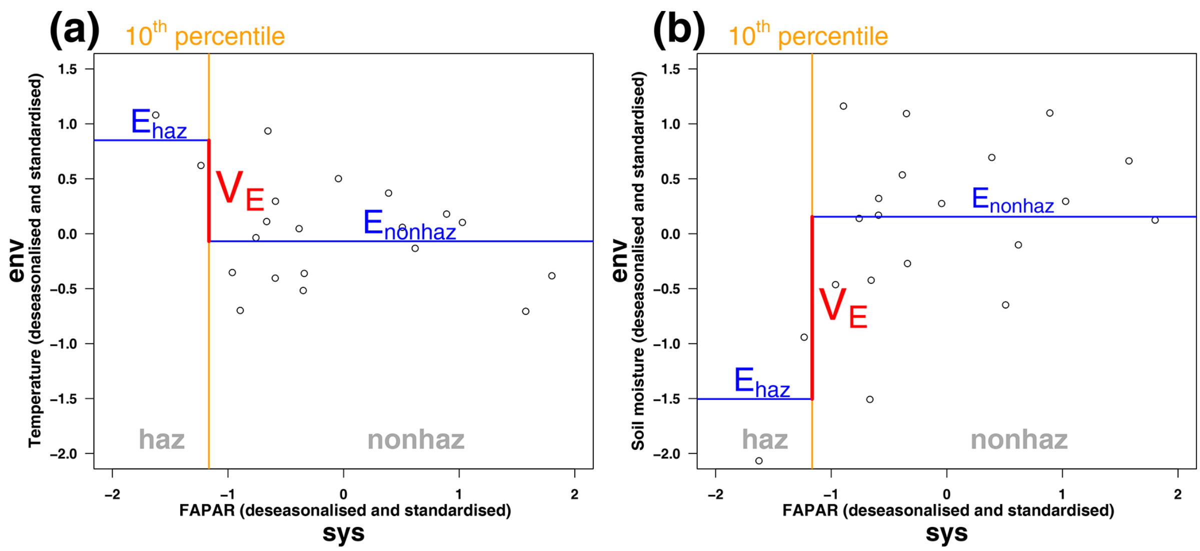

Figure 4. Schematic display of ecosystem vulnerability V_E for an exemplary grid point for **(a)** temperature and **(b)** soil moisture as environmental drivers for the month of July.

These land cover classes and subregions are less affected by the characteristic dry period in summer. Forests have better access to soil moisture because they develop deeper roots (Bréda et al., 2006; Zhang et al., 2016), whereas irrigated areas obviously have an external water supply. The northern subregions are also moister than the southern Mediterranean.

Satellite-derived soil moisture data sets are prone to uncertainty, even though there have been considerable improvements in the last years (Gruber et al., 2019). Therefore, ecosystem vulnerability was also assessed for all land cover classes and subregions using soil moisture layers at 0–7, 7–28 and 28–100 cm depth from the ERA5-Land reanalysis data set and compared to results obtained from the ESA CCI soil moisture product to verify the robustness of our results and whether specific biases are apparent (see Appendix A). Furthermore, certain land cover classes and subregions encompass a relatively small subset of grid points, and thus non-significant ecosystem vulnerability might be related to data scarcity in some of these cases.

The spatial patterns of ecosystem vulnerability are displayed for four exemplary months of the year (see Fig. 7), whereas all 12 months can be found in the Appendix (see Fig. B1). In March in most western Mediterranean regions, low FAPAR values are associated with cold and wet conditions (blue colouring), whereas in the eastern Mediterranean vulnerability to hot conditions (purple and orange colouring) are already emerging at this time of the year. In June, almost all regions are vulnerable to hot conditions and often also to dry conditions (purple and orange colouring), with exceptions in the northernmost regions such as the French Riviera as well as mountainous regions such as the Peloponnese in Greece and the High Atlas in central Morocco. In September, there are often no low FAPAR anomalies occurring (black colouring), particularly in southern and inland regions, which are the hottest regions of the Mediterranean. The reason for this is that this time usually corresponds to the dormant season in these areas. In regions where events are detected during this time of the year, vulnerability to cold and dry conditions (green colouring) prevails in most of the Mediterranean. In December, in most areas in the central Mediterranean, low FAPAR values coincide with cold and wet conditions (blue colouring), whereas in central Turkey and the southern Iberian Peninsula, vulnerability to hot conditions (purple and orange colouring) occurs. It is noteworthy that for a given grid point at a given month, only 21 observations are available. Therefore, the robustness of the magnitude of ecosystem vulnerability of individual grid points is limited and should thus be interpreted with care. The maps in Figs. 7 and B1 primarily aim to identify large-scale spatial patterns but do not provide information on statistical significance at a grid point scale.

4 Discussion

4.1 Interpretation of temporal and spatial patterns in the Mediterranean

Our findings are in accordance with the characteristics of the Mediterranean climate regime, which is primarily energy-limited during winter and soil-moisture-limited during summer (Schwingshackl et al., 2017). The vulnerability analysis allows a more detailed investigation of the changes in ecosystem vulnerability to soil moisture and temperature throughout the course of the year for different land cover classes and subregions. In a wet regime, ecosystem activ-

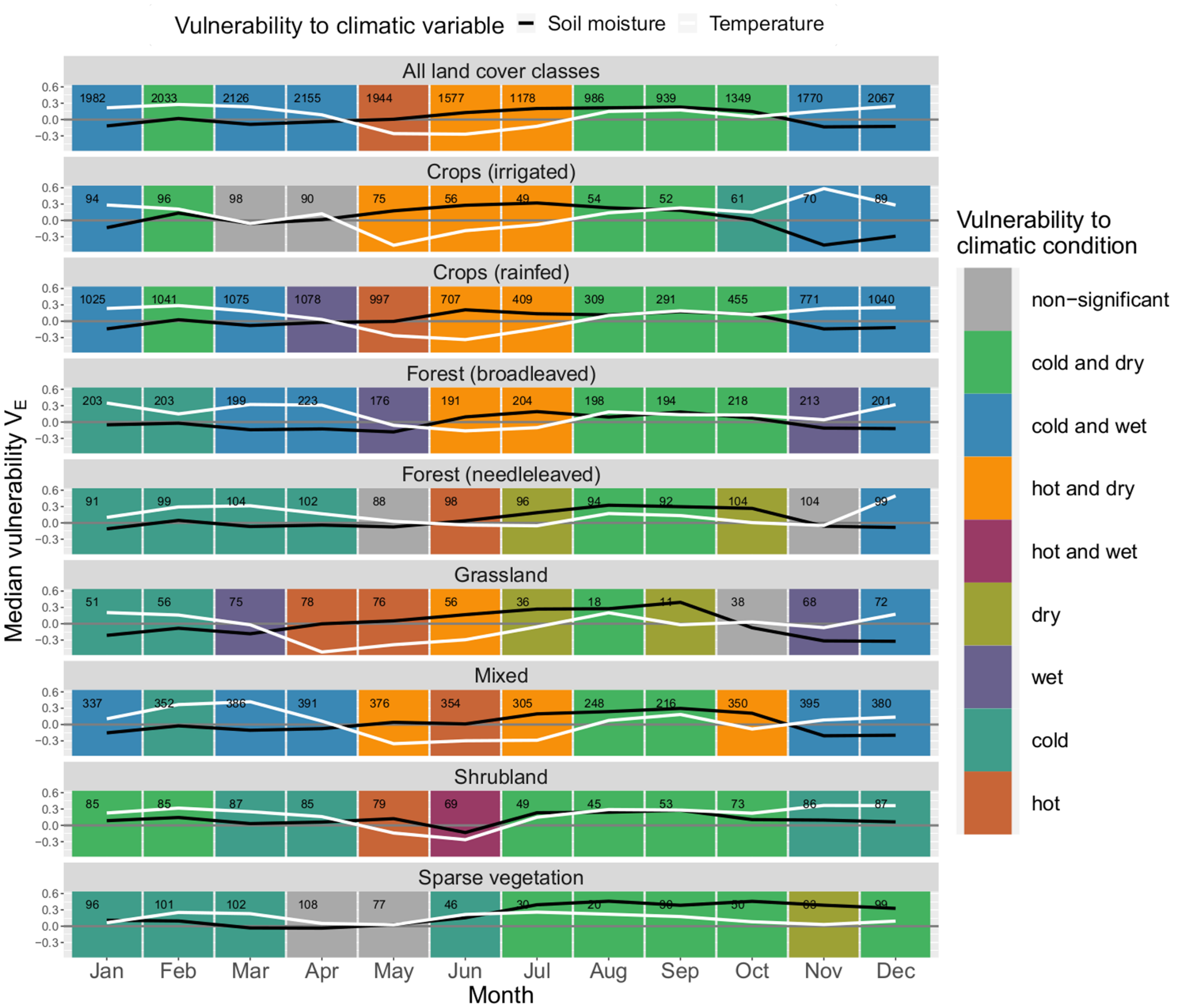

Figure 5. Median monthly ecosystem vulnerability per land cover: vulnerability to temperature (ERA5-Land) is shown in white, and vulnerability to soil moisture (ESA CCI) is shown in black for each month of the year (columns) for each land cover (rows). Months with statistically significant deviation in climatic drivers during non-hazardous and hazardous ecosystem conditions according to the Mann–Whitney U test based on a significance level $\alpha = 0.05$ are shown in colour (see legend); all other months are shown in grey. The number of grid points in which an event has occurred in this month and land cover within the period 1999–2019 is shown in the upper left corner of each panel.

ity is energy-limited, depending primarily on temperature and radiation, whereas in a transitional or dry system, soil moisture content is reduced, and thus ecosystem activity is water-limited (Seneviratne et al., 2010; Zscheischler et al., 2015). From May to July, the Mediterranean is often vulnerable to hot and dry conditions, which is a typical feature of a soil-moisture-limited regime (Seneviratne et al., 2010). Heat waves are a frequent characteristic of the Mediterranean summer (Conte et al., 2002) and are often connected to persistent anti-cyclonic regimes and droughts (Mueller and Seneviratne, 2012; Ulbrich et al., 2012). The vulnerability to dry conditions in autumn indicates that moisture reservoirs are often still depleted after the summer, impairing the onset of the next vegetation cycle. By contrast, plant growth is inhibited by too-low temperatures in autumn, which distinguishes it from the antecedent summer period. The general transition to vulnerability to cold conditions already in August is astonishing. However, it should be noted that especially for the warmer regions – e.g. north-western Africa, Turkey and the interior of Spain – either vulnerability to hot conditions prevails or no FAPAR anomalies are detected during this time (see Figs. 6 and B1) because August is outside of the growing season and the FAPAR values are usually at their annual minimum at this time of the year. During the phase of the water-limited regime, soil moisture depletion in combination with high atmospheric evaporative demand leads to plant water stress and can ultimately cause plant mortality due to hydraulic failure or carbon starvation

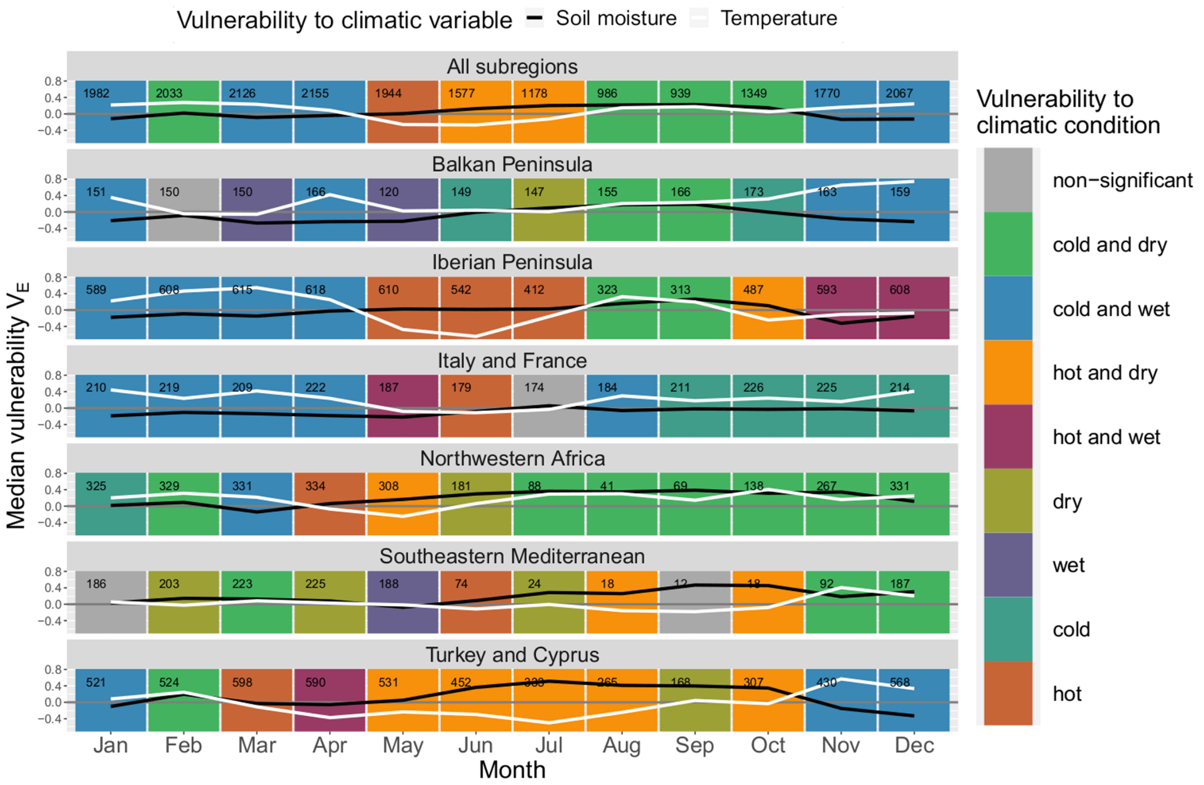

Figure 6. Median monthly ecosystem vulnerability per subregion: vulnerability to temperature (ERA5-Land) is shown in white, and vulnerability to soil moisture (ESA CCI) is shown in black for each month of the year (columns) for each land cover (rows). Months with statistically significant deviation in climatic drivers during non-hazardous and hazardous ecosystem conditions according to the Mann–Whitney U test based on a significance level $\alpha = 0.05$ are shown in colour (see legend); all other months are shown in grey. The number of grid points in which an event has occurred in this month and subregion within the period 1999–2019 is shown in the upper left corner of each panel.

(van der Molen et al., 2011; Vicente-Serrano et al., 2020). As a coping strategy, plants, for example, reduce stomatal conductance to avoid hydraulic failure due to water loss by leaf transpiration, which consequently leads to reduced carbon uptake and thus decreased photosynthetic activity (van der Molen et al., 2011; Reichstein et al., 2013; Piao et al., 2019; Vicente-Serrano et al., 2020). The vulnerability to cold conditions in most months from November to April confirms that ecosystems are energy-limited in this period and is probably related to frost damage during cold spells. Related to the Cyprus Low, cold spells often co-occur with heavy precipitation in the eastern Mediterranean during this time (de Luca et al., 2020). Presumably, wet conditions only coincide with cold conditions but are not damaging ecosystems as such. However, vulnerability of crops to wet conditions in winter was observed, for example, on the Iberian Peninsula in a study by Páscoa et al. (2017). While ecosystem activity in the northern Mediterranean is low during winter, this does not hold true for the southern Mediterranean; e.g. for some regions in Tunisia the NDVI peaks as early as December (Le Page and Zribi, 2019). Cloudiness during precipitation leads to reduced solar radiation and consequently lower surface temperature (Berg et al., 2015). This way, cold and wet conditions can lead to low transpiration rates of plants accompanied by low photosynthetic activity, leading to reduced extraction of soil moisture during that time period (Zscheischler et al., 2015). This highlights the bidirectional relation between vegetation and soil moisture; i.e. not only is the state of the vegetation dependent on soil moisture but also vice versa. This mutual linkage is neglected in many studies (Dorigo et al., 2017).

Energy-limited regimes merge gradually into water-limited regimes from Scandinavia southwards to the Mediterranean in Europe (Teuling et al., 2009). Karnieli et al. (2019) investigated the relationship of the NDVI and land surface temperature at the European scale, hypothesising that a positive relationship indicates an energy-limited condition and a negative one a water-limited condition. Our results are mostly in agreement with the findings of their study that temperature and the NDVI are comprehensively negatively related in summer in Mediterranean Europe, whereas in spring this is only the case in the southernmost regions of Mediterranean Europe, while in other areas either neutral or negative relationships prevail. According to Le Page and Zribi

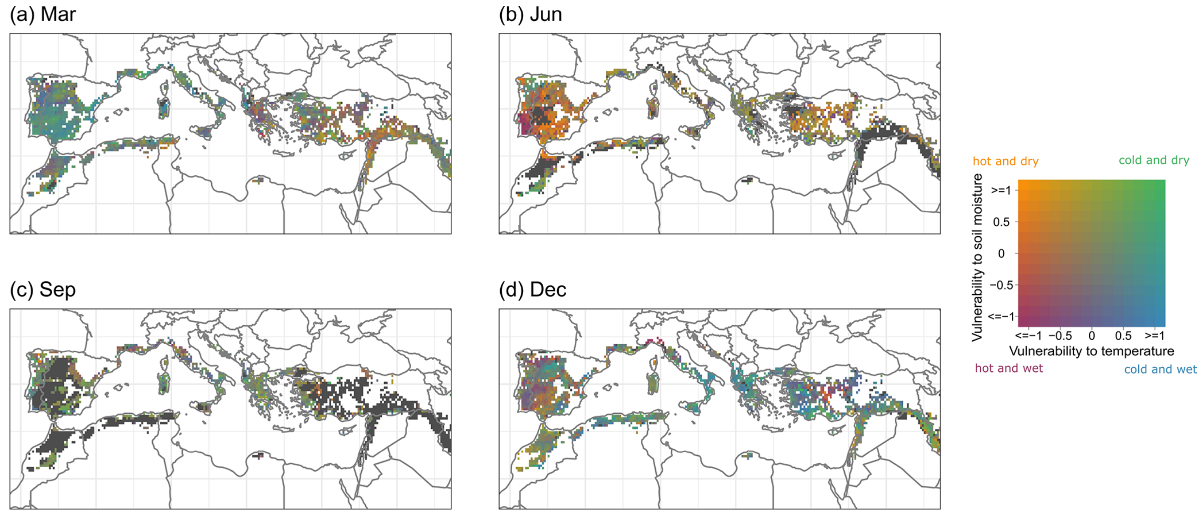

Figure 7. Average monthly vulnerability to soil moisture (ESA CCI) and temperature (ERA5-Land) in the Mediterranean Basin for **(a)** March, **(b)** June, **(c)** September and **(d)** December. Grid points without any events during the respective month are displayed in black.

(2019), temperature and the NDVI are always negatively correlated in north-western Africa, while soil moisture and the NDVI are positively correlated. This indicates that this region is soil-moisture-limited year-round, which is in good agreement with our results obtained using the ESA CCI soil moisture data set. However, the ERA5-Land soil moisture data set exhibits vulnerability to wet conditions in north-western Africa in several months of the year, which might indicate lower suitability of this reanalysis data set to represent the soil moisture conditions in this region (see Figs. 6 and A2).

Extreme ecosystem impacts are not always connected to climatic extremes but can also be caused by a combination of concurrent moderate climatic drivers (Pan et al., 2020; van der Wiel et al., 2020). Furthermore, extreme ecosystem impacts are not solely related to soil moisture and temperature anomalies. Other potential causes are, for example, windthrow, pest outbreaks and fires, which often exhibit synergistic effects in combination with droughts and heat waves (Gouveia et al., 2012; Reichstein et al., 2013; Batllori et al., 2017; Ruffault et al., 2018). Furthermore, many ecosystems are managed, which also affects ecosystem productivity (Smit et al., 2008). These additional drivers should be taken into consideration when interpreting the results of this study.

The impact of climate extremes on ecosystems depends highly on their timing (Smith, 2011; Wolf et al., 2016; Piao et al., 2019). The sensitivity to heat varies with phenophase (Hatfield and Prueger, 2015), and the effect on the carbon cycle can differ seasonally. High temperatures might, for example, increase carbon uptake by advancing spring onset but may lead to uptake reductions in summer (Piao et al., 2019). In the same way, droughts can either accelerate the phenological cycle or inhibit plant productivity, and their impact on vegetation is strongly connected to the seasonal variations in the water balance (Spano et al., 2013; Gouveia et al., 2017). The highest detrimental impacts on ecosystems by droughts in the Mediterranean have been reported at the beginning of the year at the peak of the growing season (Ivits et al., 2016; Peña-Gallardo et al., 2019). The drought and heat wave in 2003 were comparably not that harmful to Mediterranean ecosystems as they occurred in August, which is outside the main growing season (Ivits et al., 2016). The approach presented in this study helps to gain a better understanding of which stages of the year are vulnerable to which climatic condition. To our knowledge, none of the previous studies which applied the framework for ecosystem vulnerability accounted for the effects of seasonality so far. However, ecosystem responses are highly sensitive to the timing of events; therefore, it is crucial to consider this.

Climate change leads to seasonal shifts, which already becomes apparent in the strong phenological changes in the Mediterranean (Menzel et al., 2006; Gordo and Sanz, 2009, 2010). For example, higher temperatures lead to increased ecosystem productivity and subsequently higher evapotranspiration earlier in the growing season. Due to this, soil moisture is depleted faster, and therefore more energy is transferred into sensible heat instead of latent heat. As a consequence of these hot and dry conditions, the growing season might end prematurely (Seneviratne et al., 2010; Lian et al., 2020). The time series used here encompasses 21 years and is thus still too short for analysing long-term trends. Nevertheless, our approach can potentially be used to monitor how vulnerability changes in future for all 12 months of the year by comparing vulnerability during different multi-year time spans if time series of sufficient length are available. Hot and dry days are getting more persistent in summer, and unprecedented heat waves associated with Saharan warm air intrusions have occurred within the last years (Sousa et al., 2019; de Luca et al., 2020). Nevertheless, droughts and warm spells are increasing in spring as well (Vogel et al., 2021), which can have detrimental implications for the Mediterranean ecosystems as spring is the main growing season. With temperature increases in future, vulnerability to cold conditions might be constrained to a shorter time frame, whereas the time span with vulnerability to hot conditions might expand within the year. Increasing aridity is projected in the Mediterranean, especially during winter and spring (Samaniego et al., 2018), while at the same time heavy precipitation events are projected to increase (Toreti and Naveau, 2015). Thus, it remains difficult to determine how vulnerability to dry and wet conditions will evolve in future.

4.2 Potential limitations of the methodological procedure

The presented method depends heavily on the quality of the employed data types for both the two drivers and the impact proxy. Several limitations regarding moisture data are well known; e.g. the coarse spatial resolution impairs assessments at local scales. Furthermore, satellite-based soil moisture is limited to the retrieval of surface soil moisture, while deeper-reaching root-zone soil moisture is the actual ecologically relevant variable. Satellite-based soil moisture is only representative of the first 2–5 cm of the soil layer. The root zone of plants is usually deeper, which reduces the explanatory power of satellite-based soil moisture for drought impacts on ecosystems (Liu et al., 2016; Dorigo et al., 2017; West et al., 2019). For example, soil drying during summer affects primarily the top soil layer, while drying in deeper layers shows a lagged response because upward capillary flow from these layers is comparatively slow (Berg et al., 2017). Nicolai-Shaw et al. (2017) found that soil moisture data from ESA CCI were a good indicator for drought in grasslands, while forests exhibited weaker responses, probably due to access to deeper soil layers for forests compared to grasslands. However, we also assessed vulnerability to soil moisture at the depths 0–7, 7–28 and 28–100 cm using reanalysis data from ERA5-Land, and the patterns obtained at the deeper layers 7–28 and 28–100 cm are in large part similar to the ones of the layer at 0–7 cm (see Appendix A). This indicates that the assessment of the top soil layer is able to yield results which are valid for a larger proportion of the soil column. Coupling of land surface models with satellite-based surface soil moisture can further enhance knowledge on the status of root-zone soil moisture in future (Dorigo et al., 2017; Tramblay et al., 2020). Furthermore, it should be noted that validations of the ESA CCI soil moisture data set with in situ observations from Mediterranean sites in Spain, France and Turkey showed high agreement (Albergel et al., 2013; Dorigo et al., 2015; Bulut et al., 2019). Also the FAPAR product from the CGLS has been validated with observation data from Tunisia, Italy, Spain and France, primarily for a variety of crop types as well as a deciduous broadleaf forest in Italy and a needleleaf forest in Spain (Fuster et al., 2020). The FAPAR is often assumed to be directly linked to productivity. However, droughts might lead to physiological changes such as stomata closure, which are not apparent in the spectral characteristics of the canopy and thus in the FAPAR but nevertheless invoke a decreased productivity. This was the case, for example, in forest ecosystems during the drought-and-heat-wave event in 2003 in Europe (Reichstein et al., 2007; Zhang et al., 2016).

The Mediterranean Basin is characterised by large spatial variability because of its complex topography (Lionello et al., 2006). The relatively coarse resolution of the ESA CCI soil moisture data set is currently limiting the representation of this high spatial complexity (Crocetti et al., 2020). Many land cover classes express similar patterns over the course of the year according to our results. This could potentially indicate that grid points are sometimes not homogeneous enough but rather represent a mixture of several land cover classes due to the coarse resolution of 0.25°. The ESA CCI land cover product applied in this study is a state-of-the-art data set; a more detailed data set is currently not available for the Mediterranean Basin as a whole. The ESA CCI land cover classification allows only for the differentiation of major plant functional types, and future studies might benefit from a more refined land cover classification scheme with a broader variety of land cover classes. Furthermore, the subregions used in this study are not fully homogeneous, and there is a certain variability within a given subregion. Thus, the patterns identified in this study (see Figs. 5 and 6) cannot always be inferred for an entire subregion. Therefore, the ecosystem vulnerability maps (Figs. 7 and B1) should be additionally examined for the identification of potentially deviating patterns within subregions.

Many studies do not consider lagged effects in their design and the choice of a suitable timescale to account for such effects is not trivial and under debate (Zeng et al., 2013; Ivits et al., 2016). Response time varies depending on the type of event and the affected ecosystem. The response lag of vegetation is land-cover-specific as plants have various regulatory physiological functions to react to changes in soil moisture such as stress memory, water storage and stabilisation activities at the community level (van der Molen et al., 2011; Niu et al., 2014; Zhang et al., 2017). Faster response times to droughts are observed for pasture and crops compared to shrubs and forests (Chen et al., 2014; Bachmair et al., 2018). Generally, responses to drought are slower in semi-arid and sub-humid biomes compared to arid biomes (Vicente-Serrano et al., 2013). A study by Ivits et al. (2016) at the European scale found that vegetation in the Mediterranean responds slowly to meteorological droughts compared to most other European regions. Impacts on vegetation by meteorological and soil moisture droughts are often largest within the preceding 1 to 2 months (Zeng et al., 2013; Chen et al., 2014; Wu et al., 2015; Papagiannopoulou et al., 2017; Bachmair et al., 2018), which is the reason we decided on a 3-month timescale in the moving average applied to the environmental drivers in our approach. Temperature responses are usually faster than responses to drought but can still exhibit lagged responses up to a few months (Zeng et al., 2013; Papagiannopoulou et al., 2017). Temperature and soil moisture anomalies are usually analysed on different timescales (typically on a daily scale for temperature and on a monthly scale for soil moisture), which renders their joint assessment difficult. Ecosystem impacts can also vary substantially on a temporal scale from, for example, temporary changes in productivity to persistent regime shifts (Crausbay et al., 2017). Therefore, using a single timescale might not capture all relevant temporal dynamics. The choice of the optimal timescale is non-trivial, and, for example, timescales of less than a month for investigating drought impacts on vegetation have also been suggested (West et al., 2019).

Our analysis is year-round without being explicitly restricted to the months of the growing season, which makes it easily transferable to any study area. We decided this for two reasons. First, it is complex to account only for the months of the growing season as there is a large variability depending on latitude and longitude within the Mediterranean Basin (Lionello et al., 2006). Second, the analysis is implicitly limited to the growing season because FAPAR deviations during the dormant season are expected to be small and thus will exceed the extremeness threshold only on rare occasions. In our study, it can be clearly noted that the number of detected events is not distributed equally throughout the course of the year. They are at a minimum at the transition from summer to autumn, when ecosystem activity is low in the Mediterranean (see Sect. 3.2). Therefore, large areas – especially in the interior of the countries – are under-represented in these months. Results for months during the dormant season should be interpreted cautiously (Ivits et al., 2016), taking into account that they depend on a considerably lower number of events. These events might be representative solely of specific ecosystems that are still active at this time of the year or may partially result from noise in the data.

5 Conclusions

The seasonal ecosystem vulnerability analysis presented in this study helps identify the time of the year at which vulnerability to a certain climatic condition occurs. The vulnerability of Mediterranean ecosystems to the concurrent climatic drivers temperature and soil moisture was successfully assessed using the FAPAR as a proxy for ecosystem productivity, with a focus on the variation in impacts with seasonality. Our results are in line with the characteristic intra-annual change between an energy-limited and a water-limited regime from winter to summer in the Mediterranean (Schwingshackl et al., 2017). In general, three seasonal stages of vulnerability are identified throughout the year: (1) vulnerability to hot and dry conditions in late spring to midsummer, (2) vulnerability to cold and dry conditions from the end of summer to mid-autumn, and (3) vulnerability during cold and wet conditions from the end of autumn to mid-spring. There are several regions which deviate from this pattern; e.g. the “hot and dry” regime is extended from spring to autumn in Turkey, whereas the Balkan Peninsula is continuously energy-limited throughout the year and not vulnerable to hot conditions. Our results point out the necessity to incorporate seasonality in the vulnerability analysis concept as well as to examine vulnerability at a subregional scale to account for the large spatial and temporal variability in the Mediterranean. Increasing aridity and fast changes in the phenological cycle are observed in the Mediterranean Basin due to climate change (Gao and Giorgi, 2008; Gordo and Sanz, 2010). The approach for detecting seasonal ecosystem vulnerability opens novel opportunities for developing early-warning tools to identify detrimental ecosystem conditions, water limitations and irrigation demand in near-real time and for performing long-term assessments of ecosystem vulnerability and change for the near- and mid-future climate scenarios.

Appendix A: Comparison of ecosystem vulnerability using soil moisture from ESA CCI and ERA5-Land

The ERA5-Land soil moisture layer at 0–7 cm gives very similar results compared to the ESA CCI data set in the second half of the year (August–December) for most land cover classes (see Fig. A1), where the patterns are identical in most cases; for “all land cover classes” they are in agreement from June to December. However, in spring they often deviate, e.g. in May, when dry conditions arise in the ERA5-Land data set, whereas using ESA CCI there is no significant vulnerability to dry conditions for many land cover classes. For land cover classes such as “crops (rainfed)” vulnerability to dry conditions in May seems realistic as various crops are prone to drought in their reproductive phase (Zhang and Oweis, 1999; Daryanto et al., 2016), which indicates that ERA5-Land might give more plausible results for the month of May. “Shrubland” is often prone to dry conditions in the second half of the year in the ESA CCI data set, whereas according to the ERA5-Land data set it is not. Also “forest (broadleaved)” is prone to dry conditions from June to October in the ESA CCI data set, unlike in the ERA5-Land data set, where it is vulnerable to dry conditions from September to October but not during summer. However, there is no apparent systematic bias over all classes, but rather it changes by month. So, in February, vulnerability in the ERA5-Land data set, for example, leans more towards dry conditions, whereas in July this pattern is reversed.

During most of the year, the majority of subregions coincide well in both data sets, but there are exceptions (see Fig. A2). There is vulnerability to dry conditions in August in the Balkans, the Iberian Peninsula and in north-western

Africa for ESA CCI soil moisture, whereas for ERA5-Land this is reversed or insignificant. For north-western Africa, ERA5-Land detects lower vulnerability to dry conditions than ESA CCI throughout the course of the year. In addition, in the Iberian Peninsula vulnerability to wet conditions is pronounced at the beginning of the year for ESA CCI, whereas for ERA5-Land most months during this period show vulnerability to dry conditions.

In addition to the soil moisture layer corresponding to 0–7 cm soil depth, vulnerability to soil moisture was also analysed for the layers at 7–28 and 28–100 cm (see Figs. A3, A4, A5, A6). The patterns at these deeper layers largely coincide with the surface soil moisture layer (see Figs. A1, A2).

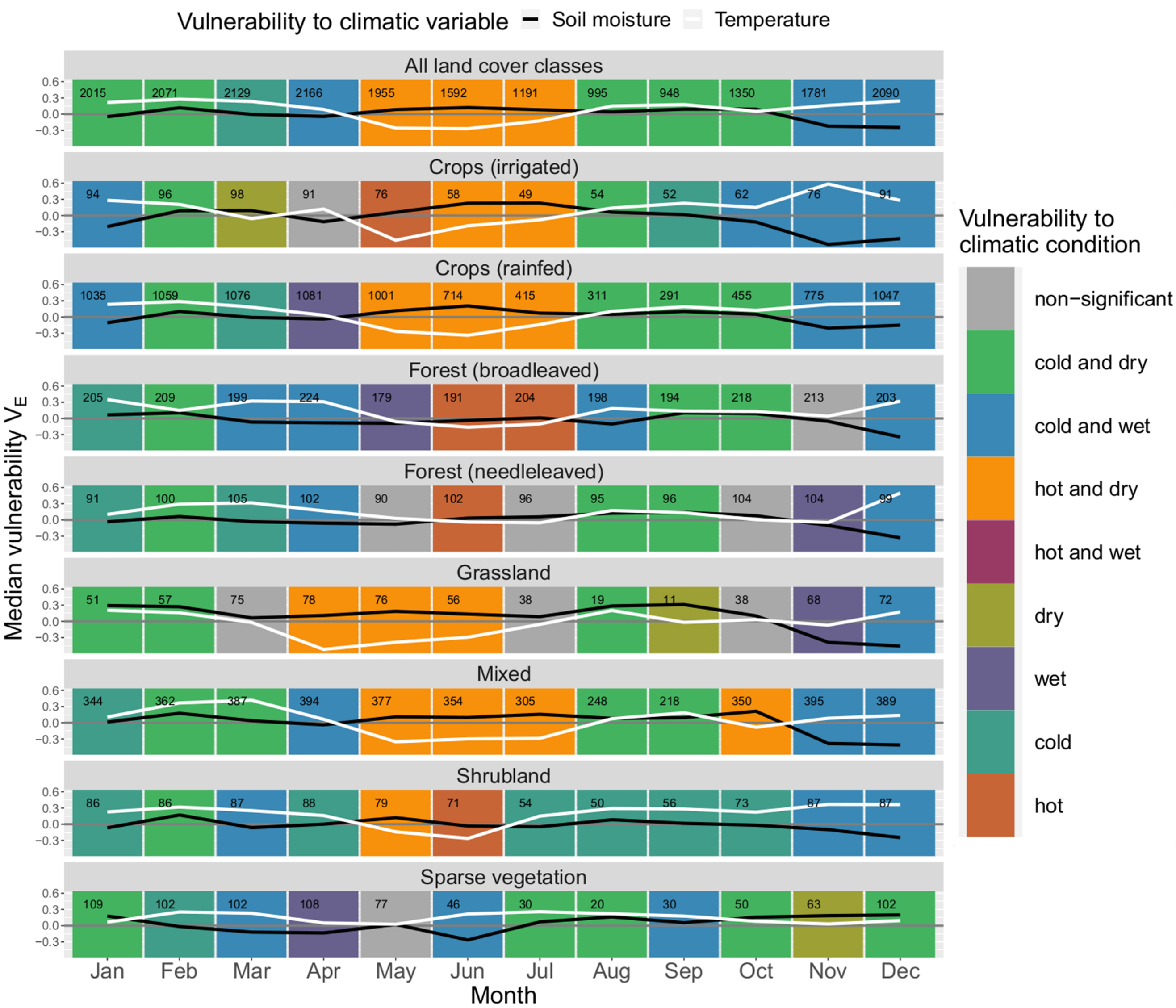

Figure A1. Median monthly ecosystem vulnerability per land cover. Vulnerability to temperature (ERA5-Land) is shown in white, and vulnerability to soil moisture (ERA5-Land at depth 0–7 cm) is shown in black for each month of the year (columns) for each land cover (rows). Months with statistically significant deviation in climatic drivers during non-hazardous and hazardous ecosystem conditions according to the Mann–Whitney U test based on a significance level $\alpha = 0.05$ are shown in colour (see legend); all other months are shown in grey. The number of grid points in which an event has occurred in this month and land cover within the period 1999–2019 is shown in the upper left corner of each panel.

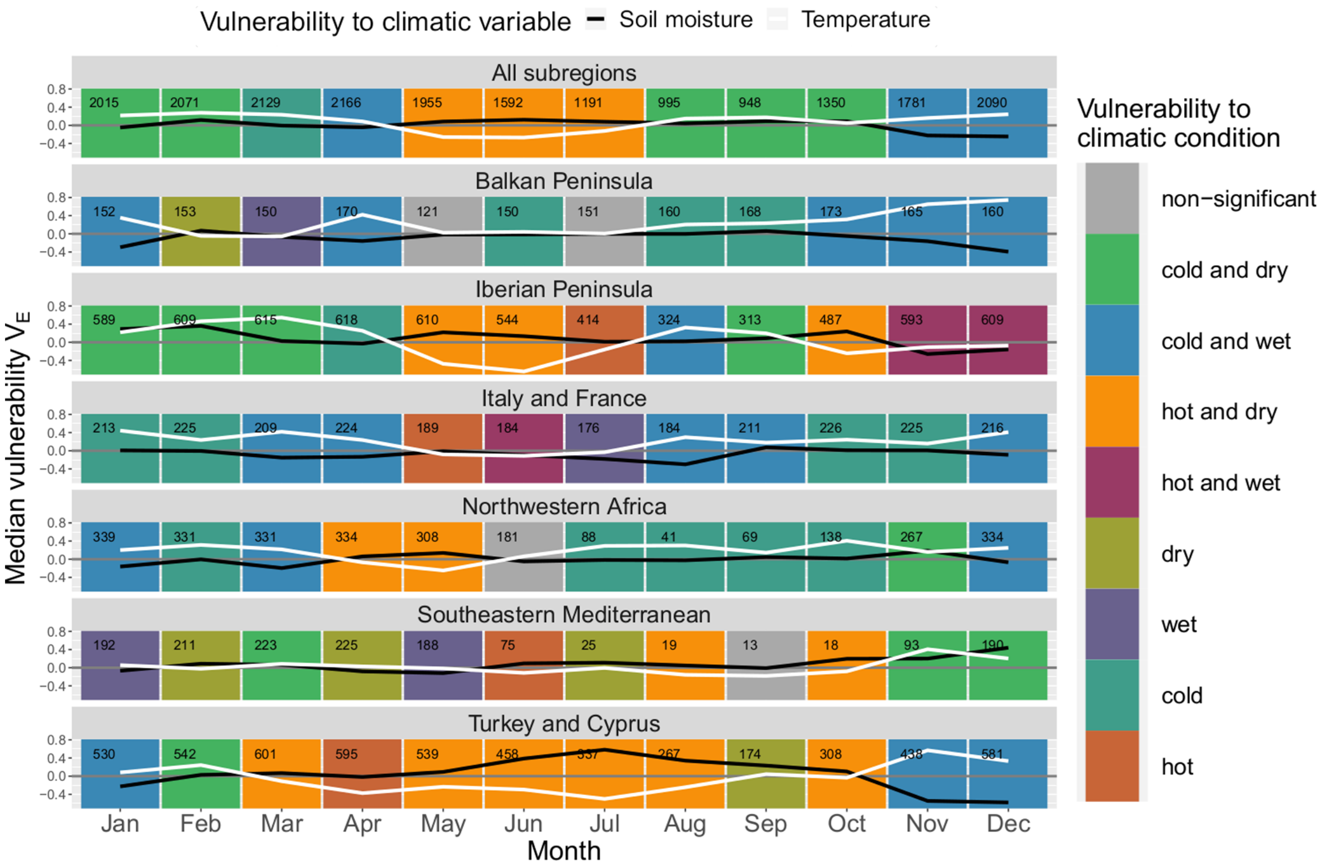

Figure A2. Median monthly ecosystem vulnerability per subregion. Vulnerability to temperature (ERA5-Land) is shown in white, and vulnerability to soil moisture (ERA5-Land at depth 0–7 cm) is shown in black for each month of the year (columns) for each land cover (rows). Months with statistically significant deviation in climatic drivers during non-hazardous and hazardous ecosystem conditions according to the Mann–Whitney U test based on a significance level $\alpha = 0.05$ are shown in colour (see legend); all other months are shown in grey. The number of grid points in which an event has occurred in this month and land cover within the period 1999–2019 is shown in the upper left corner of each panel.

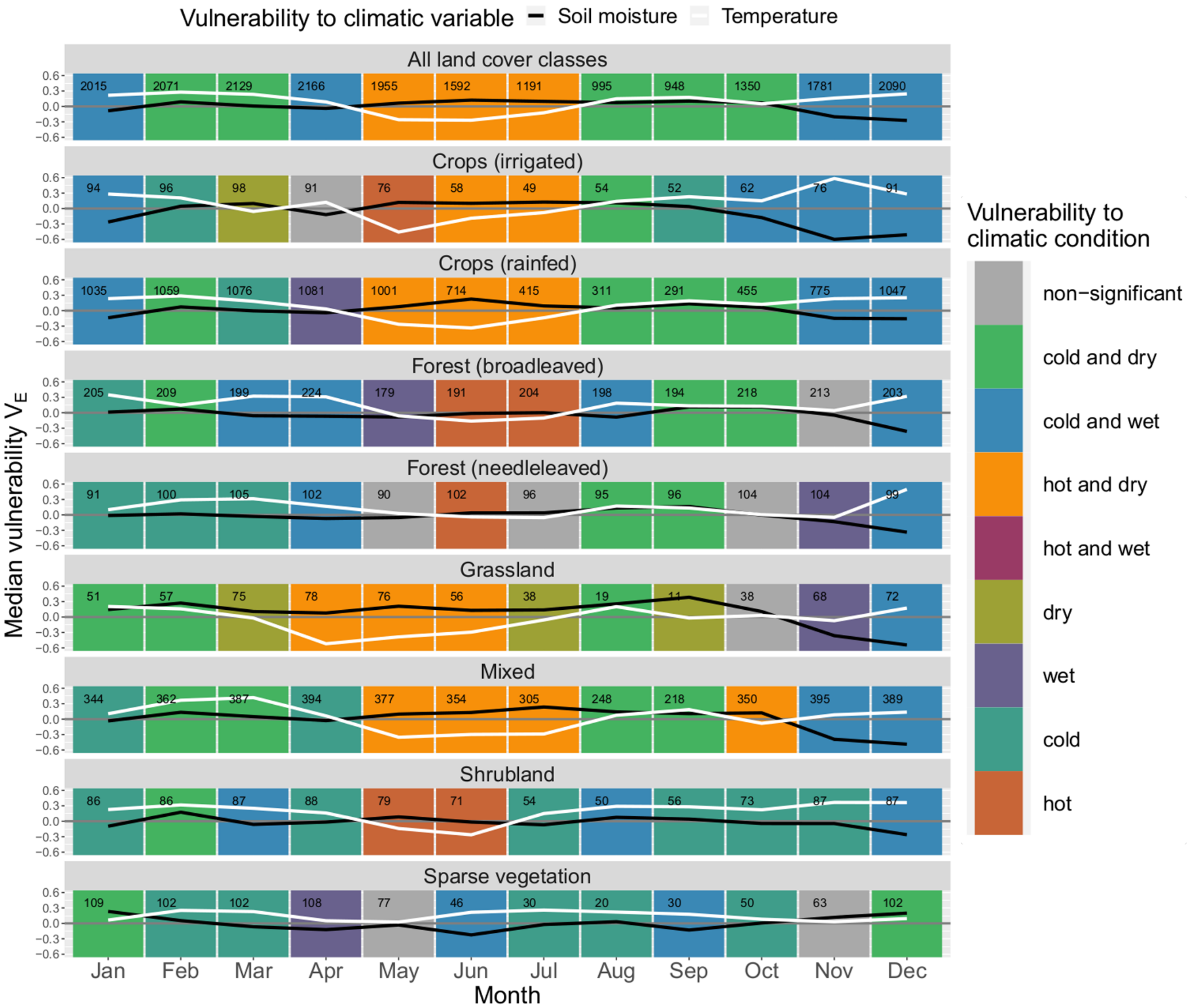

Figure A3. Median monthly ecosystem vulnerability per land cover. Vulnerability to temperature (ERA5-Land) is shown in white, and vulnerability to soil moisture (ERA5-Land at depth 7–28 cm) is shown in black for each month of the year (columns) for each land cover (rows). Months with statistically significant deviation in climatic drivers during non-hazardous and hazardous ecosystem conditions according to the Mann–Whitney U test based on a significance level $\alpha = 0.05$ are shown in colour (see legend); all other months are shown in grey. The number of grid points in which an event has occurred in this month and land cover within the period 1999–2019 is shown in the upper left corner of each panel.

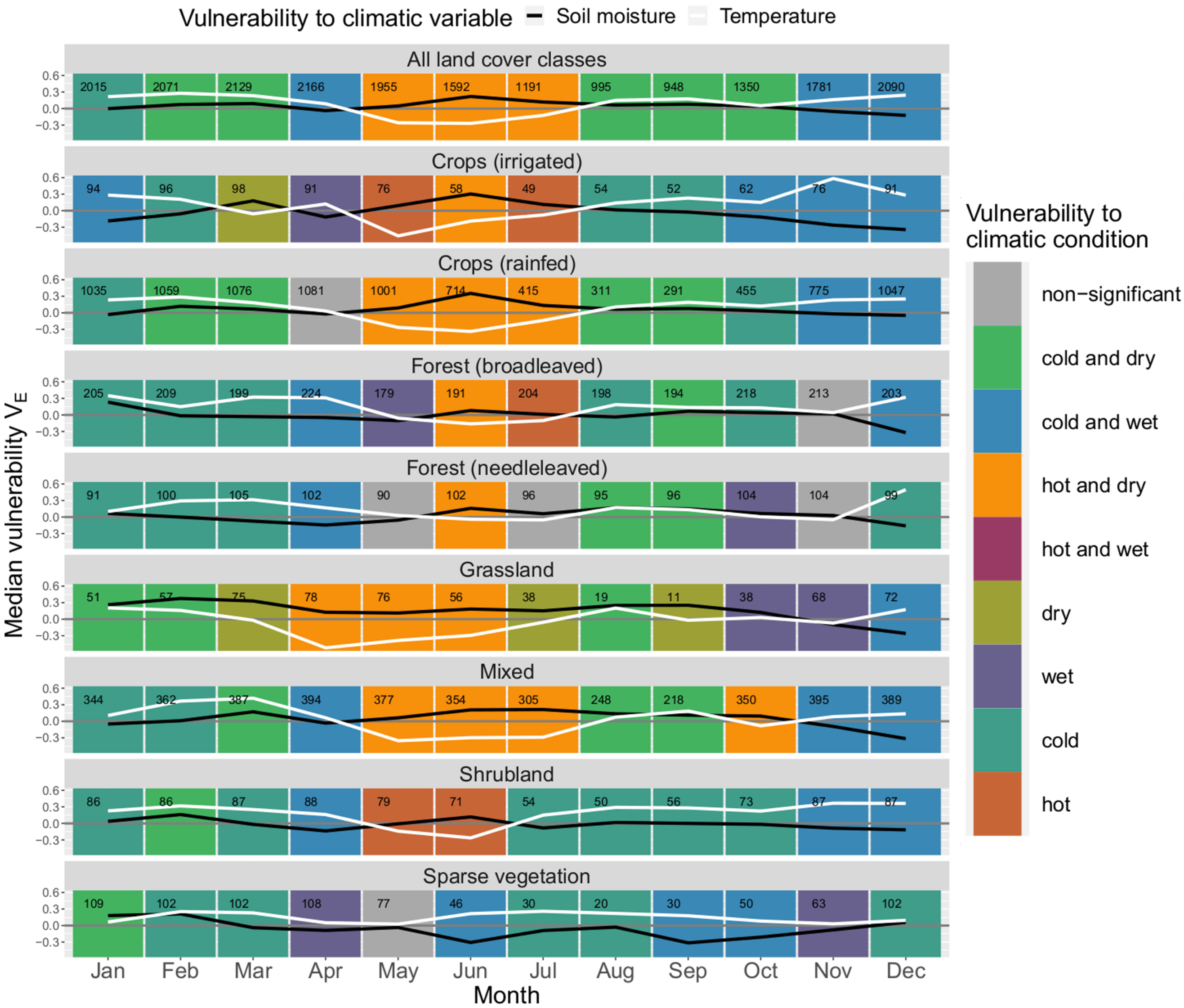

Figure A4. Median monthly ecosystem vulnerability per land cover. Vulnerability to temperature (ERA5-Land) is shown in white, and vulnerability to soil moisture (ERA5-Land at depth 28–100 cm) is shown in black for each month of the year (columns) for each land cover (rows). Months with statistically significant deviation in climatic drivers during non-hazardous and hazardous ecosystem conditions according to the Mann–Whitney U test based on a significance level $\alpha = 0.05$ are shown in colour (see legend); all other months are shown in grey. The number of grid points in which an event has occurred in this month and land cover within the period 1999–2019 is shown in the upper left corner of each panel.

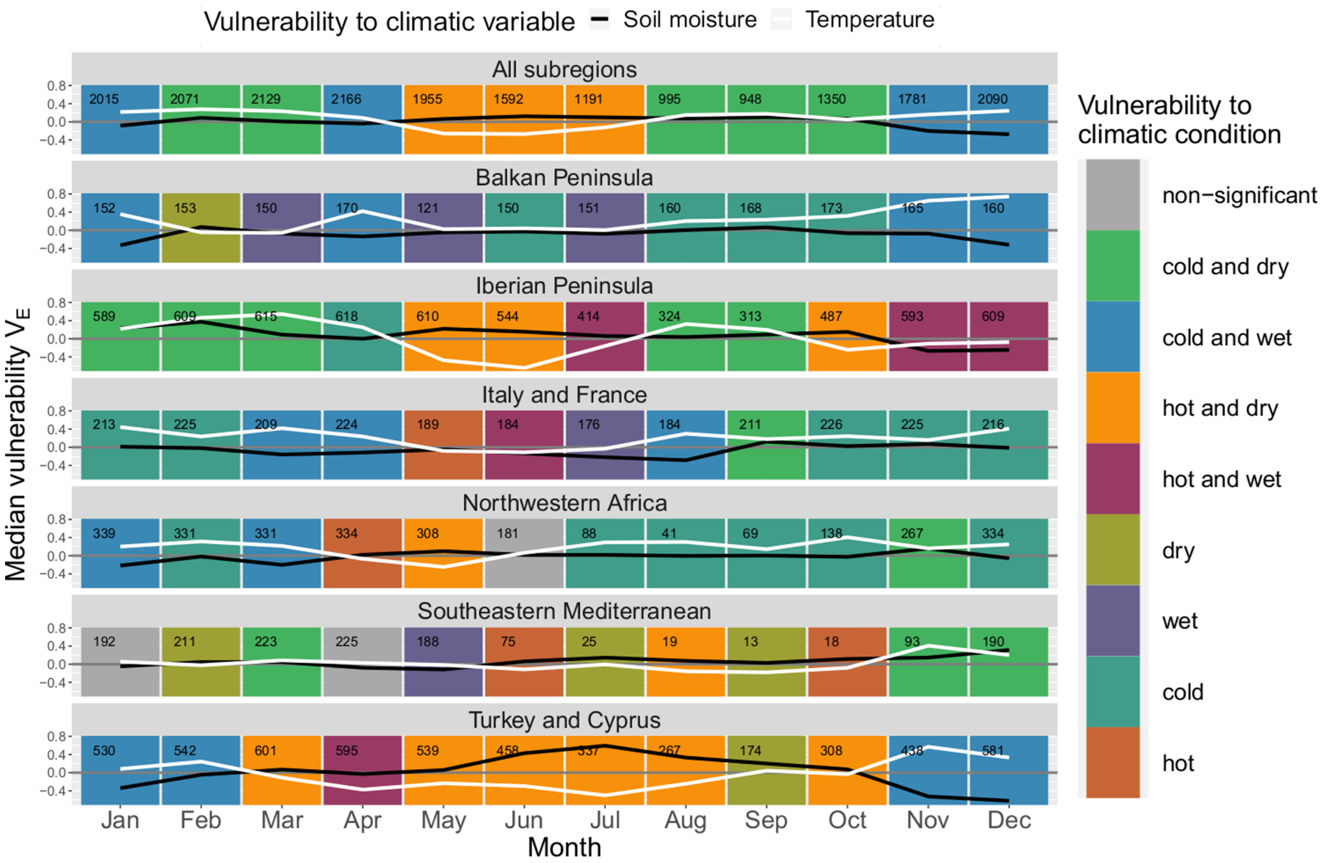

Figure A5. Median monthly ecosystem vulnerability per subregion. Vulnerability to temperature (ERA5-Land) is shown in white, and vulnerability to soil moisture (ERA5-Land at depth 7–28 cm) is shown in black for each month of the year (columns) for each land cover (rows). Months with statistically significant deviation in climatic drivers during non-hazardous and hazardous ecosystem conditions according to the Mann–Whitney U test based on a significance level $\alpha = 0.05$ are shown in colour (see legend); all other months are shown in grey. The number of grid points in which an event has occurred in this month and land cover within the period 1999–2019 is shown in the upper left corner of each panel.

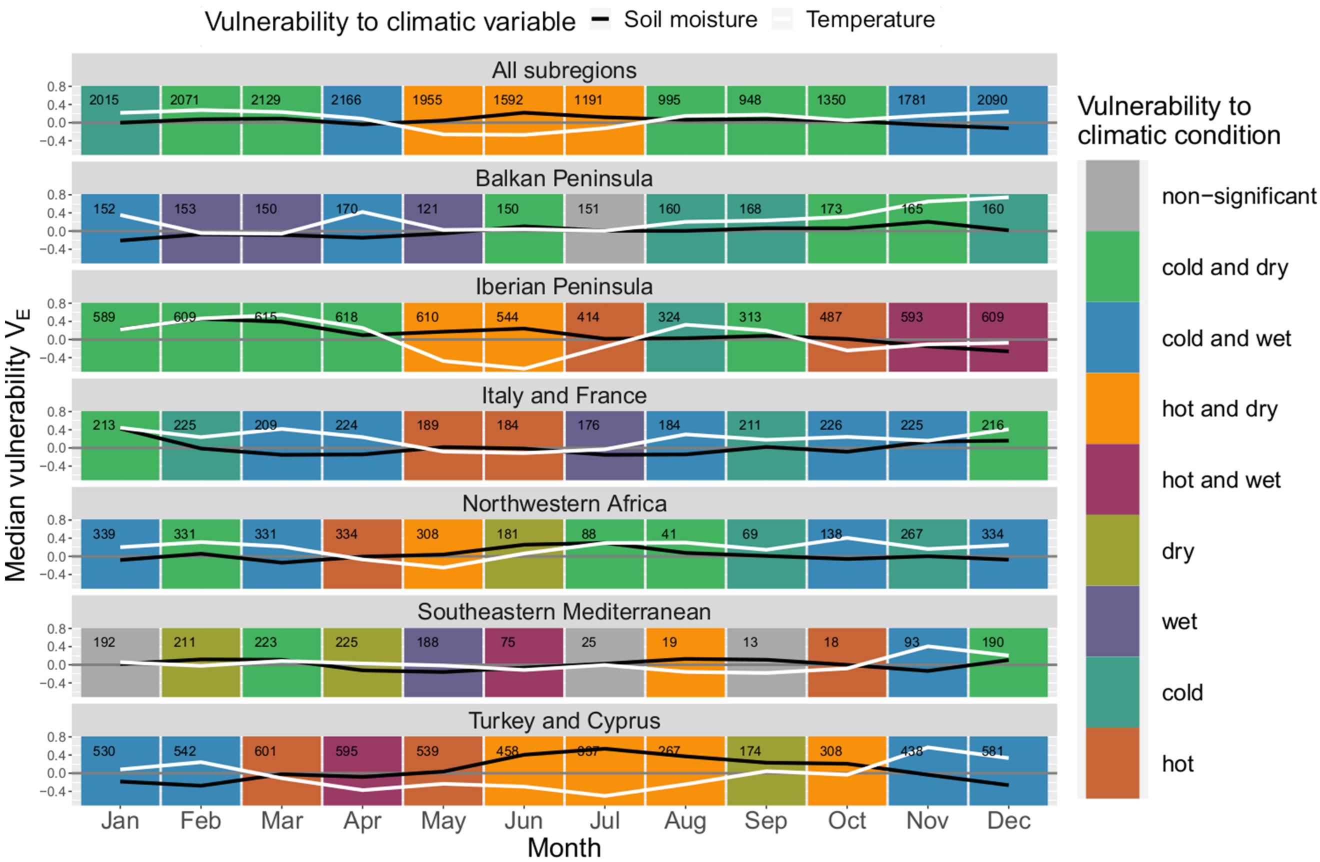

Figure A6. Median monthly ecosystem vulnerability per subregion. Vulnerability to temperature (ERA5-Land) is shown in white, and vulnerability to soil moisture (ERA5-Land at depth 28–100 cm) is shown in black for each month of the year (columns) for each land cover (rows). Months with statistically significant deviation in climatic drivers during non-hazardous and hazardous ecosystem conditions according to the Mann–Whitney U test based on a significance level $\alpha = 0.05$ are shown in colour (see legend); all other months are shown in grey. The number of grid points in which an event has occurred in this month and land cover within the period 1999–2019 is shown in the upper left corner of each panel.

Appendix B: Further materials

Table B1. Overview of the aggregation of land cover classes.

Number	Original class	Aggregated class
10	Cropland, rainfed	Crops (rainfed)
11	Cropland, rainfed, herbaceous cover	
12	Cropland, rainfed, tree or shrub cover	
20	Cropland, irrigated or postflooding	Crops (irrigated)
30	Mosaic cropland (> 50 %) or natural vegetation (tree, shrub, herbaceous cover) (< 50 %)	Mixed
40	Mosaic natural vegetation (tree, shrub, herbaceous cover) (> 50 %) or cropland (< 50 %)	
100	Mosaic tree and shrub (> 50 %) or herbaceous cover (< 50 %)	
60	Tree cover, broadleaved, deciduous, closed to open (> 15 %)	Forest (broadleaved)
62	Tree cover, broadleaved, deciduous, open (15 %–40 %)	
70	Tree cover, needleleaved, evergreen, closed to open (> 15 %)	Forest (needleleaved)
120	Shrubland	Shrubland
130	Grassland	Grassland
150	Sparse vegetation (tree, shrub, herbaceous cover) (< 15 %)	Sparse vegetation
153	Sparse herbaceous cover (< 15 %)	
200	Bare areas	
190	Urban areas	None (Omitted)
210	Water bodies	None (Omitted)

Table B2. Overview of the six subregions and the corresponding countries used in this study.

Short name	Long name	Countries
IBE	Iberian Peninsula	Portugal, Spain
IAF	Italy and France	France, Italy
BAL	Balkan Peninsula	Albania, Bosnia and Herzegovina, Bulgaria, Croatia, Greece, North Macedonia, Montenegro
TAC	Turkey and Cyprus	Cyprus, Turkey
SEM	South-eastern Mediterranean	Iran, Iraq, Israel and Palestinian territories, Jordan, Lebanon, Libya, Syria
NWA	North-western Africa	Algeria, Morocco, Tunisia

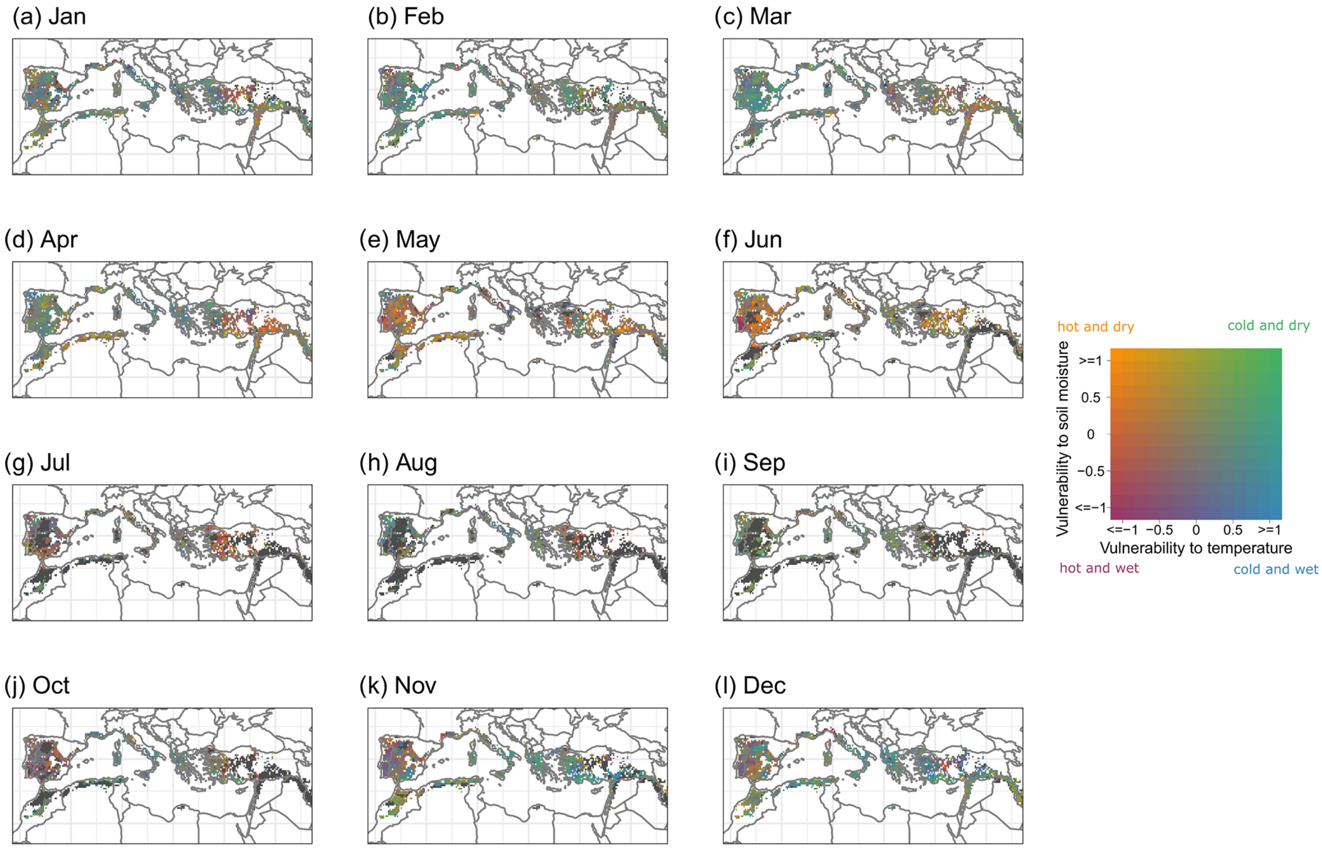

Figure B1. Average monthly vulnerability to soil moisture (ESA CCI) and temperature (ERA5-Land) in the Mediterranean Basin for **(a)** January, **(b)** February, **(c)** March, **(d)** April, **(e)** May, **(f)** June, **(g)** July, **(h)** August, **(i)** September, **(j)** October, **(k)** November and **(l)** December. Grid points without any events during the respective month are displayed in black.

Code and data availability. The code can be retrieved from https://gitup.uni-potsdam.de/joschavogel/ecosystem_vulnerability (Vogel, 2021). All data sets used in this study are publicly available.

Author contributions. JV, EP and VA designed the study and the methodology. JV developed the computer code, performed the analysis and visualised the results. EP supervised the research project. JV wrote the original draft with contributions from all co-authors.

Competing interests. The authors declare that they have no conflict of interest.

Disclaimer. Publisher's note: Copernicus Publications remains neutral with regard to jurisdictional claims in published maps and institutional affiliations.

Special issue statement. This article is part of the special issue "Understanding compound weather and climate events and related impacts (BG/ESD/HESS/NHESS inter-journal SI)". It is not associated with a conference.

Acknowledgements. We would like to thank the guest editor Bart van den Hurk and the co-editor-in-chief Michael Bahn as well as Niko Wanders and the other two anonymous reviewers for their valuable feedback to the manuscript.

Financial support. This research has been supported by the Deutsche Forschungsgemeinschaft (grant no. NatRiskChange GRK 2043).

Review statement. This paper was edited by Bart van den Hurk and reviewed by Niko Wanders and two anonymous referees.

References

Ahlström, A., Raupach, M. R., Schurgers, G., Smith, B., Arneth, A., Jung, M., Reichstein, M., Canadell, J. G., Friedlingstein, P., Jain, A. K., Kato, E., Poulter, B., Sitch, S., Stocker, B. D., Viovy, N., Wang, Y. P., Wiltshire, A., Zaehle, S., and Zeng, N.: Carbon cycle. The dominant role of semi-arid ecosystems in the trend and variability of the land CO_2 sink, Science (New York, N.Y.), 348, 895–899, https://doi.org/10.1126/science.aaa1668, 2015.

Albergel, C., Dorigo, W., Reichle, R. H., Balsamo, G., de Rosnay, P., Muñoz-Sabater, J., Isaksen, L., de Jeu, R., and Wagner, W.: Skill and Global Trend Analysis of Soil Moisture from Reanalyses and Microwave Remote Sensing, J. Hydrometeorol., 14, 1259–1277, https://doi.org/10.1175/JHM-D-12-0161.1, 2013.

Bachmair, S., Tanguy, M., Hannaford, J., and Stahl, K.: How well do meteorological indicators represent agricultural and forest drought across Europe?, Environ. Res. Lett., 13, 034042, https://doi.org/10.1088/1748-9326/aaafda, 2018.

Baret, F., Weiss, M., Lacaze, R., Camacho, F., Makhmara, H., Pacholcyzk, P., and Smets, B.: GEOV1: LAI and FAPAR essential climate variables and FCOVER global time series capitalizing over existing products, Part 1: Principles of development and production, Remote Sens. Environ., 137, 299–309, https://doi.org/10.1016/j.rse.2012.12.027, 2013.

Batllori, E., de Cáceres, M., Brotons, L., Ackerly, D. D., Moritz, M. A., and Lloret, F.: Cumulative effects of fire and drought in Mediterranean ecosystems, Ecosphere, 8, e01906, https://doi.org/10.1002/ecs2.1906, 2017.

Baumbach, L., Siegmund, J. F., Mittermeier, M., and Donner, R. V.: Impacts of temperature extremes on European vegetation during the growing season, Biogeosciences, 14, 4891–4903, https://doi.org/10.5194/bg-14-4891-2017, 2017.

Benjamini, Y. and Hochberg, Y.: Controlling the False Discovery Rate: A Practical and Powerful Approach to Multiple Testing, J. R. Statist. Soc. B, 57, 289–300, 1995.

Berg, A., Lintner, B. R., Findell, K., Seneviratne, S. I., van den Hurk, B., Ducharne, A., Chéruy, F., Hagemann, S., Lawrence, D. M., Malyshev, S., Meier, A., and Gentine, P.: Interannual Coupling between Summertime Surface Temperature and Precipitation over Land: Processes and Implications for Climate Change, J. Clim., 28, 1308–1328, https://doi.org/10.1175/JCLI-D-14-00324.1, 2015.

Berg, A., Sheffield, J., and Milly, P. C. D.: Divergent surface and total soil moisture projections under global warming, Geophys. Res. Lett., 44, 236–244, https://doi.org/10.1002/2016GL071921, 2017.

Bréda, N., Huc, R., Granier, A., and Dreyer, E.: Temperate forest trees and stands under severe drought: a review of ecophysiological responses, adaptation processes and long-term consequences, Ann. Forest Sci., 63, 625–644, https://doi.org/10.1051/forest:2006042, 2006.

Bulut, B., Yilmaz, M. T., Afshar, M. H., Şorman, A. Ü., Yücel, İ., Cosh, M. H., and Şimşek, O.: Evaluation of Remotely-Sensed and Model-Based Soil Moisture Products According to Different Soil Type, Vegetation Cover and Climate Regime Using Station-Based Observations over Turkey, Remote Sens., 11, 1875, https://doi.org/10.3390/rs11161875, 2019.

Chen, T., de Jeu, R., Liu, Y. Y., van der Werf, G. R., and Dolman, A. J.: Using satellite based soil moisture to quantify the water driven variability in NDVI: A case study over mainland Australia, Remote Sens. Environ.t, 140, 330–338, https://doi.org/10.1016/j.rse.2013.08.022, 2014.

Conte, M., Sorani, N., and Piervitali, E.: Extreme climatic events over the Mediterranean, in: Mediterranean desertification, edited by: Geeson, N., Brandt, C. J., and Thornes, J. B., Vol. 1, John Wiley & Sons, Chichester West Sussex England and Hoboken NJ USA, 15–31, 2002.

Crausbay, S. D., Ramirez, A. R., Carter, S. L., Cross, M. S., Hall, K. R., Bathke, D. J., Betancourt, J. L., Colt, S., Cravens, A. E., Dalton, M. S., Dunham, J. B., Hay, L. E., Hayes, M. J., McEvoy, J., McNutt, C. A., Moritz, M. A., Nislow, K. H., Raheem, N., and Sanford, T.: Defining Ecological Drought for the Twenty-First Century, Bull. Am. Meteorol. Soc., 98, 2543–2550, https://doi.org/10.1175/BAMS-D-16-0292.1, 2017.

Crocetti, L., Forkel, M., Fischer, M., Jurečka, F., Grlj, A., Salentinig, A., Trnka, M., Anderson, M., Ng, W.-T., Kokalj, Ž., Bucur, A., and Dorigo, W.: Earth Observation for agricultural drought monitoring in the Pannonian Basin (southeastern Europe): current state and future directions, Reg. Environ. Change, 20, 123, 1–17, https://doi.org/10.1007/s10113-020-01710-w, 2020.

Daryanto, S., Wang, L., and Jacinthe, P.-A.: Global Synthesis of Drought Effects on Maize and Wheat Production, PloS one, 11, e0156362, https://doi.org/10.1371/journal.pone.0156362, 2016.

de Boeck, H. J., Dreesen, F. E., Janssens, I. A., and Nijs, I.: Whole-system responses of experimental plant communities to climate extremes imposed in different seasons, New Phytol., 189, 806–817, https://doi.org/10.1111/j.1469-8137.2010.03515.x, 2011.

de Jeu, R. and Dorigo, W.: On the importance of satellite observed soil moisture, Int. J. Appl. Earth Obs., 45, 107–109, https://doi.org/10.1016/j.jag.2015.10.007, 2016.

de Luca, P., Messori, G., Faranda, D., Ward, P. J., and Coumou, D.: Compound warm–dry and cold–wet events over the Mediterranean, Earth Syst. Dynam., 11, 793–805, https://doi.org/10.5194/esd-11-793-2020, 2020.

Denton, E. M., Dietrich, J. D., Smith, M. D., and Knapp, A. K.: Drought timing differentially affects above- and belowground productivity in a mesic grassland, Plant Ecol., 218, 317–328, https://doi.org/10.1007/s11258-016-0690-x, 2017.

Dorigo, W. and de Jeu, R.: Satellite soil moisture for advancing our understanding of earth system processes and climate change, Int. J. Appl. Earth Obs., 48, 1–4, https://doi.org/10.1016/j.jag.2016.02.007, 2016.

Dorigo, W., Wagner, W., Albergel, C., Albrecht, F., Balsamo, G., Brocca, L., Chung, D., Ertl, M., Forkel, M., Gruber, A., Haas, E., Hamer, P. D., Hirschi, M., Ikonen, J., de Jeu, R., Kidd, R., Lahoz, W., Liu, Y. Y., Miralles, D., Mistelbauer, T., Nicolai-Shaw, N., Parinussa, R., Pratola, C., Reimer, C., van der Schalie, R., Seneviratne, S. I., Smolander, T., and Lecomte, P.: ESA CCI Soil Moisture for improved Earth system understanding: State-of-the art and future directions, Remote Sens. Environ., 203, 185–215, https://doi.org/10.1016/j.rse.2017.07.001, 2017.

Dorigo, W. A., Gruber, A., de Jeu, R., Wagner, W., Stacke, T., Loew, A., Albergel, C., Brocca, L., Chung, D., Parinussa, R. M., and Kidd, R.: Evaluation of the ESA CCI soil moisture product using ground-based observations, Remote Sens. Environ., 162, 380–395, https://doi.org/10.1016/j.rse.2014.07.023, 2015.

ESA: Land Cover CCI Product User Guide Version 2: Tech. Rep, available at: http://maps.elie.ucl.ac.be/CCI/viewer/index.php (last access: 5 November 2021), 2017.

Feng, S. and Fu, Q.: Expansion of global drylands under a warming climate, Atmos. Chem. Phys., 13, 10081–10094, https://doi.org/10.5194/acp-13-10081-2013, 2013.

Fraga, H., Pinto, J. G., Viola, F., and Santos, J. A.: Climate change projections for olive yields in the Mediterranean Basin, Int. J. Climatol., 40, 769–781, https://doi.org/10.1002/joc.6237, 2020.

Fuster, B., Sánchez-Zapero, J., Camacho, F., García-Santos, V., Verger, A., Lacaze, R., Weiss, M., Baret, F., and Smets, B.: Quality Assessment of PROBA-V LAI, fAPAR and fCOVER Collection 300 m Products of Copernicus Global Land Service, Remote Sens., 12, 1017, https://doi.org/10.3390/rs12061017, 2020.

Gao, X. and Giorgi, F.: Increased aridity in the Mediterranean region under greenhouse gas forcing estimated from high resolution simulations with a regional climate model, Glob. Planet. Change, 62, 195–209, https://doi.org/10.1016/j.gloplacha.2008.02.002, 2008.

Gobron, N., Belward, A., Pinty, B., and Knorr, W.: Monitoring biosphere vegetation 1998–2009, Geophys. Res. Lett., 37, 1–6, https://doi.org/10.1029/2010GL043870, 2010.

Gordo, O. and Sanz, J. J.: Long-term temporal changes of plant phenology in the Western Mediterranean, Glob. Change Biol., 15, 1930–1948, https://doi.org/10.1111/j.1365-2486.2009.01851.x, 2009.

Gordo, O. and Sanz, J. J.: Impact of climate change on plant phenology in Mediterranean ecosystems, Glob. Change Biol., 16, 1082–1106, https://doi.org/10.1111/j.1365-2486.2009.02084.x, 2010.

Gouveia, C. M., Bastos, A., Trigo, R. M., and DaCamara, C. C.: Drought impacts on vegetation in the pre- and post-fire events over Iberian Peninsula, Nat. Hazards Earth Syst. Sci., 12, 3123–3137, https://doi.org/10.5194/nhess-12-3123-2012, 2012.

Gouveia, C. M., Trigo, R. M., Beguería, S., and Vicente-Serrano, S. M.: Drought impacts on vegetation activity in the Mediterranean region: An assessment using remote sensing data and multi-scale drought indicators, Glob. Planet. Change, 151, 15–27, https://doi.org/10.1016/j.gloplacha.2016.06.011, 2017.

Green, J. K., Konings, A. G., Alemohammad, S. H., Berry, J., Entekhabi, D., Kolassa, J., Lee, J.-E., and Gentine, P.: Regionally strong feedbacks between the atmosphere and terrestrial biosphere, Nat. Geosci., 10, 410–414, https://doi.org/10.1038/ngeo2957, 2017.

Gruber, A., Scanlon, T., van der Schalie, R., Wagner, W., and Dorigo, W.: Evolution of the ESA CCI Soil Moisture climate data records and their underlying merging methodology, Earth Syst. Sci. Data, 11, 717–739, https://doi.org/10.5194/essd-11-717-2019, 2019.

Hatfield, J. L. and Prueger, J. H.: Temperature extremes: Effect on plant growth and development, Weather and Climate Extremes, 10, 4–10, https://doi.org/10.1016/j.wace.2015.08.001, 2015.

IPCC (Ed.): Climate Change and Land: an IPCC special report on climate change, desertification, land degradation, sustainable land management, food security, and greenhouse gas fluxes in terrestrial ecosystems, edited by: Shukla, P. R., Skea, J., Calvo Buendia, E., Masson-Delmotte, V., Pörtner, H.-O., Roberts, D. C., Zhai, P., Slade, R., Connors, S., van Diemen, R., Ferrat, M., Haughey, E., Luz, S., Neogi, S., Pathak, M., Petzold, J., Portugal Pereira, J., Vyas, P., Huntley, E., Kissick, K., Belkacemi, M., Malley, J., https://www.ipcc.ch/srccl/, 2019.

Ivits, E., Horion, S., Erhard, M., and Fensholt, R.: Assessing European ecosystem stability to drought in the vegetation growing season, Glob. Ecol. Biogeogr., 25, 1131–1143, https://doi.org/10.1111/geb.12472, 2016.

Jentsch, A., Kreyling, J., and Beierkuhnlein, C.: A new generation of climate-change experiments: events, not trends, Front. Ecol. Environ., 5, 365–374, 2007.

Karnieli, A., Ohana-Levi, N., Silver, M., Paz-Kagan, T., Panov, N., Varghese, D., Chrysoulakis, N., and Provenzale, A.: Spatial and Seasonal Patterns in Vegetation Growth-Limiting Factors over Europe, Remote Sens., 11, 2406, https://doi.org/10.3390/rs11202406, 2019.

Kidd, R. and Haas, E.: ESA Climate Change Initiative Plus Soil Moisture: Soil Moisture ECV Product User Guide (PUG) Revision 3: D3.3.1 Version 4.5, Earth Observation Data Centre for Water Resources Monitoring (EODC) GmbH, available at: https:

//www.esa-soilmoisture-cci.org/node/145 (last access: 5 November 2021), 2018.

Kottek, M., Grieser, J., Beck, C., Rudolf, B., and Rubel, F.: World Map of the Köppen-Geiger climate classification updated, Meteorol. Z., 15, 259–263, https://doi.org/10.1127/0941-2948/2006/0130, 2006.

Le Page, M. and Zribi, M.: Analysis and Predictability of Drought In Northwest Africa Using Optical and Microwave Satellite Remote Sensing Products, Sci. Rep., 9, 1466, https://doi.org/10.1038/s41598-018-37911-x, 2019.

Lian, X., Piao, S., Li, L. Z. X., Li, Y., Huntingford, C., Ciais, P., Cescatti, A., Janssens, I. A., Peñuelas, J., Buermann, W., Chen, A., Li, X., Myneni, R. B., Wang, X., Wang, Y., Yang, Y., Zeng, Z., Zhang, Y., and McVicar, T. R.: Summer soil drying exacerbated by earlier spring greening of northern vegetation, Sci. Adv., 6, eaax0255, https://doi.org/10.1126/sciadv.aax0255, 2020.

Lionello, P., Malanotte-Rizzoli P., Boscolo, R., Alpert, P., Artale, V., Li, L., Luterbacher, J., May, W., Trigo, R., Tsimplis, M., Ulbrich, U., and Xoplaki, E.: The Mediterranean Climate: An Overview of the Main Characteristics and Issues, in: Mediterranean climate variability, edited by: Lionello, P., Malanotte-Rizzoli, P., and Boscolo, R., Developments in earth & environmental sciences, Elsevier, Amsterdam, 1–26, 2006.

Lionello, P., Abrantes, F., Congedi, L., Dulac, F., Gacic, M., Gomis, D., Goodess, C., Hoff, H., Kutiel, H., Luterbacher, J., Planton, S., Reale, M., Schröder, K., Struglia, M. V., Toreti, A., Tsimplis, M., Ulbrich, U., and Xoplaki, E.: Mediterranean Climate: Background Information, in: The climate of the Mediterranean region, edited by Lionello, P., Elsevier insights, Elsevier Science, Amsterdam, xxxv–xc, 2012.

Liu, D., Ogaya, R., Barbeta, A., Yang, X., and Peñuelas, J.: Long-term experimental drought combined with natural extremes accelerate vegetation shift in a Mediterranean holm oak forest, Environ. Exp. Bot., 151, 1–11, https://doi.org/10.1016/j.envexpbot.2018.02.008, 2018.

Liu, X., Zhu, X., Pan, Y., Li, S., Liu, Y., and Ma, Y.: Agricultural drought monitoring: Progress, challenges, and prospects, J. Geogr. Sci., 26, 750–767, https://doi.org/10.1007/s11442-016-1297-9, 2016.

McWilliam, J. R.: The National and International Importance of Drought and Salinity Effects on Agricultural Production, Aust. J. Plant Physiol., 13, 1–13, 1986.

Menzel, A., Sparks, T. H., Estrella, N., Koch, E., Aasa, A., Ahas, R., Alm-Kübler, K., Bissolli, P., Braslavská, O., Briede, A., Chmielewski, F.-M., Crepinsek, Z., Curnel, Y., Dahl, Å., Defila, C., Donnelly, A., Filella, I., Jatzcak, K., Måge, F., Mestre, A., Nordli, Ø., Peñuelas, J., Pirinen, P., Remišová, V., Scheifinger, H., Striz, M., Susnik, A., van Vliet, A. J. H., Wielgolaski, F.-E., Zach, S., and Zust, A.: European phenological response to climate change matches the warming pattern, Glob. Change Biol., 12, 1969–1976, https://doi.org/10.1111/j.1365-2486.2006.01193.x, 2006.

Mueller, B. and Seneviratne, S. I.: Hot days induced by precipitation deficits at the global scale, P. Natl. Acad. Sci. USA, 109, 12398–12403, https://doi.org/10.1073/pnas.1204330109, 2012.

Muñoz-Sabater, J.: ERA5-Land monthly averaged data from 1981 to present, Copernicus Climate Change Service (C3S) Climate Data Store (CDS) [data set], https://doi.org/10.24381/cds.68d2bb30, 2019.

Myneni, R. B. and Williams, D. L.: On the relationship between FAPAR and NDVI, Remote Sens. Environ., 49, 200–211, https://doi.org/10.1016/0034-4257(94)90016-7, 1994.

Nicolai-Shaw, N., Zscheischler, J., Hirschi, M., Gudmundsson, L., and Seneviratne, S. I.: A drought event composite analysis using satellite remote-sensing based soil moisture, Remote Sens. Environ., 203, 216–225, https://doi.org/10.1016/j.rse.2017.06.014, 2017.

Niu, S., Luo, Y., Li, D., Cao, S., Xia, J., Li, J., and Smith, M. D.: Plant growth and mortality under climatic extremes: An overview, Environ. Exp. Bot., 98, 13–19, https://doi.org/10.1016/j.envexpbot.2013.10.004, 2014.

Ogaya, R. and Peñuelas, J.: Tree growth, mortality, and aboveground biomass accumulation in a holm oak forest under a five-year experimental field drought, Plant Ecol., 189, 291–299, https://doi.org/10.1007/s11258-006-9184-6, 2007.

Orth, R., Destouni, G., Jung, M., and Reichstein, M.: Large-scale biospheric drought response intensifies linearly with drought duration in arid regions, Biogeosciences, 17, 2647–2656, https://doi.org/10.5194/bg-17-2647-2020, 2020.

Pan, S., Yang, J., Tian, H., Shi, H., Chang, J., Ciais, P., Francois, L., Frieler, K., Fu, B., Hickler, T., Ito, A., Nishina, K., Ostberg, S., Reyer, C. P., Schaphoff, S., Steinkamp, J., and Zhao, F.: Climate Extreme Versus Carbon Extreme: Responses of Terrestrial Carbon Fluxes to Temperature and Precipitation, J. Geophys. Res.-Biogeo., 125, e2019JG005252, https://doi.org/10.1029/2019JG005252, 2020.

Papagiannopoulou, C., Miralles, D. G., Dorigo, W. A., Verhoest, N. E. C., Depoorter, M., and Waegeman, W.: Vegetation anomalies caused by antecedent precipitation in most of the world, Environ. Res. Lett., 12, 074016, https://doi.org/10.1088/1748-9326/aa7145, 2017.

Páscoa, P., Gouveia, C. M., Russo, A., and Trigo, R. M.: The role of drought on wheat yield interannual variability in the Iberian Peninsula from 1929 to 2012, Int. J. Biometeorol., 61, 439–451, https://doi.org/10.1007/s00484-016-1224-x, 2017.

Peña-Gallardo, M., Vicente-Serrano, S. M., Domínguez-Castro, F., and Beguería, S.: The impact of drought on the productivity of two rainfed crops in Spain, Nat. Hazards Earth Syst. Sci., 19, 1215–1234, https://doi.org/10.5194/nhess-19-1215-2019, 2019.

Peñuelas, J., Sardans, J., Filella, I., Estiarte, M., Llusià, J., Ogaya, R., Carnicer, J., Bartrons, M., Rivas-Ubach, A., Grau, O., Peguero, G., Margalef, O., Pla-Rabés, S., Stefanescu, C., Asensio, D., Preece, C., Liu, L., Verger, A., Barbeta, A., Achotegui-Castells, A., Gargallo-Garriga, A., Sperlich, D., Farré-Armengol, G., Fernández-Martínez, M., Liu, D., Zhang, C., Urbina, I., Camino-Serrano, M., Vives-Ingla, M., Stocker, B., Balzarolo, M., Guerrieri, R., Peaucelle, M., Marañón-Jiménez, S., Bórnez-Mejías, K., Mu, Z., Descals, A., Castellanos, A., and Terradas, J.: Impacts of Global Change on Mediterranean Forests and Their Services, Forests, 8, 463, https://doi.org/10.3390/f8120463, 2017.

Perkins-Kirkpatrick, S. E. and Gibson, P. B.: Changes in regional heatwave characteristics as a function of increasing global temperature, Sci. Repo., 7, 12256, https://doi.org/10.1038/s41598-017-12520-2, 2017.

Piao, S., Zhang, X., Chen, A., Liu, Q., Lian, X., Wang, X., Peng, S., and Wu, X.: The impacts of climate extremes on the terrestrial carbon cycle: A review, Sci. China Earth Sci., 1, 1285, https://doi.org/10.1007/s11430-018-9363-5, 2019.

Pinty, B., Lavergne, T., Widlowski, J.-L., Gobron, N., and Verstraete, M. M.: On the need to observe vegetation canopies in the near-infrared to estimate visible light absorption, Remote Sens. Environ., 113, 10–23, https://doi.org/10.1016/j.rse.2008.08.017, 2009.

Potter, C., Tan, P. N., Steinbach, M., Klooster, S., Kumar, V., Myneni, R., and Genovese, V.: Major disturbance events in terrestrial ecosystems detected using global satellite data sets, Glob. Change Biol., 9, 1005–1021, 2003.

R Core Team: R: A Language and Environment for Statistical Computing, available at: https://www.R-project.org/ (last access: 5 November 2021), 2020.

Reichstein, M., Ciais, P., Papale, D., Valentini, R., Running, S., Viovy, N., Cramer, W., Granier, A., Ogée, J., Allard, V., Aubinet, M., Bernhofer, C., Buchmann, N., Carrara, A., Grünwald, T., Heimann, M., Heinesch, B., Knohl, A., Kutsch, W., Loustau, D., Manca, G., Matteucci, G., Miglietta, F., Ourcival, J. M., Pilegaard, K., Pumpanen, J., Rambal, S., Schaphoff, S., Seufert, G., Soussana, J.-F., Sanz, M. J., Vesala, T., and Zhao, M.: Reduction of ecosystem productivity and respiration during the European summer 2003 climate anomaly: a joint flux tower, Remote Sensing and Modelling Analysis, Glob. Change Biol., 13, 634–651, https://doi.org/10.1111/j.1365-2486.2006.01224.x, 2007.

Reichstein, M., Bahn, M., Ciais, P., Frank, D., Mahecha, M. D., Seneviratne, S. I., Zscheischler, J., Beer, C., Buchmann, N., Frank, D. C., Papale, D., Rammig, A., Smith, P., Thonicke, K., van der Velde, M., Vicca, S., Walz, A., and Wattenbach, M.: Climate extremes and the carbon cycle, Nature, 500, 287–295, https://doi.org/10.1038/nature12350, 2013.

Reyer, C. P. O., Leuzinger, S., Rammig, A., Wolf, A., Bartholomeus, R. P., Bonfante, A., de Lorenzi, F., Dury, M., Gloning, P., Abou Jaoudé, R., Klein, T., Kuster, T. M., Martins, M., Niedrist, G., Riccardi, M., Wohlfahrt, G., de Angelis, P., de Dato, G., François, L., Menzel, A., and Pereira, M.: A plant's perspective of extremes: terrestrial plant responses to changing climatic variability, Glob. Change Biol., 19, 75–89, https://doi.org/10.1111/gcb.12023, 2013.

Ribeiro, A. F., Russo, A., Gouveia, C. M., and Pires, C. A.: Drought-related hot summers: A joint probability analysis in the Iberian Peninsula, Weather and Climate Extremes, 30, 100279, https://doi.org/10.1016/j.wace.2020.100279, 2020.

Rolinski, S., Rammig, A., Walz, A., von Bloh, W., van Oijen, M., and Thonicke, K.: A probabilistic risk assessment for the vulnerability of the European carbon cycle to weather extremes: the ecosystem perspective, Biogeosciences, 12, 1813–1831, https://doi.org/10.5194/bg-12-1813-2015, 2015.

Rubel, F., Brugger, K., Haslinger, K., and Auer, I.: The climate of the European Alps: Shift of very high resolution Köppen-Geiger climate zones 1800–2100, Meteorol. Z., 26, 115–125, https://doi.org/10.1127/metz/2016/0816, 2017.

Ruffault, J., Curt, T., Martin-StPaul, N. K., Moron, V., and Trigo, R. M.: Extreme wildfire events are linked to global-change-type droughts in the northern Mediterranean, Nat. Hazards Earth Syst. Sci., 18, 847–856, https://doi.org/10.5194/nhess-18-847-2018, 2018.

Samaniego, L., Thober, S., Kumar, R., Wanders, N., Rakovec, O., Pan, M., Zink, M., Sheffield, J., Wood, E. F., and Marx, A.: Anthropogenic warming exacerbates European soil moisture droughts, Nat. Clim. Change, 8, 421–426, https://doi.org/10.1038/s41558-018-0138-5, 2018.

Sarris, D., Christodoulakis, D., and Körner, C.: Recent decline in precipitation and tree growth in the eastern Mediterranean, Glob. Change Biol., 13, 1187–1200, https://doi.org/10.1111/j.1365-2486.2007.01348.x, 2007.

Sarris, D., Christodoulakis, D., and Körner, C.: Impact of recent climatic change on growth of low elevation eastern Mediterranean forest trees, Climatic Change, 106, 203–223, https://doi.org/10.1007/s10584-010-9901-y, 2011.

Sarris, D., Christopoulou, A., Angelonidi, E., Koutsias, N., Fulé, P. Z., and Arianoutsou, M.: Increasing extremes of heat and drought associated with recent severe wildfires in southern Greece, Reg. Environ. Change, 14, 1257–1268, https://doi.org/10.1007/s10113-013-0568-6, 2014.

Schulzweida, U.: CDO Climate Data Operator, Zenodo, https://doi.org/10.5281/zenodo.3539275, 2019.

Schwingshackl, C., Hirschi, M., and Seneviratne, S. I.: Quantifying Spatiotemporal Variations of Soil Moisture Control on Surface Energy Balance and Near-Surface Air Temperature, J. Clim., 30, 7105–7124, https://doi.org/10.1175/JCLI-D-16-0727.1, 2017.

Seneviratne, S. I., Lüthi, D., Litschi, M., and Schär, C.: Land-atmosphere coupling and climate change in Europe, Nature, 443, 205–209, https://doi.org/10.1038/nature05095, 2006.

Seneviratne, S. I., Corti, T., Davin, E. L., Hirschi, M., Jaeger, E. B., Lehner, I., Orlowsky, B., and Teuling, A. J.: Investigating soil moisture–climate interactions in a changing climate: A review, Earth-Sci. Rev., 99, 125–161, https://doi.org/10.1016/j.earscirev.2010.02.004, 2010.

Sherry, R. A., Weng, E., Arnone, J. A., Johnson, D. W., Schimel, D. S., Verburg, P. S., Wallace, L. L., and Luo, Y.: Lagged effects of experimental warming and doubled precipitation on annual and seasonal aboveground biomass production in a tallgrass prairie, Glob. Change Biol., 14, 2923–2936, https://doi.org/10.1111/j.1365-2486.2008.01703.x, 2008.

Sippel, S., Zscheischler, J., and Reichstein, M.: Ecosystem impacts of climate extremes crucially depend on the timing, P. Natl. Acad. Sci. USA, 113, 5768–5770, https://doi.org/10.1073/pnas.1605667113, 2016.

Sippel, S., Forkel, M., Rammig, A., Thonicke, K., Flach, M., Heimann, M., Otto, F. E. L., Reichstein, M., and Mahecha, M. D.: Contrasting and interacting changes in simulated spring and summer carbon cycle extremes in European ecosystems, Environ. Res. Lett., 12, 075006, https://doi.org/10.1088/1748-9326/aa7398, 2017.

Sippel, S., Reichstein, M., Ma, X., Mahecha, M. D., Lange, H., Flach, M., and Frank, D.: Drought, Heat, and the Carbon Cycle: a Review, Curr. Clim. Change Rep., 4, 266–286, https://doi.org/10.1007/s40641-018-0103-4, 2018.

Smit, H. J., Metzger, M. J., and Ewert, F.: Spatial distribution of grassland productivity and land use in Europe, Agr. Syst., 98, 208–219, https://doi.org/10.1016/j.agsy.2008.07.004, 2008.

Smith, M. D.: An ecological perspective on extreme climatic events: a synthetic definition and framework to guide future research, J. Ecol., 99, 656–663, https://doi.org/10.1111/j.1365-2745.2011.01798.x, 2011.

Sousa, P. M., Barriopedro, D., Ramos, A. M., García-Herrera, R., Espírito-Santo, F., and Trigo, R. M.: Saharan air intrusions as a relevant mechanism for Iberian heatwaves: The record breaking events of August 2018 and June 2019, Weather and Climate Extremes, 26, 100224, https://doi.org/10.1016/j.wace.2019.100224, 2019.

Spano, D., Snyder, R. L., and Cesaraccio, C.: Mediterranean Phenology, in: Phenology: An Integrative Environmental Science, edited by: Schwartz, M. D., Springer Netherlands, Dordrecht, 173–196, https://doi.org/10.1007/978-94-007-6925-0_10, 2013.

Szczypta, C., Calvet, J.-C., Maignan, F., Dorigo, W., Baret, F., and Ciais, P.: Suitability of modelled and remotely sensed essential climate variables for monitoring Euro-Mediterranean droughts, Geosci. Model Dev., 7, 931–946, https://doi.org/10.5194/gmd-7-931-2014, 2014.

Teuling, A. J., Hirschi, M., Ohmura, A., Wild, M., Reichstein, M., Ciais, P., Buchmann, N., Ammann, C., Montagnani, L., Richardson, A. D., Wohlfahrt, G., and Seneviratne, S. I.: A regional perspective on trends in continental evaporation, Geophys. Res. Lett., 36, 1–5, https://doi.org/10.1029/2008GL036584, 2009.

Toreti, A. and Naveau, P.: On the evaluation of climate model simulated precipitation extremes, Environ. Res. Lett., 10, 014012, https://doi.org/10.1088/1748-9326/10/1/014012, 2015.

Tramblay, Y., Koutroulis, A., Samaniego, L., Vicente-Serrano, S. M., Volaire, F., Boone, A., Le Page, M., Llasat, M. C., Albergel, C., Burak, S., Cailleret, M., Kalin, K. C., Davi, H., Dupuy, J.-L., Greve, P., Grillakis, M., Hanich, L., Jarlan, L., Martin-StPaul, N., Martínez-Vilalta, J., Mouillot, F., Pulido-Velazquez, D., Quintana-Seguí, P., Renard, D., Turco, M., Türkeş, M., Trigo, R., Vidal, J.-P., Vilagrosa, A., Zribi, M., and Polcher, J.: Challenges for drought assessment in the Mediterranean region under future climate scenarios, Earth-Sci. Rev., 210, 103348, https://doi.org/10.1016/j.earscirev.2020.103348, 2020.

Ulbrich, U., Lionello, P., Belušić, D., Jacobeit, J., Knippertz, P., Kuglitsch, F. G., Leckebusch, G. C., Luterbacher, J., Maugeri, M., Maheras, P., Nissen, K. M., Pavan, V., Pinto, J. G., Saaroni, H., Seubert, S., Toreti, A., Xoplaki, E., and Ziv, B.: Climate of the Mediterranean, in: The climate of the Mediterranean region, edited by: Lionello, P., Elsevier insights, Elsevier Science, Amsterdam, 301–346, https://doi.org/10.1016/B978-0-12-416042-2.00005-7, 2012.

van der Molen, M. K., Dolman, A. J., Ciais, P., Eglin, T., Gobron, N., Law, B. E., Meir, P., Peters, W., Phillips, O. L., Reichstein, M., Chen, T., Dekker, S. C., Doubková, M., Friedl, M. A., Jung, M., van den Hurk, B., de Jeu, R., Kruijt, B., Ohta, T., Rebel, K. T., Plummer, S., Seneviratne, S. I., Sitch, S., Teuling, A. J., van der Werf, G. R., and Wang, G.: Drought and ecosystem carbon cycling, Agr. Forest Meteorol., 151, 765–773, https://doi.org/10.1016/j.agrformet.2011.01.018, 2011.

van der Wiel, K., Selten, F. M., Bintanja, R., Blackport, R., and Screen, J. A.: Ensemble climate-impact modelling: extreme impacts from moderate meteorological conditions, Environ. Res. Lett., 15, 034050, https://doi.org/10.1088/1748-9326/ab7668, 2020.

van Oijen, M., Beer, C., Cramer, W., Rammig, A., Reichstein, M., Rolinski, S., and Soussana, J.-F.: A novel probabilistic risk analysis to determine the vulnerability of ecosystems to extreme climatic events, Environ. Res. Lett., 8, 015032, https://doi.org/10.1088/1748-9326/8/1/015032, 2013.

van Oijen, M., Balkovi, J., Beer, C., Cameron, D. R., Ciais, P., Cramer, W., Kato, T., Kuhnert, M., Martin, R., Myneni, R., Rammig, A., Rolinski, S., Soussana, J.-F., Thonicke, K., van der Velde, M., and Xu, L.: Impact of droughts on the carbon cycle in European vegetation: a probabilistic risk analysis using six vegetation models, Biogeosciences, 11, 6357–6375, https://doi.org/10.5194/bg-11-6357-2014, 2014.

Verger, A., Baret, F., and Weiss, M.: Near Real-Time Vegetation Monitoring at Global Scale, IEEE Journal of Selected Topics in Applied Earth Observations and Remote Sensing, 7, 3473–3481, https://doi.org/10.1109/JSTARS.2014.2328632, 2014.

Verger, A., Baret, F., and Weiss, M.: Copernicus Global Land Operations "Vegetation and Energy" "CGLOPS-1": Algorithm Theorethical Basis Document: Leaf Area Index (LAI) Fraction of Absorbed Photosynthetically Active Radiation (FAPAR) Fraction of green Vegetation Cover (FCover) Collection 1 km Version 2 Issue I1.41, Copernicus Global Land Operations, available at: https://land.copernicus.eu/global/products/fapar (last access: 5 November 2021), 2019.

Vicente-Serrano, S. M., Gouveia, C., Camarero, J. J., Beguería, S., Trigo, R., López-Moreno, J. I., Azorín-Molina, C., Pasho, E., Lorenzo-Lacruz, J., Revuelto, J., Morán-Tejeda, E., and Sanchez-Lorenzo, A.: Response of vegetation to drought time-scales across global land biomes, P. Natl. Acad. Sci. USA, 110, 52–57, https://doi.org/10.1073/pnas.1207068110, 2013.

Vicente-Serrano, S. M., McVicar, T. R., Miralles, D. G., Yang, Y., and Tomas-Burguera, M.: Unraveling the influence of atmospheric evaporative demand on drought and its response to climate change, WIREs Climate Change, 11, e632, https://doi.org/10.1002/wcc.632, 2020.

Vogel, J.: Ecosystem_vulnerability, GitLab [code], available at: https://gitup.uni-potsdam.de/joschavogel/ecosystem_vulnerability, last access: 5 November 2021.

Vogel, J., Paton, E., Aich, V., and Bronstert, A.: Increasing compound warm spells and droughts in the Mediterranean Basin, Weather and Climate Extremes, 32, 100312, https://doi.org/10.1016/j.wace.2021.100312, 2021.

von Buttlar, J., Zscheischler, J., Rammig, A., Sippel, S., Reichstein, M., Knohl, A., Jung, M., Menzer, O., Arain, M. A., Buchmann, N., Cescatti, A., Gianelle, D., Kiely, G., Law, B. E., Magliulo, V., Margolis, H., McCaughey, H., Merbold, L., Migliavacca, M., Montagnani, L., Oechel, W., Pavelka, M., Peichl, M., Rambal, S., Raschi, A., Scott, R. L., Vaccari, F. P., van Gorsel, E., Varlagin, A., Wohlfahrt, G., and Mahecha, M. D.: Impacts of droughts and extreme-temperature events on gross primary production and ecosystem respiration: a systematic assessment across ecosystems and climate zones, Biogeosciences, 15, 1293–1318, https://doi.org/10.5194/bg-15-1293-2018, 2018.

Weißhuhn, P., Müller, F., and Wiggering, H.: Ecosystem Vulnerability Review: Proposal of an Interdisciplinary Ecosystem Assessment Approach, Environ. Manag., 61, 904–915, https://doi.org/10.1007/s00267-018-1023-8, 2018.

West, H., Quinn, N., and Horswell, M.: Remote sensing for drought monitoring & impact assessment: Progress, past challenges and future opportunities, Remote Sens. Environ., 232, 111291, https://doi.org/10.1016/j.rse.2019.111291, 2019.

Wolf, S., Keenan, T. F., Fisher, J. B., Baldocchi, D. D., Desai, A. R., Richardson, A. D., Scott, R. L., Law, B. E., Litvak, M. E., Brunsell, N. A., Peters, W., and van der Laan-Luijkx, I. T.: Warm spring reduced carbon cycle impact of the 2012

US summer drought, P. Natl. Acad. Sci. USA, 113, 5880–5885, https://doi.org/10.1073/pnas.1519620113, 2016.

Wu, D., Zhao, X., Liang, S., Zhou, T., Huang, K., Tang, B., and Zhao, W.: Time-lag effects of global vegetation responses to climate change, Glob. Change Biol., 21, 3520–3531, https://doi.org/10.1111/gcb.12945, 2015.

Zdruli, P.: Desertification in the Mediterranean region, in: Mediterranean Yearbook, edited by: IEMed, Girona, 250–254, available at: https://www.iemed.org/med-yearbook/iemed-mediterranean-yearbook-2011/ (last access: 5 November 2021), 2011.

Zeng, F.-W., Collatz, G., Pinzon, J., and Ivanoff, A.: Evaluating and Quantifying the Climate-Driven Interannual Variability in Global Inventory Modeling and Mapping Studies (GIMMS) Normalized Difference Vegetation Index (NDVI3g) at Global Scales, Remote Sens., 5, 3918–3950, https://doi.org/10.3390/rs5083918, 2013.

Zhang, H. and Oweis, T.: Water–yield relations and optimal irrigation scheduling of wheat in the Mediterranean region, Agr. Water Manag., 38, 195–211, https://doi.org/10.1016/S0378-3774(98)00069-9, 1999.

Zhang, L., Jiao, W., Zhang, H., Huang, C., and Tong, Q.: Studying drought phenomena in the Continental United States in 2011 and 2012 using various drought indices, Remote Sens. Environ., 190, 96–106, https://doi.org/10.1016/j.rse.2016.12.010, 2017.

Zhang, Y., Xiao, X., Zhou, S., Ciais, P., McCarthy, H., and Luo, Y.: Canopy and physiological controls of GPP during drought and heat wave, Geophys. Res. Lett., 43, 3325–3333, https://doi.org/10.1002/2016GL068501, 2016.

Zscheischler, J., Mahecha, M. D., Harmeling, S., and Reichstein, M.: Detection and attribution of large spatiotemporal extreme events in Earth observation data, Ecol. Inform., 15, 66–73, https://doi.org/10.1016/j.ecoinf.2013.03.004, 2013.

Zscheischler, J., Reichstein, M., von Buttlar, J., Mu, M., Randerson, J. T., and Mahecha, M. D.: Carbon cycle extremes during the 21st century in CMIP5 models: Future evolution and attribution to climatic drivers, Geophys. Res. Lett., 41, 8853–8861, https://doi.org/10.1002/2014GL062409, 2014.

Zscheischler, J., Orth, R., and Seneviratne, S. I.: A submonthly database for detecting changes in vegetation-atmosphere coupling, Geophys. Res. Lett., 42, 9816–9824, https://doi.org/10.1002/2015GL066563, 2015.

Zscheischler, J., Westra, S., van den Hurk, B. J. J. M., Seneviratne, S. I., Ward, P. J., Pitman, A., AghaKouchak, A., Bresch, D. N., Leonard, M., Wahl, T., and Zhang, X.: Future climate risk from compound events, Nat. Clim. Change, 8, 469–477, https://doi.org/10.1038/s41558-018-0156-3, 2018.

Chapter 4

Identifying meteorological drivers of extreme impacts: an application to simulated crop yields

Johannes Vogel, Pauline Rivoire, Cristina Deidda, Leila Rahimi, Christoph A. Sauter, Elisabeth Tschumi, Karin van der Wiel, Tianyi Zhang and Jakob Zscheischler

Earth System Dynamics, 12, 151–172, https://doi.org/10.5194/esd-12-151-2021, 2021

Earth Syst. Dynam., 12, 151–172, 2021
https://doi.org/10.5194/esd-12-151-2021

Earth System Dynamics
Open Access

Identifying meteorological drivers of extreme impacts: an application to simulated crop yields

Johannes Vogel[1,2,★], **Pauline Rivoire**[3,4,★], **Cristina Deidda**[5], **Leila Rahimi**[5,6], **Christoph A. Sauter**[7], **Elisabeth Tschumi**[3,8], **Karin van der Wiel**[9], **Tianyi Zhang**[10], **and Jakob Zscheischler**[3,8,11]

[1]Institute of Environmental Science and Geography, University of Potsdam, Potsdam, Germany
[2]Institute of Ecology, Technical University of Berlin, Berlin, Germany
[3]Oeschger Centre for Climate Change Research, University of Bern, Bern, Switzerland
[4]Institute of Geography, University of Bern, Bern, Switzerland
[5]Department of Civil and Environmental Engineering, Politecnico di Milano, Milan, Italy
[6]Department of Water Engineering, University of Tabriz, Tabriz, Iran
[7]Department of Civil and Environmental Engineering, University of Strathclyde, Glasgow, UK
[8]Climate and Environmental Physics, University of Bern, Bern, Switzerland
[9]Royal Netherlands Meteorological Institute (KNMI), De Bilt, the Netherlands
[10]Institute of Atmospheric Physics, Chinese Academy of Sciences, Beijing, China
[11]Department of Computational Hydrosystems, Helmholtz Centre for Environmental Research – UFZ, Leipzig, Germany
★These authors contributed equally to this work.

Correspondence: Johannes Vogel (joschavogel@uni-potsdam.de), Pauline Rivoire (pauline.rivoire@giub.unibe.ch), and Tianyi Zhang (zhangty@post.iap.ac.cn)

Received: 1 July 2020 – Discussion started: 27 July 2020
Revised: 1 December 2020 – Accepted: 28 December 2020 – Published: 10 February 2021

Abstract. Compound weather events may lead to extreme impacts that can affect many aspects of society including agriculture. Identifying the underlying mechanisms that cause extreme impacts, such as crop failure, is of crucial importance to improve their understanding and forecasting. In this study, we investigate whether key meteorological drivers of extreme impacts can be identified using the least absolute shrinkage and selection operator (LASSO) in a model environment, a method that allows for automated variable selection and is able to handle collinearity between variables. As an example of an extreme impact, we investigate crop failure using annual wheat yield as simulated by the Agricultural Production Systems sIMulator (APSIM) crop model driven by 1600 years of daily weather data from a global climate model (EC-Earth) under present-day conditions for the Northern Hemisphere. We then apply LASSO logistic regression to determine which weather conditions during the growing season lead to crop failure. We obtain good model performance in central Europe and the eastern half of the United States, while crop failure years in regions in Asia and the western half of the United States are less accurately predicted. Model performance correlates strongly with annual mean and variability of crop yields; that is, model performance is highest in regions with relatively large annual crop yield mean and variability. Overall, for nearly all grid points, the inclusion of temperature, precipitation and vapour pressure deficit is key to predict crop failure. In addition, meteorological predictors during all seasons are required for a good prediction. These results illustrate the omnipresence of compounding effects of both meteorological drivers and different periods of the growing season for creating crop failure events. Especially vapour pressure deficit and climate extreme indicators such as diurnal temperature range and the number of frost days are selected by the statistical model as relevant predictors for crop failure at most grid points, underlining their overarching relevance. We conclude that the LASSO regression model is a useful tool to automatically detect compound drivers of extreme impacts and could be applied to other weather impacts such as wildfires or floods. As the detected relationships are of

purely correlative nature, more detailed analyses are required to establish the causal structure between drivers and impacts.

1 Introduction

Climate extremes such as droughts, heatwaves, floods and frost events can have substantial impacts on crop health (Shah and Paulsen, 2003; Singh et al., 2011; Lesk et al., 2016; Ben-Ari et al., 2018). However, not all climate extremes lead to an extreme impact, and large impacts can be related to moderate drivers (Zscheischler et al., 2016; Van der Wiel et al., 2019a, 2020; Pan et al., 2020). Whether a large impact occurs does not only depend on a climate hazard but also on the vulnerability of the underlying system (Oppenheimer et al., 2015), which varies strongly for crops during the course of the growing season (Iizumi and Ramankutty, 2015; Ben-Ari et al., 2018). The mechanisms that translate a climate hazard into crop failure are often very complex and associated with lagged effects that are difficult to disentangle (Frank et al., 2015).

While climate extremes may lead to large impacts, extreme climate-related impacts are often the result of multiple contributing factors (Tschumi and Zscheischler, 2020). The concept of compound events has recently been promoted to address climate impacts from an impact-centred perspective. For instance, compound events have been defined as extreme impacts that depend on multiple statistically dependent drivers (Leonard et al., 2014) or, more recently, simply as the combination of multiple drivers that contributes to environmental or societal risk (Zscheischler et al., 2018). Drivers in this context refer to climate and weather processes and phenomena. With respect to yields at the local scale, multiple drivers can compound an impact through a sequence of weather events (temporally compounding); one weather event may also change the vulnerability of the crop to a subsequent weather event (preconditioning), or multiple drivers may interact and impact crops at the same time (multivariate events) (Zscheischler et al., 2020).

Understanding the drivers that lead to extreme impacts helps to better predict and mitigate the potential impacts of such events. One way of identifying the relevant drivers of an impact is to perform a bottom-up analysis, that is, start from an impact and identify key drivers through statistical analysis (Zscheischler et al., 2013; Ben-Ari et al., 2018). In this context, linear regression analysis can identify the most relevant drivers of an impact variable and reveal potential interactions between drivers (Forkel et al., 2012; Ben-Ari et al., 2018). More sophisticated approaches such as random forests might yield higher predictive power at the cost of losing explainability (Vogel et al., 2019). When the set of possible predictors is very large, suitable variable selection approaches need to be applied to reduce the number of predictors. In order to be applicable to a large number of locations and a variety of impacts, an automatic approach is desired that only requires a limited amount of expert knowledge and parameter tuning. An example of such an approach is the least absolute shrinkage and selection operator (Tibshirani, 1996), or short LASSO regression, which obtains a reduced number of predictors by penalizing the number of variables in the loss function.

The aim of this study is to present a method that can identify drivers of extreme impacts in an automatic manner and that is suitable for many applications. We use crop failure as an example of an extreme impact in a model environment; that is, we use simulated data from a climate and a crop model. End-of-season crop yield is related to climate drivers via highly complex interactions at different temporal scales. Temperature and precipitation are the two basic climate variables that regulate crop health (Lobell and Asner, 2003; Lobell et al., 2011; Leng et al., 2016). Furthermore, vapour pressure deficit (VPD), the difference of water vapour pressure at saturated condition and its actual value at a given temperature, determines crop photosynthesis and water demand (Rawson et al., 1977; Zhang et al., 2017; Yuan et al., 2019).

Here, we use 1600 years of wheat yield data from a global gridded crop model driven by simulated meteorological data under present-day conditions. Based on this large database of yield data, we showcase approaches to identify multiple drivers of crop failure in different regions of the world and highlight results for the LASSO regression. Using a model environment to explore new analytical approaches to identify drivers of extreme impacts, we circumvent common limitations associated with observational data, such as a small sample size, measurement uncertainties and data coverage. Among the large amount of information provided by the crop model simulations, the statistical model summarizes the link between crop failure and climate conditions.

This paper is structured as follows. The data and methods used in this study are introduced in Sect. 2. In this section, the reader can first find a description of the data, including an introduction to the global climate model and the crop model used in this study. We further describe which meteorological variables are considered in the statistical analysis; Sect. 2 also introduces the LASSO logistic regression to predict years of low yield based on meteorological drivers and the metrics employed to assess the performance of the statistical model. The results of the LASSO regression are shown in Sect. 3, where the performance and the summary statistics for the variables that have been selected as being critical to predict crop failure events are presented. Finally, we summarize and discuss the LASSO regression's results in Sect. 4 and give some perspective to this study in Sect. 5.

2 Data and methods

2.1 Climate and crop model simulations

To investigate the influence of natural variability and climatic extreme events, a large ensemble simulation experiment was set up with the EC-Earth global climate model (v2.3; Hazeleger et al., 2012). We use this climate model data set, consisting of 2000 years of present-day simulated weather, to investigate if we can identify the drivers of extreme low crop yield seasons. Large ensemble modelling is at the forefront of climate science (Deser et al., 2020); due to the computational expenses involved, a balance between ensemble size, horizontal resolution and number of climate models has to be found. We have found the climate data used here to be suitable for the present study. A detailed description of these climate simulations is provided in Van der Wiel et al. (2019b); here, we provide a short overview of the experimental setup. The present day was defined as the 5-year model period in which the simulated global mean surface temperature matched that observed in 2011–2015 (HadCRUT4 data; Morice et al., 2012). Because of a cold bias in EC-Earth, in the model this period is 2035–2039. To create the large ensemble, 25 ensemble members were branched off from 16 long transient climate runs (forced by Representative Concentration Pathway (RCP) 8.5). Each ensemble member was integrated for 5 years. Differences between ensemble members were forced by choosing different seeds in the atmospheric stochastic perturbations (Buizza et al., 1999). This resulted in a total of $16 \times 25 \times 5 = 2000$ years of meteorological data at T159 horizontal resolution (approximately 1°).

Biases in the EC-Earth simulations result in unrealistic growing conditions for crops. Therefore, minimum and maximum temperatures and precipitation fields were bias corrected. The Agricultural Model Intercomparison and Improvement Project (AgMIP) Modern-Era Retrospective Analysis for Research and Applications (AgMERRA) reanalysis (Ruane et al., 2015) was used as "truth". From AgMERRA, the years 1981–2010 were used as a training set, while EC-Earth uses the long transient runs (16 times for 2005–2034). Daily minimum and maximum temperatures were corrected on a grid point basis; a model bias field was defined as the difference between the model climatology and the AgMERRA climatology. The climatology was defined to be the mean plus the first three annual harmonics. Daily precipitation was corrected towards having the correct number of rainy days and total amount of precipitation. Firstly, for each month, the number of rainy days in AgMERRA was computed (threshold of $0.1\,\mathrm{mm\,d^{-1}}$); then the same threshold was determined for EC-Earth data, which resulted in the same number of rainy days. All days with simulated precipitation lower than this threshold were set to $0\,\mathrm{mm\,d^{-1}}$. Lastly, the total amount of precipitation was corrected by means of a multiplicative factor, also on a month-by-month basis. Other meteorological variables were not bias corrected.

Northern Hemisphere winter wheat yields were simulated using the Agricultural Production Systems sIMulator (APSIM)-Wheat model (Zheng et al., 2014), which is a process-based model incorporating wheat physiology, water and nitrogen processes under a wide range of growing conditions. It was previously used for field (Li et al., 2014), regional (Asseng et al., 2013) and global-scale (Rosenzweig et al., 2014) wheat studies. A grid-point-specific sowing date was used based on Sacks et al. (2010). The application of nitrogen was exacted from Mueller et al. (2012). Soil parameters (including pH, soil total nitrogen, organic carbon content, bulk density and soil moisture characteristics curves for each of five 20 cm deep soil layers) were derived from the International Soil Profile Data Set (Batjes, 2012). In addition, we also input the grid-specific thermal time accumulation parameters, which were derived from phenology (Sacks et al., 2010) and AgMERRA data. The atmospheric CO_2 concentration was set to 394 ppm. The growing season of winter wheat spans 2 calendar years (e.g. sowing in November and harvest in June). As such, each climate model integration of 5 years covers four winter-wheat-growing seasons; the 2000 years of EC-Earth climate data thus result in 1600 simulated wheat-growing seasons. Further details on the settings of the APSIM-Wheat model can be found in Appendix A. For model validation, the grid-based wheat yield simulations were aggregated to country level and then validated against the yield statistics during 2011–2015 (FAOSTAT, 2020). Most simulated yields are closely related to observed yields (Fig. B1), indicating good model performance.

2.2 Data processing

The APSIM model provided crop data for 995 grid points in the Northern Hemisphere. For our analysis, we chose to discard all grid points for which the annual mean yield is below the 10th percentile of annual mean yield across all grid points because many of these grid points were also associated with unrealistically long (> 365 d) or short (< 90 d) growing seasons, or had an overall average crop yield of $0\,\mathrm{kg\,ha^{-1}\,yr^{-1}}$. Overall, 895 grid points remained for the analysis.

At each grid point, a year with yield lower than the 5th percentile for this grid point is considered as a year with crop failure and called "bad year" in the remainder, whereas all other years are referred to as "normal years". Grid points for which the 5th percentile yield was equal to 0 were excluded to avoid the co-occurrence of years without yield in the bad and normal years. This excluded six more grid points so that 889 remained for further analysis. Figure 1a shows the simulated mean annual yield, and Fig. 1b displays the relative difference between the 5th percentile and the mean annual yield. These two figures also indicate grid points that were discarded for further analysis. Finally, we discarded individual years with a growing season longer than 365 d, leading to a slightly lower number of years than 1600 for 82 grid points, i.e. for about 5 % of the grid points.

The data were split into training and testing data sets by randomly assigning 70 % of the data to the former and 30 % to the latter. For the logistic regression (Sect. 2.4), explanatory variables and yield were normalized by rescaling them to a range of $[-1, 1]$ for each grid point individually.

2.3 Explanatory data analysis

The APSIM model uses six meteorological variables on a daily basis as input – dew-point temperature (T_d), precipitation (Pr), 10 m wind speed (Wind), incoming shortwave radiation (Rad), maximum temperature (T_max) and minimum temperature (T_min). From these variables, we additionally calculated VPD as an important variable for plant growth (Rawson et al., 1977; Zhang et al., 2017; Yuan et al., 2019). For a given grid point, the sowing date is the same for the 1600 simulated years, but the harvest dates differ. We therefore define the growing season for a given grid point as starting on the month containing the sowing date and finishing with the month containing the latest harvest date. Figure 2 illustrates the temporal evolution of composites of these seven variables over the course of a growing season for normal (blue) and bad years (red) for one grid point in France (47.7° N, 1.1° E; Fig. 2a). The composites provide some indication about which of the meteorological variables may contribute to crop failure. In addition, the temporal evolution of the two composites reveals during which part of the growing season the different variables are relevant. The various composites suggests that, for this grid point, 30 d Pr, VPD and T_max during the summer (June–August) have a high impact on crop yield (Fig. 2c, f and h). The other variables appear to be less relevant (Fig. 2b, d, e and g). Similar composites for grid points in the US (44.3° N, 90.0° W) and in China (30.8° N, 118.1° E) are shown in Figs. B2 and B3, respectively.

In addition to the seven meteorological variables, we considered seven climate extreme indicators as potential predictors of crop failure (mean diurnal temperature range, dtr; number of frost days, frs; maximum temperature, TXx; minimum temperature, TNn; maximum five day precipitation sum, Rx5day; number of warm days, TX90p; number of cold days, TN10p; following Vogel et al., 2019) (Table 1). For both the monthly means of the meteorological variables and the growing season means/totals of the indicators of climate extremes, we calculated the Pearson correlation coefficient between the variables and annual yield (Fig. 3a and b for the same grid point as in Figs. 2 and 3c and d as average correlation over all grid points). These correlations are computationally and conceptually very simple, and together with Fig. 2, they serve as a first estimation of the importance of the available variables. Some variables, such as wind speed, do not have a discernible influence on yield and thus can be neglected for this study. We use monthly means of T_max, Pr and VPD during the growing season, as well as the seven extreme indicators for further analysis.

2.4 LASSO regression

The aim of this study is to provide an interpretable statistical model that is able to predict years with extremely low yields (bad years) with meteorological variables. We use the LASSO (Tibshirani, 1996) logistic regression for an automatic selection of meteorological variables that are statistically linked to low yields. The approach is explained below.

For a given grid point, let $Y \in \{0, 1\}^n$ be the binary yield vector, with n the number of years. If the year $i \in \{1, \ldots, n\}$ is a bad year, then $Y_i = 1$; otherwise, $Y_i = 0$. Let $\boldsymbol{X}_1, \ldots, \boldsymbol{X}_p \in \mathbb{R}^n$ be the explanatory variables vectors (monthly meteorological variables and climate extreme indicators, rescaled as explained in Sect. 2.2). Using a generalized linear model and, more specifically, a logistic regression, we can identify how much of the occurrence of bad yields is explained by which explanatory variable:

$$\mathbb{P}[Y = 1] = \frac{1}{1 + \exp\left(\beta_0 + \beta_1 \boldsymbol{X}_1 + \ldots + \beta_p \boldsymbol{X}_p\right)}, \tag{1}$$

where $\beta_0, \beta_1, \ldots, \beta_p$ are the regression coefficients.

However, a simple logistic regression presents two challenges here. Firstly, some variables might be highly correlated (e.g. correlation between temperature in May and temperature in June, or the correlation of extreme indices with meteorological variables). This correlation implies a high variability of the coefficients. For instance, if the variables $\boldsymbol{X}_j$ and $\boldsymbol{X}_k$ are highly correlated, the information brought by a high absolute value of β_j and a low absolute value of β_k might be the same as the information brought by a low absolute value of β_j and a high absolute value of β_k. Another issue is the large number of potential explanatory variables (up to 43 for some grid points). The relatively straightforward relationship of a generalized linear model (simpler than the crop model equations themselves) allows us to reveal which meteorological variables explain bad yields best. However, if the number of a priori explanatory variables is very large, the regression becomes rather complex and many coefficients will be close to zero, rendering an interpretation difficult.

LASSO regression tackles both challenges with an automatic variable selection using a regularization by penalizing the number of coefficients different from 0 using the ℓ_1 norm on the vector of coefficients (Tibshirani, 1996). Thus, the regression coefficients are obtained by minimizing an objective function consisting of the sum of the usual loss function for logistic regression and a penalty term on the coefficient norm:

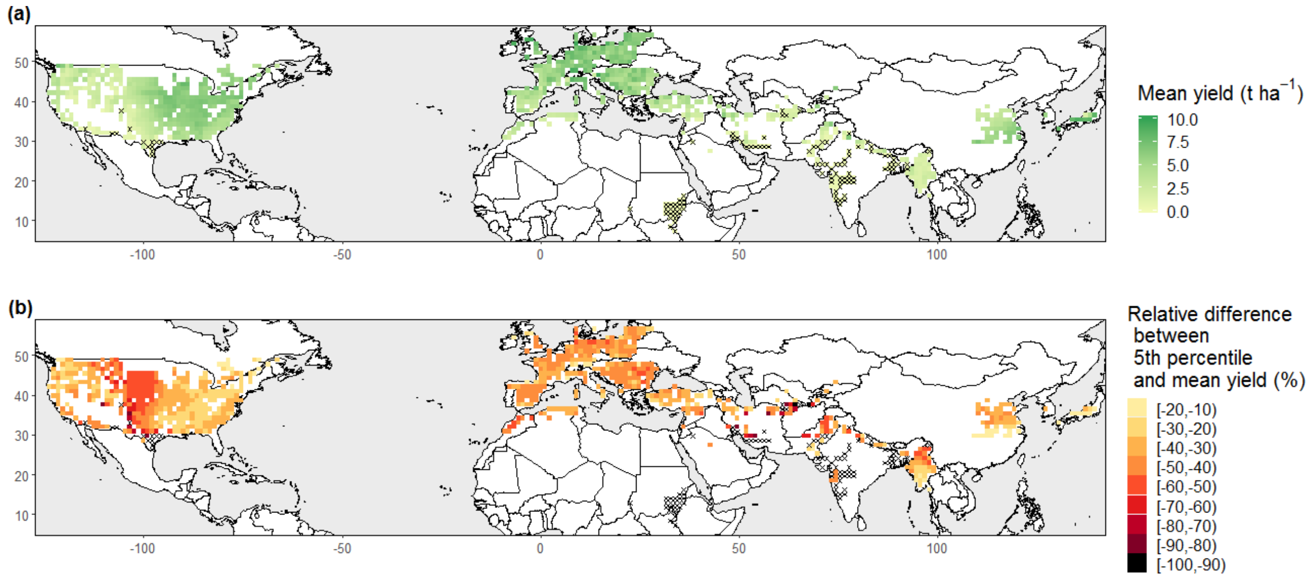

Figure 1. **(a)** Mean annual yield over the 1600 years (t ha^{-1}). **(b)** Relative difference between the 5th percentile and the mean annual yield. Grid points discarded for our study are crossed out (specified in Sect. 2.2).

Table 1. Meteorological drivers used in the analysis.

Variable name	Description	Type
T_{max}	Maximum temperature	Monthly mean
VPD	Vapour pressure deficit	Monthly mean
Pr	Precipitation	Monthly mean
dtr	Mean diurnal temperature range in the growing season	Climate extreme indicator
frs	Number of frost days in the growing season	Climate extreme indicator
TXx	Maximum temperature in the growing season	Climate extreme indicator
TNn	Minimum temperature in the growing season	Climate extreme indicator
Rx5day	Maximum 5 d precipitation sum in the growing season	Climate extreme indicator
TX90p	Number of warm days in the growing season with daily maximum temperature above the 90th percentile*	Climate extreme indicator
TN10p	Number of cold days in the growing season with daily minimum temperature below the 10th percentile*[a]	Climate extreme indicator

* Note: percentiles are grid point based; i.e. they are representative of the local climate.

$$\min_{(\beta_0,\boldsymbol{\beta})\in\mathbb{R}^{p+1}} -\left[\frac{1}{n}\sum_{i=1}^{n} y_i\left(\beta_0+\boldsymbol{x}_i^T\boldsymbol{\beta}\right) - \log\left(1+e^{\beta_0+\boldsymbol{x}_i^T\boldsymbol{\beta}}\right)\right]+\lambda\|\boldsymbol{\beta}\|_1, \qquad (2)$$

for a fixed $\lambda > 0$. The penalty term on the coefficient norms prevents a high variability of these coefficients. Furthermore, the ℓ_1 norm implies a variable selection. Coefficients associated with non-relevant explanatory variables are set to 0.

We use the R package `glmnet` (Friedman et al., 2010) to perform the LASSO regression with R version 3.6 (R Core Team, 2019). Through 10-fold cross-validation in the training data set, we obtain the optimal λ_{min} and $\lambda_{1SE} = \lambda_{min} + SE$ with "SE" the standard error of the lambda that achieves the minimum loss, and the coefficients $\boldsymbol{\beta} = (\beta_1, \ldots, \beta_p)$, which is the solution to the optimization in Eq. (2) for $\lambda = \lambda_{1SE}$. Our preference for $\lambda = \lambda_{1SE}$ is motivated by the balance between number of selected variables and accuracy of the loss function minimization (Friedman et al., 2010; Krstajic et al.,

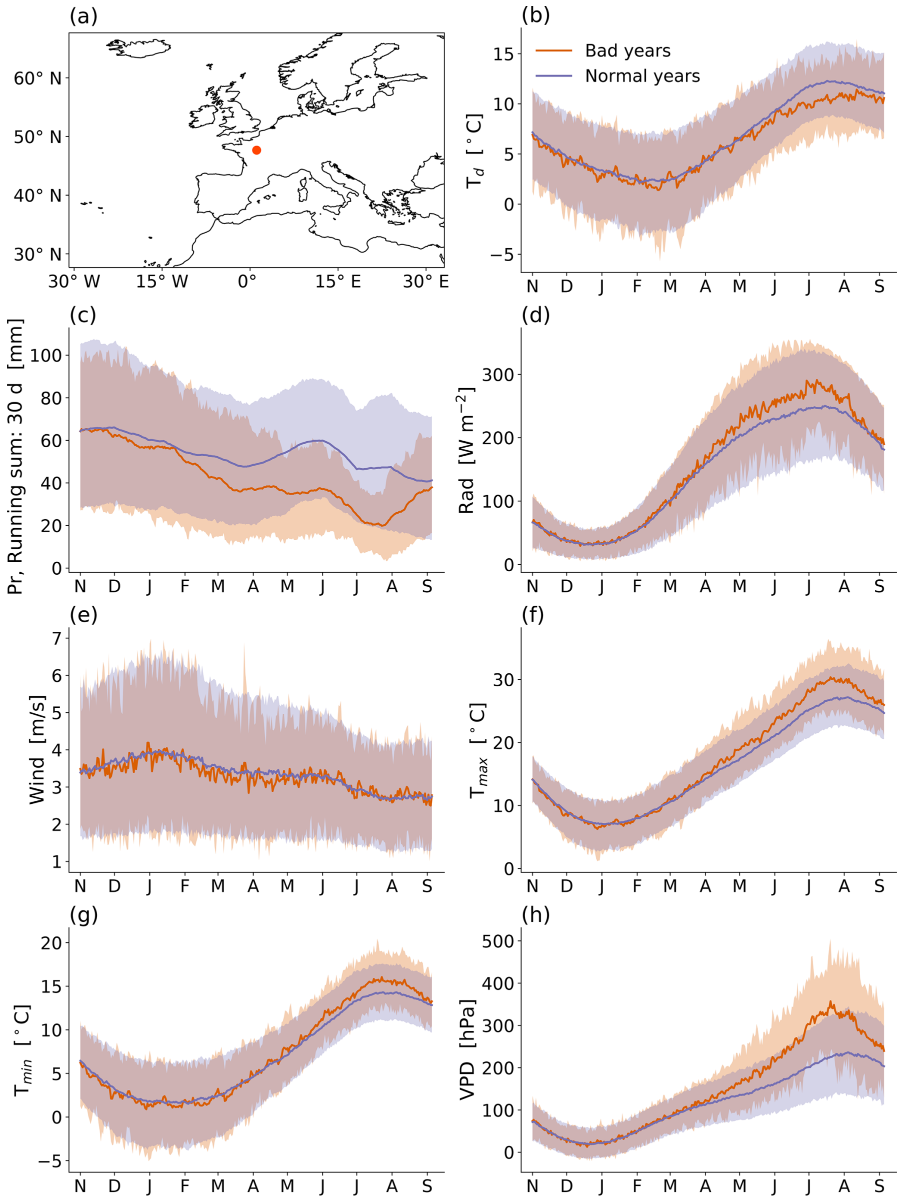

Figure 2. Daily evolution of meteorological variables used as input for the APSIM model over the course of the year for an exemplary grid point in France (47.7° N, 1.1° E; shown as a red dot in panel **a**). Red lines indicate the composite mean of the bad years (80 seasons); blue lines indicate the composite mean of the normal years (1520 seasons). Shading shows the range between the 10th and 90th percentiles of the respective years. Variables shown are **(b)** dew-point temperature, **(c)** 30 d running sum of precipitation, **(d)** incoming shortwave radiation, **(e)** wind speed, **(f)** maximum temperature, **(g)** minimum temperature and **(h)** vapour pressure deficit.

2014). Indeed, less variables are selected with λ_{1SE} than with λ_{min}, because $\lambda_{1SE} > \lambda_{min}$ and thus the penalty term on the norm of coefficient is stronger, but the minimization of the Eq. (2) is still sensible, because λ_{1SE} lies within the uncertainty range of the optimal λ.

2.5 Other models

To compare the performance of the LASSO regression with other regression methods we also perform the analysis with a generalized linear model (GLM) and a random forest binary classification.

For the application of the GLM, a pre-selection of the initial variables is required, since the number of predictors is limited. Only the variables with the highest Pearson correla-

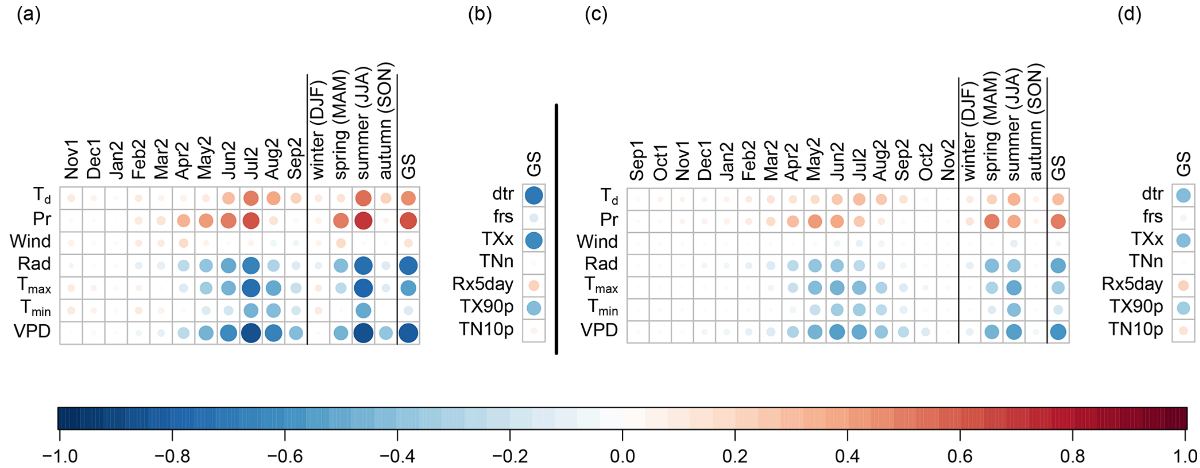

Figure 3. Linear correlations between potential meteorological predictors and annual yield. **(a)** Correlation between the monthly, seasonal and growing season (GS) averages of the meteorological variables and annual yield for a grid point in France (47.7° N, 1.1° E). **(b)** Correlation of the climate extreme indicators (Table 1) and annual yield for the same grid point. **(c, d)** Average of the same correlations across all Northern Hemisphere grid points. Note that panel **(a)** shows the correlation for all months included in the growing season of the grid point in France, while panel **(c)** shows the average correlation for a given month computed over all grid points containing this month in their growing season.

tion coefficients ($\rho > 0.30$) were selected as initial predictors from an initial data set composed of all months of the growing season for each of the three variables (T_{max}, Pr and VPD) and the seven extreme indicators. Next, the subset of best predictor variables is identified with the leaps algorithm (Furnival and Wilson, 1974). We use the implementation of the R package `bestGLM` (McLeod et al., 2020), using a binomial family with a logit link function. Overall, GLM achieves lower performance (Sect. 2.7) compared to the LASSO logistic regression (not shown). The weaknesses of this approach include its sensitivity to outliers and multicollinearity, and overfitting.

Finally, a random forest approach – a common machine learning technique – was also performed using the R package `randomForest` (Breiman, 2001; Liaw and Wiener, 2002) serving as a benchmark for the model performance of the LASSO logistic regression. The random forest binary classification achieves comparable performance (Sect. 2.7) but is not superior to the LASSO approach.

2.6 Segregation threshold adjustment

The segregation threshold for assigning a continuous prediction to either a bad or normal year was adjusted in a grid-point-wise manner to account for the unbalanced data set with 19-fold higher occurrences of normal years than bad years. Let s be the local segregation threshold between a bad year predicted and a good year predicted. In other words, if the probability $p = \mathbb{P}[Y = 1]$ predicted for a given grid point by the LASSO logistic regression model is greater or equal to s (lower than s), then the year is predicted as a bad year (normal year). We want to choose s as a good compromise in prediction of normal years and bad years, given that bad years are rare. In other words, we want to find an optimal trade-off between specificity and sensitivity. To this purpose, a cost function $\mathcal{C} = \mathcal{C}(s)$ is calculated based on the false positive rate $R_{FP} = R_{FP}(s)$, the associated cost for a false positive instance $\mathcal{C}_{FP}$, the sum of observed normal years O_{NY}, the false negative rate $R_{FN} = R_{FN}(s)$, the associated cost for a false negative instance $\mathcal{C}_{FN}$ and the sum of observed bad years O_{BY} of the training data set (Hand, 2009). A false positive means that a normal year was observed while a bad year was predicted, and a false negative refers to the observation of a bad year, whereas a normal year was predicted. For a given grid point, FP, FN, TP and TN denote the total number of false positives, false negatives, true positives and true negatives, respectively (Fig. 4). The value of $\mathcal{C}(s)$ is given by

$$\mathcal{C}(s) = R_{FP}(s)\mathcal{C}_{FP}O_{NY} + R_{FN}(s)\mathcal{C}_{FN}O_{BY}, \quad (3)$$

where $R_{FP} = \frac{FP}{FP+TN}$, $R_{FN} = \frac{FN}{FN+TP}$ and $\mathcal{C}_{FP} = \mathcal{C}_{FN} = 100$. In this study, the costs associated with false positive $\mathcal{C}_{FP}$ and false negatives $\mathcal{C}_{FN}$ are given equal weight.

The optimal segregation threshold s^* for a given grid point is $s^* = \text{argmin}_{s\in(0,1)}\mathcal{C}(s)$. The segregation threshold selected in this study is the mean value of s^* over all grid points.

2.7 Model performance assessment and sensitivity analysis

Model performance is assessed using the critical success index (CSI). The CSI is frequently used for evaluating the prediction of rare events, as it neglects the number of correct predictions of non-extremes, which dominate the confusion matrix (Mason, 1989). General performance measures such as the misclassification error are biased by the high number

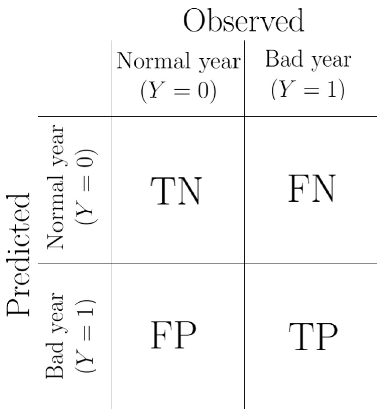

Figure 4. Confusion matrix for classification of observed and predicted normal and bad years.

of normal years and are therefore not meaningful for the assessment of model performance in unbalanced data sets with under-represented extreme events. The CSI is defined as

$$\mathrm{CSI} = \frac{\mathrm{TP}}{\mathrm{TP} + \mathrm{FP} + \mathrm{FN}}. \tag{4}$$

To evaluate the robustness of our model, in addition to the 5th percentile threshold, we repeated the analysis with thresholds of 2.5 % and 10 %, reaching qualitatively similar performance. In addition to the normalization by rescaling the data to the interval $[-1, 1]$, we also performed a z-score transformation, which yielded comparable results. Therefore, our choice of normalization is arbitrary to a degree and a z-score transformation can potentially also be applied in the LASSO logistic regression model. Moreover, we applied two more combinations of splitting training and testing data sets: a 60/40 and an 80/20 split. With increasing size of the training data set, the CSI increased slightly, however, at the expense of stochastic under-representation of bad yield years in the smaller testing data sets. As a trade-off, we decided for the 70/30 split.

The adjustment of the segregation threshold was carried out with equal weight to false positive and false negative predictions. It can be argued that the latter case – where a normal year is predicted, but crop failure is observed – is more detrimental and should therefore be given a higher weight. Due to the subjectivity in the determination of this weight, an adjustment of the weight term was not applied. However, it should be noted that the attribution of a higher weight of false negative predictions would yield a lower segregation threshold and hence improve the overall CSI.

3 Results

3.1 Overall performance

The LASSO logistic regression model can predict bad years with an average CSI = 0.43 across all grid points. Best performance is obtained in the eastern half of the United States with a maximum of CSI = 0.82 (Fig. 5), which decreases westwards in the Great Plains and is lowest in the wheat-growing regions located close to the Rocky Mountains. Furthermore, especially the most northern and southwestern grid points in North America show a lower performance in general. Also central Europe shows high performance up to CSI = 0.80. A notable regional exception with low performance can be found in the Alps. Many Asian and African growing regions show medium prediction accuracy such as northern China, Myanmar, Turkey and the Maghreb, with exceptions of some regions including Pakistan, southern China and Japan, which show a low performance in general. For 30 grid points, it is not possible to obtain reasonable predictions of bad years with our approach, indicated by a CSI equal to 0. Overall, regions with high prediction accuracy of bad years are often those that also have high mean yields (Fig. 1). CSI is positively correlated with mean yield with a Pearson correlation coefficient of $\rho = 0.46$ (Fig. 6a); an even stronger correlation is found with yield variability ($\rho = 0.57$) (Fig. 6b).

3.2 Explanatory variables

Here, we summarize properties of the variables selected by the LASSO logistic regression as relevant explanatory variables, i.e. those which are statistically linked to bad years. A median of 11 variables per grid point has been selected as explanatory variables, and for 50 % of grid points the number of selected variables lies between 7 and 14 (Fig. 7a). The inclusion of extreme indicators provides a useful addition to the monthly predictors, shown by a median number of two selected extreme indicators per grid point (Fig. 7b). Grid points without extreme indicators are found only in few areas such as eastern Europe, the Alps and southern China. In total, 72 % of all grid points include monthly predictors of VPD, Pr and T_{max}, and almost all grid points (97 %) incorporate VPD (Fig. 7c). Interestingly, in the Great Plains (USA), in many cases temperature is not included, whereas in most other regions of the US all meteorological variables are selected to achieve a good prediction. In southern China, temperature is not needed by the models, whereas in the northern areas, usually all meteorological variables are part of the model. In most wheat-growing regions, particularly in the northeastern US, southeastern Europe and Turkey, all four seasons contain relevant predictors for predicting bad years (Fig. 7d). Generally, the number of seasons included decreases towards the southeastern regions in the US, whereas in western Europe no clear pattern emerges. In lower latitudes such as in southern Asia, growing seasons are generally shorter (Fig. B4), and consequently often only predictors from one or two seasons are included in the respective models.

At the global scale, VPD in May and June, as well as Pr in April, are the predictors which are most often included in

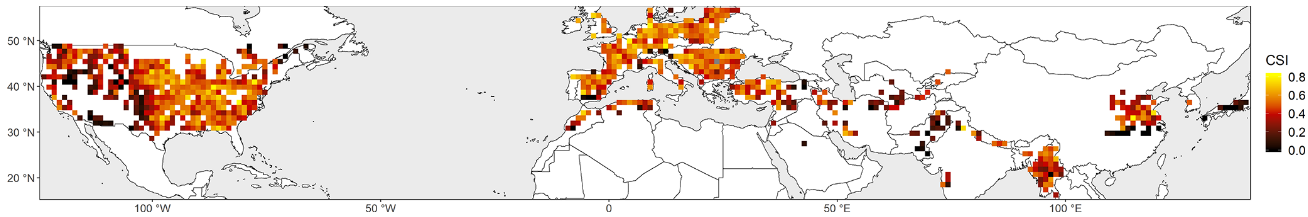

Figure 5. Critical success index (CSI; Eq. 4) of the LASSO logistic regression model (see Sect. 2.7 for definition).

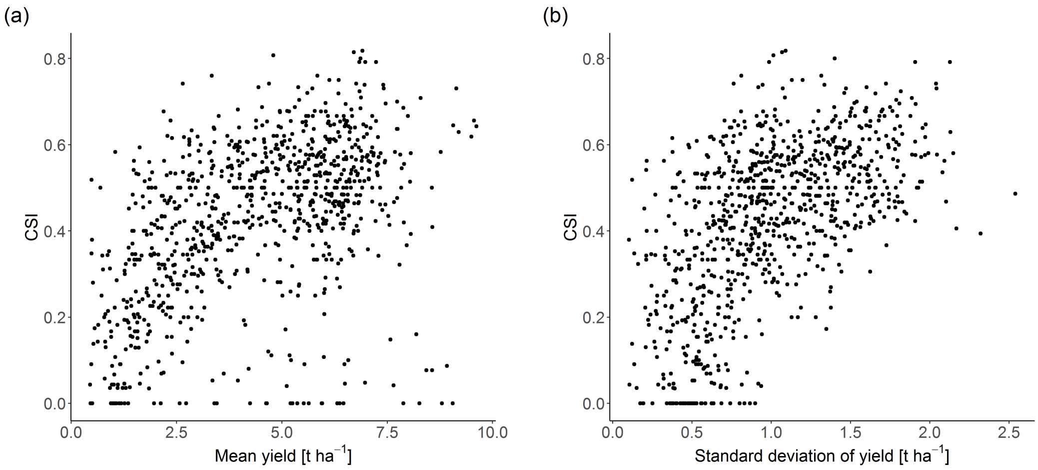

Figure 6. Correlation between CSI and annual crop yield mean and variability for the 889 grid points included in the LASSO logistic regression model. **(a)** Scatterplot between CSI and mean annual yield. **(b)** Scatterplot between CSI and annual yield standard deviation.

the LASSO regression, followed by the climate extreme indicators diurnal temperature range (dtr) and number of frost days (frs) (Fig. 8a). In nearly all cases, the sign of the coefficient is positive for VPD in May and June, and negative for Pr in April. This implicates that higher VPD increases the risk of crop failure and is similar for the other variables. In North America and Europe, in addition to dtr and frs, VPD and Pr in spring to early summer are the most frequent monthly predictors (Fig. 8b and c). The growing season for wheat varies with latitude. Consequently, in more northern regions, mostly in Europe and North America, monthly predictors from the months between March and July are included in the LASSO regression, whereas in southern regions such as in Asia and Africa, November to May are usually the most frequent months (Fig. 8d).

This clear latitudinal shift can be visually identified in North America from February to July, especially for VPD (see maps in the Supplement). In central Europe, the growing season ends latest; thus, VPD in August is usually included in the model. In addition to the most common climate extreme indicators, dtr and frs, Rx5day and TXx are among the most frequent predictors in Asia and North America, respectively. Overall, frs is mostly included in northern grid points, with notable exceptions in western Europe (Fig. B5a) and mainly with a positive coefficient (higher frs leads to more crop failure events), which can likely be attributed to the influence of mild maritime climate in those regions. In contrast, dtr is important in most Asian grid points and especially in western Europe and the Maghreb, whereas in the Pannonian Basin and Turkey it is a less common predictor (Fig. B5b). The coefficient associated with dtr in the LASSO regression is mainly positive, except in parts of India and Myanmar. Some variability in the mean diurnal temperature range might be beneficial for regions close to the Equator where the variability in diurnal temperature is usually low. Generally, both low and high dtr values can influence wheat yield beneficially depending on the growing region; e.g. a low dtr can be advantageous because of a reduced occurrence of frost days, whereas a higher dtr might also indicate a favourable effect because of increased solar radiation (Lobell, 2007). Rx5day is predominant in the western US, the western Mediterranean and central Asia (Fig. B5c), which are all growing regions with comparably low average annual precipitation. TX90p is a common variable in low latitudes with a positive coefficient, especially in the southern US and Myanmar (Fig. B5d). This indicates that in these regions physiological temperature thresholds are occasionally exceeded, making TX90p a crucial variable in these areas.

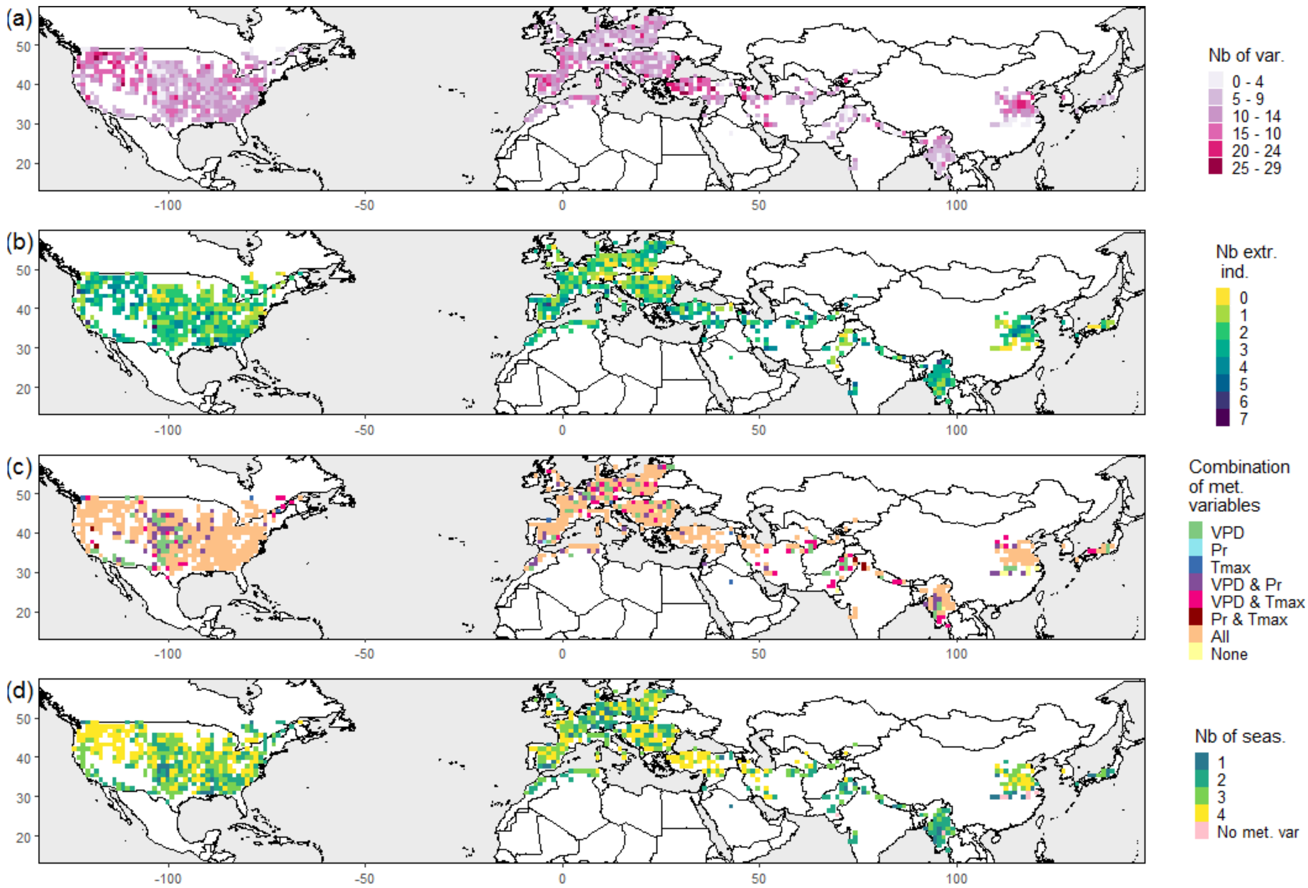

Figure 7. Maps illustrating the selected predictors by the LASSO logistical regression. **(a)** Total number of selected variables. **(b)** Number of selected climate extreme indicators. **(c)** Combination of selected meteorological variables. "None" means that only climate extreme indicators were selected; "All" means that at least 1 month from each of the three meteorological variables (VPD, Pr, $T_{\max}$) is selected. **(d)** Number of selected seasons (out of the four seasons – DJF, MAM, JJA, SON).

4 Discussion

4.1 Predicting bad yield years

In this study, we presented a method for identifying drivers of extreme impacts using crop failure as an example. Such approaches are highly sought after to identify compound drivers of large impacts (Zscheischler et al., 2020; Van der Wiel et al., 2020). Our method allows us to investigate potential drivers at a global scale using a highly automated scheme based on LASSO regression. The benefits of LASSO regression include its usage for automatic variable selection, its consideration of correlation between explanatory variables and its performance. Moreover, the statistical model obtained provides a logistic linear relationship between crop failure and selected variables, which is much simpler to interpret than the crop model equations themselves or results obtained with more complex machine learning approaches.

We defined bad years as years where the annual crop yield is below the 5th percentile and were able to predict those years by using the LASSO regression with an average CSI of 0.43. This means that on average, the sum of the numbers of false positives and false negatives is slightly higher than the number of true positives (or accurate predictions of bad years). Our model performance is somewhat comparable to results from Vogel et al. (2019), who were able to explain 46 % of variation in spring wheat anomalies using a similar set of predictors based on a random forest algorithm. In our case, more sophisticated machine learning regression models such as random forests did not yield better prediction skill, indicating that performance in the current setup using monthly predictors for a binary classification of bad years likely cannot be much improved. This is probably also related to the fact that predicting extremes of a continuous variable is challenging because no natural separation between extremes and non-extremes exists. Another challenge arises from the highly asymmetric distribution of observed bad and normal years. Even though in our case the total amount of samples per grid point is relatively large (1600, because we

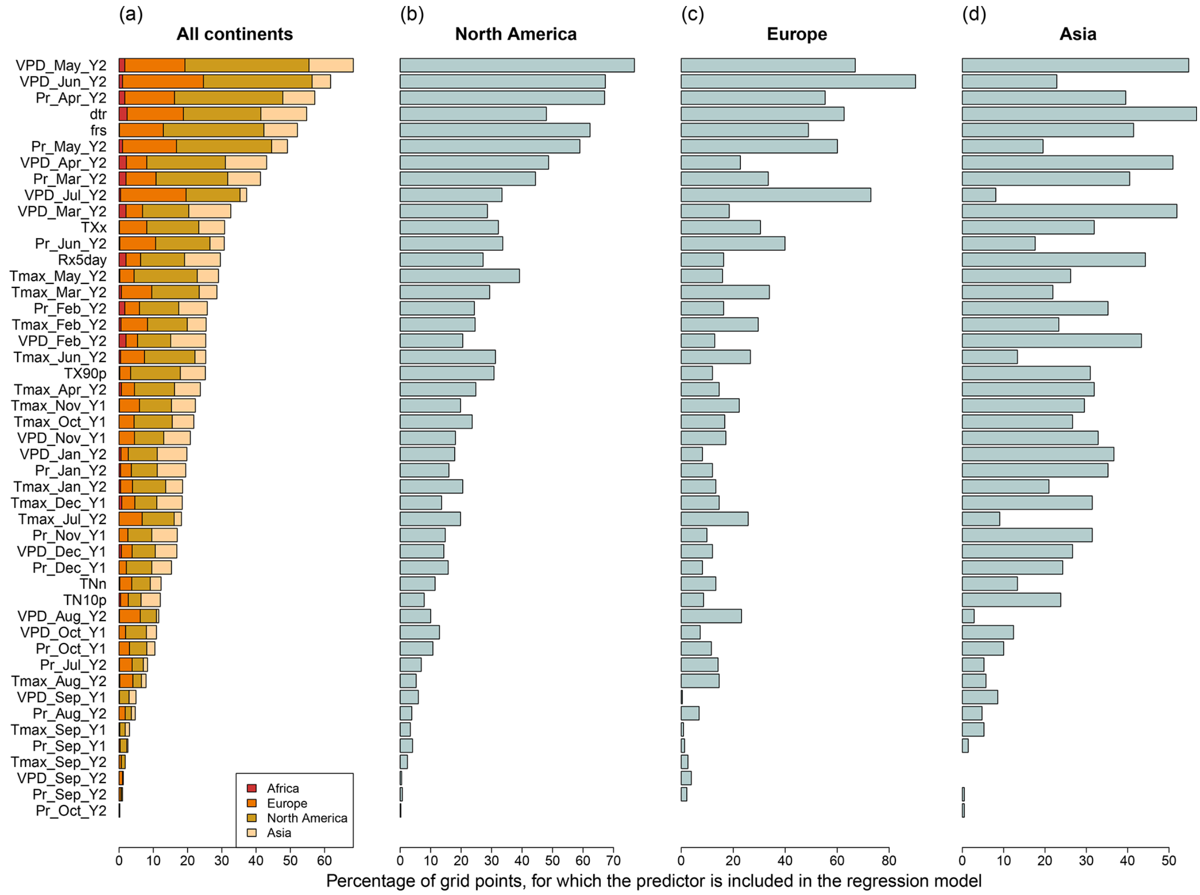

Figure 8. For each possible predictor, we show the percentage of grid points for which this predictor has a non-zero coefficient in the LASSO logistic regression. **(a)** All continents (889 grid points in total), **(b)** North America (419 grid points), **(c)** Europe (233 grid points) and **(d)** Asia (210 grid points). The extension "Y1" means that the respective month belongs to the first calendar year of the growing season, while "Y2" means it belongs to the second calendar year of the growing season.

used simulated crop yield data) the number of observed bad years is only 80 and thus can still be considered fairly small.

We analysed the robustness of our results using (a) the 10th percentile as a threshold to discriminate between bad and normal years and (b) a smaller data subset with only 400 entries per grid point (i.e. a quarter of the available data). The spatial patterns of the selected predictors and the CSI using the 10th percentile threshold are very similar compared to those of the 5th percentile, and the average CSI increases slightly from 0.43 to 0.52. Using a sample size of 400 we still obtain an average CSI of 0.33, indicating that performance decreases only slightly with decreasing data size, while the spatial patterns remain consistent (results not shown). Furthermore, the spatial coherence of our results (Fig. 7) additionally suggests robustness of our analysis. An application of the approach on real data might still be challenging, as observational sample sizes generally are much smaller than even 400 years. In addition, observational data are often not available at such spatial resolution and extent as is the case for the crop model data used in this study. This will make it difficult to use spatial coherence of the identified drivers as an indicator of model robustness when using observational data. Furthermore, modelling winter wheat yield is particularly challenging due to its long growing season (Vogel et al., 2019).

A limitation to our study design is the pre-selection of potential predictor variables. Here, we used monthly mean values and a number of climate extreme indicators. More flexible averaging time periods for the predictors might result in higher prediction accuracy due to better overlap with sensitive periods of the impact variable. For instance, in our crop yield example, meteorological predictors need to coincide with the respective phenological development stage because their impact can vary depending on the phenophase. Wheat, for example, is known to require wet conditions in the vegetative phase; however, it prefers dry conditions during ripening (Seyfert, 1960). Therefore, the application of monthly meteorological predictors might be insufficient for accurate matching of meteorological drivers to the respective phenological phases. We explored the option of automatically generating optimal time periods for the meteorological predictors by maximizing the difference between the composites between normal and bad years. For instance, 30 d cumulative precipitation differs between normal and bad years starting in February and ending in August for a grid point in France (Fig. 2c), whereas VPD only differs from May to September (Fig. 2h). Composite plots for a grid point in the US and in China are shown in Figs. B2 and B3, respectively. However, deciding when the separation between normal and bad years is large enough to start and end the optimal time periods is challenging and difficult to generalize and thus automate, which was the aim of our method design. Nevertheless, such a well-tuned selection of predictors has the potential to improve the prediction of bad years significantly and should thus be explored in future research.

We find a strong correlation of the yearly mean and standard deviation of annual yield with the LASSO regression performance indicator CSI (Fig. 6). Low model performance at grid points with low yield variability suggests that the distinction between normal and bad years is challenging at these locations, e.g. in southern China and Japan (Figs. 1b and 5). Regions with high annual yield are found primarily in central Europe and the eastern half of the United States, which also represent the regions with highest model performance. In contrast, many regions in Asia generally have lower average yields and lower prediction skill of bad years. This could be related to a calibration bias in the crop model, leading to a better representation of wheat-growing processes in regions where wheat reaches higher yields in the real world. A further explanation for this phenomenon could be that the crop model is primarily designed for crop growth at typical environmental conditions, whereas growing regions with conditions at the edge of the ecological niche of wheat might be less well represented.

Our analysis was based on fitting a local model at each location, which is one of the three principal statistical methods used to link crop yield with weather conditions, along with cross-section models and panel models, which are global models that adjust for spatial variability using fixed or random effects (Lobell and Burke, 2010; Shi et al., 2013). Collinearity between explanatory variables is a recurrent issue when using these methods (Shi et al., 2013) that we addressed with the LASSO regression. One example is VPD and T_{max}, which might be highly correlated but still might individually contribute relevant information because they have a different impact on the plant process, as explained in Kern et al. (2018). LASSO regression did not completely discard one of these two variables, despite their high correlation.

4.2 Important predictors

For most grid points, VPD is the most important monthly predictor of bad years, followed by Pr and T_{max}, in that order. While their importance in time differs between grid points, depending on the timing of the respective growing season (Sippel et al., 2016), their order changes little across space. In addition, the order of importance of extreme indicators is quite similar in North America, Europe and Asia. One notable distinction is the higher importance of Rx5day in Asian grid points compared to North America and Europe. The consistent selection of similar predictors across large spatial scales may suggest that the LASSO regression is fairly robust. However, this may also be related to the inevitable simplifications of crop-growing processes in the employed crop model. In particular, the same model is applied at all locations, likely creating certain homogeneity by default. Kern et al. (2018) conducted a comparable analysis on observed winter wheat crop yield in Hungary. With a linear regression using a step-wise selection of monthly meteorological variables, they found that a positive anomaly in VPD and T_{min} during May decreases yield. Additionally, April, May and June appear to be the most relevant months in our global analysis, which is consistent with regional studies (Kern et al., 2018; Kogan et al., 2013; Ribeiro et al., 2020).

Climate extreme indicators are important predictors as the occurrence of an extreme weather event may induce crop failure in a given year. However, in years without such extreme events, crop yields are still governed by the weather during the growing season (Iizumi and Ramankutty, 2015). We found that both climate extreme indicators as well as monthly means of common climate variables have proven to be valuable predictors of years resulting in crop failure. Droughts and heatwaves are well known to affect crop yield (Lesk et al., 2016; Jagadish et al., 2014), and temperature and precipitation explain a large fraction of interannual crop yield variability (Lobell and Burke, 2008). In contrast, VPD is often overlooked in statistical analyses of crop yield variability (Zhang et al., 2017). We show that VPD is a key predictor for crop failure. It is known to play a crucial role in plant functioning and is projected to increase as main limiting driver in the face of climate change (Novick et al., 2016; Grossiord et al., 2020). High VPD values can lead to plant mortality via carbon starvation and hydraulic failure (McDowell et al., 2011; Grossiord et al., 2020). However, its covariation with temperature and solar radiation makes it difficult to disentangle their respective effects (Stocker et al., 2019; Grossiord et al., 2020). There are well-defined temperature thresholds for wheat; e.g. a temperature of 31 °C before flowering is considered to evoke sterile grains and thus reduces yield (Porter and Gawith, 1999; Daryanto et al., 2016). T_{max} is a secondary predictor in our statistical model, which is in line with results based on observed and simulated yields (Schauberger et al., 2017), and can be attributed to the rare exceedance of critical temperature thresholds in the growing season. Crops are particularly vulnerable during key development stages, so extreme events during that time span can lead to large yield reductions, even in the event of otherwise favourable weather conditions during the growing season (Porter and Gawith, 1999; Moriondo and Bindi, 2007). The vulnerability of wheat to climatic events depends largely on phenophases, and generally wheat possesses a higher sensitivity to temperature and precipitation during its reproductive phase than during its vegetative phase (Porter and Gawith, 1999; Luo, 2011; Daryanto et al., 2016). Future research could investigate the importance of time of occurrence of extreme indicators (Vogel et al., 2019). For instance, due to climate change, false spring events may become more likely in some regions (Moriondo and Bindi, 2007; Allstadt et al., 2015), and thus the timing of frost days could provide a valuable addition to the model.

The frequent inclusion of the extreme indicators such as dtr and frs in our regression model highlights that short-term extreme events can potentially have larger impacts than gradual changes over time (Jentsch et al., 2007). The variable dtr was also identified as an important predictor by Vogel et al. (2019), whereas frs was of minor importance for explaining variation in spring wheat yield. By contrast, frs is one of the most predominant predictors in our study, which might be explained by the differing growing season of winter wheat, which is encompassing primarily the cold seasons.

We explored the relevance of interactions between predictors; however, this did not significantly improve model performance. This might hint at the inability of the APSIM crop model to account adequately for such compound effects, which is consistent with Ben-Ari et al. (2018), who linked the crop failure 2016 in France to an extraordinary combination of warm winter temperatures followed by wet spring conditions. The commonly used crop models employed for crop yield forecasts were not able to predict the 2016 yield failure in France (Ben-Ari et al., 2018).

Overall, our results illustrate the omnipresence of compounding meteorological events for crop failure. In nearly all grid points, most seasons and meteorological variables were relevant to predict years with crop failure (Fig. 7). This suggests that the co-occurrence of certain weather conditions as well as the combination of weather conditions in different seasons are associated with crop failure. With our approach we have identified meteorological conditions that are statistically linked to crop failure. Our results confirm prior findings by Van der Wiel et al. (2020) that such conditions are not necessarily extreme but can also be moderate. However, for interpretation of the selected variable set, one should be aware that the variables in our model are selected based on correlation, and thus attributing them as potential physical drivers needs further careful investigation. To identify such causal relationships, more advanced methods from the emerging field of causal inference could be employed (Runge et al., 2019).

5 Conclusions

In this paper, we presented a robust statistical approach – namely LASSO logistic regression – for predicting crop failure and automatically selecting relevant predictors among a large number of meteorological variables and climate extreme indicators. We illustrated our approach on 1600 years of simulated winter wheat yield for the Northern Hemisphere under present-day climate conditions. LASSO regression can serve as a tool for identifying important variables with automated variable selection while accounting for collinearity and achieving overall good predictive power. Consistent with earlier knowledge, we find that predicting crop failure requires accounting for a number of different meteorological drivers at different times of the growing season, which is illustrated by the large number of variables at all seasons included in our statistical model (Fig. 7). This indicates that compounding effects are ubiquitous across time and meteorological drivers, and highlights the usefulness of approaches such as LASSO regression to reveal multiple meteorological drivers of crop failure. We identified vapour pressure deficit as one key variable to predict crop failure, which underlines the importance of its consideration in statistical crop yield models, in particular because it is often overlooked in statistical analyses of crop yield variability. Furthermore, climate extreme indicators such as diurnal temperature range and the number of frost days have proven to be valuable additions to the predictive models, highlighting the necessity to address not only monthly mean conditions but especially also climatic extremes in such models. Overall, this study helps to enhance the knowledge required to improve seasonal forecasts and undertake adaptation measures against crop failure. The flexibility of our approach allows an application to other climate impacts that are influenced by a large range of variables varying with seasonality, for instance, wildfires or flooding.

Appendix A: APSIM-Wheat model settings

A total of 11 phenological phases are included in the APSIM-Wheat model, and the length of each phase is simulated based on thermal time accumulation, which is adjusted for other factors such as vernalization, photoperiod and nitrogen. To calculate thermal time, crown minimum (T_{cmin}) and maximum (T_{cmax}) temperatures are first simulated for non-freezing temperatures (T_{min} and T_{max}; Eqs. A1 and A2) and then used to compute the crown mean temperature (T_{c}; Eq. A3). Finally, daily thermal time ($\Delta\mathrm{TT}$) is calculated based on three cardinal temperatures (T_{base}, T_{opt} and T_{ceiling}; Eq. A4) (Zheng et al., 2014):

$$T_{\mathrm{cmax}} = \begin{cases} 2 + T_{\mathrm{max}}\left(0.4 + 0.0018(H_{\mathrm{snow}} - 15)^2\right) & T_{\mathrm{max}} < 0 \\ T_{\mathrm{max}} & T_{\mathrm{max}} \geq 0 \end{cases} \quad \text{(A1)}$$

$$T_{\mathrm{cmin}} = \begin{cases} 2 + T_{\mathrm{min}}\left(0.4 + 0.0018(H_{\mathrm{snow}} - 15)^2\right) & T_{\mathrm{min}} < 0 \\ T_{\mathrm{min}} & T_{\mathrm{min}} \geq 0 \end{cases} \quad \text{(A2)}$$

$$T_{\mathrm{c}} = \frac{(T_{\mathrm{cmin}} + T_{\mathrm{cmax}})}{2} \quad \text{(A3)}$$

$$\Delta\mathrm{TT} = \begin{cases} T_{\mathrm{c}} & T_{\mathrm{base}} < T_{\mathrm{c}} \leq T_{\mathrm{opt}} \\ \frac{T_{\mathrm{opt}}}{T_{\mathrm{base}}}\left(T_{\mathrm{ceiling}} - T_{\mathrm{c}}\right) & T_{\mathrm{opt}} < T_{\mathrm{c}} \leq T_{\mathrm{ceiling}} \\ 0 & T_{\mathrm{c}} \leq T_{\mathrm{base}} \text{ or } T_{\mathrm{c}} \geq T_{\mathrm{ceiling}}, \end{cases} \quad \text{(A4)}$$

where H_{snow} is set to 0, and T_{base}, T_{opt} and T_{ceiling} are set to 0, 26 and 34 °C, respectively.

The dry-matter above-ground biomass (ΔQ; Eq. A8) is calculated as a potential biomass accumulation resulting from radiation interception (ΔQ_{r}) and soil water deficiency (ΔQ_{w}) (Zheng et al., 2014). The radiation-limited dry-biomass accumulation (ΔQ_{r}; Eq. A6) is calculated by the intercepted radiation (I), radiation use efficiency (RUE), stress factor (f_{s}) and carbon dioxide factor (f_{c}). The stress factor (f_{s}) comprises stresses that crops may encounter during growth and is the minimum value of a temperature factor ($f_{T,\mathrm{photo}}$) and a nitrogen factor ($f_{\mathrm{N,photo}}$) (Eq. A5). The water-limited dry above-ground biomass (ΔQ_{w}; Eq. A7) is a function of radiation-limited dry above-ground biomass (ΔQ_{r}), the ratio between the daily water uptake (W_{u}) and demand (W_{d}):

$$f_{\mathrm{s}} = \min\left(f_{T,\mathrm{photo}}, f_{\mathrm{N,photo}}\right) \quad \text{(A5)}$$

$$\Delta Q_{\mathrm{r}} = I \cdot \mathrm{RUE} \cdot f_{\mathrm{s}} \cdot f_{\mathrm{c}} \quad \text{(A6)}$$

$$\Delta Q_{\mathrm{w}} = \Delta Q_{\mathrm{r}} \frac{W_{\mathrm{u}}}{W_{\mathrm{d}}} \quad \text{(A7)}$$

$$\Delta Q = \begin{cases} \Delta Q_{\mathrm{r}} & W_{\mathrm{u}} = W_{\mathrm{d}} \\ \Delta Q_{\mathrm{w}} & W_{\mathrm{u}} < W_{\mathrm{d}}. \end{cases} \quad \text{(A8)}$$

Appendix B: Additional figures

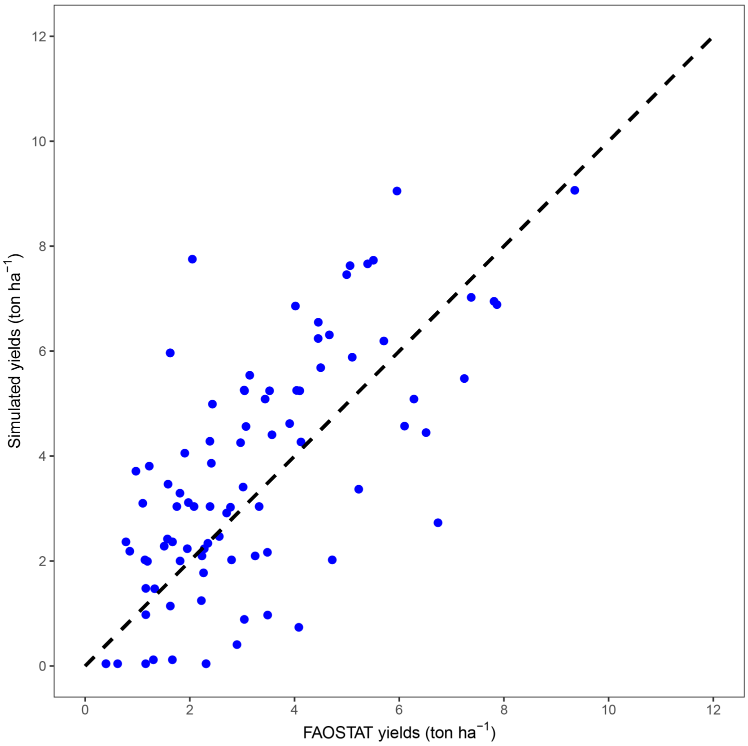

Figure B1. Comparison between the country-specific simulated yields and yield statistics (FAOSTAT, 2020). The dashed line is the 1 : 1 line.

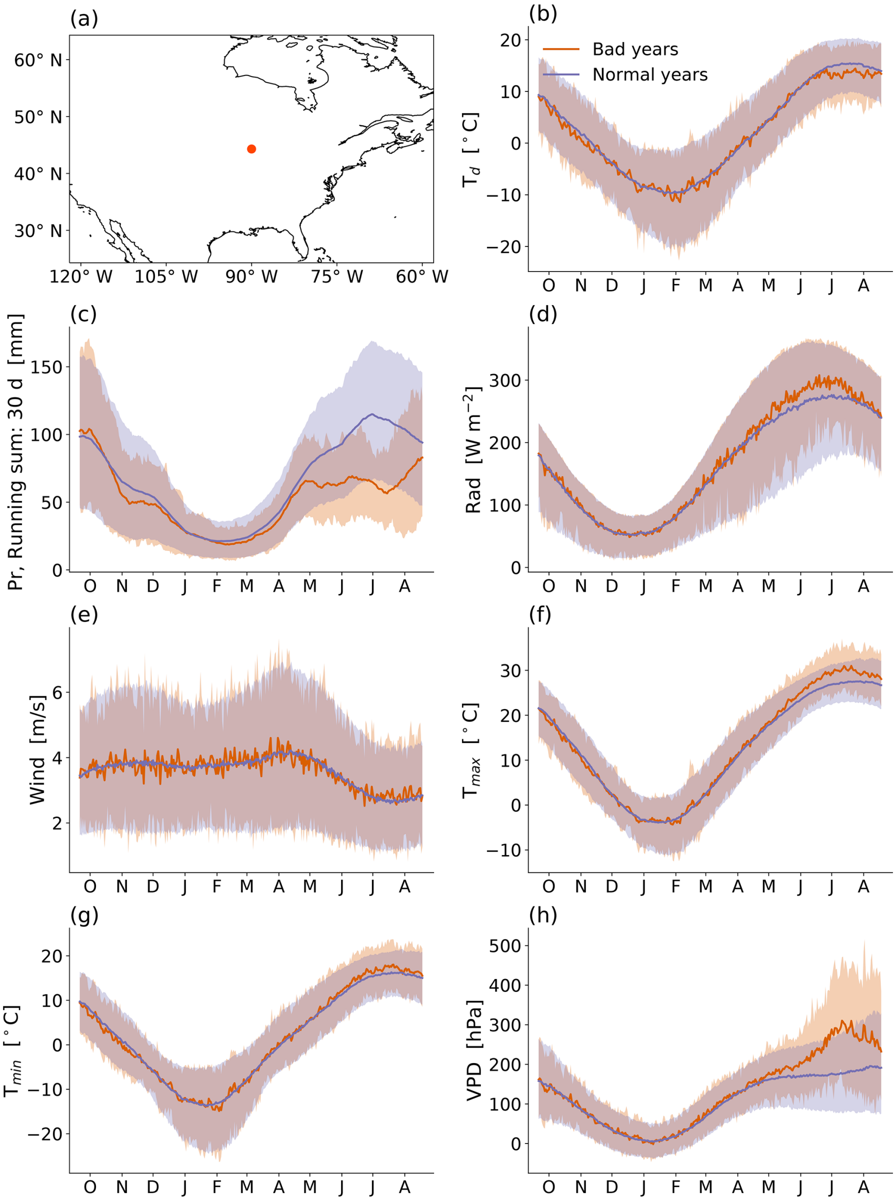

Figure B2. As Fig. 2 but for a grid point in the United States (44.3° N, 90.0° W).

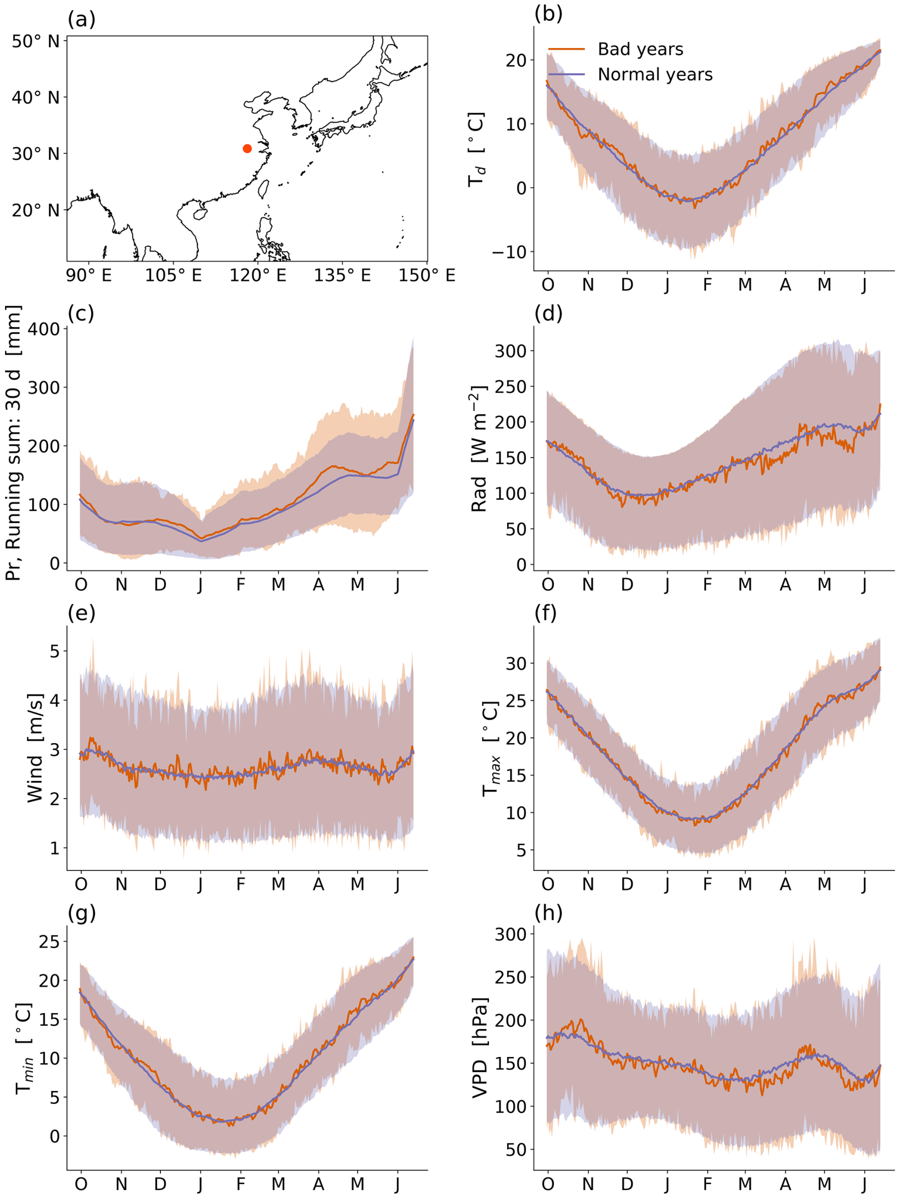

Figure B3. As Fig. 2 but for a grid point in China (30.8° N, 118.1° E).

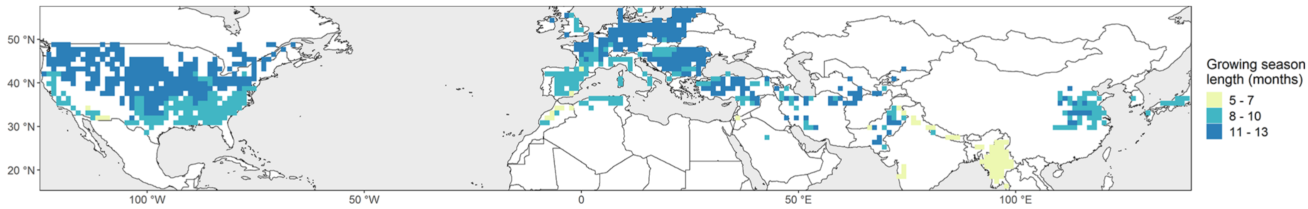

Figure B4. Number of months in the growing season (number of months between the earliest sowing date and the latest harvest date). The growing season starts at the month containing the sowing date and ends with the month containing the latest harvest date among the 1600 model years. We discarded years with harvest date later than 365 days after the sowing date. Some growing seasons are 13 months long because we include both the entire first month and the entire last month.

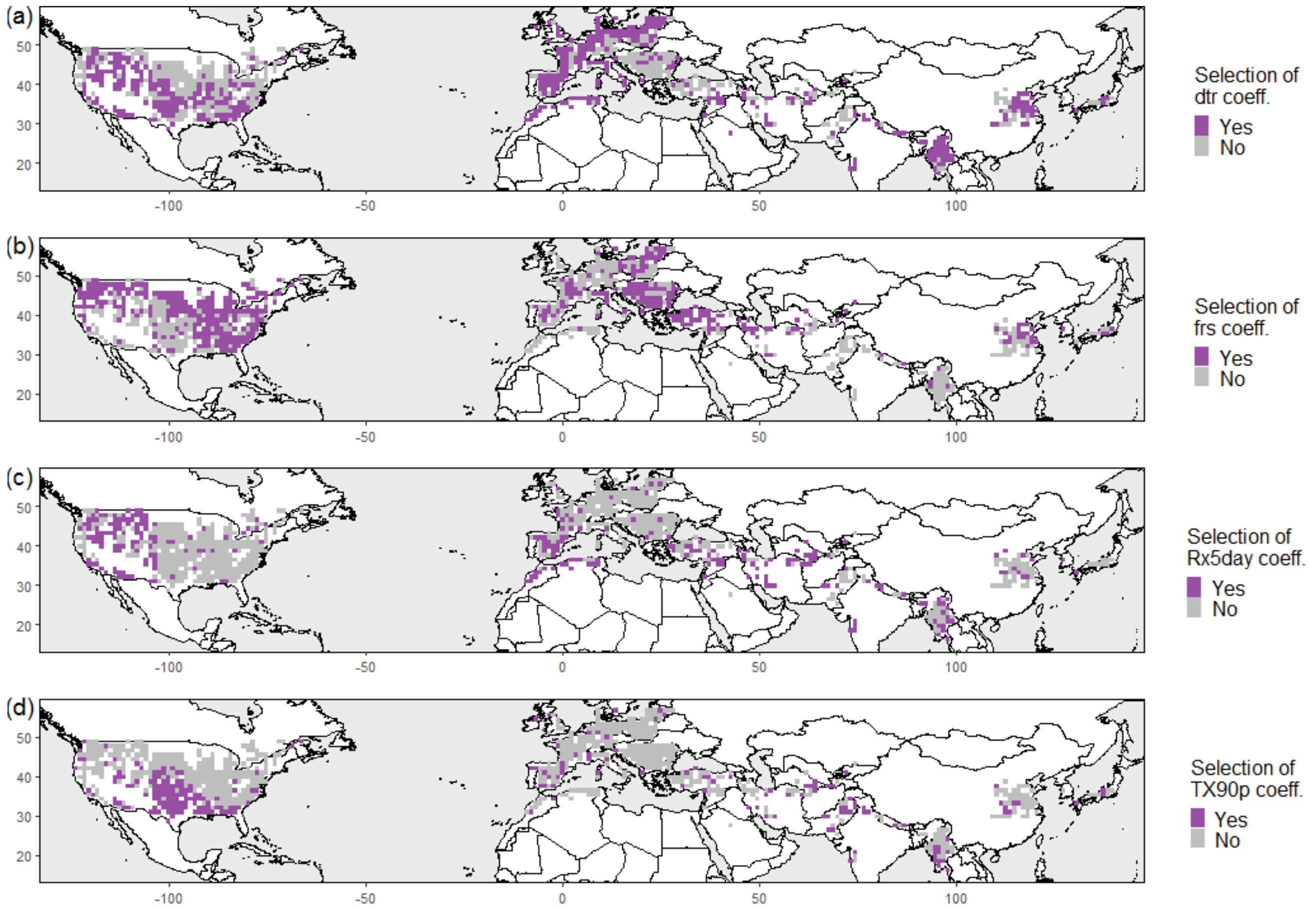

Figure B5. Selected climate extreme indicators (Table 1) in the LASSO logistic regression model for each location: dtr **(a)**, frs **(b)**, Rx5day **(c)** and TX90p **(d)**.

Code availability. The code to reproduce the figures is available from GitHub (https://github.com/jo-vogel/Identify_crop_yield_drivers, last access: February 2021) (Vogel et al., 2021).

Data availability. The climate and crop simulations are available from Karin van der Wiel (wiel@knmi.nl) and Tianyi Zhang (zhangty@post.iap.ac.cn) upon request, respectively.

Supplement. The Supplement contains monthly binary maps showing whether a specific predictor was included to predict crop failure by the LASSO logistic regression. Maps are provided for (a) VPD, (b) T_{max} and (c) Pr. The extension "Y1" means that the respective month belongs to the first calendar year of the growing season, while "Y2" means it belongs to the second calendar year of the growing season. The supplement related to this article is available online at: https://doi.org/10.5194/esd-12-151-2021-supplement.

Author contributions. JZ and KvdW conceived the project and supervised the work. JV and PR conducted most of the data analysis, including the LASSO logistic regression and creation of the key figures. KvdW performed the climate model simulations with EC-Earth. TZ performed the crop model simulations with APSIM. All authors contributed substantially to the data analysis, design of figures and writing of the manuscript.

Competing interests. The authors declare that they have no conflict of interest.

Special issue statement. This article is part of the special issue "Understanding compound weather and climate events and related impacts (BG/ESD/HESS/NHESS inter-journal SI)". It is not associated with a conference.

Acknowledgements. This work emerged from the Training School on Statistical Modelling organized by the European COST Action DAMOCLES (CA17109).

Financial support. This research has been supported by the DFG research training group "Natural Hazards and Risks in a Changing World" (grant no. GRK 2043), the EPSRC Doctoral Training Partnership (DTP) (grant no. EP/R513349/1), the Swiss National Science Foundation (grant nos. 178751, 179876, 189908), the Netherlands Organisation for Scientific Research (grant no. NWO AL45 WCL.2 016.2), the National Natural Science Foundation of China (grant no. NSFC 41661144006), the National Key Research and Development Project of China (grant no. 2019YFA0607402) and the Helmholtz Initiative and Networking Fund (Young Investigator Group COMPOUNDX; grant agreement no. VH-NG-1537).

Review statement. This paper was edited by Gabriele Messori and reviewed by Kai Kornhuber and two anonymous referees.

References

Allstadt, A. J., Vavrus, S. J., Heglund, P. J., Pidgeon, A. M., Thogmartin, W. E., and Radeloff, V. C.: Spring plant phenology and false springs in the conterminous US during the 21st century, Environ. Res. Lett., 10, 104008, https://doi.org/10.1088/1748-9326/10/10/104008, 2015.

Asseng, S., Ewert, F., Rosenzweig, C., Jones, J. W., Hatfield, J. L., Ruane, A. C., Boote, K. J., Thorburn, P. J., Rötter, R. P., Cammarano, D., Brisson, N., Basso, B., Martre, P., Aggarwal, P. K., Angulo, C., Bertuzzi, P., Biernath, C., Challinor, A. J., Doltra, J., Gayler, S., Goldberg, R., Grant, R., Heng, L., Hooker, J., Hunt, L. A., Ingwersen, J., Izaurralde, R. C., Kersebaum, K. C., Müller, C., Naresh Kumar, S., Nendel, C., O'Leary, G., Olesen, J. E., Osborne, T. M., Palosuo, T., Priesack, E., Ripoche, D., Semenov, M. A., Shcherbak, I., Steduto, P., Stöckle, C., Stratonovitch, P., Streck, T., Supit, I., Tao, F., Travasso, M., Waha, K., Wallach, D., White, J. W., Williams, J. R., and Wolf, J.: Uncertainty in simulating wheat yields under climate change, Nat. Clim. Change, 3, 827–832, https://doi.org/10.1038/nclimate1916, 2013.

Batjes, N. H.: ISRIC-WISE derived soil properties on a 5 by 5 arc-minutes global grid (ver. 1.2), Report 2012/01, ISRIC-World Soil Information, Wageningen, 2012.

Ben-Ari, T., Boé, J., Ciais, P., Lecerf, R., Van der Velde, M., and Makowski, D.: Causes and implications of the unforeseen 2016 extreme yield loss in the breadbasket of France, Nat. Commun., 9, 1–10, https://doi.org/10.1038/s41467-018-04087-x, 2018.

Breiman, L.: Random Forests, Mach. Learn., 45, 5–32, https://doi.org/10.1023/A:1010933404324, 2001.

Buizza, R., Milleer, M., and Palmer, T. N.: Stochastic representation of model uncertainties in the ECMWF ensemble prediction system, Q. J. Roy. Meteorol. Soc., 125, 2887–2908, https://doi.org/10.1002/qj.49712556006, 1999.

Daryanto, S., Wang, L., and Jacinthe, P.-A.: Global Synthesis of Drought Effects on Maize and Wheat Production, PloS One, 11, e0156362, https://doi.org/10.1371/journal.pone.0156362, 2016.

Deser, C., Lehner, F., Rodgers, K. B., Ault, T., Delworth, T. L., DiNezio, P. N., Fiore, A., Frankignoul, C., Fyfe, J. C., Horton, D. E., Kay, J. E., Knutti, R., Lovenduski, N. S., Marotzke, J., McKinnon, K. A., Minobe, S., Randerson, J., Screen, J. A., Simpson, I. R., and Ting, M.: Insights from Earth system model initial-condition large ensembles and future prospects, Nat. Clim. Change, 10, 277–286, https://doi.org/10.1038/s41558-020-0731-2, 2020.

FAOSTAT: FAO Statistics, Food and Agriculture Organization of the United Nations, Rome, available at: http://www.fao.org/faostat/en/, last access: 1 October 2020.

Forkel, M., Thonicke, K., Beer, C., Cramer, W., Bartalev, S., and Schmullius, C.: Extreme fire events are related to previous-year surface moisture conditions in permafrost-underlain larch forests of Siberia, Environ. Res. Lett., 7, 044021, https://doi.org/10.1088/1748-9326/7/4/044021, 2012.

Frank, D., Reichstein, M., Bahn, M., Thonicke, K., Frank, D., Mahecha, M. D., Smith, P., van der Velde, M., Vicca, S., Babst, F.,

Beer, C., Buchmann, N., Canadell, J. G., Ciais, P., Cramer, W., Ibrom, A., Miglietta, F., Poulter, B., Rammig, A., Seneviratne, S. I., Walz, A., Wattenbach, M., Zavala, M. A., and Zscheischler, J.: Effects of climate extremes on the terrestrial carbon cycle: concepts, processes and potential future impacts, Global Change Biol., 21, 2861–2880, https://doi.org/10.1111/gcb.12916, 2015.
Friedman, J., Hastie, T., and Tibshirani, R.: Regularization Paths for Generalized Linear Models via Coordinate Descent, J. Stat. Softw., 33, 1–22, https://doi.org/10.18637/jss.v033.i01, 2010.
Furnival, G. M. and Wilson, R. W.: Regressions by Leaps and Bounds, Technometrics, 16, 499–511, https://doi.org/10.1080/00401706.1974.10489231, 1974.
Grossiord, C., Buckley, T. N., Cernusak, L. A., Novick, K. A., Poulter, B., Siegwolf, R. T. W., Sperry, J. S., and McDowell, N. G.: Plant responses to rising vapor pressure deficit, New Phytol., 226, 1550–1566, https://doi.org/10.1111/nph.16485, 2020.
Hand, D. J.: Measuring classifier performance: a coherent alternative to the area under the ROC curve, Mach. Learn., 77, 103–123, https://doi.org/10.1007/s10994-009-5119-5, 2009.
Hazeleger, W., Wang, X., Severijns, C., Ştefănescu, S., Bintanja, R., Sterl, A., Wyser, K., Semmler, T., Yang, S., Van den Hurk, B., van Noije, T., van der Linden, E., and van der Wiel, K.: EC-Earth V2.2: description and validation of a new seamless earth system prediction model, Clim. Dynam., 39, 2611–2629, https://doi.org/10.1007/s00382-011-1228-5, 2012.
Iizumi, T. and Ramankutty, N.: How do weather and climate influence cropping area and intensity?, Global Food Secur., 4, 46–50, https://doi.org/10.1016/j.gfs.2014.11.003, 2015.
Jagadish, K. S. V., Kadam, N. N., Xiao, G., Melgar, R. J., Bahuguna, R. N., Quinones, C., Tamilselvan, A., Prasad, P. V. V., and Jagadish, K. S.: Agronomic and Physiological Responses to High Temperature, Drought, and Elevated CO_2 Interactions in Cereals, in: Advances in Agronomy, vol. 127 of Advances in Agronomy, edited by: Sparks, D. L., Elsevier Science, Burlington, 111–156, https://doi.org/10.1016/B978-0-12-800131-8.00003-0, 2014.
Jentsch, A., Kreyling, J., and Beierkuhnlein, C.: A new generation of climate-change experiments: events, not trends, Front. Ecol. Environ., 5, 365–374, https://doi.org/10.1890/1540-9295(2007)5[365:ANGOCE]2.0.CO;2, 2007.
Kern, A., Barcza, Z., Marjanović, H., Árendás, T., Fodor, N., Bónis, P., Bognár, P., and Lichtenberger, J.: Statistical modelling of crop yield in Central Europe using climate data and remote sensing vegetation indices, Agr. Forest Meteorol., 260-261, 300–320, https://doi.org/10.1016/j.agrformet.2018.06.009, 2018.
Kogan, F., Kussul, N., Adamenko, T., Skakun, S., Kravchenko, O., Kryvobok, O., Shelestov, A., Kolotii, A., Kussul, O., and Lavrenyuk, A.: Winter wheat yield forecasting in Ukraine based on Earth observation, meteorologicaldata and biophysical models, Int. J. Appl. Earth Obs. Geoinform., 23, 192–203, https://doi.org/10.1016/j.jag.2013.01.002, 2013.
Krstajic, D., Buturovic, L. J., Leahy, D. E., and Thomas, S.: Cross-validation pitfalls when selecting and assessing regression and classification models, J. Cheminform., 6, 1–15, https://doi.org/10.1186/1758-2946-6-10, 2014.
Leng, G., Zhang, X., Huang, M., Asrar, G. R., and Leung, L. R.: The Role of Climate Covariability on Crop Yields in the Conterminous United States, Sci. Rep., 6, 33160, https://doi.org/10.1038/srep33160, 2016.
Leonard, M., Westra, S., Phatak, A., Lambert, M., van den Hurk, B., Mcinnes, K., Risbey, J., Schuster, S., Jakob, D., and Stafford-Smith, M.: A compound event framework for understanding extreme impacts, Wiley Interdisciplin. Rev.: Clim. Change, 5, 113–128, https://doi.org/10.1002/wcc.252, 2014.
Lesk, C., Rowhani, P., and Ramankutty, N.: Influence of extreme weather disasters on global crop production, Nature, 529, 84–87, https://doi.org/10.1038/nature16467, 2016.
Li, K., Yang, X., Liu, Z., Zhang, T., Lu, S., and Liu, Y.: Low yield gap of winter wheat in the North China Plain, Eur. J. Agron., 59, 1–12, https://doi.org/10.1016/j.eja.2014.04.007, 2014.
Liaw, A. and Wiener, M.: Classification and Regression by randomForest, R News, 2, 18–22, available at: https://CRAN.R-project.org/doc/Rnews/ (last access: 18 November 2020), 2002.
Lobell, D. B.: Changes in diurnal temperature range and national cereal yields, Agr. Forest Meteorol., 145, 229–238, https://doi.org/10.1016/j.agrformet.2007.05.002, 2007.
Lobell, D. B. and Asner, G. P.: Climate and Management Contributions to Recent Trends in U.S. Agricultural Yields, Science, 299, 1032, https://doi.org/10.1126/science.1078475, 2003.
Lobell, D. B. and Burke, M. B.: Why are agricultural impacts of climate change so uncertain? The importance of temperature relative to precipitation, Environ. Res. Lett., 3, 034007, https://doi.org/10.1088/1748-9326/3/3/034007, 2008.
Lobell, D. B. and Burke, M. B.: On the use of statistical models to predict crop yield responses to climate change, Agr. Forest Meteorol., 150, 1443–1452, https://doi.org/10.1016/j.agrformet.2010.07.008, 2010.
Lobell, D. B., Schlenker, W., and Costa-Roberts, J.: Climate Trends and Global Crop Production Since 1980, Science, 333, 616–620, https://doi.org/10.1126/science.1204531, 2011.
Luo, Q.: Temperature thresholds and crop production: a review, Climatic Change, 109, 583–598, https://doi.org/10.1007/s10584-011-0028-6, 2011.
Mason, I.: Dependence of the Critical Success Index on sample climate and threshold probability, Aust. Meteorol. Mag., 37, 75–81, 1989.
McDowell, N. G., Beerling, D. J., Breshears, D. D., Fisher, R. A., Raffa, K. F., and Stitt, M.: The interdependence of mechanisms underlying climate-driven vegetation mortality, Trends Ecol. Evol., 26, 523–532, https://doi.org/10.1016/j.tree.2011.06.003, 2011.
McLeod, A., Xu, C., and Lai, Y.: bestglm: Best Subset GLM and Regression Utilities, r package version 0.37.3, available at: https://CRAN.R-project.org/package=bestglm, last access: 18 November 2020.
Morice, C. P., Kennedy, J. J., Rayner, N. A., and Jones, P. D.: Quantifying uncertainties in global and regional temperature change using an ensemble of observational estimates: The HadCRUT4 data set, J. Geophys. Res.-Atmos., 117, D08101, https://doi.org/10.1029/2011JD017187, 2012.
Moriondo, M. and Bindi, M.: Impact of climate change on the phenology of typical Mediterranean crops, Ital. J. Agrometeorol., 3, 5–12, 2007.
Mueller, N. D., Gerber, J. S., Johnston, M., Ray, D. K., Ramankutty, N., and Foley, J. A.: Closing yield gaps through nutrient and water management, Nature, 490, 254–257, https://doi.org/10.1038/nature11420, 2012.

Novick, K. A., Ficklin, D. L., Stoy, P. C., Williams, C. A., Bohrer, G., Oishi, A. C., Papuga, S. A., Blanken, P. D., Noormets, A., Sulman, B. N., Scott, R. L., Wang, L., and Phillips, R. P.: The increasing importance of atmospheric demand for ecosystem water and carbon fluxes, Nat. Clim. Change, 6, 1023–1027, https://doi.org/10.1038/nclimate3114, 2016.

Oppenheimer, M., Campos, M., Warren, R., Birkmann, J., Luber, G., O'Neill, B., and Takahashi, K.: Emergent risks and key vulnerabilities, in: Climate Change 2014 Impacts, Adaptation and Vulnerability: Part A: Global and Sectoral Aspects, Cambridge University Press, Cambridge, 1039–1100, https://doi.org/10.1017/CBO9781107415379.024, 2015.

Pan, S., Yang, J., Tian, H., Shi, H., Chang, J., Ciais, P., Francois, L., Frieler, K., Fu, B., Hickler, T., Ito, A., Nishina, K., Ostberg, S., Reyer, C. P., Schaphoff, S., Steinkamp, J., and Zhao, F.: Climate Extreme Versus Carbon Extreme: Responses of Terrestrial Carbon Fluxes to Temperature and Precipitation, J. Geophys. Res.-Biogeo., 125, e2019JG005252, https://doi.org/10.1029/2019JG005252, 2020.

Porter, J. R. and Gawith, M.: Temperatures and the growth and development of wheat: a review, Eur. J. Agron., 10, 23–36, https://doi.org/10.1016/S1161-0301(98)00047-1, 1999.

Rawson, H. M., Begg, J. E., and Woodward, R. G.: The Effect of Atmospheric Humidity on Photosynthesis, Transpiration and Water Use Efficiency of Leaves of Several Plant Species, Planta, 134, 5–10, https://doi.org/10.1007/BF00390086, 1977.

R Core Team: R: A Language and Environment for Statistical Computing, R Foundation for Statistical Computing, Vienna, Austria, available at: https://www.R-project.org/ (last access: 18 November 2020), 2019.

Ribeiro, A. F. S., Russo, A., Gouveia, C. M., Páscoa, P., and Zscheischler, J.: Risk of crop failure due to compound dry and hot extremes estimated with nested copulas, Biogeosciences, 17, 4815–4830, https://doi.org/10.5194/bg-17-4815-2020, 2020.

Rosenzweig, C., Elliott, J., Deryng, D., Ruane, A. C., Müller, C., Arneth, A., Boote, K. J., Folberth, C., Glotter, M., Khabarov, N., Neumann, K., Piontek, F., Pugh, T. A. M., Schmid, E., Stehfest, E., Yang, H., and Jones, J. W.: Assessing agricultural risks of climate change in the 21st century in a global gridded crop model intercomparison, P. Natl. Acad. Sci. USA, 111, 3268–3273, https://doi.org/10.1073/pnas.1222463110, 2014.

Ruane, A. C., Goldberg, R., and Chryssanthacopoulos, J.: Climate forcing datasets for agricultural modeling: Merged products for gap-filling and historical climate series estimation, Agr. Forest Meteorol., 200, 233–248, https://doi.org/10.1016/j.agrformet.2014.09.016, 2015.

Runge, J., Bathiany, S., Bollt, E., Camps-Valls, G., Coumou, D., Deyle, E., Glymour, C., Kretschmer, M., Mahecha, M. D., Muñoz-Marí, J., van Nes, E. H., Peters, J., Quax, R., Reichstein, M., Scheffer, M., Schölkopf, B., Spirtes, P., Sugihara, G., Sun, J., Zhang, K., and Zscheischler, J.: Inferring causation from time series in Earth system sciences, Nat. Commun., 10, 2553, https://doi.org/10.1038/s41467-019-10105-3, 2019.

Sacks, W. J., Deryng, D., Foley, J. A., and Ramankutty, N.: Crop planting dates: an analysis of global patterns, Global Ecol. Biogeogr., 19, 607–620, https://doi.org/10.1111/j.1466-8238.2010.00551.x, 2010.

Schauberger, B., Archontoulis, S., Arneth, A., Balkovic, J., Ciais, P., Deryng, D., Elliott, J., Folberth, C., Khabarov, N., Müller, C., Pugh, T. A. M., Rolinski, S., Schaphoff, S., Schmid, E., Wang, X., Schlenker, W., and Frieler, K.: Consistent negative response of US crops to high temperatures in observations and crop models, Nat. Commun., 8, 13931, https://doi.org/10.1038/ncomms13931, 2017.

Seyfert, F.: Phänologie, in: vol. 255 of Die neue Brehm-Bücherei, nachdr., 2. unveränd. Edn., VerlagsKG Wolf, Magdeburg, 1960.

Shah, N. and Paulsen, G.: Interaction of drought and high temperature on photosynthesis and grain-filling of wheat, Plant Soil, 257, 219–226, https://doi.org/10.1023/a:1026237816578, 2003.

Shi, W., Tao, F., and Zhang, Z.: A review on statistical models for identifying climate contributions to crop yields, J. Geogr. Sci., 23, 567–576, https://doi.org/10.1007/s11442-013-1029-3, 2013.

Singh, A., Phadke, V. S., and Patwardhan, A.: Impact of Drought and Flood on Indian Food Grain Production, in: Challenges and Opportunities in Agrometeorology, Springer, Berlin, Heidelberg, 421–433, https://doi.org/10.1007/978-3-642-19360-6_32, 2011.

Sippel, S., Zscheischler, J., and Reichstein, M.: Ecosystem impacts of climate extremes crucially depend on the timing, P. Natl. Acad. Sci. USA, 113, 5768–5770, https://doi.org/10.1073/pnas.1605667113, 2016.

Stocker, B. D., Zscheischler, J., Keenan, T. F., Prentice, I. C., Seneviratne, S. I., and Peñuelas, J.: Drought impacts on terrestrial primary production underestimated by satellite monitoring, Nat. Geosci., 12, 264–270, https://doi.org/10.1038/s41561-019-0318-6, 2019.

Tibshirani, R.: Regression Shrinkage and Selection via the Lasso, J. Roy. Stat. Soc., 58, 267–288, 1996.

Tschumi, E. and Zscheischler, J.: Countrywide climate features during recorded climate-related disasters, Climatic Change, 158, 593–609, https://doi.org/10.1007/s10584-019-02556-w, 2020.

Van der Wiel, K., Stoop, L., van Zuijlen, B., Blackport, R., van den Broek, M., and Selten, F.: Meteorological conditions leading to extreme low variable renewable energy production and extreme high energy shortfall, Renew. Sustain. Energy Rev., 111, 261–275, https://doi.org/10.1016/j.rser.2019.04.065, 2019a.

Van der Wiel, K., Wanders, N., Selten, F., and Bierkens, M.: Added value of large ensemble simulations for assessing extreme river discharge in a 2 °C warmer world, Geophys. Res. Lett., 46, 2093–2102, https://doi.org/10.1029/2019GL081967, 2019b.

Van der Wiel, K., Selten, F. M., Bintanja, R., Blackport, R., and Screen, J. A.: Ensemble climate-impact modelling: extreme impacts from moderate meteorological conditions, Environ. Res. Lett., 15, 034050, https://doi.org/10.1088/1748-9326/ab7668, 2020.

Vogel, E., Donat, M. G., Alexander, L. V., Meinshausen, M., Ray, D. K., Karoly, D., Meinshausen, N., and Frieler, K.: The effects of climate extremes on global agricultural yields, Environ. Res. Lett., 14, 054010, https://doi.org/10.1088/1748-9326/ab154b, 2019.

Vogel, J., Rivoire, P., Deidda, C., Sauter, C. A., Tschumi, E.: Identify_crop_yield_drivers, available at: https://github.com/jo-vogel/Identify_crop_yield_drivers, last access: February 2021.

Yuan, W., Zheng, Y., Piao, S., Ciais, P., Lombardozzi, D., Wang, Y., Ryu, Y., Chen, G., Dong, W., Hu, Z., Jain, A. K., Jiang, C., Kato, E., Li, S., Lienert, S., Liu, S., Nabel, J. E., Qin, Z., Quine, T., Sitch, S., Smith, W. K., Wang, F., Wu, C., Xiao, Z., and Yang, S.: Increased atmospheric vapor pressure deficit reduces global vegetation growth, Sci. Adv., 5, eaax1396, https://doi.org/10.1126/sciadv.aax1396, 2019.

Zhang, S., Tao, F., and Zhang, Z.: Spatial and temporal changes in vapor pressure deficit and their impacts on crop yields in China during 1980–2008, J. Meteorol. Res., 31, 800–808, https://doi.org/10.1007/s13351-017-6137-z, 2017.

Zheng, B., Chenu, K., Doherty, A., and Chapman, S.: The APSIM-wheat module (7.5 R3008), Agricultural Production Systems Simulator (APSIM) Initiative, Toowoomba, Australia, available at: https://www.apsim.info/documentation/model-documentation/crop-module-documentation/wheat/ (last access: 18 November 2020), 2014.

Zscheischler, J., Mahecha, M. D., Harmeling, S., and Reichstein, M.: Detection and attribution of large spatiotemporal extreme events in Earth observation data, Ecol. Inform., 15, 66–73, https://doi.org/10.1016/j.ecoinf.2013.03.004, 2013.

Zscheischler, J., Fatichi, S., Wolf, S., Blanken, P. D., Bohrer, G., Clark, K., Desai, A. R., Hollinger, D., Keenan, T., Novick, K. A., and Seneviratne, S. I.: Short-term favorable weather conditions are an important control of interannual variability in carbon and water fluxes, J. Geophys. Res.-Biogeo., 121, 2186–2198, https://doi.org/10.1002/2016JG003503, 2016.

Zscheischler, J., Westra, S., van den Hurk, B., Seneviratne, S. I., Ward, P. J., Pitman, A., AghaKouchak, A., Bresch, D. N., Leonard, M., Wahl, T., and Zhang, X.: Future climate risk from compound events, Nat. Clim. Change, 8, 469–477, https://doi.org/10.1038/s41558-018-0156-3, 2018.

Zscheischler, J., Martius, O., Westra, S., Bevacqua, E. R. C., Horton, R. M., van den Hurk, B., AghaKouchak, A., Jézéquel, A., Mahecha, M. D., Maraun, D., Ramos, A. M., Ridder, N., Thiery, W., and Vignotto, E.: A typology of compound weather and climate events, Nat. Rev. Earth Environ., 1, 333–347, https://doi.org/10.1038/s43017-020-0060-z, 2020.

Chapter 5

Synthesis

5.1 Main findings and conclusions

This thesis presents three articles, which are all connected by temperature and water availability in the face of climate change and the ecological impacts related to them (see objectives in section 1.5). While the main aspect of the first study lies on the investigation of changes in compound weather events, the other two studies focus on the identification of meteorological drivers of extreme ecological impacts, namely ecosystem productivity and agricultural yields in the former and latter case.

The first study (see chapter 2) analysed changes in compound warm spells and droughts in the Mediterranean Basin within the last 40 years. The number of such events increased significantly within this time period with an annual growth rate of 3.9% and 3.5% for warm season (extreme in absolute terms) and deseasonalised (extreme relative to their time of occurrence during the course of the year) compound events, respectively. Especially in recent years, a high frequency of deseasonalised events has occurred, shown by the fact that the years 2014–2017 all belong to the six years with the highest number of such events. Temperature extremes are increasing faster than the temperature mean due to land-atmosphere feedbacks in the Mediterranean Basin (Orlowsky and Seneviratne, 2012, Lewis et al., 2019). This is in line with the findings of this study, which showed that the highest increase in compound events is found for the definition with the highest level of extremeness regarding duration and magnitude (7-Day and 95^{th} percentile). In many regions, events exceeding this threshold have occurred exclusively within the last two decades. This illustrates that unprecedented climatic conditions are arising in the Mediterranean Basin, which are outside the previous climatic variability. The frequency of warm season and deseasonalised compound warm spells and droughts between the periods 1979–1998 and 1999–2018 increased for almost the entire Mediterranean Basin, with few exceptions such as the Atlantic coast of Portugal and Galicia, where decreases occurred. The frequency between these two time spans has particularly increased in Morocco, south-eastern Spain and western Turkey. The absolute change in the number of warm season compound events from 1979 to 2019 was highest in the Western Balkan.

Both warm spells and SPEI droughts showed a significant increase, whereas no significant trend was detected for SPI droughts. This indicates that while precipitation amounts remain unchanged, atmospheric evaporative demand is increasing and as a consequence the Mediterranean is getting drier despite the stagnant rainfalls. The findings from the change vector analysis showed that the rising number of compound events can primarily be attributed to an increase in temperature and not to a lack of precipitation. The analysis of deseasonalised compound warm spells and droughts particularly showed increased frequencies in late spring and early summer with potentially harmful impacts on ecosystems and agriculture since this is the main growing season in the Mediterranean Basin. This increase in deseasonalised compound events could be explained by higher evapotranspiration levels caused by the overall temperature rise. As a consequence, water resources are potentially depleted earlier in the year, which in turn fortifies the occurrence of warm spells. However, such increases during this time of the year were not noticeable in the absolute extremes, i.e. the warm season compound events, which highlights the importance to consider also increases in relative extremes and to account for the seasonality in the joint assessment of warm spells and droughts. Furthermore, the differing patterns of SPI and SPEI droughts showed that the choice of the drought index is essential. The SPI is presumably not an adequate choice to investigate drought impacts on vegetation, as it does not incorporate evapotranspiration. The SPEI is an improvement in that regard, however, it only accounts for potential evapotranspiration, not actual evapotranspiration. These shortcomings formed the motivation to use satellite-derived measurements of soil moisture instead of indices such as SPI and SPEI in the ecoclimatological context of the subsequent ecosystem vulnerability analysis. Nevertheless, it should be noted that remote sensing products of soil moisture also have several downsides, which are addressed in section 5.2.1 and chapter 3.

The second study (see chapter 3) investigated the seasonal pattern of ecosystem vulnerability to temperature and soil moisture anomalies in the Mediterranean Basin. Three main regimes of ecosystem vulnerability during the course of the year were identified: a) vulnerability to hot and dry conditions in late spring to midsummer, b) vulnerability to cold and dry conditions from the end of summer to mid-autumn and c) vulnerability during cold and wet conditions from the end of autumn to mid-spring. The general transition from an energy-limited regime in winter to a soil-moisture-limited one in summer is well reflected in the annual cycle of ecosystem vulnerability to temperature and soil moisture anomalies depicted in this study. However, there are regional differences from this pattern. In Turkey, vulnerability to hot and dry conditions is present from spring to autumn, longer than in any other subregion. By contrast, the Balkan Peninsula exhibits an energy-limited regime almost year-round and vulnerability to hot conditions is nearly absent. However, the preceding study on compound warm spells and droughts presented in chapter 2 showed high increases of compound events in the Western Balkan, so it is likely that vulnerability to heat will become more prevalent in the near future. Ecosystems in north-western Africa are soil-moisture-limited almost year-round according to the results obtained from the ESA CCI satellite-based data set. This diverges from the findings received from the ERA5-Land reanalysis product, where vulnerability to dry conditions is much less pronounced. This suggests that the reanalysis data set is not as well-suited as the satellite-derived data set to represent ecosystem vulnerability to soil moisture in this region. The patterns of seasonal vulnerability are often similar to one another for many land cover classes. Grasslands are the only land cover class exhibiting vulnerability to hot conditions already in April, whereas for half of the land cover classes the onset occurs in May. This indicates that grasslands might show a faster response time to adverse climatic conditions compared to other land cover classes.

Not only climate conditions affect ecosystems but also vice versa: an example hereof is the mechanism of land-atmosphere feedbacks described earlier with temperature increases leading to higher transpiration rates of the vegetation, which in turn can lead to the onset of compound warm spells and droughts. In addition, the coincidence of wet conditions and low ecosystem productivity in winter, which is prevalent in the study on ecosystem vulnerability, depicts a case where the direction of causal relation is uncertain. While wet conditions can be harmful to ecosystems, it is also plausible that transpiration is reduced during states of low ecosystem productivity and therefore less soil moisture is extracted, leading to overall wetter conditions. In conclusion, this study provides a suitable approach to identify at which stage of the year ecosystem vulnerability to certain climatic conditions occurs for various land cover classes and subregions of the Mediterranean Basin.

The third study (see chapter 4) aimed to develop a method for the automated selection of relevant meteorological drivers of crop failure of winter wheat in the Northern Hemisphere. This requires the consideration of a variety of different meteorological drivers at different times of the growing season. It was shown that LASSO logistic regression is a suitable tool for automated variable selection, which accounts for multicollinearity while at the same time achieving good model performance. The approach was designed in a way that it is transferable to other multivariate ecoclimatological settings with a focus on seasonality of the respective variables. The most important predictors of crop failure include VPD at late stages of the growing season – i.e. during the reproductive phase – as well as the diurnal temperature range and the number of frost days. Interestingly, the regional model performance correlates strongly with the annual mean and standard deviation of wheat crop yield. This suggests that the discrimination of years with normal and bad yield is more challenging when there is generally a low interannual variability of crop yields. Good model performance is achieved in Central Europe and the eastern half of the USA, whereas prediction accuracy is relatively low in Asia and the western half of the USA.

The selection of some of the climate extreme indicators follow temperature gradients, for example the number of frost days is less often included in southern grid points. Furthermore, the number of frost days has a higher importance in eastern European grid points compared to western European ones, which can potentially be linked to the increasingly continental climate eastward. It is also notable that the number of warm days with daily maximum temperature above the 90^{th} percentile is predominantly included as a predictor in southern grid points, especially in the United States. This shows that frost generally poses a lower risk in hotter as well as in maritime climate zones, whereas critical high-temperature thresholds for crop growth are primarily surpassed in southern regions. However, this is likely to shift due to climate change and thus critical high temperatures might be reached in temperate regions in future, where they were previously uncommon.

All three articles highlight the importance of incorporating seasonality for a better understanding of year-round dynamics. Studies often only concentrate on a single season, while an examination of the entire growing season could provide additional insights in many ecological contexts. The first two studies illustrate that it is crucial to account for the seasonality of climate extreme events. The third study also accounts for the seasonality of mean climatic conditions, however, the aspect of seasonality of extremes is not specifically addressed here and thus further research could complement this by explicitly addressing the timing of extremes. The two ecoclimatological studies presented in chapter 3 and 4 account for all combinations of temperature and water availability, whereas the first study presented in chapter 2 has a more narrow focus on hot and dry extremes solely since these are of particular interest due to their increasing joint occurrence with climate change (Zscheischler and Seneviratne, 2017). While the study on crop failure is based exclusively on model data, the vulnerability analysis applies primarily remote sensing data sets. This illustrates the main difference between both studies. The study on crop failure encompasses 1600 growing season simulations, whereas only a fraction of this time span is available for the second study, which covers 21 years. Due to this data scarcity, only few extremes are present in each of the time series and a much longer temporal coverage of satellite products would be required to be able to utilise more sophisticated methods such as the LASSO logistic regression, which was applied in the study on crop failure, at a pixel level. Both studies differentiate between extreme and non-extreme states based on percentile threshold. While a sensitivity analysis using other percentiles was carried out in both cases, such a threshold is nevertheless a purely statistical choice and thus its meaningfulness for real-world applications might be limited in that regard. This is discussed further in section 5.2.3.

5.2 Challenges and future research

5.2.1 Challenges and opportunities of remote sensing for ecoclimatological studies

The rapid advancement of remote sensing technologies enables to quantify variables such as soil moisture and the FAPAR consistently at large spatial scales for multiple decades. Satellite-based soil moisture and the FAPAR are recognised as important variables for terrestrial earth observation and are part of the essential climate variables (ECV) according to the Global Climate Observing System (GCOS) (GCOS-138, 2010, Dorigo et al., 2017, Smets et al., 2019). Despite facilitating new ways to investigate interactions between climate and the biosphere, there are still some constraints regarding the usage of satellite-based soil moisture and the FAPAR.

The retrieval of soil moisture data is inhibited by frozen soils and dense vegetation (Dorigo et al., 2017). Furthermore, the optimal hydrologic variable referring to ecosystem vulnerability is plant available water within the root zone, rather than surface soil moisture (Wagner et al., 2007). However, observations of this variable are not available for large spatial scales. Satellite-based soil moisture data is only obtainable for approximately the first centimetres of the top soil and thus it is not representative of the entire root zone (Kidd and Haas, 2018). While soil water dynamics of deeper soil layers show dampened and delayed dynamics compared to the surface layer, there is nevertheless a significant correlation between these layers (Akbar et al., 2018). Furthermore, Denissen et al. (2020) state that satellite-derived surface soil moisture is well suited to infer the state of the vegetation and corresponding land-atmosphere interactions during climate extremes. In addition, the satellite-based ESA CCI soil moisture data set was used to create a global precipitation product, which was compared to state-of-the-art precipitation data sets and showed relatively good performance (Ciabatta et al., 2018). In conclusion, remote sensing has enabled large-scale long-term drought monitoring and thus contributed tremendously to the progress in this field (West et al., 2019).

Within the last decade, Cosmic-Ray Neutron Sensing (CRNS) has been established as a complementary technique to retrieve soil moisture (Andreasen et al., 2017). It operates at a scale of several hectares and has a penetration depth of tens of centimetres (Desilets and Zreda, 2013, Köhli et al., 2015), which renders it useful for assessing root-zone soil moisture. It is therefore a promising tool for agricultural applications and can also be used for the validation of soil moisture products from satellites or hydrological models (Andreasen et al., 2017, Stevanato et al., 2019).

Before the emergence of biophysical variables such as the FAPAR, studies on vegetation dynamics had to rely on vegetation indices such as the normalised difference vegetation index (NDVI) (Gobron et al., 2010). The NDVI serves as a proxy for net primary productivity and is commonly used for ecological applications (Kerr and Ostrovsky, 2003, Pettorelli, 2013). It can be calculated for sensors with only few spectral bands such as the Advanced Very-High-Resolution Radiometer (AVHRR) and can therefore be obtained for comparably long time spans (Scholze et al., 2017). However, the NDVI has certain limitations, e.g. there are potential biases in sparse vegetation (the signal gets impaired due to noise from soil reflectance) and dense vegetation canopies (the NDVI value saturates under such conditions) (Asrar et al., 1984, Huete, 1988, Pettorelli et al., 2005).

Biophysical variables such as the FAPAR are alternatives to overcome the limitations of the NDVI. The FAPAR is defined as "the fraction of the photosynthetically active radiation (i.e. incoming solar radiation in the spectral region 0.4-–0.7 μm) that is absorbed by the vegetation canopy" (Scholze et al., 2017). Nevertheless, there is not always a linear relationship between the FAPAR and drought conditions. Anisohydric grass species only loosely control the closure of their stomata during droughts and tend to dry out, turning from green to yellow colour and thus there is a direct relation between drought severity and the FAPAR. However, isohydric tree species might close their stomata, which prevents water loss but also CO_2 assimilation. This way, absorbed radiation is directly dissipated again, leading to a reduced photosynthetic productivity, while at the same time changes in the FAPAR are comparably small (Reichstein et al., 2007).

Vegetation optical depth (VOD) and sun-induced fluorescence (SIF) provide recent promising alternatives for the observation of vegetation activity from space (Sippel et al., 2018b, Crocetti et al., 2020). VOD measures the degree of attenuation of microwave radiation evoked by vegetation (Jackson and Schmugge, 1991, Moesinger et al., 2020). It depends on vegetation density, biomass and water content and is related to plant productivity (Owe et al., 2008, Konings et al., 2019, Teubner et al., 2019). The comparatively short life span of individual microwave sensors is a challenge for the long-term investigation of VOD dynamics. The creation of a merged product incorporating input from several sensors is demanding, but such products have become publicly available in recent years (Moesinger et al., 2020). SIF is defined as “an electromagnetic signal emitted as a two-peak spectrum between 650 and 850 nm by the chlorophyll α of green plants under solar radiation” (Scholze et al., 2017). Its exact relationship to gross primary productivity is still unclear and data quality is not satisfying so far (Gu et al., 2020). Moreover, long-term time series of SIF are not available yet and there is no operational satellite designed for its measurement currently (Duveiller et al., 2020). However, the European Space Agency plans to launch the Fluorescence Explorer in 2024, which is designed for this purpose (Moreno, 2021).

5.2.2 Methodological tools in the context of ecoclimatological studies

The methods used in the first and second study are focussing on the simultaneous occurrence of events within several time series and can be denominated as event coincidence analyses (Donges et al., 2016). An event coincidence analysis is a common statistical approach for investigating compound events (Raymond et al., 2020). In recent years the application of copulas has also become more popular for studying compound events e.g. in the context of agrometeorological studies (Ribeiro et al., 2019, Raymond et al., 2020). Besides such statistical approaches, process-based models are frequently applied in such contexts. Such models have the advantage that they possess physical meaning, but they usually require a large amount of input data (Tilloy et al., 2019). Machine learning tools such as the LASSO regression (Tibshirani, 1996) presented in the third article in this thesis are promising for ecoclimatological studies. While they usually provide high performance, limited interpretability often is a major disadvantage of machine learning approaches (Reichstein et al., 2019, Roscher et al., 2020). Although interpretability of machine learning has often been neglected (Mateo-Sanchis et al., 2021), there is an increasing number of ways how to enhance model interpretability. By now there are various crop science studies applying machine learning to determine variable importance of environmental drivers and gain an understanding of their relationship to crop yields, e.g. using accumulated local effects, Shapley additive explanations, partial dependence and pseudosample plots (Sanz et al., 2018, Vogel et al., 2019, Peichl et al., 2021, Zhu et al., 2021, Lischeid et al., 2022).

The risk of simultaneous crop failure in several breadbasket regions will increase disproportionately due to climate change and thus pose a threat to global food security (Gaupp et al., 2019, Kornhuber et al., 2020). Investigation of such spatial compounds using a set-up similar to the one presented in the third study in this thesis is therefore a relevant field of future research (Bevacqua et al., 2021).

5.2.3 Choice of appropriate time scales and thresholds for extreme impacts

The definition of an adequate time scale for attributing meteorological drivers to ecological impacts posed a main challenge in both ecoclimatological studies presented in the chapters 3 and 4. The choice for the study on crop failure is more straightforward compared to the study on ecosystem vulnerability: the relevant time frame was given by the length of the growing season of winter wheat for each respective grid point and the impact is represented by a single variable for each year, i.e. annual crop yield. However, the inclusion of several months preceding the beginning of the growing season might arguably also be relevant, since e.g. VPD and precipitation before the beginning of the growing season affect soil moisture contents in the following months. In the case of the vulnerability analysis, the entire course of the year is analysed for each pixel, rather than a fixed growing season and the impact variable – the FAPAR, a proxy for ecosystem productivity – is investigated independently for each of the 12 months of the year. This adds further complexity to the choice of an adequate time scale. In addition, droughts usually operate on longer time scales than heat waves, which makes it challenging to find an optimal time scale (Miralles et al., 2019). Finally, it was decided to link ecosystem productivity to climatic conditions in the same and the two preceding months, a time scale commonly used in the scientific literature.

Nevertheless, clear guidelines on how to define an optimal time span for the attribution of climatic impacts on ecosystems are lacking and many scientific studies do not provide a sound argument for the choice of their respective time span. Moreover, the choice of a monthly time step is convenient and widely used but nevertheless debatable. Plants exhibit varying sensitivity to climatic conditions depending on the phenological stage of their growing cycle (Seyfert, 1960). Due to the coarseness of the temporal scale, e.g. the start of the growing season might not be well-aligned with a calendar month (Wu et al., 2021). Furthermore, some important growth stages such as anthesis and grain-filling (Prasad and Djanaguiraman, 2014) might be too short to be captured well using a monthly time scale (Lischeid et al., 2022). Accounting for the time intervals of the actual phenophases instead of using a monthly time step would likely improve the explanatory power of ecoclimatological studies. However, this requires precise information on crop phenology at a given location. Based on the literature examined in the course of this thesis, the consideration of compound events and the importance of seasonal timing of events during critical growth stages appears to be well recognised in agricultural science, whereas these topics seem to be not as broadly investigated in other ecological contexts yet. When studying ecological impacts of climate change, many problems require multivariate solutions. Furthermore, accounting for seasonal differences and choosing an appropriate time scale is crucial. Both approaches presented in chapters 3 and 4 illustrate ways to account for multiple climatic drivers and their seasonal timing. In addition, they are flexible and can easily be transferred to other ecoclimatological settings.

The definition of critical thresholds of ecosystem responses is challenging. Scientific studies are often restricted to case studies focussing on single outstanding events or they apply a definition of extremes using either percentiles or absolute values. However, the universal application of an absolute threshold to a multitude of ecosystems might not be equally representative for all of them (Flach et al., 2021). On the other hand, a percentile-based threshold is arbitrary to a degree and does not have any direct physical interpretation (Horton et al., 2016). Nonetheless, the vast majority of studies uses percentile-based thresholds (van Oijen et al., 2013, Ahlström et al., 2015, Baumbach et al., 2017, Nicolai-Shaw et al., 2017, von Buttlar et al., 2018, Sutanto et al., 2020). Percentile-based thresholds are presumably widely used because alternative, ecologically meaningful thresholds are often not readily obtainable. For example, heat stress levels leading to plant mortality are often not well quantified (Niu et al., 2014). An exception are major staple crops such as maize, wheat and soybean, for which thresholds for heat, frost and drought stress are well-known (Porter and Gawith, 1999, Luo, 2011, Hatfield and Prueger, 2015, Horton et al., 2016, Strer et al., 2018). Both studies in chapters 3 and 4 applied percentile-based thresholds and might benefit from alternative thresholds. Another approach is presented by Liu et al. (2013), who developed a method based on Student's t-test for the detection of significant vegetation extremes events. Furthermore, it is possible to use a setting for the assessment of ecosystem vulnerability, which does not require the definition of a threshold for extremeness. For example, Simelton et al. (2009) use an approach for detecting regions of crop-drought vulnerability, which is based on the ratio of a crop failure index and a drought index. These two indices are based on harvest and precipitation anomalies, respectively. Another example is depicted in the assessment of vegetation sensitivity to climatic drivers by Wu et al. (2021), who link vegetation index anomalies to air temperature, solar radiation and soil moisture using the partial correlation coefficient.

Due to the complexity of the concept of drought, a large variety of drought indices exists (Heim, 2002, Svoboda and Fuchs, 2016). A general agreement on which drought index is most preferential for which kind of impact is missing (Bachmair et al., 2016). Thresholds for drought definition are usually arbitrary and lack a sound theoretical or empirical basis. Furthermore, their choice also depends on the drought impact under investigation (Bachmair et al., 2016). There is a need for a paradigm shift from the focus on extremeness of hazards to the extremeness of impacts (see also section 1.3.4 in the introduction). Definition of droughts only rarely consider their impact, although the impacts are usually the subject of interest (Wilhite and Glantz, 1985, Tramblay et al., 2020). Assessing drought severity using solely thresholds derived from indices like the SPI falls short of adequately assessing drought impacts. Instead, it is recommendable to design thresholds that are meaningful for the respective sector of interest e.g. "agro-ecological drought indices" to evaluate the impact of droughts across various agroecosystems in the Mediterranean Basin (Tramblay et al., 2020). Such indices should account for plant-available soil water, plant functional responses and plant density as well as species composition (Tramblay et al., 2020). However, impacts of droughts are considerably more difficult to identify in comparison to instantaneous events (Vicente-Serrano and Beguería-Portugués, 2003, Hayes et al., 2011). There is a need for drought impact data bases (Tramblay et al., 2020), but long-term information on impacts is currently still lacking and to date, a standard framework for the assessment of drought impacts and standards for different sectors are still missing (Kreibich et al., 2019). One step towards a systematic assessment of drought impacts is the European Drought Impact Inventory, which also includes ecological impacts (Stahl et al., 2016). Nevertheless, the usage of such inventories for attribution of drought impacts to climatic drivers remains difficult. For example, increasing trends in drought impacts might also be attributed to rising awareness and easier and faster distribution of information through the internet, creating a reporting bias over time (Stahl et al., 2016).

The results of the first study in this thesis stress the importance to view drought indices in the context of their impacts. The frequency of SPI droughts has not significantly decreased over the last 40 years in the Mediterranean Basin, whereas SPEI droughts showed a significant decrease (see chapter 2). This indicates that the region has become drier due to increasing atmospheric evaporative demand, despite negligible changes in precipitation. Thus, the SPEI seems a more adequate choice for assessing ecosystem impacts in this setting. This illustrates that it is crucial to identify a suitable drought index for the problem at hand. While the usage of indices such as the SPI and SPEI is typical at large spatial scales, the emergence of satellite-based soil moisture products with long-term coverage, which are thoroughly validated has given new opportunities to investigate droughts, which are especially promising for the monitoring of ecosystem states.

Bibliography

AghaKouchak, A., Cheng, L., Mazdiyasni, O., and Farahmand, A.: Global warming and changes in risk of concurrent climate extremes: Insights from the 2014 California drought, Geophysical Research Letters, 41, 8847–8852, https://doi.org/10.1002/2014GL062308, 2014.

AghaKouchak, A., Farahmand, A., Melton, F. S., Teixeira, J., Anderson, M. C., Wardlow, B. D., and Hain, C. R.: Remote sensing of drought: Progress, challenges and opportunities, Reviews of Geophysics, 53, 452–480, https://doi.org/10.1002/2014RG000456, 2015.

AghaKouchak, A., Huning, L. S., Chiang, F., Sadegh, M., Vahedifard, F., Mazdiyasni, O., Moftakhari, H., and Mallakpour, I.: How do natural hazards cascade to cause disasters?, Nature, 561, 458–460, https://doi.org/10.1038/d41586-018-06783-6, 2018.

AghaKouchak, A., Chiang, F., Huning, L. S., Love, C. A., Mallakpour, I., Mazdiyasni, O., Moftakhari, H., Papalexiou, S. M., Ragno, E., and Sadegh, M.: Climate Extremes and Compound Hazards in a Warming World, Annual Review of Earth and Planetary Sciences, 48, https://doi.org/10.1146/annurev-earth-071719-055228, 2020.

Ahlström, A., Raupach, M. R., Schurgers, G., Smith, B., Arneth, A., Jung, M., Reichstein, M., Canadell, J. G., Friedlingstein, P., Jain, A. K., Kato, E., Poulter, B., Sitch, S., Stocker, B. D., Viovy, N., Wang, Y. P., Wiltshire, A., Zaehle, S., and Zeng, N.: Carbon cycle. The dominant role of semi-arid ecosystems in the trend and variability of the land CO_2 sink, Science (New York, N.Y.), 348, 895–899, https://doi.org/10.1126/science.aaa1668, 2015.

Ainsworth, E. A. and Long, S. P.: What have we learned from 15 years of free-air CO_2 enrichment (FACE)? A meta-analytic review of the responses of photosynthesis, canopy properties and plant production to rising CO_2, New Phytologist, 165, 351–371, https://doi.org/10.1111/j.1469-8137.2004.01224.x, 2005.

Akbar, R., Short Gianotti, D., McColl, K. A., Haghighi, E., Salvucci, G. D., and Entekhabi, D.: Hydrological Storage Length Scales Represented by Remote Sensing Estimates of Soil Moisture and Precipitation, Water Resources Research, 54, 1476–1492, https://doi.org/10.1002/2017WR021508, 2018.

Alessandri, A., de Felice, M., Zeng, N., Mariotti, A., Pan, Y., Cherchi, A., Lee, J.-Y., Wang, B., Ha, K.-J., Ruti, P., and Artale, V.: Robust assessment of the expansion and retreat of Mediterranean climate in the 21st century, Scientific reports, 4, 7211, https://doi.org/10.1038/srep07211, 2014.

Allakhverdiev, S. I., Kreslavski, V. D., Klimov, V. V., Los, D. A., Carpentier, R., and Mohanty, P.: Heat stress: an overview of molecular responses in photosynthesis, Photosynthesis research, 98, 541–550, https://doi.org/10.1007/s11120-008-9331-0, 2008.

Allen, C. D., Macalady, A. K., Chenchouni, H., Bachelet, D., McDowell, N., Vennetier, M., Kitzberger, T., Rigling, A., Breshears, D. D., Hogg, E. H., Gonzalez, P., Fensham, R., Zhang, Z., Castro, J., Demidova, N., Lim, J.-H., Allard, G., Running, S. W., Semerci, A., and Cobb, N.: A global overview of drought and heat-induced tree mortality reveals emerging climate change risks for forests, Forest Ecology and Management, 259, 660–684, https://doi.org/10.1016/j.foreco.2009.09.001, 2010.

Allen, C. D., Breshears, D. D., and McDowell, N. G.: On underestimation of global vulnerability to tree mortality and forest die-off from hotter drought in the Anthropocene, Ecosphere, 6, 1–55, https://doi.org/10.1890/ES15-00203.1, 2015.

Allen, M. R., de Coninck, H., Dube, O. P., Hoegh-Guldberg, O., Jacob, D., Jiang, K., Revi, A., Rogelj, J., Roy, J., and Shindell, D.: Technical Summary, in: Global warming of 1.5 °C. An IPCC Special Report on the impacts of global warming of 1.5°C above pre-industrial levels and related global greenhouse gas emission pathways, in the context of strengthening the global response to the threat of climate change, sustainable development, and efforts to eradicate poverty, edited by Masson-Delmotte, V., Zhai, P., Pörtner, H.-O., Roberts, D., Skea, J., Shukla, P. R., Pirani, A., Moufouma-Okia, W., Péan, C., Pidcock, R., Connors, S., Matthews, J., Chen, Y., Zhou, X., Gomis, M. I., Lonnoy, E., Maycock, T., Tignor, M., and Waterfield, T., pp. 27–46, URL `https://www.ipcc.ch/sr15/`, last access: 19/12/2021, 2018.

Anderegg, W. R. L., Kane, J. M., and Anderegg, L. D. L.: Consequences of widespread tree mortality triggered by drought and temperature stress, Nature Climate Change, 3, 30–36, https://doi.org/10.1038/nclimate1635, 2013.

Andreasen, M., Jensen, K. H., Desilets, D., Franz, T. E., Zreda, M., Bogena, H. R., and Looms, M. C.: Status and Perspectives on the Cosmic-Ray Neutron Method for Soil Moisture Estimation and Other Environmental Science Applications, Vadose Zone Journal, 16, vzj2017.04.0086, https://doi.org/10.2136/vzj2017.04.0086, 2017.

Archibold, O. W.: Mediterranean ecosystems, in: Ecology of world vegetation, edited by Archibold, O. W., pp. 131–164, Springer-Science+Business Media B.V, Dordrecht, Netherlands, https://doi.org/10.1007/978-94-011-0009-0_5, 1995.

Asrar, G., Fuchs, M., Kanemasu, E. T., and Hatfield, J. L.: Estimating Absorbed Photosynthetic Radiation and Leaf Area Index from Spectral Reflectance in Wheat, Agronomy Journal, 76, 300–306, https://doi.org/10.2134/agronj1984.00021962007600020029x, 1984.

Asseng, S., Ewert, F., Martre, P., Rötter, R. P., Lobell, D. B., Cammarano, D., Kimball, B. A., Ottman, M. J., Wall, G. W., White, J. W., Reynolds, M. P., Alderman, P. D., Prasad, P. V. V., Aggarwal, P. K., Anothai, J., Basso, B., Biernath, C., Challinor, A. J., de Sanctis, G., Doltra, J., Fereres, E., Garcia-Vila, M., Gayler, S., Hoogenboom, G., Hunt, L. A., Izaurralde, R. C., Jabloun, M., Jones, C. D., Kersebaum, K. C., Koehler, A.-K., Müller, C., Naresh Kumar, S., Nendel, C., O'Leary, G., Olesen, J. E., Palosuo, T., Priesack, E., Eyshi Rezaei, E., Ruane, A. C., Semenov, M. A., Shcherbak, I., Stöckle, C., Stratonovitch, P., Streck, T., Supit, I., Tao, F., Thorburn, P. J., Waha, K., Wang, E., Wallach, D., Wolf, J., Zhao, Z., and Zhu, Y.: Rising temperatures reduce global wheat production, Nature Climate Change, 5, 143–147, https://doi.org/10.1038/nclimate2470, 2015.

Bachmair, S., Svensson, C., Hannaford, J., Barker, L. J., and Stahl, K.: A quantitative analysis to objectively appraise drought indicators and model drought impacts, Hydrology and Earth System Sciences, 20, 2589–2609, https://doi.org/10.5194/hess-20-2589-2016, 2016.

Bahn, M., Reichstein, M., Dukes, J. S., Smith, M. D., and McDowell, N. G.: Climate-biosphere interactions in a more extreme world, New Phytologist, 202, 356–359, https://doi.org/10.1111/nph.12662, 2014.

Baret, F., Weiss, M., Lacaze, R., Camacho, F., Makhmara, H., Pacholcyzk, P., and Smets, B.: GEOV1: LAI and FAPAR essential climate variables and FCOVER global time series capitalizing over existing products. Part1: Principles of development and production, Remote Sensing of Environment, 137, 299–309, https://doi.org/10.1016/j.rse.2012.12.027, 2013.

Barnabás, B., Jäger, K., and Fehér, A.: The effect of drought and heat stress on reproductive processes in cereals, Plant, Cell and Environment, 31, 11–38, https://doi.org/10.1111/j.1365-3040.2007.01727.x, 2008.

Basso, F., Pisante, M., and Basso, B.: Soil Erosion and Land Degradation, in: Mediterranean desertification, edited by Geeson, N., Brandt, C. J., and Thornes, J. B., pp. 347–359, John Wiley & Sons, Chichester West Sussex England and Hoboken NJ USA, 2002.

Baumbach, L., Siegmund, J. F., Mittermeier, M., and Donner, R. V.: Impacts of temperature extremes on European vegetation during the growing season, Biogeosciences, 14, 4891–4903, https://doi.org/10.5194/bg-14-4891-2017, 2017.

Beguería, S. and Vicente-Serrano, S. M.: SPEI: Calculation of the Standardised Precipitation-Evapotranspiration Index, URL `https://CRAN.R-project.org/web/packages/SPEI/index.html`, last access: 19/12/2021, 2017.

Ben-Ari, T., Boé, J., Ciais, P., Lecerf, R., van der Velde, M., and Makowski, D.: Causes and implications of the unforeseen 2016 extreme yield loss in the breadbasket of France, Nature communications, 9, 1627, https://doi.org/10.1038/s41467-018-04087-x, 2018.

Beniston, M., Stephenson, D. B., Christensen, O. B., Ferro, C. A. T., Frei, C., Goyette, S., Halsnaes, K., Holt, T., Jylhä, K., Koffi, B., Palutikof, J., Schöll, R., Semmler, T., and Woth, K.: Future extreme events in European climate: an exploration of regional climate model projections, Climatic change, 81, 71–95, https://doi.org/10.1007/s10584-006-9226-z, 2007.

Berg, A., Lintner, B. R., Findell, K., Seneviratne, S. I., van den Hurk, B., Ducharne, A., Chéruy, F., Hagemann, S., Lawrence, D. M., Malyshev, S., Meier, A., and Gentine, P.: Interannual Coupling between Summertime Surface Temperature and Precipitation over Land: Processes and Implications for Climate Change, Journal of Climate, 28, 1308–1328, https://doi.org/10.1175/JCLI-D-14-00324.1, 2015.

Bernal, M., Estiarte, M., and Peñuelas, J.: Drought advances spring growth phenology of the Mediterranean shrub Erica multiflora, Plant biology (Stuttgart, Germany), 13, 252–257, https://doi.org/10.1111/j.1438-8677.2010.00358.x, 2011.

Bevacqua, E., de Michele, C., Manning, C., Couasnon, A., Ribeiro, A. F. S., Ramos, A. M., Vignotto, E., Bastos, A., Blesić, S., Durante, F., Hillier, J., Oliveira, S. C., Pinto, J. G., Ragno, E., Rivoire, P., Saunders, K., Wiel, K., Wu, W., Zhang, T., and Zscheischler, J.: Guidelines for Studying Diverse Types of Compound Weather and Climate Events, Earth's Future, 9, https://doi.org/10.1029/2021EF002340, 2021.

Blondel, J. and Aronson, J.: Biodiversity and Ecosystem Function in the Mediterranean Basin: Human and Non-Human Determinants, in: Mediterranean-Type Ecosystems, pp. 43–119, Springer, Berlin, Heidelberg, https://doi.org/10.1007/978-3-642-78881-9_2, 1995.

Bonada, N. and Resh, V. H.: Mediterranean-climate streams and rivers: geographically separated but ecologically comparable freshwater systems, Hydrobiologia, 719, 1–29, https://doi.org/10.1007/s10750-013-1634-2, 2013.

Bréda, N., Huc, R., Granier, A., and Dreyer, E.: Temperate forest trees and stands under severe drought: a review of ecophysiological responses, adaptation processes and long-term consequences, Annals of Forest Science, 63, 625–644, https://doi.org/10.1051/forest:2006042, 2006.

Breiman, L.: Random Forests, Machine Learning, 45, 5–32, https://doi.org/10.1023/A:1010933404324, 2001.

Breshears, D. D., Cobb, N. S., Rich, P. M., Price, K. P., Allen, C. D., Balice, R. G., Romme, W. H., Kastens, J. H., Floyd, M. L., Belnap, J., Anderson, J. J., Myers, O. B., and Meyer, C. W.: Regional vegetation die-off in response to global-change-type drought, Proceedings of the National Academy of Sciences, 102, 15 144–15 148, https://doi.org/10.1073/pnas.0505734102, 2005.

Camarero, J. J., Olano, J. M., and Parras, A.: Plastic bimodal xylogenesis in conifers from continental Mediterranean climates, New Phytologist, 185, 471–480, https://doi.org/10.1111/j.1469-8137.2009.03073.x, 2010.

Camarero, J. J., Valeriano, C., Gazol, A., Colangelo, M., and Sánchez-Salguero, R.: Climate Differently Impacts the Growth of Coexisting Trees and Shrubs under Semi-Arid Mediterranean Conditions, Forests, 12, 381, https://doi.org/10.3390/f12030381, 2021.

Cherubini, P., Gartner, B. L., Tognetti, R., Bräker, O. U., Schoch, W., and Innes, J. L.: Identification, measurement and interpretation of tree rings in woody species from mediterranean climates, Biological reviews of the Cambridge Philosophical Society, 78, 119–148, https://doi.org/10.1017/s1464793102006000, 2003.

Ciabatta, L., Massari, C., Brocca, L., Gruber, A., Reimer, C., Hahn, S., Paulik, C., Dorigo, W., Kidd, R., and Wagner, W.: SM2RAIN-CCI: a new global long-term rainfall data set derived from ESA CCI soil moisture, Earth System Science Data, 10, 267–280, https://doi.org/10.5194/essd-10-267-2018, 2018.

Ciais, P., Reichstein, M., Viovy, N., Granier, A., Ogée, J., Allard, V., Aubinet, M., Buchmann, N., Bernhofer, C., Carrara, A., Chevallier, F., de Noblet, N., Friend, A. D., Friedlingstein, P., Grünwald, T., Heinesch, B., Keronen, P., Knohl, A., Krinner, G., Loustau, D., Manca, G., Matteucci, G., Miglietta, F., Ourcival, J. M., Papale, D., Pilegaard, K., Rambal, S., Seufert, G., Soussana, J. F., Sanz, M. J., Schulze, E. D., Vesala, T., and Valentini, R.: Europe-wide reduction in primary productivity caused by the heat and drought in 2003, Nature, 437, 529–533, https://doi.org/10.1038/nature03972, 2005.

Conte, M., Sorani, N., and Piervitali, E.: Extreme climatic events over the Mediterranean, in: Mediterranean desertification, edited by Geeson, N., Brandt, C. J., and Thornes, J. B., pp. 15–31, John Wiley & Sons, Chichester West Sussex England and Hoboken NJ USA, 2002.

Cook, B. I., Anchukaitis, K. J., Touchan, R., Meko, D. M., and Cook, E. R.: Spatiotemporal drought variability in the Mediterranean over the last 900 years, Journal of geophysical research. Atmospheres, 121, 2060–2074, https://doi.org/10.1002/2015JD023929, 2016.

Copernicus Climate Change Service: ERA5: Fifth generation of ECMWF atmospheric reanalyses of the global climate: Copernicus Climate Change Service Climate Data Store (CDS), https://doi.org/10.24381/cds.adbb2d47, 2017.

Crafts-Brandner, S. J. and Salvucci, M. E.: Rubisco activase constrains the photosynthetic potential of leaves at high temperature and CO_2, Proceedings of the National Academy of Sciences, 97, 13 430–13 435, https://doi.org/10.1073/pnas.230451497, 2000.

Cramer, W., Guiot, J., Fader, M., Garrabou, J., Gattuso, J.-P., Iglesias, A., Lange, M. A., Lionello, P., Llasat, M. C., Paz, S., Peñuelas, J., Snoussi, M., Toreti, A., Tsimplis, M. N., and Xoplaki, E.: Climate change and interconnected risks to sustainable development in the Mediterranean, Nature Climate Change, 8, 972–980, https://doi.org/10.1038/s41558-018-0299-2, 2018.

Crausbay, S. D., Ramirez, A. R., Carter, S. L., Cross, M. S., Hall, K. R., Bathke, D. J., Betancourt, J. L., Colt, S., Cravens, A. E., Dalton, M. S., Dunham, J. B., Hay, L. E., Hayes, M. J., McEvoy, J., McNutt, C. A., Moritz, M. A., Nislow, K. H., Raheem, N., and Sanford, T.: Defining Ecological Drought for the Twenty-First Century, Bulletin of the American Meteorological Society, 98, 2543–2550, https://doi.org/10.1175/BAMS-D-16-0292.1, 2017.

Crocetti, L., Forkel, M., Fischer, M., Jurečka, F., Grlj, A., Salentinig, A., Trnka, M., Anderson, M., Ng, W.-T., Kokalj, Ž., Bucur, A., and Dorigo, W.: Earth Observation for agricultural drought monitoring in the Pannonian Basin (southeastern Europe): current state and future directions, Regional Environmental Change, 20, 123, https://doi.org/10.1007/s10113-020-01710-w, 2020.

Dale, V. H., Joyce, L. A., Mcnulty, S., Neilson, R. P., Ayres, M. P., Flannigan, M. D., Hanson, P. J., Irland, L. C., Lugo, A. E., Peterson, C. J., Simberloff, D., Swanson, F. J., Stocks, B. J., and Michael Wotton, B.: Climate Change and Forest Disturbances, BioScience, 51, 723–734, https://doi.org/10.1641/0006-3568(2001)051[0723:CCAFD]2.0.CO;2, 2001.

Daryanto, S., Wang, L., and Jacinthe, P.-A.: Global Synthesis of Drought Effects on Maize and Wheat Production, PloS one, 11, e0156 362, https://doi.org/10.1371/journal.pone.0156362, 2016.

de Boeck, H. J., Dreesen, F. E., Janssens, I. A., and Nijs, I.: Whole-system responses of experimental plant communities to climate extremes imposed in different seasons, The New Phytologist, 189, 806–817, https://doi.org/10.1111/j.1469-8137.2010.03515.x, 2011.

de Boeck, H. J., Bassin, S., Verlinden, M., Zeiter, M., and Hiltbrunner, E.: Simulated heat waves affected alpine grassland only in combination with drought, The New Phytologist, 209, 531–541, https://doi.org/10.1111/nph.13601, 2016.

Denissen, J. M., Teuling, A. J., Reichstein, M., and Orth, R.: Critical Soil Moisture Derived From Satellite Observations Over Europe, Journal of Geophysical Research: Atmospheres, 125, https://doi.org/10.1029/2019JD031672, 2020.

Denton, E. M., Dietrich, J. D., Smith, M. D., and Knapp, A. K.: Drought timing differentially affects above- and belowground productivity in a mesic grassland, Plant Ecology, 218, 317–328, https://doi.org/10.1007/s11258-016-0690-x, 2017.

Desilets, D. and Zreda, M.: Footprint diameter for a cosmic-ray soil moisture probe: Theory and Monte Carlo simulations, Water Resources Research, 49, 3566–3575, https://doi.org/10.1002/wrcr.20187, 2013.

Diffenbaugh, N. S. and Giorgi, F.: Climate change hotspots in the CMIP5 global climate model ensemble, Climatic change, 114, 813–822, https://doi.org/10.1007/s10584-012-0570-x, 2012.

Donges, J. F., Schleussner, C.-F., Siegmund, J. F., and Donner, R. V.: Event coincidence analysis for quantifying statistical interrelationships between event time series, The European Physical Journal Special Topics, 225, 471–487, https://doi.org/10.1140/epjst/e2015-50233-y, 2016.

Dorigo, W., Wagner, W., Albergel, C., Albrecht, F., Balsamo, G., Brocca, L., Chung, D., Ertl, M., Forkel, M., Gruber, A., Haas, E., Hamer, P. D., Hirschi, M., Ikonen, J., de Jeu, R., Kidd, R., Lahoz, W., Liu, Y. Y., Miralles, D., Mistelbauer, T., Nicolai-Shaw, N., Parinussa, R., Pratola, C., Reimer, C., van der Schalie, R., Seneviratne, S. I., Smolander, T., and Lecomte, P.: ESA CCI Soil Moisture for improved Earth system understanding: State-of-the art and future directions, Remote Sensing of Environment, 203, 185–215, https://doi.org/10.1016/j.rse.2017.07.001, 2017.

Dünkeloh, A. and Jacobeit, J.: Circulation dynamics of Mediterranean precipitation variability 1948-98, International Journal of Climatology, 23, 1843–1866, https://doi.org/10.1002/joc.973, 2003.

Duveiller, G., Filipponi, F., Walther, S., Köhler, P., Frankenberg, C., Guanter, L., and Cescatti, A.: A spatially downscaled sun-induced fluorescence global product for enhanced monitoring of vegetation productivity, Earth System Science Data, 12, 1101–1116, https://doi.org/10.5194/essd-12-1101-2020, 2020.

Erşahin, S., Bilgili, B. C., Dikmen, Ü., and Ercanli, İ.: Net Primary Productivity of Anatolian Forests in Relation to Climate, 2000–2010, Forest Science, 62, 698–709, https://doi.org/10.5849/forsci.15-171, 2016.

ESA: Land Cover CCI Product User Guide Version 2: Tech. Rep., URL `maps.elie.ucl.ac.be/CCI/viewer/download/ESACCI-LC-Ph2-PUGv2_2.0.pdf`, last access: 19/12/2021, 2017.

FAOSTAT: FAO Statistics, Food and Agriculture Organization of the United Nations, Rome, URL `https://www.fao.org/faostat/en/`, last access: 19/12/2021, 2019.

Feng, S., Hao, Z., Wu, X., Zhang, X., and Hao, F.: A multi-index evaluation of changes in compound dry and hot events of global maize areas, Journal of Hydrology, 602, 126 728, https://doi.org/10.1016/j.jhydrol.2021.126728, 2021.

Fenner, D., Holtmann, A., Krug, A., and Scherer, D.: Heat waves in Berlin and Potsdam, Germany – Long–term trends and comparison of heat wave definitions from 1893 to 2017, International Journal of Climatology, 39, 2422–2437, https://doi.org/10.1002/joc.5962, 2019.

Field, C. B., Barros, V., Stocker, T. F., Qin, D., Dokken, D. J., Ebi, K. L., Mastrandrea, M., Mach, J., Plattner, G.-K., Allen, K., Tignor, M., and Midgley, P. M., eds.: Managing the Risks of Extreme Events and Disasters to Advance Climate Change Adaptation: A Special Report of Working Groups I and II of the Intergovernmental Panel on Climate Change, Cambridge University Press, Cambridge, UK, and New York, NY, USA, 2012.

Fischer, E. M. and Knutti, R.: Robust projections of combined humidity and temperature extremes, Nature Climate Change, 3, 126–130, https://doi.org/10.1038/nclimate1682, 2013.

Flach, M., Brenning, A., Gans, F., Reichstein, M., Sippel, S., and Mahecha, M. D.: Vegetation modulates the impact of climate extremes on gross primary production, Biogeosciences, 18, 39–53, https://doi.org/10.5194/bg-18-39-2021, 2021.

Fraga, H., Pinto, J. G., Viola, F., and Santos, J. A.: Climate change projections for olive yields in the Mediterranean Basin, International Journal of Climatology, 40, 769–781, https://doi.org/10.1002/joc.6237, 2020.

Frank, D., Reichstein, M., Bahn, M., Thonicke, K., Frank, D., Mahecha, M. D., Smith, P., van der Velde, M., Vicca, S., Babst, F., Beer, C., Buchmann, N., Canadell, J. G., Ciais, P., Cramer, W., Ibrom, A., Miglietta, F., Poulter, B., Rammig, A., Seneviratne, S. I., Walz, A., Wattenbach, M., Zavala, M. A., and Zscheischler, J.: Effects of climate extremes on the terrestrial carbon cycle: concepts, processes and potential future impacts, Global Change Biology, 21, 2861–2880, https://doi.org/10.1111/gcb.12916, 2015.

Friedman, J., Hastie, T., and Tibshirani, R.: Regularization Paths for Generalized Linear Models via Coordinate Descent, Journal of Statistical Software, 33, 1–22, https://doi.org/10.18637/jss.v033.i01, 2010.

Gao, X. and Giorgi, F.: Increased aridity in the Mediterranean region under greenhouse gas forcing estimated from high resolution simulations with a regional climate model, Global and Planetary Change, 62, 195–209, https://doi.org/10.1016/j.gloplacha.2008.02.002, 2008.

García-Plazaola, J. I., Esteban, R., Hormaetxe, K., Fernández-Marín, B., and Becerril, J. M.: Photoprotective responses of Mediterranean and Atlantic trees to the extreme heat-wave of summer 2003 in Southwestern Europe, Trees, 22, 385–392, https://doi.org/10.1007/s00468-007-0199-y, 2008.

Gaupp, F., Hall, J., Mitchell, D., and Dadson, S.: Increasing risks of multiple breadbasket failure under 1.5 and 2 °C global warming, Agricultural Systems, 175, 34–45, https://doi.org/10.1016/j.agsy.2019.05.010, 2019.

GCOS-138: Implementation Plan for the Global Observing System for Climate in support of the UNFCCC - 2010 Update, World Meteorological Organization, URL `https://climate.esa.int/sites/default/files/gcos-138.pdf`, last access: 19/12/2021, 2010.

Giorgi, F.: Climate change hot-spots, Geophysical Research Letters, 33, L08 707, https://doi.org/10.1029/2006GL025734, 2006.

Gobron, N., Belward, A., Pinty, B., and Knorr, W.: Monitoring biosphere vegetation 1998-2009, Geophysical Research Letters, 37, L15 402, https://doi.org/10.1029/2010GL043870, 2010.

Gordo, O. and Sanz, J. J.: Long-term temporal changes of plant phenology in the Western Mediterranean, Global Change Biology, 15, 1930–1948, https://doi.org/10.1111/j.1365-2486.2009.01851.x, 2009.

Gordo, O. and Sanz, J. J.: Impact of climate change on plant phenology in Mediterranean ecosystems, Global Change Biology, 16, 1082–1106, https://doi.org/10.1111/j.1365-2486.2009.02084.x, 2010.

Gourdji, S. M., Sibley, A. M., and Lobell, D. B.: Global crop exposure to critical high temperatures in the reproductive period: historical trends and future projections, Environmental Research Letters, 8, 024 041, https://doi.org/10.1088/1748-9326/8/2/024041, 2013.

Gouveia, C. M., Bistinas, I., Liberato, M. L., Bastos, A., Koutsias, N., and Trigo, R.: The outstanding synergy between drought, heatwaves and fuel on the 2007 Southern Greece exceptional fire season, Agricultural and Forest Meteorology, 218-219, 135–145, https://doi.org/10.1016/j.agrformet.2015.11.023, 2016.

Green, J. K., Konings, A. G., Alemohammad, S. H., Berry, J., Entekhabi, D., Kolassa, J., Lee, J.-E., and Gentine, P.: Regionally strong feedbacks between the atmosphere and terrestrial biosphere, Nature Geoscience, 10, 410–414, https://doi.org/10.1038/ngeo2957, 2017.

Grossiord, C., Buckley, T. N., Cernusak, L. A., Novick, K. A., Poulter, B., Siegwolf, R. T. W., Sperry, J. S., and McDowell, N. G.: Plant responses to rising vapor pressure deficit, New Phytologist, 226, 1550–1566, https://doi.org/10.1111/nph.16485, 2020.

Gruber, A., Scanlon, T., van der Schalie, R., Wagner, W., and Dorigo, W.: Evolution of the ESA CCI Soil Moisture climate data records and their underlying merging methodology, Earth System Science Data, 11, 717–739, https://doi.org/10.5194/essd-11-717-2019, 2019.

Gu, L., Chen, J., Yin, J., Sullivan, S. C., Wang, H.-M., Guo, S., Zhang, L., and Kim, J.-S.: Projected increases in magnitude and socioeconomic exposure of global droughts in 1.5 and 2 °C warmer climates, Hydrology and Earth System Sciences, 24, 451–472, https://doi.org/10.5194/hess-24-451-2020, 2020.

Guiot, J. and Cramer, W.: Climate change: The 2015 Paris Agreement thresholds and Mediterranean basin ecosystems, Science (New York, N.Y.), 354, 465–468, https://doi.org/10.1126/science.aah5015, 2016.

Guiot, J. and Kaniewski, D.: The Mediterranean Basin and Southern Europe in a warmer world: what can we learn from the past?, Frontiers in Earth Science, 3, https://doi.org/10.3389/feart.2015.00028, 2015.

Gutiérrez, E., Campelo, F., Camarero, J. J., Ribas, M., Muntán, E., Nabais, C., and Freitas, H.: Climate controls act at different scales on the seasonal pattern of Quercus ilex L. stem radial increments in NE Spain, Trees, 25, 637–646, https://doi.org/10.1007/s00468-011-0540-3, 2011.

Hamed, R., van Loon, A. F., Aerts, J., and Coumou, D.: Impacts of compound hot–dry extremes on US soybean yields, Earth System Dynamics, 12, 1371–1391, https://doi.org/10.5194/esd-12-1371-2021, 2021.

Hao, Z. and AghaKouchak, A.: A Nonparametric Multivariate Multi-Index Drought Monitoring Framework, Journal of Hydrometeorology, 15, 89–101, https://doi.org/10.1175/JHM-D-12-0160.1, 2014.

Hao, Z., Singh, V., and Hao, F.: Compound Extremes in Hydroclimatology: A Review, Water, 10, 718, https://doi.org/10.3390/w10060718, 2018.

Hartmann, D. L., Tank, A. M. K., Rusticucci, M., Alexander, L. V., Brönnimann, S., Charabi, Y. A. R., Dentener, F. J., Dlugokencky, E. J., Easterling, D. R., Kaplan, A., et al.: Observations: atmosphere and surface, in: Climate Change 2013: The Physical Science Basis. Contribution of Working Group I to the Fifth Assessment Report of the Intergovernmental Panel on Climate Change, edited by Stocker, T. F., Qin, D., Plattner, G. K., Tignor, M., Allen, S. K., Boschung, J., Nauels, A., Xia, Y., Bex, V., and Midgley, P. M., pp. 159–254, Cambridge University Press, New York, 2013.

Hatfield, J. L. and Prueger, J. H.: Temperature extremes: Effect on plant growth and development, Weather and Climate Extremes, 10, 4–10, https://doi.org/10.1016/j.wace.2015.08.001, 2015.

Hayes, M., Svoboda, M., Wall, N., and Widhalm, M.: The Lincoln Declaration on Drought Indices: Universal Meteorological Drought Index Recommended, Bulletin of the American Meteorological Society, 92, 485–488, https://doi.org/10.1175/2010BAMS3103.1, 2011.

Hazeleger, W., Wang, X., Severijns, C., Ştefănescu, S., Bintanja, R., Sterl, A., Wyser, K., Semmler, T., Yang, S., van den Hurk, B., van Noije, T., van der Linden, E., and van der Wiel, K.: EC-Earth V2.2: description and validation of a new seamless earth system prediction model, Climate Dynamics, 39, 2611–2629, https://doi.org/10.1007/s00382-011-1228-5, 2012.

He, Q., Silliman, B. R., Liu, Z., and Cui, B.: Natural enemies govern ecosystem resilience in the face of extreme droughts, Ecology Letters, 20, 194–201, https://doi.org/10.1111/ele.12721, 2017.

Hegerl, G. C., Hanlon, H., and Beierkuhnlein, C.: Elusive extremes, Nature Geoscience, 4, 142–143, https://doi.org/10.1038/ngeo1090, 2011.

Heim, R. R.: A Review of Twentieth-Century Drought Indices Used in the United States, Bulletin of the American Meteorological Society, 83, 1149–1166, https://doi.org/10.1175/1520-0477-83.8.1149, 2002.

Hersbach, H., Bell, W., Berrisford, P., Horányi, A., J., M.-S., Nicolas, J., Radu, R., Schepers, D., Simmons, A., Soci, C., and Dee, D.: Global reanalysis: goodbye ERA-Interim, hello ERA5, ECMWF (European Centre for Medium-Range Weather Forecasts), Newsletter 159, 17–24, https://doi.org/10.21957/VF291HEHD7, 2019.

Hoegh-Guldberg, O., Jacob, D., Taylor, M., Bindi, M., Brown, S., Camilloni, I., and Zhou, G.: Impacts of 1.5 °C Global Warming on Natural and Human Systems, in: Global warming of 1.5 °C. An IPCC Special Report on the impacts of global warming of 1.5°C above pre-industrial levels and related global greenhouse gas emission pathways, in the context of strengthening the global response to the threat of climate change, sustainable development, and efforts to eradicate poverty, edited by Masson-Delmotte, V., Zhai, P., Pörtner, H.-O., Roberts, D., Skea, J., Shukla, P. R., Pirani, A., Moufouma-Okia, W., Péan, C., Pidcock, R., Connors, S., Matthews, J., Chen, Y., Zhou, X., Gomis, M. I., Lonnoy, E., Maycock, T., Tignor, M., and Waterfield, T., pp. 175–311, URL `https://www.ipcc.ch/sr15/`, last access: 19/12/2021, 2018.

Horton, R. M., Mankin, J. S., Lesk, C., Coffel, E., and Raymond, C.: A Review of Recent Advances in Research on Extreme Heat Events, Current Climate Change Reports, 2, 242–259, https://doi.org/10.1007/s40641-016-0042-x, 2016.

Huete, A.: A soil-adjusted vegetation index (SAVI), Remote Sensing of Environment, 25, 295–309, https://doi.org/10.1016/0034-4257(88)90106-X, 1988.

Iizumi, T., Shiogama, H., Imada, Y., Hanasaki, N., Takikawa, H., and Nishimori, M.: Crop production losses associated with anthropogenic climate change for 1981-2010 compared with preindustrial levels, International Journal of Climatology, 38, 5405–5417, https://doi.org/10.1002/joc.5818, 2018.

Jackson, T. J. and Schmugge, T. J.: Vegetation effects on the microwave emission of soils, Remote Sensing of Environment, 36, 203–212, https://doi.org/10.1016/0034-4257(91)90057-D, 1991.

Jagadish, K. S. V., Kadam, N. N., Xiao, G., Melgar, R. J., Bahuguna, R. N., Quinones, C., Tamilselvan, A., Prasad, P. V. V., and Jagadish, K. S.: Agronomic and Physiological

Responses to High Temperature, Drought, and Elevated CO_2 Interactions in Cereals, in: Advances in Agronomy, edited by Sparks, D. L., vol. 127 of *Advances in Agronomy*, pp. 111–156, Elsevier Science, Burlington, https://doi.org/10.1016/B978-0-12-800131-8.00003-0, 2014.

Jentsch, A., Kreyling, J., and Beierkuhnlein, C.: A new generation of climate-change experiments: events, not trends, Frontiers in Ecology and the Environment, 5, 365–374, 2007.

Jentsch, A., Kreyling, J., Elmer, M., Gellesch, E., Glaser, B., Grant, K., Hein, R., Lara, M., Mirzae, H., Nadler, S. E., Nagy, L., Otieno, D., Pritsch, K., Rascher, U., Schädler, M., Schloter, M., Singh, B. K., Stadler, J., Walter, J., Wellstein, C., Wöllecke, J., and Beierkuhnlein, C.: Climate extremes initiate ecosystem-regulating functions while maintaining productivity, Journal of Ecology, 99, 689–702, https://doi.org/10.1111/j.1365-2745.2011.01817.x, 2011.

Kaniewski, D., van Campo, E., and Weiss, H.: Drought is a recurring challenge in the Middle East, Proceedings of the National Academy of Sciences, 109, 3862–3867, https://doi.org/10.1073/pnas.1116304109, 2012.

Kaniewski, D., Guiot, J., and van Campo, E.: Drought and societal collapse 3200 years ago in the Eastern Mediterranean: a review, WIREs Climate Change, 6, 369–382, https://doi.org/10.1002/wcc.345, 2015.

Kappes, M. S., Keiler, M., von Elverfeldt, K., and Glade, T.: Challenges of analyzing multi-hazard risk: a review, Natural Hazards, 64, 1925–1958, https://doi.org/10.1007/s11069-012-0294-2, 2012.

Keenan, T. F., Sabate, S., and Gracia, C.: The importance of mesophyll conductance in regulating forest ecosystem productivity during drought periods, Global Change Biology, 16, 1019–1034, https://doi.org/10.1111/j.1365-2486.2009.02017.x, 2010.

Kelley, C. P., Mohtadi, S., Cane, M. A., Seager, R., and Kushnir, Y.: Climate change in the Fertile Crescent and implications of the recent Syrian drought, Proceedings of the National Academy of Sciences, 112, 3241–3246, https://doi.org/10.1073/pnas.1421533112, 2015.

Kerr, J. T. and Ostrovsky, M.: From space to species: ecological applications for remote sensing, Trends in Ecology & Evolution, 18, 299–305, https://doi.org/10.1016/S0169-5347(03)00071-5, 2003.

Kidd, R. and Haas, E.: ESA Climate Change Initiative Plus Soil Moisture: Soil Moisture ECV Product User Guide (PUG) Revision 3: D3.3.1 Version 4.5, Earth Observation Data Centre for Water Resources Monitoring (EODC) GmbH, URL `https://www.esa-soilmoisture-cci.org/node/145`, last access: 19/12/2021, 2018.

Köhli, M., Schrön, M., Zreda, M., Schmidt, U., Dietrich, P., and Zacharias, S.: Footprint characteristics revised for field–scale soil moisture monitoring with cosmic–ray neutrons, Water Resources Research, 51, 5772–5790, https://doi.org/10.1002/2015WR017169, 2015.

Konings, A. G., Rao, K., and Steele-Dunne, S. C.: Macro to micro: microwave remote sensing of plant water content for physiology and ecology, New Phytologist, 223, 1166–1172, https://doi.org/10.1111/nph.15808, 2019.

Kornhuber, K., Coumou, D., Vogel, E., Lesk, C., Donges, J. F., Lehmann, J., and Horton, R. M.: Amplified Rossby waves enhance risk of concurrent heatwaves in major breadbasket regions, Nature Climate Change, 10, 48–53, https://doi.org/10.1038/s41558-019-0637-z, 2020.

Kotsias, G., Lolis, C. J., Hatzianastassiou, N., Lionello, P., and Bartzokas, A.: An objective definition of seasons for the Mediterranean region, International Journal of Climatology, 41, E1889–E1905, https://doi.org/10.1002/joc.6819, 2020.

Kottek, M., Grieser, J., Beck, C., Rudolf, B., and Rubel, F.: World Map of the Köppen-Geiger climate classification updated, Meteorologische Zeitschrift, 15, 259–263, https://doi.org/10.1127/0941-2948/2006/0130, 2006.

Kreibich, H., Blauhut, V., Aerts, J. C., Bouwer, L. M., van Lanen, H. A., Mejia, A., Mens, M., and van Loon, A. F.: How to improve attribution of changes in drought and flood impacts, Hydrological Sciences Journal, 64, 1–18, https://doi.org/10.1080/02626667.2018.1558367, 2019.

Kreyling, J., Wenigmann, M., Beierkuhnlein, C., and Jentsch, A.: Effects of Extreme Weather Events on Plant Productivity and Tissue Die-Back are Modified by Community Composition, Ecosystems, 11, 752–763, https://doi.org/10.1007/s10021-008-9157-9, 2008.

Kurz, W. A., Dymond, C. C., Stinson, G., Rampley, G. J., Neilson, E. T., Carroll, A. L., Ebata, T., and Safranyik, L.: Mountain pine beetle and forest carbon feedback to climate change, Nature, 452, 987–990, https://doi.org/10.1038/nature06777, 2008.

Le Gouis, J., Oury, F.-X., and Charmet, G.: How changes in climate and agricultural practices influenced wheat production in Western Europe, Journal of Cereal Science, 93, 102 960, https://doi.org/10.1016/j.jcs.2020.102960, 2020.

Lemordant, L., Gentine, P., Stéfanon, M., Drobinski, P., and Fatichi, S.: Modification of land-atmosphere interactions by CO_2 effects: Implications for summer dryness and heat wave amplitude, Geophysical Research Letters, 43, 10,240–10,248, https://doi.org/10.1002/2016GL069896, 2016.

Leonard, M., Westra, S., Phatak, A., Lambert, M., van den Hurk, B., McInnes, K., Risbey, J., Schuster, S., Jakob, D., and Stafford-Smith, M.: A compound event framework for understanding extreme impacts, WIREs Climate Change, 5, 113–128, https://doi.org/10.1002/wcc.252, 2014.

Lesk, C., Rowhani, P., and Ramankutty, N.: Influence of extreme weather disasters on global crop production, Nature, 529, 84–87, https://doi.org/10.1038/nature16467, 2016.

Lesk, C., Coffel, E., Winter, J., Ray, D., Zscheischler, J., Seneviratne, S. I., and Horton, R.: Stronger temperature–moisture couplings exacerbate the impact of climate warming on global crop yields, Nature Food, 2, 683–691, https://doi.org/10.1038/s43016-021-00341-6, 2021.

Leutner, B., Horning, N., and Schwalb-Willmann, J.: RStoolbox: Tools for Remote Sensing Data Analysis, URL `http://bleutner.github.io/RStoolbox`, last access: 19/12/2021, 2019.

Lewis, S. C., King, A. D., Perkins-Kirkpatrick, S. E., and Mitchell, D. M.: Regional hotspots of temperature extremes under 1.5 °C and 2 °C of global mean warming, Weather and Climate Extremes, 26, 100 233, https://doi.org/10.1016/j.wace.2019.100233, 2019.

Liaw, A. and Wiener, M.: Classification and Regression by randomForest, R News, 2, 18–22, URL `https://cran.r-project.org/doc/Rnews/`, last access: 19/12/2021, 2002.

Lionello, P. and Scarascia, L.: The relation between climate change in the Mediterranean region and global warming, Regional Environmental Change, 18, 1481–1493, https://doi.org/10.1007/s10113-018-1290-1, 2018.

Lionello, P., Malanotte-Rizzoli P., Boscolo, R., Alpert, P., Artale, V., Li, L., Luterbacher, J., May, W., Trigo, R., Tsimplis, M., Ulbrich, U., and Xoplaki, E.: The Mediterranean Climate: An Overview of the Main Characteristics and Issues, in: Mediterranean climate variability, edited by Lionello, P., Malanotte-Rizzoli, P., and Boscolo, R., Developments in earth & environmental sciences, pp. 1–26, Elsevier, Amsterdam, 2006.

Lionello, P., Abrantes, F., Congedi, L., Dulac, F., Gacic, M., Gomis, D., Goodess, C., Hoff, H., Kutiel, H., Luterbacher, J., Planton, S., Reale, M., Schröder, K., Struglia, M. V., Toreti, A., Tsimplis, M., Ulbrich, U., and Xoplaki, E.: Mediterranean Climate: Background Information, in: The climate of the Mediterranean region, edited by Lionello, P., Elsevier insights, pp. xxxv–xc, Elsevier Science, Amsterdam, 2012.

Lischeid, G., Webber, H., Sommer, M., Nendel, C., and Ewert, F.: Machine learning in crop yield modelling: A powerful tool, but no surrogate for science, Agricultural and Forest Meteorology, 312, 108 698, https://doi.org/10.1016/j.agrformet.2021.108698, 2022.

Little, C. M., Horton, R. M., Kopp, R. E., Oppenheimer, M., Vecchi, G. A., and Villarini, G.: Joint projections of US East Coast sea level and storm surge, Nature Climate Change, 5, 1114–1120, https://doi.org/10.1038/nclimate2801, 2015.

Liu, B., Siu, Y. L., Mitchell, G., and Xu, W.: The danger of mapping risk from multiple natural hazards, Natural Hazards, 82, 139–153, https://doi.org/10.1007/s11069-016-2184-5, 2016.

Liu, G., Liu, H., and Yin, Y.: Global patterns of NDVI-indicated vegetation extremes and their sensitivity to climate extremes, Environmental Research Letters, 8, 025 009, https://doi.org/10.1088/1748-9326/8/2/025009, 2013.

Lloret, F., Peñuelas, J., and Estiarte, M.: Experimental evidence of reduced diversity of seedlings due to climate modification in a Mediterranean–type community, Global Change Biology, 10, 248–258, https://doi.org/10.1111/j.1365-2486.2004.00725.x, 2004.

Lloret, F., Escudero, A., Iriondo, J. M., Martínez-Vilalta, J., and Valladares, F.: Extreme climatic events and vegetation: the role of stabilizing processes, Global Change Biology, 18, 797–805, https://doi.org/10.1111/j.1365-2486.2011.02624.x, 2012.

Lobell, D. B., Schlenker, W., and Costa-Roberts, J.: Climate trends and global crop production since 1980, Science (New York, N.Y.), 333, 616–620, https://doi.org/10.1126/science.1204531, 2011.

Lobell, D. B., Hammer, G. L., McLean, G., Messina, C., Roberts, M. J., and Schlenker, W.: The critical role of extreme heat for maize production in the United States, Nature Climate Change, 3, 497–501, https://doi.org/10.1038/nclimate1832, 2013.

Luo, Q.: Temperature thresholds and crop production: a review, Climatic change, 109, 583–598, https://doi.org/10.1007/s10584-011-0028-6, 2011.

Luo, Y., El-Madany, T., Ma, X., Nair, R., Jung, M., Weber, U., Filippa, G., Bucher, S. F., Moreno, G., Cremonese, E., Carrara, A., Gonzalez-Cascon, R., Cáceres Escudero, Y., Galvagno, M., Pacheco-Labrador, J., Martín, M. P., Perez-Priego, O., Reichstein, M., Richardson, A. D., Menzel, A., Römermann, C., and Migliavacca, M.: Nutrients and water availability constrain the seasonality of vegetation activity in a Mediterranean ecosystem, Global Change Biology, 26, 4379–4400, https://doi.org/10.1111/gcb.15138, 2020.

Mahony, C. R. and Cannon, A. J.: Wetter summers can intensify departures from natural variability in a warming climate, Nature communications, 9, 783, https://doi.org/10.1038/s41467-018-03132-z, 2018.

Mäkinen, H., Kaseva, J., Trnka, M., Balek, J., Kersebaum, K. C., Nendel, C., Gobin, A., Olesen, J. E., Bindi, M., Ferrise, R., Moriondo, M., Rodríguez, A., Ruiz-Ramos, M., Takáč, J., Bezák, P., Ventrella, D., Ruget, F., Capellades, G., and Kahiluoto, H.: Sensitivity of European wheat to extreme weather, Field Crops Research, 222, 209–217, https://doi.org/10.1016/j.fcr.2017.11.008, 2018.

Manning, C., Widmann, M., Bevacqua, E., van Loon, A. F., Maraun, D., and Vrac, M.: Soil Moisture Drought in Europe: A Compound Event of Precipitation and Potential Evapotranspiration on Multiple Time Scales, Journal of Hydrometeorology, 19, 1255–1271, https://doi.org/10.1175/JHM-D-18-0017.1, 2018.

Masson-Delmotte, V., Zhai, P., Pirani, A., Connors, S. L., Péan, C., Berger, S., Caud, N., Chen, Y., Goldfarb, L., Gomis, M. I., Huang, M., Leitzell, K., Lonnoy, E., Matthews, J., Maycock, T. K., Waterfield, T., Yelekçi, O., Yu, R., and Zhou, B., eds.: Climate Change 2021: The Physical Science Basis: Summary for Policymakers, Cambridge University Press, URL https://www.ipcc.ch/report/sixth-assessment-report-working-group-i/, last access: 19/12/2021, 2021.

Mateo-Sanchis, A., Piles, M., Amorós-López, J., Muñoz-Marí, J., Adsuara, J. E., Moreno-Martínez, Á., and Camps-Valls, G.: Learning main drivers of crop progress and failure in Europe with interpretable machine learning, International Journal of Applied Earth Observation and Geoinformation, 104, 102 574, https://doi.org/10.1016/j.jag.2021.102574, 2021.

Mathbout, S., Lopez-Bustins, J. A., Royé, D., and Martin-Vide, J.: Mediterranean-Scale Drought: Regional Datasets for Exceptional Meteorological Drought Events during 1975–2019, Atmosphere, 12, 941, https://doi.org/10.3390/atmos12080941, 2021.

Matusick, G., Ruthrof, K. X., Kala, J., Brouwers, N. C., Breshears, D. D., and Hardy, G. E. S. J.: Chronic historical drought legacy exacerbates tree mortality and crown dieback during acute heatwave-compounded drought, Environmental Research Letters, 13, 095 002, https://doi.org/10.1088/1748-9326/aad8cb, 2018.

Mbow, C., Rosenzweig, C., Barioni, L. G., Benton, T. G., Herrero, M., Krishnapillai, M., Liwenga, E., Pradhan, P., Rivera-Ferre, M. G., Sapkota, TB, Tubiello, FN, and Xu, Y.: Food security, in: Climate Change and Land: an IPCC special report on climate change, desertification, land degradation, sustainable land management, food security, and greenhouse gas fluxes in terrestrial ecosystems, edited by Shukla, P. R., Skea, J., Calvo Buendia, E., Masson-Delmotte, V., Pörtner, H.-O., Roberts, D. C., Zhai, P., Slade, R., Connors, S., van Diemen, R., Ferrat, M., Haughey, E., Luz, S., Neogi, S., Pathak, M., Petzold, J., Portugal Pereira, J., Vyas, P., Huntley, E., Kissick, K., Belkacemi, M., and Malley, J., URL https://www.ipcc.ch/srccl/, last access: 19/12/2021, 2019.

McDowell, N., Pockman, W. T., Allen, C. D., Breshears, D. D., Cobb, N., Kolb, T., Plaut, J., Sperry, J., West, A., Williams, D. G., and Yepez, E. A.: Mechanisms of plant survival and mortality during drought: why do some plants survive while others succumb to drought?, New Phytologist, 178, 719–739, https://doi.org/10.1111/j.1469-8137.2008.02436.x, 2008.

McLeod, A., Xu, C., and Lai, Y.: Best Subset GLM and Regression Utilities, URL https://CRAN.R-project.org/package=bestglm, last access: 19/12/2021, 2020.

McPhillips, L. E., Chang, H., Chester, M. V., Depietri, Y., Friedman, E., Grimm, N. B., Kominoski, J. S., McPhearson, T., Méndez-Lázaro, P., Rosi, E. J., and Shafiei Shiva, J.: Defining Extreme Events: A Cross-Disciplinary Review, Earth's Future, 6, 441–455, https://doi.org/10.1002/2017EF000686, 2018.

Miao, S., Zou, C. B., and Breshears, D. D.: Vegetation responses to extreme hydrological events: sequence matters, The American naturalist, 173, 113–118, https://doi.org/10.1086/593307, 2009.

Miralles, D. G., Gentine, P., Seneviratne, S. I., and Teuling, A. J.: Land-atmospheric feedbacks during droughts and heatwaves: state of the science and current challenges, Annals of the New York Academy of Sciences, 1436, 19–35, https://doi.org/10.1111/nyas.13912, 2019.

Mishra, A. K. and Singh, V. P.: A review of drought concepts, Journal of Hydrology, 391, 202–216, https://doi.org/10.1016/j.jhydrol.2010.07.012, 2010.

Moesinger, L., Dorigo, W., de Jeu, R., van der Schalie, R., Scanlon, T., Teubner, I., and Forkel, M.: The global long-term microwave Vegetation Optical Depth Climate Archive (VODCA), Earth System Science Data, 12, 177–196, https://doi.org/10.5194/essd-12-177-2020, 2020.

Monneveux, P., Jing, R., and Misra, S. C.: Phenotyping for drought adaptation in wheat using physiological traits, Frontiers in physiology, 3, 429, https://doi.org/10.3389/fphys.2012.00429, 2012.

Moreno, J. F.: The Fluorescence Explorer (FLEX) Mission: From Spectral Measurements to High-Level Science Products, in: IEEE International Geoscience and Remote Sensing Symposium IGARSS, 7/11/2021 - 7/16/2021, pp. 115–118, IEEE, https://doi.org/10.1109/IGARSS47720.2021.9553537, 2021.

Moriondo, M., Jones, G. V., Bois, B., Dibari, C., Ferrise, R., Trombi, G., and Bindi, M.: Projected shifts of wine regions in response to climate change, Climatic change, 119, 825–839, https://doi.org/10.1007/s10584-013-0739-y, 2013a.

Moriondo, M., Trombi, G., Ferrise, R., Brandani, G., Dibari, C., Ammann, C. M., Lippi, M. M., and Bindi, M.: Olive trees as bio-indicators of climate evolution in the Mediterranean Basin, Global Ecology and Biogeography, 22, 818–833, https://doi.org/10.1111/geb.12061, 2013b.

Mueller, B. and Seneviratne, S. I.: Hot days induced by precipitation deficits at the global scale, Proceedings of the National Academy of Sciences, 109, 12 398–12 403, https://doi.org/10.1073/pnas.1204330109, 2012.

Muñoz-Sabater, J.: ERA5-Land monthly averaged data from 1981 to present, Copernicus Climate Change Service (C3S) Climate Data Store (CDS), https://doi.org/10.24381/CDS.68D2BB30, 2019.

Nicolai-Shaw, N., Zscheischler, J., Hirschi, M., Gudmundsson, L., and Seneviratne, S. I.: A drought event composite analysis using satellite remote-sensing based soil moisture, Remote Sensing of Environment, 203, 216–225, https://doi.org/10.1016/j.rse.2017.06.014, 2017.

Niu, S., Luo, Y., Li, D., Cao, S., Xia, J., Li, J., and Smith, M. D.: Plant growth and mortality under climatic extremes: An overview, Environmental and Experimental Botany, 98, 13–19, https://doi.org/10.1016/j.envexpbot.2013.10.004, 2014.

Norby, R. J. and Zak, D. R.: Ecological Lessons from Free-Air CO_2 Enrichment (FACE) Experiments, Annual Review of Ecology, Evolution, and Systematics, 42, 181–203, https://doi.org/10.1146/annurev-ecolsys-102209-144647, 2011.

Novick, K. A., Ficklin, D. L., Stoy, P. C., Williams, C. A., Bohrer, G., Oishi, A. C., Papuga, S. A., Blanken, P. D., Noormets, A., Sulman, B. N., Scott, R. L., Wang, L., and Phillips, R. P.: The increasing importance of atmospheric demand for ecosystem water and carbon fluxes, Nature Climate Change, 6, 1023–1027, https://doi.org/10.1038/nclimate3114, 2016.

Orlowsky, B. and Seneviratne, S. I.: Global changes in extreme events: regional and seasonal dimension, Climatic change, 110, 669–696, https://doi.org/10.1007/s10584-011-0122-9, 2012.

Owe, M., de Jeu, R., and Holmes, T.: Multisensor historical climatology of satellite-derived global land surface moisture, Journal of Geophysical Research, 113, F01 002, https://doi.org/10.1029/2007JF000769, 2008.

Pausas, J. G. and Millán, M. M.: Greening and Browning in a Climate Change Hotspot: The Mediterranean Basin, BioScience, 69, 143–151, https://doi.org/10.1093/biosci/biy157, 2019.

Peichl, M., Thober, S., Samaniego, L., Hansjürgens, B., and Marx, A.: Machine learning methods to assess the effects of a non-linear damage spectrum taking into account soil moisture on winter wheat yields in Germany, Hydrology and Earth System Sciences Discussions, 1–28, https://doi.org/10.5194/hess-2021-9, 2021.

Peña-Bautista, R. J., Hernandez-Espinosa, N., Jones, J. M., Guzmán, C., and Braun, H. J.: CIMMYT Series on Carbohydrates, Wheat, Grains, and Health: Wheat-Based Foods: Their Global and Regional Importance in the Food Supply, Nutrition, and Health, Cereal Foods World, 62, 231–249, https://doi.org/10.1094/CFW-62-5-0231, 2017.

Peña-Gallardo, M., Vicente-Serrano, S. M., Domínguez-Castro, F., and Beguería, S.: The impact of drought on the productivity of two rainfed crops in Spain, Natural Hazards and Earth System Sciences, 19, 1215–1234, https://doi.org/10.5194/nhess-19-1215-2019, 2019.

Peñuelas, J., Sardans, J., Filella, I., Estiarte, M., Llusià, J., Ogaya, R., Carnicer, J., Bartrons, M., Rivas-Ubach, A., Grau, O., Peguero, G., Margalef, O., Pla-Rabés, S., Stefanescu, C., Asensio, D., Preece, C., Liu, L., Verger, A., Barbeta, A., Achotegui-Castells, A., Gargallo-Garriga, A., Sperlich, D., Farré-Armengol, G., Fernández-Martínez, M., Liu, D., Zhang, C., Urbina, I., Camino-Serrano, M., Vives-Ingla, M., Stocker, B., Balzarolo, M., Guerrieri, R., Peaucelle, M., Marañón-Jiménez, S., Bórnez-Mejías, K., Mu, Z., Descals, A., Castellanos, A., and Terradas, J.: Impacts of Global Change on Mediterranean Forests and Their Services, Forests, 8, 463, https://doi.org/10.3390/f8120463, 2017.

Perkins, S. E.: A review on the scientific understanding of heatwaves—Their measurement, driving mechanisms, and changes at the global scale, Atmospheric Research, 164-165, 242–267, https://doi.org/10.1016/j.atmosres.2015.05.014, 2015.

Perkins, S. E. and Alexander, L. V.: On the Measurement of Heat Waves, Journal of Climate, 26, 4500–4517, https://doi.org/10.1175/JCLI-D-12-00383.1, 2013.

Perkins-Kirkpatrick, S. E. and Gibson, P. B.: Changes in regional heatwave characteristics as a function of increasing global temperature, Scientific reports, 7, 12 256, https://doi.org/10.1038/s41598-017-12520-2, 2017.

Pettorelli, N.: The normalized difference vegetation index, Oxford Univ. Press, Oxford, 1 edn., https://doi.org/10.1093/acprof:osobl/9780199693160.001.0001, 2013.

Pettorelli, N., Vik, J. O., Mysterud, A., Gaillard, J.-M., Tucker, C. J., and Stenseth, N. C.: Using the satellite-derived NDVI to assess ecological responses to environmental change, Trends in Ecology & Evolution, 20, 503–510, https://doi.org/10.1016/j.tree.2005.05.011, 2005.

Phoenix, G. K., Emmett, B. A., Britton, A. J., Caporn, S. J. M., Dise, N. B., Helliwell, R., Jones, L., Leake, J. R., Leith, I. D., Sheppard, L. J., Sowerby, A., Pilkington, M. G., Rowe, E. C., Ashmore, M. R., and Power, S. A.: Impacts of atmospheric nitrogen deposition: responses of multiple plant and soil parameters across contrasting ecosystems in long-term field experiments, Global Change Biology, 18, 1197–1215, https://doi.org/10.1111/j.1365-2486.2011.02590.x, 2012.

Piao, S., Zhang, X., Chen, A., Liu, Q., Lian, X., Wang, X., Peng, S., and Wu, X.: The impacts of climate extremes on the terrestrial carbon cycle: A review, Science China Earth Sciences, 1, 1285, https://doi.org/10.1007/s11430-018-9363-5, 2019.

Porter, J. R. and Gawith, M.: Temperatures and the growth and development of wheat: a review, European Journal of Agronomy, 10, 23–36, https://doi.org/10.1016/S1161-0301(98)00047-1, 1999.

Postiglione, L.: Soil Salinization in the Mediterranean: Soils, Processes and Implications, in: Mediterranean desertification, edited by Geeson, N., Brandt, C. J., and Thornes, J. B., pp. 163–173, John Wiley & Sons, Chichester West Sussex England and Hoboken NJ USA, 2002.

Potter, C., Tan, P. N., Steinbach, M., Klooster, S., Kumar, V., Myneni, R., and Genovese, V.: Major disturbance events in terrestrial ecosystems detected using global satellite data sets, Global Change Biology, 9, 1005–1021, 2003.

Prasad, P. V. V. and Djanaguiraman, M.: Response of floret fertility and individual grain weight of wheat to high temperature stress: sensitive stages and thresholds for temperature and duration, Functional plant biology, 41, 1261–1269, https://doi.org/10.1071/FP14061, 2014.

Prasad, P. V. V., Pisipati, S. R., Ristic, Z., Bukovnik, U., and Fritz, A. K.: Impact of Nighttime Temperature on Physiology and Growth of Spring Wheat, Crop Science, 48, 2372–2380, https://doi.org/10.2135/cropsci2007.12.0717, 2008.

R Core Team: R: A Language and Environment for Statistical Computing, Vienna, Austria, URL `https://www.R-project.org/`, last access: 19/12/2021, 2020.

Rahmstorf, S. and Coumou, D.: Increase of extreme events in a warming world, Proceedings of the National Academy of Sciences, 108, 17 905–17 909, https://doi.org/10.1073/pnas.1201491109, 2011.

Rajsekhar, D., Singh, V. P., and Mishra, A. K.: Multivariate drought index: An information theory based approach for integrated drought assessment, Journal of Hydrology, 526, 164–182, https://doi.org/10.1016/j.jhydrol.2014.11.031, 2015.

Raymond, C., Horton, R. M., Zscheischler, J., Martius, O., AghaKouchak, A., Balch, J., Bowen, S. G., Camargo, S. J., Hess, J., Kornhuber, K., Oppenheimer, M., Ruane, A. C., Wahl, T., and White, K.: Understanding and managing connected extreme events, Nature Climate Change, 10, 611–621, https://doi.org/10.1038/s41558-020-0790-4, 2020.

Reichstein, M., Ciais, P., Papale, D., Valentini, R., Running, S., Viovy, N., Cramer, W., Granier, A., Ogée, J., Allard, V., Aubinet, M., Bernhofer, C., Buchmann, N., Carrara, A., Grünwald, T., Heimann, M., Heinesch, B., Knohl, A., Kutsch, W., Loustau, D., Manca, G., Matteucci, G., Miglietta, F., Ourcival, J. M., Pilegaard, K., Pumpanen, J., Rambal, S., Schaphoff, S., Seufert, G., Soussana, J.-F., Sanz, M. J., Vesala, T., and Zhao, M.: Reduction of ecosystem productivity and respiration during the European summer 2003 climate anomaly: a joint flux tower, remote sensing and modelling analysis, Global Change Biology, 13, 634–651, https://doi.org/10.1111/j.1365-2486.2006.01224.x, 2007.

Reichstein, M., Bahn, M., Ciais, P., Frank, D., Mahecha, M. D., Seneviratne, S. I., Zscheischler, J., Beer, C., Buchmann, N., Frank, D. C., Papale, D., Rammig, A., Smith, P., Thonicke, K., van der Velde, M., Vicca, S., Walz, A., and Wattenbach, M.: Climate extremes and the carbon cycle, Nature, 500, 287–295, https://doi.org/10.1038/nature12350, 2013.

Reichstein, M., Camps-Valls, G., Stevens, B., Jung, M., Denzler, J., Carvalhais, N., and Prabhat: Deep learning and process understanding for data-driven Earth system science, Nature, 566, 195–204, https://doi.org/10.1038/s41586-019-0912-1, 2019.

Rennenberg, H., Loreto, F., Polle, A., Brilli, F., Fares, S., Beniwal, R. S., and Gessler, A.: Physiological responses of forest trees to heat and drought, Plant biology (Stuttgart, Germany), 8, 556–571, https://doi.org/10.1055/s-2006-924084, 2006.

Rezaei, E. E., Siebert, S., and Ewert, F.: Intensity of heat stress in winter wheat—phenology compensates for the adverse effect of global warming, Environmental Research Letters, 10, 024 012, https://doi.org/10.1088/1748-9326/10/2/024012, 2015.

Ribeiro, A. F. S., Russo, A., Gouveia, C. M., Páscoa, P., and Pires, C. A. L.: Probabilistic modelling of the dependence between rainfed crops and drought hazard, Natural Hazards and Earth System Sciences, 19, 2795–2809, https://doi.org/10.5194/nhess-19-2795-2019, 2019.

Ribeiro, A. F. S., Russo, A., Gouveia, C. M., Páscoa, P., and Zscheischler, J.: Risk of crop failure due to compound dry and hot extremes estimated with nested copulas, Biogeosciences, 17, 4815–4830, https://doi.org/10.5194/bg-17-4815-2020, 2020a.

Ribeiro, A. F. S., Russo, A., Gouveia, C. M., and Pires, C. A.: Drought-related hot summers: A joint probability analysis in the Iberian Peninsula, Weather and Climate Extremes, 30, 100 279, https://doi.org/10.1016/j.wace.2020.100279, 2020b.

Ribot, J.: Cause and response: vulnerability and climate in the Anthropocene, The Journal of Peasant Studies, 41, 667–705, https://doi.org/10.1080/03066150.2014.894911, 2014.

Rolinski, S., Rammig, A., Walz, A., von Bloh, W., van Oijen, M., and Thonicke, K.: A probabilistic risk assessment for the vulnerability of the European carbon cycle to weather extremes: the ecosystem perspective, Biogeosciences, 12, 1813–1831, https://doi.org/10.5194/bg-12-1813-2015, 2015.

Roscher, R., Bohn, B., Duarte, M. F., and Garcke, J.: Explainable Machine Learning for Scientific Insights and Discoveries, IEEE Access, 8, 42 200–42 216, https://doi.org/10.1109/ACCESS.2020.2976199, 2020.

Rosenzweig, C., Iglesias, A., Yang, X. B., Epstein, P. R., and Chivian, E.: Climate change and extreme weather events - Implications for food production, plant diseases, and pests, Global Change and Human Health, 2, 90–104, 2001.

Röthlisberger, M. and Martius, O.: Quantifying the Local Effect of Northern Hemisphere Atmospheric Blocks on the Persistence of Summer Hot and Dry Spells, Geophysical Research Letters, 46, 10 101–10 111, https://doi.org/10.1029/2019GL083745, 2019.

Rowland, L., Da Costa, A. C. L., Galbraith, D. R., Oliveira, R. S., Binks, O. J., Oliveira, A. A. R., Pullen, A. M., Doughty, C. E., Metcalfe, D. B., Vasconcelos, S. S., Ferreira, L. V., Malhi, Y., Grace, J., Mencuccini, M., and Meir, P.: Death from drought in tropical forests is triggered by hydraulics not carbon starvation, Nature, 528, 119–122, https://doi.org/10.1038/nature15539, 2015.

Rubel, F., Brugger, K., Haslinger, K., and Auer, I.: The climate of the European Alps: Shift of very high resolution Köppen-Geiger climate zones 1800–2100, Meteorologische Zeitschrift, 26, 115–125, https://doi.org/10.1127/metz/2016/0816, 2017.

Rubio, J. L., ed.: Water scarcity, land degradation and desertification in the Mediterranean Region: Environmental and security aspects: proceedings of the NATO Advanced Research Workshop on Water Scarcity, Land Degradation and Desertification in the Mediterranean Region - Environment and Security Linkages, Valencia, Spain, 10 - 11 December 2007, NATO Science for Peace and Security Series - C Environmental Security, Springer, Dordrecht, URL `https://link.springer.com/book/10.1007/978-90-481-2526-5`, last access: 19/12/2021, 2009.

Ruffault, J., Curt, T., Martin-StPaul, N. K., Moron, V., and Trigo, R. M.: Extreme wildfire events are linked to global-change-type droughts in the northern Mediterranean, Natural Hazards and Earth System Sciences, 18, 847–856, https://doi.org/10.5194/nhess-18-847-2018, 2018.

Samaniego, L., Thober, S., Kumar, R., Wanders, N., Rakovec, O., Pan, M., Zink, M., Sheffield, J., Wood, E. F., and Marx, A.: Anthropogenic warming exacerbates European soil moisture droughts, Nature Climate Change, 8, 421–426, https://doi.org/10.1038/s41558-018-0138-5, 2018.

Sanz, H., Valim, C., Vegas, E., Oller, J. M., and Reverter, F.: SVM-RFE: selection and visualization of the most relevant features through non-linear kernels, BMC bioinformatics, 19, 432, https://doi.org/10.1186/s12859-018-2451-4, 2018.

Sarris, D., Christodoulakis, D., and Körner, C.: Impact of recent climatic change on growth of low elevation eastern Mediterranean forest trees, Climatic change, 106, 203–223, https://doi.org/10.1007/s10584-010-9901-y, 2011.

Schauberger, B., Archontoulis, S., Arneth, A., Balkovic, J., Ciais, P., Deryng, D., Elliott, J., Folberth, C., Khabarov, N., Müller, C., Pugh, T. A. M., Rolinski, S., Schaphoff, S., Schmid, E., Wang, X., Schlenker, W., and Frieler, K.: Consistent negative response of US crops to high temperatures in observations and crop models, Nature communications, 8, 13 931, https://doi.org/10.1038/ncomms13931, 2017.

Schilling, J., Hertig, E., Tramblay, Y., and Scheffran, J.: Climate change vulnerability, water resources and social implications in North Africa, Regional Environmental Change, 20, https://doi.org/10.1007/s10113-020-01597-7, 2020.

Schlenker, W. and Roberts, M. J.: Nonlinear temperature effects indicate severe damages to U.S. crop yields under climate change, Proceedings of the National Academy of Sciences, 106, 15 594–15 598, https://doi.org/10.1073/pnas.0906865106, 2009.

Schleussner, C.-F., Lissner, T. K., Fischer, E. M., Wohland, J., Perrette, M., Golly, A., Rogelj, J., Childers, K., Schewe, J., Frieler, K., Mengel, M., Hare, W., and Schaeffer, M.: Differential climate impacts for policy-relevant limits to global warming: the case of 1.5 °C and 2 °C, Earth System Dynamics, 7, 327–351, https://doi.org/10.5194/esd-7-327-2016, 2016.

Scholze, M., Buchwitz, M., Dorigo, W., Guanter, L., and Quegan, S.: Reviews and syntheses: Systematic Earth observations for use in terrestrial carbon cycle data assimilation systems, Biogeosciences, 14, 3401–3429, https://doi.org/10.5194/bg-14-3401-2017, 2017.

Schönfelder, P. and Schönfelder, I.: Die Kosmos Mittelmeerflora, Kosmos-Naturführer, Kosmos, Stuttgart, 2018.

Schrader, S. M., Wise, R. R., Wacholtz, W. F., Ort, D. R., and Sharkey, T. D.: Thylakoid membrane responses to moderately high leaf temperature in Pima cotton, Plant, Cell and Environment, 27, 725–735, https://doi.org/10.1111/j.1365-3040.2004.01172.x, 2004.

Schulzweida, U.: CDO Climate Data Operator, Zenodo, https://doi.org/10.5281/zenodo.3539275, 2019.

Sedlmeier, K., Feldmann, H., and Schädler, G.: Compound summer temperature and precipitation extremes over central Europe, Theoretical and Applied Climatology, 131, 1493–1501, https://doi.org/10.1007/s00704-017-2061-5, 2018.

Seneviratne, S. I., Corti, T., Davin, E. L., Hirschi, M., Jaeger, E. B., Lehner, I., Orlowsky, B., and Teuling, A. J.: Investigating soil moisture–climate interactions in a changing climate: A review, Earth-Science Reviews, 99, 125–161, https://doi.org/10.1016/j.earscirev.2010.02.004, 2010.

Seneviratne, S. I., N. Nicholls, D. Easterling, C.M. Goodess, S. Kanae, J. Kossin, Y. Luo, J. Marengo, K. McInnes, and M. Rahimi: Changes in climate extremes and their impacts on the natural physical environment, in: Managing the Risks of Extreme Events and Disasters to Advance Climate Change Adaptation: A Special Report of Working Groups I and II of the Intergovernmental Panel on Climate Change, edited by Field, C. B., Barros, V., Stocker, T. F., Qin, D., Dokken, D. J., Ebi, K. L., Mastrandrea, M., Mach, J., Plattner, G.-K., Allen, K., Tignor, M., and Midgley, P. M., pp. 109–230, Cambridge University Press, Cambridge, UK, and New York, NY, USA, 2012.

Seneviratne, S. I., Donat, M. G., Mueller, B., and Alexander, L. V.: No pause in the increase of hot temperature extremes, Nature Climate Change, 4, 161–163, https://doi.org/10.1038/nclimate2145, 2014.

Seyfert, F.: Phänologie, vol. 255 of *Die neue Brehm-Bücherei*, VerlagsKG Wolf, Magdeburg, 2 edn., 1960.

Sheffield, J. and Wood, E. F.: Projected changes in drought occurrence under future global warming from multi-model, multi-scenario, IPCC AR4 simulations, Climate Dynamics, 31, 79–105, https://doi.org/10.1007/s00382-007-0340-z, 2008.

Shiferaw, B., Smale, M., Braun, H.-J., Duveiller, E., Reynolds, M., and Muricho, G.: Crops that feed the world 10. Past successes and future challenges to the role played by wheat in global food security, Food Security, 5, 291–317, https://doi.org/10.1007/s12571-013-0263-y, 2013.

Shukla, P. R., Skea, J., Slade, R., van Diemen, R., Haughey, E., Malley, J., Pathak, M., and Portugal Pereira J.: Technical Summary, in: Climate Change and Land: an IPCC special report on climate change, desertification, land degradation, sustainable land management, food security, and greenhouse gas fluxes in terrestrial ecosystems, edited by Shukla, P. R., Skea, J., Calvo Buendia, E., Masson-Delmotte, V., Pörtner, H.-O., Roberts, D. C., Zhai, P., Slade, R., Connors, S., van Diemen, R., Ferrat, M., Haughey, E., Luz, S., Neogi, S., Pathak, M., Petzold, J., Portugal Pereira, J., Vyas, P., Huntley, E., Kissick, K., Belkacemi, M., and Malley, J., URL `https://www.ipcc.ch/srccl/`, last access: 19/12/2021, 2019.

Simelton, E., Fraser, E. D., Termansen, M., Forster, P. M., and Dougill, A. J.: Typologies of crop-drought vulnerability: an empirical analysis of the socio-economic factors that influence the sensitivity and resilience to drought of three major food crops in China (1961–2001), Environmental Science & Policy, 12, 438–452, https://doi.org/10.1016/j.envsci.2008.11.005, 2009.

Sippel, S., Zscheischler, J., and Reichstein, M.: Ecosystem impacts of climate extremes crucially depend on the timing, Proceedings of the National Academy of Sciences, 113, 5768–5770, https://doi.org/10.1073/pnas.1605667113, 2016.

Sippel, S., El-Madany, T. S., Migliavacca, M., Mahecha, M. D., Carrara, A., Flach, M., Kaminski, T., Otto, F. E. L., Thonicke, K., Vossbeck, M., and Reichstein, M.: Warm Winter, Wet Spring, and an Extreme Response in Ecosystem Functioning on the Iberian Peninsula, Bulletin of the American Meteorological Society, 99, S80–S85, https://doi.org/10.1175/BAMS-D-17-0135.1, 2018a.

Sippel, S., Reichstein, M., Ma, X., Mahecha, M. D., Lange, H., Flach, M., and Frank, D.: Drought, Heat, and the Carbon Cycle: a Review, Current Climate Change Reports, 4, 266–286, https://doi.org/10.1007/s40641-018-0103-4, 2018b.

Smets, B., Verger, A., Camacho, F., van der Goten, R., and Jacobs, T.: Copernicus Global Land Operations “Vegetation and Energy”: Product User Manual: Leaf Area Index (LAI) Fraction Of Absorbed Photosynthetically Active Radiation (FAPAR) Fraction Of Vegetation Cover (FCOVER) Collection 1km Version 2 Issue 1.33, Copernicus Global Land Operations, URL `https://land.copernicus.eu/global/products/fapar`, last access: 19/12/2021, 2019.

Smith, M. D.: An ecological perspective on extreme climatic events: a synthetic definition and framework to guide future research, Journal of Ecology, 99, 656–663, https://doi.org/10.1111/j.1365-2745.2011.01798.x, 2011.

Spano, D., Snyder, R. L., and Cesaraccio, C.: Mediterranean Phenology, in: Phenology: An Integrative Environmental Science, edited by Schwartz, M. D., pp. 173–196, Springer Netherlands, Dordrecht, https://doi.org/10.1007/978-94-007-6925-0_10, 2013.

Stahl, K., Kohn, I., Blauhut, V., Urquijo, J., De Stefano, L., Acácio, V., Dias, S., Stagge, J. H., Tallaksen, L. M., Kampragou, E., van Loon, A. F., Barker, L. J., Melsen, L. A., Bifulco, C., Musolino, D., de Carli, A., Massarutto, A., Assimacopoulos, D., and van Lanen, H. A. J.: Impacts of European drought events: insights from an international database of text-based reports, Natural Hazards and Earth System Sciences, 16, 801–819, https://doi.org/10.5194/nhess-16-801-2016, 2016.

Stevanato, L., Baroni, G., Cohen, Y., Fontana, C. L., Gatto, S., Lunardon, M., Marinello, F., Moretto, S., and Morselli, L.: A Novel Cosmic-Ray Neutron Sensor for Soil Moisture Estimation over Large Areas, Agriculture, 9, 202, https://doi.org/10.3390/agriculture9090202, 2019.

Strer, M., Svoboda, N., and Herrmann, A.: Abundance of adverse environmental conditions during critical stages of crop production in Northern Germany, Environmental sciences Europe, 30, 10, https://doi.org/10.1186/s12302-018-0138-0, 2018.

Sutanto, S. J., Vitolo, C., Di Napoli, C., D'Andrea, M., and van Lanen, H. A. J.: Heatwaves, droughts, and fires: Exploring compound and cascading dry hazards at the pan-European scale, Environment international, 134, 105 276, https://doi.org/10.1016/j.envint.2019.105276, 2020.

Svoboda, M. and Fuchs, B. A.: Handbook of Drought Indicators and Indices, World Meteorological Organization and Global Water Partnership, Integrated Drought Management Programme (IDMP), Integrated Drought Management Tools and Guidelines Series 2, Geneva, 2016.

Terradas, J. and Savé, R.: The influence of summer and winter stress and water relationships on the distribution of Quercus ilex L., Vegetatio, 99-100, 137–145, https://doi.org/10.1007/978-94-017-2836-2_14, 1992.

Teskey, R., Wertin, T., Bauweraerts, I., Ameye, M., McGuire, M. A., and Steppe, K.: Responses of tree species to heat waves and extreme heat events, Plant, cell & environment, 38, 1699–1712, https://doi.org/10.1111/pce.12417, 2015.

Teubner, I. E., Forkel, M., Camps-Valls, G., Jung, M., Miralles, D. G., Tramontana, G., van der Schalie, R., Vreugdenhil, M., Mösinger, L., and Dorigo, W. A.: A carbon sink-driven approach to estimate gross primary production from microwave satellite observations, Remote Sensing of Environment, 229, 100–113, https://doi.org/10.1016/j.rse.2019.04.022, 2019.

Teuling, A. J., Seneviratne, S. I., Stöckli, R., Reichstein, M., Moors, E., Ciais, P., Luyssaert, S., van den Hurk, B., Ammann, C., Bernhofer, C., Dellwik, E., Gianelle, D., Gielen, B., Grünwald, T., Klumpp, K., Montagnani, L., Moureaux, C., Sottocornola, M., and Wohlfahrt, G.: Contrasting response of European forest and grassland energy exchange to heatwaves, Nature Geoscience, 3, 722–727, https://doi.org/10.1038/ngeo950, 2010.

Thornes, J. B.: The Evolving Context of Mediterranean Desertification, in: Mediterranean desertification, edited by Geeson, N., Brandt, C. J., and Thornes, J. B., pp. 5–11, John Wiley & Sons, Chichester West Sussex England and Hoboken NJ USA, 2002.

Tibshirani, R.: Regression Shrinkage and Selection via the Lasso, Journal of the Royal Statistical Society: Series B (Statistical Methodology), 58, 267–288, 1996.

Tilloy, A., Malamud, B. D., Winter, H., and Joly-Laugel, A.: A review of quantification methodologies for multi-hazard interrelationships, Earth-Science Reviews, 196, 102 881, https://doi.org/10.1016/j.earscirev.2019.102881, 2019.

Toreti, A. and Naveau, P.: On the evaluation of climate model simulated precipitation extremes, Environmental Research Letters, 10, 014 012, https://doi.org/10.1088/1748-9326/10/1/014012, 2015.

Tramblay, Y., Koutroulis, A., Samaniego, L., Vicente-Serrano, S. M., Volaire, F., Boone, A., Le Page, M., Llasat, M. C., Albergel, C., Burak, S., Cailleret, M., Kalin, K. C., Davi, H., Dupuy, J.-L., Greve, P., Grillakis, M., Hanich, L., Jarlan, L., Martin-StPaul, N., Martínez-Vilalta, J., Mouillot, F., Pulido-Velazquez, D., Quintana-Seguí, P., Renard, D., Turco, M., Türkeş, M., Trigo, R., Vidal, J.-P., Vilagrosa, A., Zribi, M., and Polcher, J.: Challenges for drought assessment in the Mediterranean region under future climate scenarios, Earth-Science Reviews, 210, 103 348, https://doi.org/10.1016/j.earscirev.2020.103348, 2020.

Trigo, R. M., Gouveia, C. M., and Barriopedro, D.: The intense 2007–2009 drought in the Fertile Crescent: Impacts and associated atmospheric circulation, Agricultural and Forest Meteorology, 150, 1245–1257, https://doi.org/10.1016/j.agrformet.2010.05.006, 2010.

Trnka, M., Olesen, J. E., Kersebaum, K. C., Skjelvåg, A. O., Eitzinger, J., Seguin, B., Peltonen-Sainio, P., Rötter, R. P., Iglesias, A., Orlandini, S., Dubrovsky, M., Hlavinka, P., Balek, J., Eckersten, H., Cloppet, E., Calanca, P., Gobin, A., Vučetič, V., Nejedlik, P., Kumar, S., Lalic, B., Mestre, A., Rossi, F., Kozyra, J., Alexandrov, V., Semerádová, D., and Žalud, Z.: Agroclimatic conditions in Europe under climate change, Global Change Biology, 17, 2298–2318, https://doi.org/10.1111/j.1365-2486.2011.02396.x, 2011.

Trnka, M., Rötter, R. P., Ruiz-Ramos, M., Kersebaum, K. C., Olesen, J. E., Žalud, Z., and Semenov, M. A.: Adverse weather conditions for European wheat production will become more frequent with climate change, Nature Climate Change, 4, 637–643, https://doi.org/10.1038/nclimate2242, 2014.

Tuel, A. and Eltahir, E. A. B.: Why Is the Mediterranean a Climate Change Hot Spot?, Journal of Climate, 33, 5829–5843, https://doi.org/10.1175/JCLI-D-19-0910.1, 2020.

Ulbrich, U., Lionello, P., Belušić, D., Jacobeit, J., Knippertz, P., Kuglitsch, F. G., Leckebusch, G. C., Luterbacher, J., Maugeri, M., Maheras, P., Nissen, K. M., Pavan, V., Pinto, J. G., Saaroni, H., Seubert, S., Toreti, A., Xoplaki, E., and Ziv, B.: Climate of the Mediterranean, in: The climate of the Mediterranean region, edited by Lionello, P., Elsevier insights, pp. 301–346, Elsevier Science, Amsterdam, https://doi.org/10.1016/B978-0-12-416042-2.00005-7, 2012.

van der Molen, M. K., Dolman, A. J., Ciais, P., Eglin, T., Gobron, N., Law, B. E., Meir, P., Peters, W., Phillips, O. L., Reichstein, M., Chen, T., Dekker, S. C., Doubková, M., Friedl, M. A., Jung, M., van den Hurk, B., de Jeu, R., Kruijt, B., Ohta, T., Rebel, K. T., Plummer, S., Seneviratne, S. I., Sitch, S., Teuling, A. J., van der Werf, G. R., and Wang, G.: Drought and ecosystem carbon cycling, Agricultural and Forest Meteorology, 151, 765–773, https://doi.org/10.1016/j.agrformet.2011.01.018, 2011.

van der Velde, M., Baruth, B., Bussay, A., Ceglar, A., Garcia Condado, S., Karetsos, S., Lecerf, R., Lopez, R., Maiorano, A., Nisini, L., Seguini, L., and van den Berg, M.: In-season performance of European Union wheat forecasts during extreme impacts, Scientific reports, 8, 15 420, https://doi.org/10.1038/s41598-018-33688-1, 2018.

van Oijen, M., Beer, C., Cramer, W., Rammig, A., Reichstein, M., Rolinski, S., and Soussana, J.-F.: A novel probabilistic risk analysis to determine the vulnerability of ecosystems to extreme climatic events, Environmental Research Letters, 8, 015 032, https://doi.org/10.1088/1748-9326/8/1/015032, 2013.

van Oldenborgh, G. J., Krikken, F., Lewis, S., Leach, N. J., Lehner, F., Saunders, K. R., van Weele, M., Haustein, K., Li, S., Wallom, D., Sparrow, S., Arrighi, J., Singh, R. K., van Aalst, M. K., Philip, S. Y., Vautard, R., and Otto, F. E. L.: Attribution of the Australian bushfire risk to anthropogenic climate change, Natural Hazards and Earth System Sciences, 21, 941–960, https://doi.org/10.5194/nhess-21-941-2021, 2021.

van Rossum, G. and Drake, F. L.: Python 3 Reference Manual, CreateSpace, Scotts Valley, CA, 2009.

Vayreda, J., Martinez-Vilalta, J., Gracia, M., and Retana, J.: Recent climate changes interact with stand structure and management to determine changes in tree carbon stocks in Spanish forests, Global Change Biology, 18, 1028–1041, https://doi.org/10.1111/j.1365-2486.2011.02606.x, 2012.

Verger, A., Baret, F., and Weiss, M.: Near Real-Time Vegetation Monitoring at Global Scale, IEEE Journal of Selected Topics in Applied Earth Observations and Remote Sensing, 7, 3473–3481, https://doi.org/10.1109/JSTARS.2014.2328632, 2014.

Vicente-Serrano, S. M. and Beguería-Portugués, S.: Estimating extreme dry-spell risk in the middle Ebro valley (northeastern Spain): a comparative analysis of partial duration series with a general Pareto distribution and annual maxima series with a Gumbel distribution, International Journal of Climatology, 23, 1103–1118, https://doi.org/10.1002/joc.934, 2003.

Vicente-Serrano, S. M., McVicar, T. R., Miralles, D. G., Yang, Y., and Tomas-Burguera, M.: Unraveling the influence of atmospheric evaporative demand on drought and its response to climate change, WIREs Climate Change, 11, e632, https://doi.org/10.1002/wcc.632, 2020.

Vilà-Cabrera, A., Martínez-Vilalta, J., Vayreda, J., and Retana, J.: Structural and climatic determinants of demographic rates of Scots pine forests across the Iberian Peninsula, Ecological Applications, 21, 1162–1172, https://doi.org/10.1890/10-0647.1, 2011.

Vogel, E., Donat, M. G., Alexander, L. V., Meinshausen, M., Ray, D. K., Karoly, D., Meinshausen, N., and Frieler, K.: The effects of climate extremes on global agricultural yields, Environmental Research Letters, 14, 054 010, https://doi.org/10.1088/1748-9326/ab154b, 2019.

Vogel, J.: Ecosystem_vulnerability, URL `https://github.com/jo-vogel/ecosystem_vulnerability`, last access: 19/12/2021, 2021a.

Vogel, J.: compound_events_mediterranean, URL `https://github.com/jo-vogel/compound_events_mediterranean`, last access: 19/12/2021, 2021b.

Vogel, J., Rivoire, P., Deidda, C., Sauter, C. A., and Tschumi, E.: Identify_crop_yield_drivers, URL `https://github.com/jo-vogel/Identify_crop_yield_drivers`, last access: 19/12/2021, 2021.

von Buttlar, J., Zscheischler, J., Rammig, A., Sippel, S., Reichstein, M., Knohl, A., Jung, M., Menzer, O., Arain, M. A., Buchmann, N., Cescatti, A., Gianelle, D., Kieley, G., Law, B. E., Magliulo, V., Margolis, H., McCaughey, H., Merbold, L., Migliavacca, M., Montagnani, L., Oechel, W., Pavelka, M., Peichl, M., Rambal, S., Raschi, A., Scott, R. L., Vaccari, F. P., van Gorsel, E., Varlagin, A., Wohlfahrt, G., and Mahecha, M. D.: Impacts of droughts and extreme temperature events on gross primary production and ecosystem respiration: a systematic assessment across ecosystems and climate zones, Biogeosciences, 15, 1293–1318, https://doi.org/10.5194/bg-15-1293-2018, 2018.

Wagner, W., Blöschl, G., Pampaloni, P., Calvet, J.-C., Bizzarri, B., Wigneron, J.-P., and Kerr, Y.: Operational readiness of microwave remote sensing of soil moisture for hydrologic applications, Hydrology Research, 38, 1–20, https://doi.org/10.2166/nh.2007.029, 2007.

Walter, J., Jentsch, A., Beierkuhnlein, C., and Kreyling, J.: Ecological stress memory and cross stress tolerance in plants in the face of climate extremes, Environmental and Experimental Botany, 94, 3–8, https://doi.org/10.1016/j.envexpbot.2012.02.009, 2013.

West, H., Quinn, N., and Horswell, M.: Remote sensing for drought monitoring & impact assessment: Progress, past challenges and future opportunities, Remote Sensing of Environment, 232, 111 291, https://doi.org/10.1016/j.rse.2019.111291, 2019.

Wilhite, D. A. and Glantz, M. H.: Understanding: the Drought Phenomenon: The Role of Definitions, Water International, 10, 111–120, https://doi.org/10.1080/02508068508686328, 1985.

Wolf, S., Keenan, T. F., Fisher, J. B., Baldocchi, D. D., Desai, A. R., Richardson, A. D., Scott, R. L., Law, B. E., Litvak, M. E., Brunsell, N. A., Peters, W., and van der Laan-Luijkx, I. T.: Warm spring reduced carbon cycle impact of the 2012 US summer drought, Proceedings of the National Academy of Sciences, 113, 5880–5885, https://doi.org/10.1073/pnas.1519620113, 2016.

Wu, M., Vico, G., Manzoni, S., Cai, Z., Bassiouni, M., Tian, F., Zhang, J., Ye, K., and Messori, G.: Early growing season anomalies in vegetation activity determine the large–scale climate–vegetation coupling in Europe, Journal of Geophysical Research: Biogeosciences, 126, e2020JG006 167, https://doi.org/10.1029/2020JG006167, 2021.

Yordanov, I.: Response of photosynthetic apparatus to temperature stress and molecular mechanisms of its adaptations, Photosynthetica, 26, 517–531, 1992.

Zampieri, M., Ceglar, A., Dentener, F., and Toreti, A.: Wheat yield loss attributable to heat waves, drought and water excess at the global, national and subnational scales, Environmental Research Letters, 12, 064 008, https://doi.org/10.1088/1748-9326/aa723b, 2017.

Zdruli, P.: Desertification in the Mediterranean region, in: Mediterranean Yearbook, edited by IEMed, pp. 250–254, Girona, URL `https://www.iemed.org/med-yearbook/iemed-mediterranean-yearbook-2011/`, last access: 19/12/2021, 2011.

Zhang, S., Tao, F., and Zhang, Z.: Spatial and temporal changes in vapor pressure deficit and their impacts on crop yields in China during 1980–2008, Journal of Meteorological Research, 31, 800–808, https://doi.org/10.1007/s13351-017-6137-z, 2017.

Zheng, B., Chenu, K., Doherty, A., and Chapman, S.: The APSIM-Wheat Module (7.5 R3008), Agricultural Production Systems Simulator (APSIM) Initiative, Toowoomba, Australia, URL `https://www.apsim.info/documentation/model-documentation/crop-module-documentation/wheat/`, last access: 19/12/2021, 2014.

Zhu, P., Abramoff, R., Makowski, D., and Ciais, P.: Uncovering the Past and Future Climate Drivers of Wheat Yield Shocks in Europe With Machine Learning, Earth's Future, 9, e2020EF001 815, https://doi.org/10.1029/2020EF001815, 2021.

Zscheischler, J. and Seneviratne, S. I.: Dependence of drivers affects risks associated with compound events, Science advances, 3, e1700 263, https://doi.org/10.1126/sciadv.1700263, 2017.

Zscheischler, J., Mahecha, M. D., Harmeling, S., and Reichstein, M.: Detection and attribution of large spatiotemporal extreme events in Earth observation data, Ecological Informatics, 15, 66–73, https://doi.org/10.1016/j.ecoinf.2013.03.004, 2013.

Zscheischler, J., Reichstein, M., von Buttlar, J., Mu, M., Randerson, J. T., and Mahecha, M. D.: Carbon cycle extremes during the 21st century in CMIP5 models: Future evolution and attribution to climatic drivers, Geophysical Research Letters, 41, 8853–8861, https://doi.org/10.1002/2014GL062409, 2014.

Zscheischler, J., Westra, S., van den Hurk, B. J. J. M., Seneviratne, S. I., Ward, P. J., Pitman, A., AghaKouchak, A., Bresch, D. N., Leonard, M., Wahl, T., and Zhang, X.: Future climate risk from compound events, Nature Climate Change, 8, 469–477, https://doi.org/10.1038/s41558-018-0156-3, 2018.

Zscheischler, J., Martius, O., Westra, S., Bevacqua, E., Raymond, C., Horton, R. M., van den Hurk, B., AghaKouchak, A., Jézéquel, A., Mahecha, M. D., Maraun, D., Ramos, A. M., Ridder, N. N., Thiery, W., and Vignotto, E.: A typology of compound weather and climate events, Nature Reviews Earth & Environment, 1, 333–347, https://doi.org/10.1038/s43017-020-0060-z, 2020a.

Zscheischler, J., van den Hurk, B., Ward, P. J., and Westra, S.: Multivariate extremes and compound events, in: Climate extremes and their implications for impact and risk assessment, edited by Sillmann, J., Sippel, S., and Russo, S., pp. 59–76, Elsevier, Amsterdam, https://doi.org/10.1016/B978-0-12-814895-2.00004-5, 2020b.

Zscheischler, J., Sillmann, J., and Alexander, L.: Introduction to the special issue: Compound weather and climate events, Weather and Climate Extremes, 100381, https://doi.org/10.1016/j.wace.2021.100381, 2021.

Appendix

Code availability

The code corresponding to the article in chapter 2 is available from `https://github.com/jo-vogel/compound_events_mediterranean` (Vogel, 2021b).
The code corresponding to the article in chapter 3 is available from `https://github.com/jo-vogel/ecosystem_vulnerability` (Vogel, 2021a).
The code corresponding to the article in chapter 4 is available from `https://github.com/jo-vogel/Identify_crop_yield_drivers` (Vogel et al., 2021).

Software and packages

The work was carried out using R version 3.6 (R Core Team, 2020), Python version 3.7 (van Rossum and Drake, 2009) and Climate Data Operators (CDO) version 1.9 (Schulzweida, 2019). The R package `SPEI` was used for calculating the SPI and SPEI (Beguería and Vicente-Serrano, 2017) and the R package `RStoolbox` was used to perform the change vector analysis (Leutner et al., 2019) for the article in chapter 2. The R packages `glmnet`, `bestglm`, and `randomForest` were applied to perform the analysis for the article in chapter 4 using a LASSO regression (Friedman et al., 2010), a generalized linear model (McLeod et al., 2020) and a random forest approach (Breiman, 2001, Liaw and Wiener, 2002).

Data availability

Table A1 provides an overview of all data sets, which were used in this thesis.

Table A1: Overview of datasets

Data set	Reference	Availability	Variable
ECMWF Reanalysis (ERA5)	Copernicus Climate Change Service (2017), Hersbach et al. (2019)	Publicly available	2 m air temperature Total precipitation Potential evaporation
ERA5-Land	Muñoz-Sabater (2019)	Publicly available	2 m air temperature Soil moisture
European Space Agency's Climate Change Initiative	Dorigo et al. (2017), Gruber et al. (2019)	Publicly available	Soil moisture
	ESA (2017)	Publicly available	Land cover
Copernicus Global Land Service	Baret et al. (2013), Verger et al. (2014)	Publicly available	FAPAR
–	Kottek et al. (2006), Rubel et al. (2017)	Publicly available	Köppen-Geiger climate classification
EC-Earth	Hazeleger et al. (2012)	Available on request from Karin van der Wiel (wiel@knmi.nl)	Dew-point temperature Precipitation 10 m wind speed Incoming shortwave radiation Maximum temperature Minimum temperature
APSIM	Zheng et al. (2014)	Available on request from Tianyi Zhang (zhangty@post.iap.ac.cn)	Wheat yield